AN ABSTRACT OF THE DISSERTATION OF

Nason J. McCullough for the degree of Doctor of Philosophy in Civil Engineering presented on June 2, 2003.

Title: The Seismic Geotechnical Modeling, Performance, and Analysis of Pile-Supported Wharves.

Abstract Approved:

Redacted for Privacy

Stephen E. Dickenson

This dissertation presents the results of a research effort conducted to better understand the seismic performance and analysis of pile-supported wharves. Given the limited number of well-documented field case histories, the seismic performance of pile-supported wharves has been poorly quantified, and the analysis methods commonly employed in engineering practice have generally not been validated. Field case histories documenting the seismic performance of pile-supported wharves commonly contain only limited information, such as approximations of wharf and embankment deformations and peak ground surface accelerations. In order to supplement the field data, five centrifuge models were dynamically tested, with each

model containing close to 100 instruments monitoring pile bending moments, excess pore pressures, displacements, and accelerations.

The combined field and model database was used to develop seismic performance relationships between permanent lateral deformations, maximum and residual bending moments and peak ground surface displacements. Key issues such as the seismic performance of batter piles, the development of large moments at depth, and the need to account for permanent lateral deformations for high levels of shaking, even for very stable geometries, are discussed.

The field data and model studies were also used to validate two geotechnical seismic performance analysis methods: 1) the limit-equilibrium based rigid, sliding block (Newmark) method, and 2) an advanced finite-difference effective stress based numerical model (FLAC). Favorable predictions were generally obtained for both methods, yet there was a large variability in the results predicted using the rigid, sliding block method. The numerical model predicted the permanent deformations, pore pressure generation, and accelerations fairly well, however, pile bending moments were poorly predicted. The results of this research clearly highlighted the need for analysis validation studies, and note the uncertainty and variability inherent in the seismic performance of complex structures. The lack of adequate validation may lead to an over-confidence and false sense of security in the results of the seismic analysis methods.

This dissertation specifically addresses pile-supported wharves, yet the results presented herein are applicable to other pile-supported structures located near, or on,

slopes adjacent to the waterfront, such as: bridge abutments, railroad trestles, and pile-supported buildings near open slopes. Performance and analysis issues common to all of these structures are addressed, such as: liquefiable soils, lateral pile response in horizontal and sloping soils, the lateral behavior of piles in rock fill, and global slope stability, as well as the general observed seismic behavior.

THE SEISMIC GEOTECHNICAL MODELING, PERFORMANCE, AND ANALYSIS OF PILE-SUPPORTED WHARVES

by

Nason J. McCullough

A DISSERTATION

submitted to

Oregon State University

in partial fulfillment of

the requirements for the

degree of

Doctor of Philosophy

Presented June 2, 2003

Commencement June 2004

Doctor of Philosophy dissertation of Nason J. McCullough presented on June 2, 2003.

APPROVED:

Redacted for Privacy

Major Professor, representing Civil Engineering

Redacted for Privacy

Head of the Department of Civil, Construction, and Environmental Engineering

Redacted for Privacy

Dean of the Graduate School

I understand that my dissertation will become part of the permanent collection of Oregon State University libraries. My signature below authorizes release of my dissertation to any reader upon request.

Redacted for Privacy

Nason J. McCullough, Author

ACKNOWLEDGEMENTS

The author expresses his sincere gratitude to Steve Dickenson, who has been a friend and mentor during his graduate studies at Oregon State University. I thank him for his guidance and allowing me to be a part of the interesting and practical research presented herein. I also want to acknowledge my fellow students at Oregon State University, who have been both colleagues and friends over the years. I am most grateful to Brian Nicholas who provided much friendship and academic competition during my undergraduate studies, and Scott Schlechter, a good friend and graduate colleague, who helped design, construct, test and diagnose the centrifuge models presented herein.

I also want express my gratitude to my parents, Patrick and Susan, who instilled in me the love of learning and a confidence that nothing was beyond my reach, proven by completion of this dissertation. My sister Leaf, who has been my friend and companion since her birth, not only providing sibling rivalry, but also the support and love of a truly dear friend. And lastly, and most importantly, my wife Amelia and children Ruth and Nicholas, who are the joy of my life. Amelia has provided love, support, patience, and encouragement during these graduate study years, while Ruth and Nicholas have shown me the importance of life.

CONTRIBUTION OF AUTHORS

Mr. Scott M. Schlechter and Mr. Jonathon C. Boland contributed much effort in designing, building, testing, and evaluating the centrifuge models, and are therefore listed as co-authors on the manuscript contained herein documenting the centrifuge models.

TABLE OF CONTENTS

Page

CHAPTER 1 – INTRODUCTION 1

SUMMARY OF PAST RESEARCH 4

Lateral Response of Piles in Soil 5
Physical Modeling 6
Numerical Modeling 7

PHYSICAL SCALE MODELING 10

NUMERICAL MODELING 11

General Formulation of FLAC 11
Constitutive Soil Model 14
Pore Pressure Generation 16
Soil Strength and Elastic Modulus 24
Modeling of Structural Elements 24
Modeling of the Water (Pore Fluid) 32
Boundary Conditions 34
Modeling of the Earthquake Motions 35

CHAPTER 2 – MANUSCRIPT NO. 1: THE DYNAMIC CENTRIFUGE MODELING OF PILE-SUPPORTED WHARVES 39

ABSTRACT 40

INTRODUCTION 41

DESCRIPTION OF THE CENTRIFUGE FACILITY 43

MODEL CONTAINER 44

MODEL SCALING 44

PORE FLUID 47

DESIGN OF THE MODELS 48

Geometry 48
Structural Elements 57
Nevada Sand 59

TABLE OF CONTENTS (continued)

INSTRUMENTATION 62

MODEL CONSTRUCTION 64

Soil Placement 64
Placement of the Piles and Wharf Deck 67
Saturation 67

MODEL TESTING 68

TEST RESULTS 69

ACKNOWLEDGEMENTS 75

REFERENCES 76

CHAPTER 3 – MANUSCRIPT NO. 2: THE SEISMIC PERFORMANCE OF PILE-SUPPORTED WHARVES 79

ABSTRACT 80

INTRODUCTION 81

FIELD CASE HISTORY SUMMARY 81

MODEL CASE HISTORIES 90

GENERAL PERFORMANCE OF PILE-SUPPORTED WHARVES 95

SUMMARY 107

ACKNOWLEDGEMENTS 109

REFERENCES 110

CHAPTER 4 – MANUSCRIPT NO. 3: THE SEISMIC ANALYSIS OF PILE-SUPPORTED STRUCTURES ON SLOPES 113

ABSTRACT 114

INTRODUCTION 115

METHODS OF ANALYSIS 118

Rigid, sliding block method 118

TABLE OF CONTENTS (continued)

Finite-difference numerical analyses 122

RESULTS OF THE SLIDING BLOCK VALIDATION STUDY 126

RESULTS OF THE NUMERICAL MODEL VALIDATION STUDY 133

Lateral Pile Behavior in Sloping Rock Fill 133
Port of Oakland 135
Centrifuge Models 140

DISCUSSION 146

SUMMARY 148

ACKNOWLEDGEMENTS 149

REFERENCES 150

CHAPTER 5 – SUMMARY AND CONCLUSIONS 154

CHAPTER 6 – RECOMMENDATIONS FOR FUTURE RESEARCH 159

BIBLIOGRAPHY 162

APPENDICES 171

APPENDIX A – RESULTS OF THE LIMIT EQUILIBRIUM SLOPE STABILITY ANALYSES AND THE NEWMARK RIGID, SLIDING BLOCK ANALYSES 172
APPENDIX B – NUMERICAL MODEL PREDICTIONS OF THE CENTRIFUGE MODEL PERFORMANCE 193

LIST OF FIGURES

Figure		Page
1.	Typical Pile-Supported Wharf Geometries.	3
2.	Basic Explicit Calculation Cycle (after Itasca 2000).	12
3.	Cyclic Strength Curve.	17
4.	Simplified Base Curve Recommended for Calculation of CRR from SPT Data along with Empirical Liquefaction Data for a M_w 7.5 earthquake (modified From Seed et al. 1985, as presented by Youd et al. 1997).	19
5.	K_σ correction factor, as recommended by Harder and Boulanger (1997).	21
6.	K_α correction factor, as recommended by Harder and Boulanger (1997), where τ_s is the initial static shear stress, and σ'_{vo} is the initial effective overburden stress.	22
7.	Relationship between the excess pore pressure ratio and the damage parameter.	23
8.	Graphical Illustration of the shear pile interface springs used in FLAC.	26
9.	Graphical Illustration of the normal pile interface springs used in FLAC.	26
10.	A typical FLAC model used to estimate the normal pile interface spring stiffness and strength values.	28
11.	Data from a FLAC analysis to determine the normal pile interface spring stiffness and strength values.	29
12.	Centrifuge Model Geometries for Lateral Pile Load Tests of Models SMS02 and JCB01.	30
13.	Comparison between the predicted moments and displacements using FLAC and the measured values from the centrifuge models SMS02 and JCB01 for the piles in the sloping rock fill	33
14.	Comparison between the predicted moments and displacements using FLAC and the measured values from centrifuge models for the pile in the sloping rock fill for one cycle of the load sequence.	34

LIST OF FIGURES (Continued)

15. Comparison between the predicted bending moments and displacements using FLAC and the measured values from the centrifuge models SMS02 and JCB01 for the piles in the horizontally layered backland soils 37

16. Comparison between the predicted moments and displacements using FLAC and the measured values from the centrifuge models for the pile in the horizontally layered backland for one cycle of the load sequence. 38

17. Typical pile-supported wharf structures. 42

18. Plan and profile views of the container utilized for the suite of centrifuge models. 45

19. Plan and profile of centrifuge model NJM01. 51

20. Plan and profile of centrifuge model NJM02. 52

21. Plan and profile of centrifuge model SMS01. 53

22. Plan and profile of centrifuge model SMS02. 54

23. Plan and profile of centrifuge model JCB01. 55

24. Plan views showing the locations of the single piles in models a) SMS02, and b) JCB01 that were used for the cyclic lateral load tests. 56

25. Rock Gradations used in the models. 61

26. Un-scaled input acceleration time histories 69

27. Measured and observed permanent lateral wharf deformation for various levels of shaking.. 71

28. NJM02 post-test ground cracks and separation between the piles and soils. 72

29. Post-test ground cracks in SMS01 due to lateral slope movement. 72

30. Post-test ground surface settlement in the backland of SMS01 due to liquefaction. 73

31. Typical Pile-Supported Wharf Geometries. 82

LIST OF FIGURES (Continued)

32. Port of Oakland damaged batter pile during the 1989 Loma Prieta Earthquake. 85

33. Port of Kobe Takahama Wharf damaged during the 1995 Hyogoken-Nambu Earthquake (Iai 1998). 87

34. Permanent lateral deformations Takahama Wharf at the Port of Kobe measured following the 1995 Hyogoken-Nambu Earthquake (Iai 1998). 88

35. Port of Kobe Takahama Wharf damaged during the 1995 Hyogoken-Nambu Earthquake piles extracted from the wharf for inspection. 89

36. Centrifuge model NJM01. 92

37. Centrifuge model NJM02. 93

38. Centrifuge model SMS01. 93

39. Centrifuge model SMS02. 94

40. Centrifuge model JCB01. 94

41. Relationship between the ground surface peak ground acceleration in the backland and the permanent lateral deformation of the wharf deck 96

42. Maximum cyclic and residual moments for three piles for centrifuge model NJM01. 99

43. Maximum cyclic and residual moments for three piles for centrifuge model NJM02. 100

44. Maximum cyclic and residual moments for two piles for centrifuge model SMS01. 101

45. Maximum cyclic and residual moments for two piles for centrifuge model SMS02. 102

46. Maximum cyclic and residual moments for two piles for centrifuge model JCB01. 103

47. Relationship between the peak ground surface acceleration and the maximum dynamic pile moments. 104

LIST OF FIGURES (Continued)

48. The normalized residual moment recorded at depth, plotted against the permanent lateral deformation of the wharf deck..... 106

49. Ratio of the moments recorded adjacent to the pile/deck connection to the maximum pile moments recorded at depth, plotted against the peak ground surface acceleration in the backland. 107

50. Typical Pile-Supported Wharf Geometries. 116

51. Simplified cyclic strength curve. 125

52. Centrifuge model NJM01. 128

53. Centrifuge model NJM02. 128

54. Centrifuge model SMS01. 129

55. Centrifuge model SMS02. 129

56. Centrifuge model JCB01. 130

57. Results of the rigid, sliding block validation study. 132

58. Centrifuge Model Geometries for Lateral Pile Load Tests. 134

59. Comparison between the predicted moments and displacements for the pile in the sloping rock fill..... 135

60. Pile-supported wharf at the Port of Oakland Seventh Street Terminal, prior to the 1989 Loma Prieta Earthquake (Egan et al. 1992)..... 137

61. Geometry, grid and structural elements that were used in the numerical model of the Port of Oakland Seventh Street Terminal, Berth 38..... 138

62. Input acceleration time history for the numerical model (El. –21 m). 139

63. Numerical model predicted performance of Berth 38, Seventh Street Terminal, Port of Oakland during the 1989 Loma Prieta Earthquake..... 140

64. Results of the FLAC validation study using the centrifuge model test data. 145

65. Comparison between the Centrifuge measured and FLAC predicted residual moments in piles number 2 and 5 for centrifuge model SMS01. 147

LIST OF TABLES

Table		Page
1.	Recommended values for the *CRR* correction factor, c_r.	18
2.	Model scaling factors and values.	47
3.	Model summary.	49
4.	Pile properties for all of the centrifuge models, including the prototype target pile properties.	58
5.	Wharf deck properties for all of the centrifuge models, including the prototype target wharf deck properties.	59
6.	Summary of Nevada Sand properties.	60
7.	In-situ soil properties.	66
8.	Centrifuge model summary.	91
9.	Parameters used in the rigid, sliding block analyses, and results of the validation study.	131
10.	Soil properties used in the FLAC validation of the Port of Oakland seismic case history	137
11.	Structural properties used in the FLAC validation of the Port of Oakland seismic case history	139
12.	Cohesionless soil properties for the centrifuge models.	142
13.	Cohesive soil properties for the centrifuge models.	142

CHAPTER 1 – INTRODUCTION

The research presented in this dissertation is the culmination of an extensive investigation examining the seismic performance of pile-supported wharves. Given the predominance of pile-supported wharves at western United States ports, the moderate to high seismicity of the western United States, and the limited information addressing the seismic performance and analysis of pile-supported wharves, this research program was initiated with several primary goals:

1) Examine the seismic performance of pile-supported wharves using field case histories, physical model studies, and numerical model studies.
2) Examine the effect of soil improvement on the seismic behavior of pile-supported wharves.
3) Examine the ability of simplified and advanced analysis methods to predict the seismic performance of pile-supported wharves.

This research project focused primarily on geotechnical issues, such as soil liquefaction, slope stability, and soil/structure interaction. Bending moments in the piles were also examined. However, other structural design issues, such as pile/deck connections, detailing, and pile degradation were not examined.

A pile-supported wharf structure, as presented herein, consists of a wharf deck supported on piles installed in sloping ground at the waterfront. The sloping ground generally consists of either native soils overlain by a rock armor layer, or a perimeter rock dike used to contain backfill soils. The piles are driven and/or jetted through the

rock dike and into the foundation soils. The term pile-supported wharf, as used herein, refers to the entire pile/wharf/dike/soil system, as illustrated in Figure 1.

This dissertation is organized and presented in manuscript format, with three submitted journal articles linked together with the Introduction, and Summary and Conclusions chapters. The remaining sections of the Introduction chapter provide background information on centrifuge modeling and the advanced numerical model that was used for this research. This is information that may be useful to the reader, but could not be included in the manuscripts due to length limitations. Following this chapter, the three journal manuscripts present the details and results of this research program.

The first manuscript, "The Dynamic Centrifuge Modeling of Pile-Supported Wharves," is presented in Chapter 2, and provides details and select results of the small-scale physical models that were tested dynamically in a centrifuge. These well-instrumented model tests supplement the limited field case history database on the seismic performance of pile-supported wharves.

The second manuscript, "The Seismic Performance of Pile-Supported Wharves," is presented in Chapter 3, and provides a background summary on the seismic performance of pile-supported wharves. Included are field case histories, as well as the centrifuge modeling case histories presented in the first manuscript. The manuscript summarizes the seismic performance as a series of figures illustrating permanent ground deformations, peak ground accelerations, and maximum cyclic and residual bending moments in the piles.

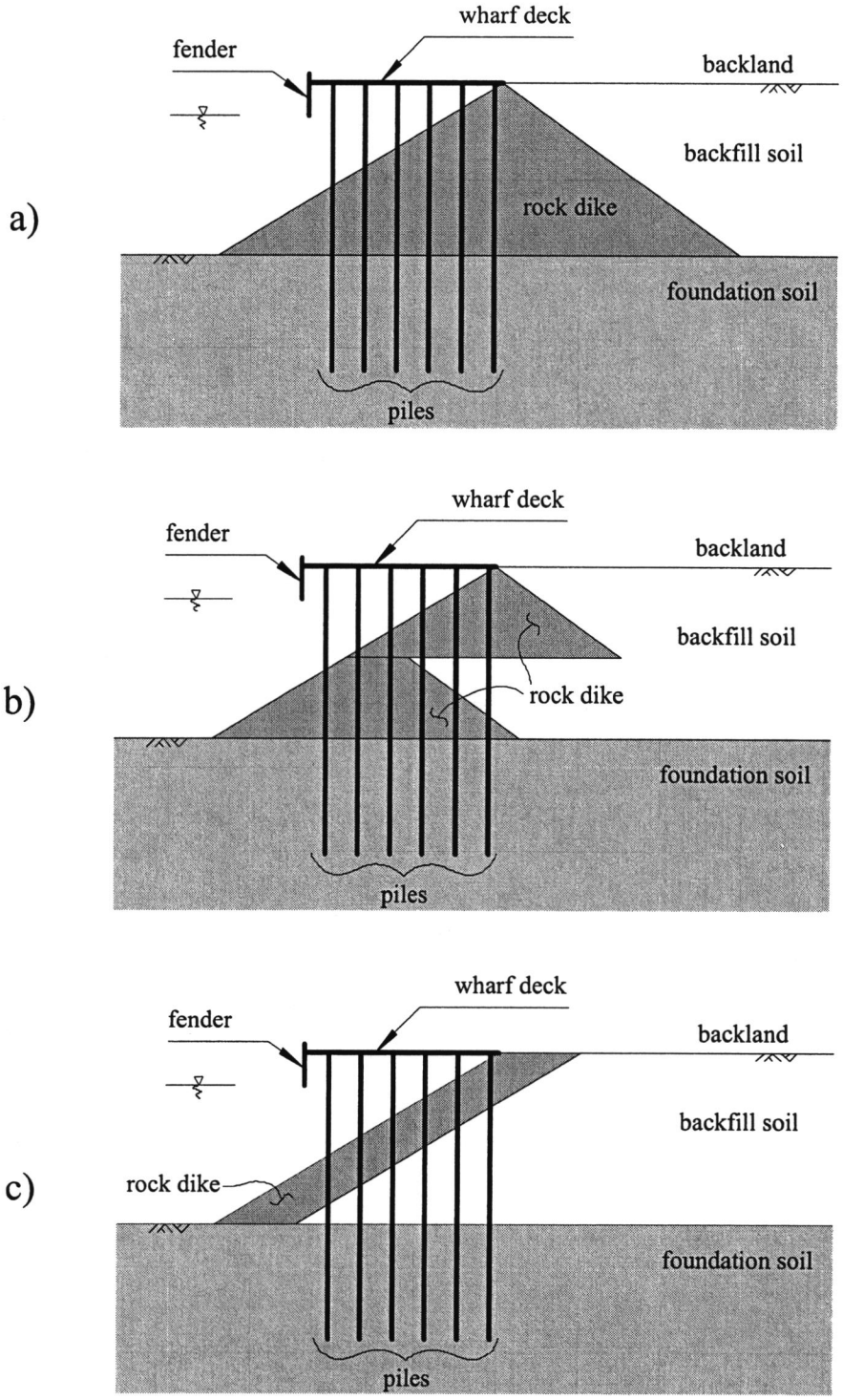

Figure 1. Typical pile-supported wharf geometries; a) single lift, b) multi-lift, and c) sliver (cut-slope) rock dike configurations.

The third manuscript, "The Seismic Analysis of Pile-Supported Structures on Slopes," presented in Chapter 4 provides the validation results of two geotechnical seismic analysis methods for pile-supported wharves. One method was relatively simple, based on the rigid, sliding block (Newmark) method of estimating permanent slope displacements. In order to better model the seismic behavior of pile-supported wharves, pore pressure generation and the effect of the piles were accounted for in the analyses. The other method was an advanced effective-stress based numerical model that was used to perform time history analyses. The advanced analysis method included the full soil/structure interaction, as well as the dynamic response of the soils and structure and the cyclically induced generation of excess pore pressures.

Chapter 5 provides a summary and conclusions of the research, while Chapter 6 includes recommendations for future research.

Appendix A includes the full results of the simplified method validation study, while Appendix B includes graphical results of the advanced model validation study.

SUMMARY OF PAST RESEARCH

There are several examples of pertinent past research on the seismic performance, modeling, and/or analysis of pile-supported wharves. However, to the author's knowledge, complete pile-supported wharf models have never been physically modeled, though numerical computer programs have been used to evaluate complete pile-supported wharf structures. In addition, there are portions of full-scale modeling, physical modeling, and numerical modeling efforts applicable to the

seismic behavior, performance, and analysis of pile-supported wharves. Presented below are summaries of these research efforts applicable to the research presented herein.

Lateral Response of Piles in Soil

The lateral response of piles in sands, silts, and clays has been well documented, including cyclic behavior and the behavior in sloping ground (Ensoft 1999). However, the vast majority of piles in pile-supported wharves are installed through sloping rock fill, a case that has not been well documented. Diaz et al. (1984) present the results of full-scale lateral pile load tests conducted at the Port of Los Angeles using reinforced concrete piles in rock fill. The tests were conducted to estimate the static lateral pile behavior in sloping rock fill. The tests were conducted at the top of a rock dike, with the pile being forced into the horizontal backland in one direction and downslope into the rock fill in the other direction. Diaz et al. (1984) then used COM624 to predict the measured pile deformations and bending moments. The p-y curves where then adjusted in COM624 until the predicted results were representative of the measured results. The authors presented a chart illustrating the required modifications to p-y curves developed for horizontally layered profiles to accurately model the case of piles in sloping rock fill.

The results indicated that the p-y springs should be adjusted to account for sloping conditions, in that there is a reduced lateral resistance in the downslope direction due to the smaller effective confining stresses, in comparison to the

horizontal or upslope direction. This is in agreement with the general recommendations for analyzing piles in slopes (Ensoft 1999). However, the factors presented by Diaz et al. (1984) were specific for rock fill, and indicated that the load (p) in the downslope direction wasas low as 5 percent of the value in horizontal profiles. It is also interesting to note that the back-calculated p-y reduction was only noted for depths below approximately 10 pile diameters, above this depth, there was an increase in resistance. The increase in lateral resistance was attributed by Diaz et al. (1984) to be due to individual rock particles being pushed over each other as the pile was pushed through the rock fill. This appears to be due to particle size effects, with the diameter of the rock particles being approximately the same diameter as the piles, thus representing discrete particle behavior. However, the standard p-y springs were developed for pile diameter to soil particle diameter ratios much greater than 1.0. This is discussed in more detail in Chapter 4.

Physical Modeling

There are no known physical models of complete pile-supported wharf systems, however, Scott et al. (1993) and Muraleetharan et al. (1997) presented the results of a centrifuge modeling study examining the seismic performance of a rock dike retaining a loose liquefiable backfill. This model was constructed to represent Pier 400 at the Port of Los Angeles. This centrifuge model did not include any structural elements, but did illustrate the general pattern of seismic deformations of rock dikes. The results of the model indicated liquefaction-induced volumetric strains

in the backland, lateral movement of the rock dike on the underlying silt, and the densification and deformation of the rock dike. This model represented the most similar centrifuge model to the research presented herein. Even though the model did not include structural elements and was of a fairly simple geometry, it illustrated the capability of modeling waterfront rock dike structures in a centrifuge.

There are numerous other research efforts documenting the seismic modeling of piles in horizontally layered liquefiable soils. Ko et al. (1984), Abdoun et al. (1997), Goh and O'Rourke (1999), and Wilson (1998) are several of the documented research efforts. These efforts provided the basis for the centrifuge modeling of piles. In addition, Abdoun et al. (1997) and Goh and O'Rourke (199) illustrated the development of large moments at depth due to pile pinning and the ability to model this effect in a centrifuge. These studies also illustrated the capability of modeling heavily instrumented piles in a centrifuge, and the ability to reduce recorded strain gauge data to back-calculate pile bending moments, shear, displacements, slopes, and applied soil pressures. In addition, the presented research illustrated methods of heavily and durably instrumenting piles to obtain accurate bending moment measurements.

Numerical Modeling

Roth et al. (1992) and Inel et al. (1993) describe the use of an advanced numerical program (FLAC) for modeling the seismic behavior of pile-supported wharves. The modeling method and constitutive model (Roth et al. 1986, Roth et al.

1991) utilized in the analyses was capable of modeling the cyclic generation of excess pore pressures and was the predecessor of the constitutive model used for the analyses presented herein. Roth et al. (1992) described two validation studies for the constitutive model, one involving horizontally layered backfill soil, and one involving the seismic response of the San Fernando Dam. Also described was the use of the numerical and constitutive model to analyze and design a pier at the Port of Long Beach (Inel et al. 1993). The papers contained validation studies of the constitutive model using field case histories, and highlighted the necessity of accounting for soil-structure interaction during the seismic analysis of pile-supported wharves. Also included was a discussion on the use of batter piles for the lateral resistance of pile-supported wharves. The constitutive model used for modeling the cyclic generation of excess pore pressures is discussed in more detail towards the end of Chapter 1, and the seismic behavior of batter piles is discussed in Chapter 3.

A numerical study on the seismic behavior of a pile-supported wharf (Seventh Street Terminal) at the Port of Oakland during the 1989 Loma Prieta earthquake by Singh et al. (2001, 2002) also highlights the importance of modeling the soil-structure interaction for pile-supported wharves. The authors also presented a parametric study on using various liquefied soil strengths. The authors had difficulty in predicting both pile deformations and the pattern of pile damage. For example, a good deformation prediction resulted in poor pile performance predictions. The authors also highlighted the necessity of accurately accounting for the soil behavior in structural seismic analysis of pile-supported wharves.

Roth and Dawson (2003) also present the results of validation studies on the seismic performance of pile-supported wharves at the Port of Oakland during the 1989 Loma Prieta earthquake, including the performance of several different wharves. Roth et al. (2003) presented the results of comparing structural analysis using FLAC, SAP2000 and Perform-2D, concluding that FLAC is capable of adequately modeling structural behavior. The authors also highlighted the necessity of interaction between the structural and geotechnical seismic analysis and design of pile-supported wharves.

McCullough and Dickenson (1998) and McCullough (1998) describe the use of FLAC and the same constitutive model utilized herein to model the seismic performance of sheet pile bulkheads. Presented were the satisfactory validation studies based on field case histories, and the development of simple design and screening tools for predicting the seismic performance of sheet pile bulkheads.

Numerical models have also been used extensively for the prediction of measured centrifuge model behavior. These validation studies have highlighted both the necessity of performing validation studies, and the capability of performing such studies. Some of the documented research efforts to predict the seismic behavior of centrifuge models include: Muraleetharan et al. (1997) presented the results of using DYSAC2 to predict the seismic behavior of rock dike containing liquefiable soils, Curras et al. (2001) presented the results of using GeoFEAP to predict the seismic lateral response of single piles and piles supporting a super-structure in liquefiable soils, Abdoun et al. (1997) and Goh and O'Rourke (1999) presented the results of using FLAC and BSTRUCT to predict the lateral behavior of piles in liquefied soil

during lateral spreading conditions. There are numerous other documented comparisons between numerical and centrifuge models, including the VELACS study (Arulanandan and Scott 1993), however, the several studies presented above are the most applicable to the research presented herein.

PHYSICAL SCALE MODELING

Scale modeling provides a method of examining the seismic behavior and performance of port structures, at a reduced scale. Given the limited number of field case histories, scale modeling is an attractive method to build a base of performance data for use in validating numerical models. There are two types of physical scale modeling, as presented herein. The first is centrifuge scale modeling in which a model is subjected to an increased *gravity* (centrifugal acceleration), producing a stress field within the model representative of a field stress state. Since the strength and elastic moduli values of soils are a function of confining stress, the increased *gravity* leads to a scale model representative of the prototype condition. The second type of modeling utilizes geometric scaling (also called one-g scaling). This type of modeling requires modification of the soil void ratio and density to arrive at soil strength and modulus values within the scale model that are representative of the prototype values. Geometric scale modeling was utilized in addition to centrifuge scaling for several of the model tests presented herein. The physical scale modeling for this research project is presented in Chapter 2.

NUMERICAL MODELING

The research presented herein utilized the advanced numerical model FLAC (Fast Lagrangian Analysis of Continua; Itasca 2000). FLAC is a non-linear, two-dimensional finite-difference computer program, developed for the continuum analysis of geotechnical materials. Results of the FLAC analysis of pile-supported wharf case histories are presented in Chapter 4, but due to length limitations of the manuscript, specifics of the FLAC modeling used for the project are summarized in the following sections. For a complete description of the mechanics of FLAC, the reader is directed to the FLAC User's Manual (Itasca 2000).

General Formulation of FLAC

FLAC is capable of modeling both static and dynamic situations. Elements or zones represent the materials (structural and soil), with all of the elements and zones constituting the grid (mesh). The numerical formulation of FLAC utilizes a time-stepping approach, where the following steps take place within FLAC (Figure 2) during each timestep:

1) Nodal velocities and displacements are calculated from stresses and forces using Newton's second law of motion given by:

$$m\frac{\partial \dot{u}}{\partial t} = F \tag{1}$$

where m is mass, $\partial \dot{u} / \partial t$ is acceleration, u is displacement, and F is force. Using the definition of a derivative, $\partial \dot{u} / \partial t$ is given by:

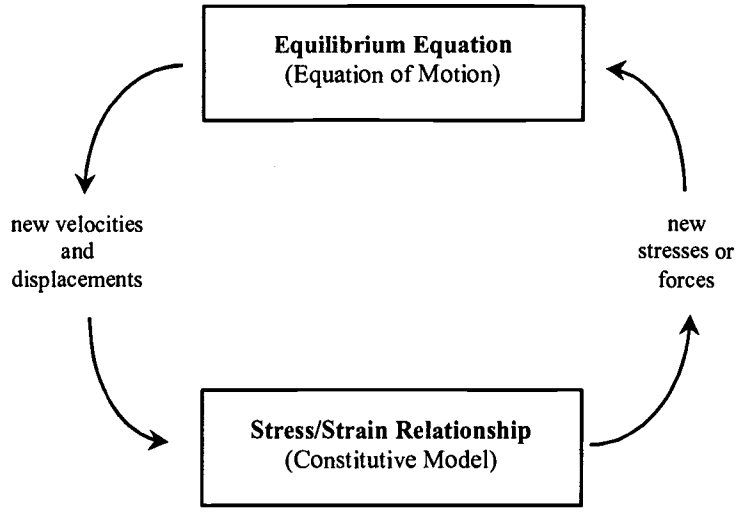

Figure 2. Basic explicit calculation cycle (after Itasca 2000)

$$\frac{\partial \dot{u}}{\partial t} = \lim_{\Delta t \to 0} \frac{\dot{u}^{(t+\Delta t/2)} - \dot{u}^{(t-\Delta t/2)}}{\Delta t} \tag{2}$$

By making the timestep (Δt) small, but finite, $\partial \dot{u} / \partial t$ is approximated as:

$$\frac{\partial \dot{u}}{\partial t} \approx \frac{\dot{u}^{(t+\Delta t/2)} - \dot{u}^{(t-\Delta t/2)}}{\Delta t} \tag{3}$$

Substituting equation 3 into equation 1 results in the nodal (gridpoint) velocity:

$$\dot{u}^{(t+\Delta t/2)} = \dot{u}^{(t-\Delta t/2)} + F^{(t)} \frac{\Delta t}{m} \tag{4}$$

where $F^{(t)}$ is the summation of the applied and body (gravitational) forces acting on the corresponding node at time t. Displacements are subsequently calculated as:

$$u^{(t+\Delta t)} = u^{(t)} + \dot{u}^{(t+\Delta t/2)}\Delta t \tag{5}$$

2) A constitutive model then calculates new stresses from the strain rates and current stresses:

$$\sigma_{ij}^{(t+\Delta t)} = \sigma_{ij}^{(t)} + \Delta\sigma_{ij} \tag{6}$$

where i and j denote the coordinates in a Cartesian coordinate plane, and the change in stress ($\Delta\sigma_{ij}$) is determined using the constitutive model ($M[\ ]$):

$$\Delta\sigma_{ij}^{(t+\Delta t)} = M\left[\Delta e_{ij}^{(t+\Delta t/2)}\right] \tag{7}$$

where $M[\ ]$ represents the constitutive relationship and the change in strain (Δe) is given by the average of the velocity gradients:

$$\Delta e_{ij}^{(t+\Delta t/2)} = \frac{1}{2}\left[\frac{\partial \dot{u}_i}{\partial x_j}^{(t+\Delta t/2)} + \frac{\partial \dot{u}_j}{\partial x_i}^{(t+\Delta t/2)}\right]\Delta t \tag{8}$$

These two steps are repeated until the sum of the forces acting on the node is below a set tolerance for static solutions. For dynamic solutions, the scheme is followed for a specific period of time.

FLAC uses an explicit method, where the calculation timestep is very short compared with the time necessary for information (e.g. acceleration, velocity, displacement) to physically pass from one element to another. For soils, the maximum

speed at which information can physically propagate is typically taken as the pressure wave velocity.

FLAC also utilizes a *Lagrangian* formulation, in which the incremental displacements are added to the coordinates at each timestep so that the grid moves and deforms with the material that it represents. Because of the explicit Lagrangian methodology, and the explicit use of the equations of motion, FLAC is advantageous in modeling nonlinear, large strain, physically unstable situations (Itasca 2000). In addition, with the use of an excess pore pressure generation constitutive model, the ability to model soil-structure interaction, and the seismic analysis capabilities, FLAC is advantageous for modeling the seismic performance of pile-supported wharves.

Constitutive Soil Model

Two constitutive soil models were used during this research project. The first was an effective stress Mohr-Coulomb constitutive model, which was capable of modeling plastic deformations utilizing a plastic flow rule. The second was identical to the Mohr-Coulomb constitutive model, but had the added functionality of modeling pore pressure generation, and is denoted herein as the SEED.FIS constitutive model. The elastic soil behavior for both constitutive models was defined by the bulk and shear modulus values of the soil, while the soil strength was defined by the effective angle of friction and cohesion, and the volumetric shear behavior was defined by a dilation angle.

The fundamental elastic relationships are given by Hooke's law in plane strain in the incremental form as:

$$\begin{aligned}
\Delta\sigma_{11} &= \alpha_1 \Delta e_{11} + \alpha_2 \Delta e_{22} \\
\Delta\sigma_{22} &= \alpha_1 \Delta e_{22} + \alpha_2 \Delta e_{11} \\
\Delta\sigma_{12} &= 2G\Delta e_{12} \\
\Delta\sigma_{33} &= \alpha_2 \left(\Delta e_{11} + \Delta e_{22}\right)
\end{aligned} \tag{9}$$

where α_1 and α_2 represent functions of the bulk modulus (K) and shear modulus (G), and are given by:

$$\begin{aligned}
\alpha_1 &= K + \frac{4}{3}G \\
\alpha_2 &= K - \frac{2}{3}G \\
K &= \frac{E}{3(1-2\nu)} \\
G &= \frac{E}{2(1+\nu)}
\end{aligned} \tag{10}$$

where E is the elastic modulus and ν is Poisson's Ratio. Rewriting equation 9 in terms of principle stresses and strains:

$$\begin{aligned}
\Delta\sigma_1 &= \alpha_1 \Delta e_1 + \alpha_2 \left(\Delta e_2 + \Delta e_3\right) \\
\Delta\sigma_2 &= \alpha_1 \Delta e_2 + \alpha_2 \left(\Delta e_1 + \Delta e_3\right) \\
\Delta\sigma_3 &= \alpha_1 \Delta e_3 + \alpha_2 \left(\Delta e_1 + \Delta e_2\right)
\end{aligned} \tag{11}$$

The strains noted in equations 9 and 11 are elastic strains. Corrections to the stresses are made if either shear or tensile failure occurs. If the stress state for the new

timestep lies outside the failure envelope, corrections are made to the stress state until it lies on or within the failure envelope.

Pore Pressure Generation

The SEED.FIS constitutive model utilized a pore pressure generation scheme based on empirical cyclic stress ratio parameters (Martin et al. 1975; Seed et al. 1976; Seed 1979). Shear stress cycles were tracked during the analyses, and pore pressures were incrementally generated in liquefiable soils as a function of the liquefaction resistance of the soil. The incremental pore pressures were added to the hydrostatic pore pressures, resulting in decreased effective stresses as excess pore pressures were generated.

The liquefaction resistance of the soil was defined by a cyclic strength curve, relating the cyclic resistance ratio of the soil to the number of cycles necessary to cause liquefaction (Figure 3). The cyclic resistance ratio (*CRR*) is the cyclic shear stress (τ_{cyc}) required to cause liquefaction, normalized by the initial effective overburden stress (σ'_{vo}). In the SEED.FIS constitutive model, the resistance curve was simplified as a tri-linear line, with an upper plateau at the cyclic resistance ratio required to cause liquefaction in 3 cycles (CRR_3) and the lower bound the cyclic resistance ratio required to cause liquefaction in 30 cycles (CRR_{30}).

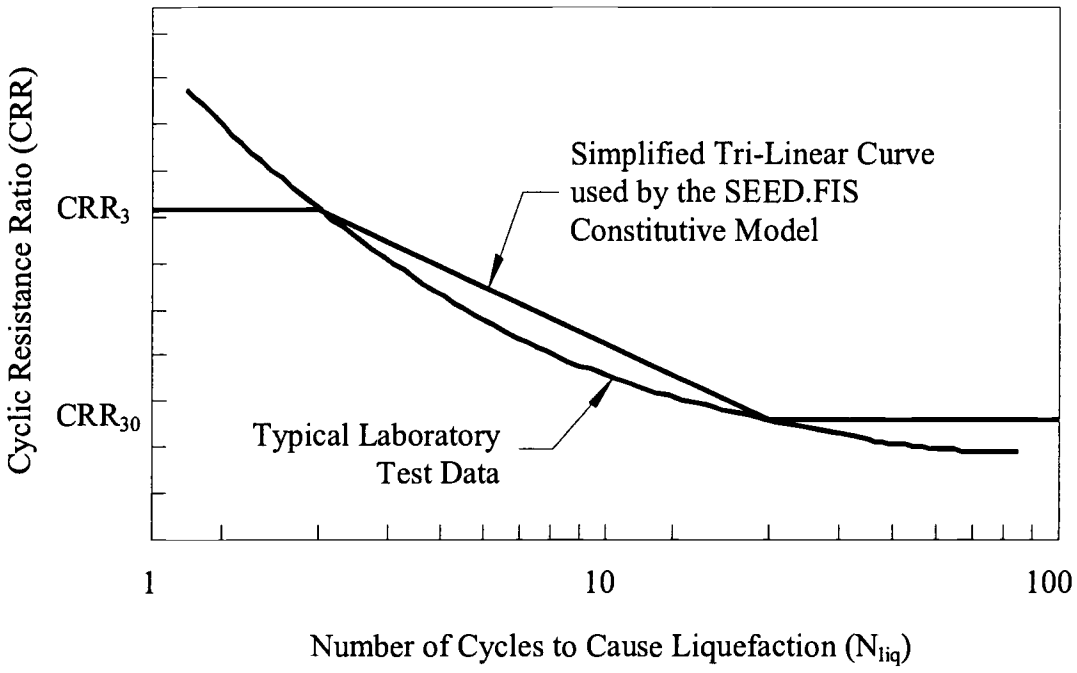

Figure 3. Cyclic strength curve.

If laboratory test data was used to develop the cyclic strength curve, adjustments were made to convert the laboratory values to field values. Cyclic triaxial tests (CRR_{tx}) and cyclic simple shear (CRR_{ss}) tests are the most common laboratory methods of developing cyclic strength curves, but these two test methods impose different loadings. In addition, cyclic triaxial and cyclic simple shear laboratory tests are unidirectional, and it has been noted that the bi-directional shaking in the field results in approximately a 10 percent decrease in resistance. Incorporation of these corrections leads to the following relationship between the *CRR* values used to develop the cyclic strength curves and the values determined from laboratory testing:

$$CRR = 0.9(CRR_{ss}) = 0.9(c_r)(CSR_{tx}) \quad (12)$$

where published values of the correction factor (c_r) are provided in Table 1.

Table 1. Recommended values for the *CRR* correction factor, c_r.

Reference	Equation	c_r for the following at rest earth pressures (K_0)	
		K_0 = 0.4	K_0 = 1.0
Finn et al. (1971)	$c_r = (1 + K_0)/2$	0.7	1.0
Seed and Peacock (1971)	Varies	0.55-0.72	1.0
Castro (1975)	$c_r = 2(1 + 2K_0)/(3\sqrt{3})$	0.69	1.15

In many cases, laboratory specific cyclic resistance data were not available, and for these cases the following procedures were used to estimate the cyclic strength curve.

1) For the soil layer in question, the corrected *SPT* blowcount, $(N_1)_{60}$ was used to estimate the cyclic resistance for a M_w 7.5 earthquake ($CRR_{7.5}$) using Figure 4. A M_w 7.5 earthquake was assumed to produce 15 equivalent uniform cycles of shaking (Youd et al. 1997).
2) Magnitude scaling factors (*MSF*) were then used to estimate the *CRR* values at 3 and 30 cycles, assuming that a M_w 5.4 earthquake represented 3 equivalent uniform cycles of shaking and that a M_w 8.9 earthquake represented 30 equivalent uniform cycles of shaking. The *MSF* values were determined using the following equation (Youd et al. 1997):

$$MSF = \frac{10^{2.24}}{M_w^{2.56}} \tag{13}$$

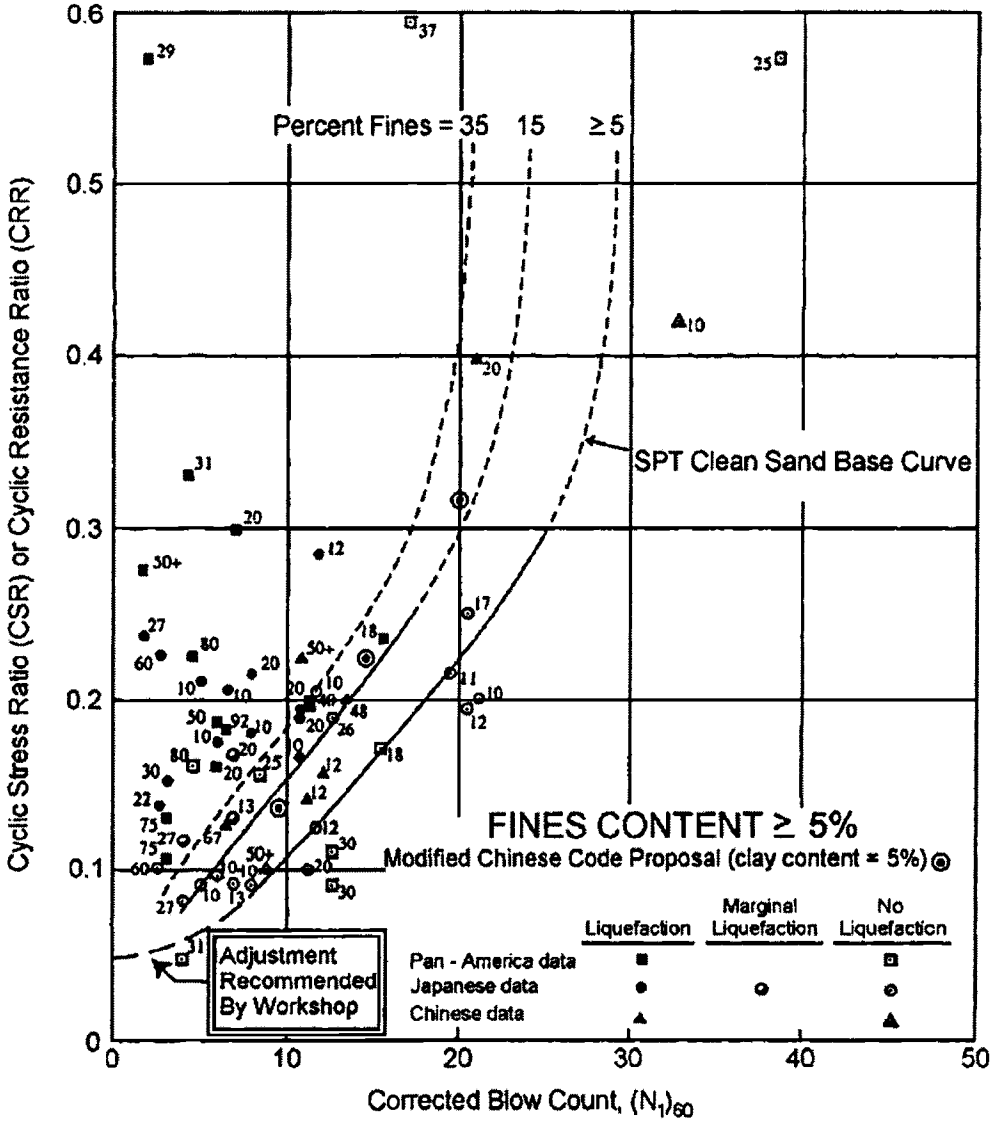

Figure 4. Simplified base curve recommended for calculation of *CRR* from *SPT* data along with empirical liquefaction data for a M_w 7.5 earthquake (modified From Seed et al. 1985, as presented by Youd et al. 1997).

Cyclically loaded laboratory tests have indicated that liquefaction resistance is also a function of confining stress. The cyclic resistance of soils increases with increased confining stress, but the relationship between *CRR* and confining stress is nonlinear. Therefore, a correction was required to adjust the *CRR* values at high confining stresses. In addition, the cyclic resistance is a function of initial static shear stresses. For loose soils, initial static shear stresses tend to de-stabilize the soil and reduce the liquefaction resistance, whereas for dense soils initial static shear stresses tend to increase the resistance to liquefaction. The overburden and initial static shear stress corrections are termed the K_σ and K_α corrections, respectively, and were determined using Figure 5 and Figure 6, respectively.

The estimated *CRR* for input into the SEED.FIS model was therefore calculated as:

$$CRR = CRR_{7.5} \cdot MSF \cdot K_\sigma \cdot K_\alpha \tag{14}$$

During the dynamic solution, shear stress cycles were monitored within each potentially liquefiable soil zone using the SEED.FIS constitutive model. When a stress reversal was detected, the induced cyclic stress ratio (*CSR*) was calculated. The *CSR* value was then used to determine the number of equivalent cycles to cause liquefaction for the particular shear stress cycle (*N*) from the simplified cyclic resistance curve presented in Figure 3.

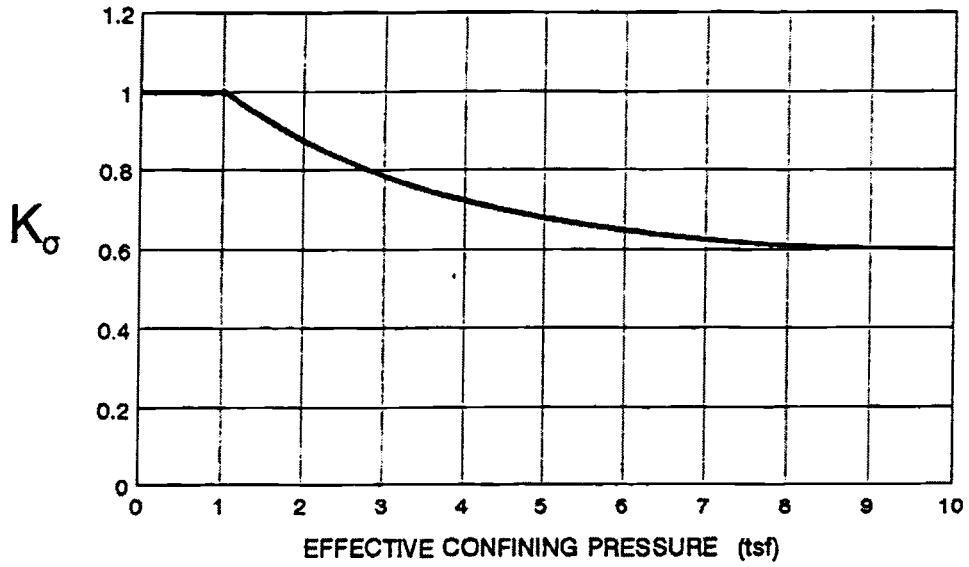

Figure 5. K_σ correction factor (Harder and Boulanger 1997).

The summation of the inverse of the number of cycles to liquefaction recorded for each stress cycle for each zone was represented by an incremental damage parameter, ΔD (Annaki and Lee 1977), as follows:

$$\Delta D = \frac{1}{N} \tag{15}$$

The incremental damage parameter was linearly related to the excess pore pressure ratio (r_u) as:

$$r_u = D = \sum \Delta D \tag{16}$$

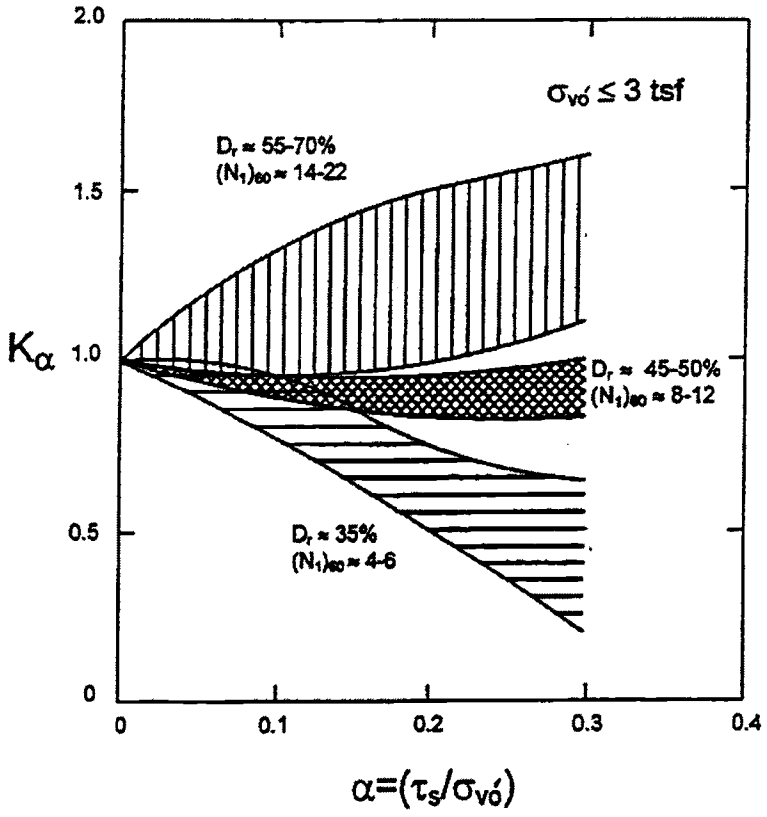

Figure 6. K_α correction factor (Harder and Boulanger (1997). τ_s is the initial static shear stress, and σ'_{vo} is the initial effective vertical stress.

The actual relationship between r_u and D is nonlinear (Figure 7), but for sands the relationship is fairly well predicted by the linear relationship used in the SEED.FIS model. However, it should be noted that the relationship is much more nonlinear for finer (silt) or coarser (gravel) soils. It has also been noted that the actual pore pressure generation path (linear or nonlinear) has little effect on the resulting liquefaction induced deformation predictions (Inel et al. 1993).

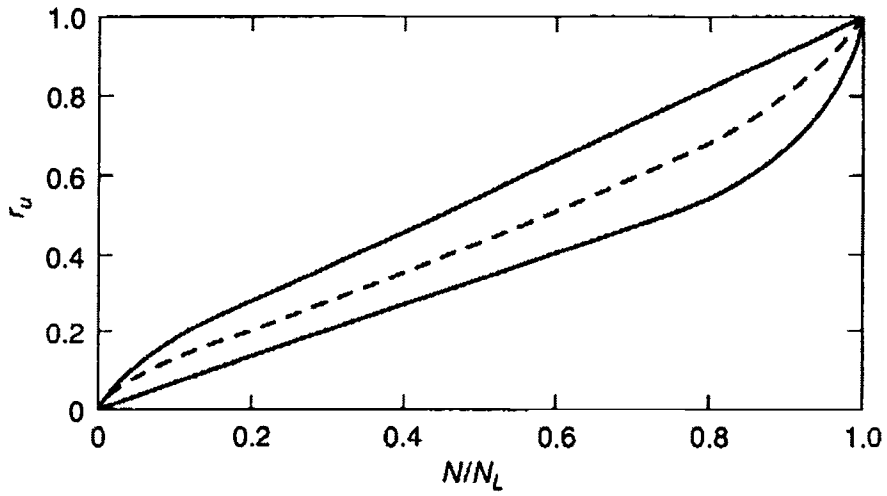

Figure 7. Relationship between the excess pore pressure ratio and the damage parameter (equivalent to N/N_L), showing an approximate linear, one-to-one relationship (after De Alba et al. 1975).

Excess pore pressures were then calculated and added to hydrostatic pore pressures (u_h) to obtain the total pore pressure (u):

$$u_{excess} = r_u \cdot \sigma'_{vo}$$
$$u = u_g + u_{excess} \tag{17}$$

Therefore, as the pore pressures in the model increased, the effective stresses decreased, and the effects of earthquake-induced pore pressure generation were modeled.

One-dimensional volumetric strains due to the dissipation of pore pressures were also calculated at the end of each dynamic analysis following the recommendations of Ishihara and Yoshimine (1992) using a post-processing routine.

Soil Strength and Elastic Modulus

As mentioned above, the Mohr-Coulomb constitutive model requires the bulk and shear modulus values to represent the elastic behavior, the cohesion and angle of internal friction to model soil failure, and the dilation angle to model shear strain induced volumetric strains. These properties were determined from laboratory tests, empirical correlations with field tests, or from published correlations.

Liquefied soil strengths (S_r) were modeled following the recommendations of Stark and Mesri (1992) as a function of initial effective overburden stress and energy, overburden stress, and fines corrected SPT blowcount ($(N_1)_{60-cs}$):

$$S_r = 0.011 \cdot \sigma_{vo}' \cdot (N_1)_{60-cs} \tag{18}$$

Alternatively, the relationship provided by Seed and Harder (1990) was utilized in some instances. In the SEED.FIS model the strength of a liquefied zone of soil was the maximum of the liquefied soil strength, or the value calculated from the Mohr-Coulomb strength criteria:

$$S = \sigma' \cdot tan(\phi) \tag{19}$$

Modeling of Structural Elements

FLAC has several options for the modeling of structural elements, including beam and pile elements, both of which were utilized for this project. Beam and pile elements are identical, except that pile elements include an interface element to model

soil-structure interaction (SSI). The interface element utilizes springs to model both the shear and normal SSI behavior. The procedures used to estimate the normal spring stiffness and a validation study are outlined in the following sections.

Estimation of the Pile Interface Spring Stiffness and Strength Values

There are two interface elements, normal and shear, each having a stiffness and strength. The stiffness and strength values represent the load-displacement relationship between the piles and the soil. The normal interface elements are analogous to p-y springs, and the shear interface elements are analogous to t-z springs, commonly used in the lateral and vertical analysis of piles, except that p-y and t-z springs empirically represent both the interface behavior and the adjacent soil behavior, whereas the FLAC interface springs represent only the interface behavior. The values of the springs are graphically illustrated in Figure 8 and Figure 9 for the shear and normal springs, respectively.

The normal spring stiffness and strength values were estimated using a FLAC model of the pile in plan view, through cross-sections at various depths. A typical model is shown in Figure 10. In the model, stresses were applied, representing the in-situ condition, and the pile was forced at a constant velocity through the soil. In Figure 10 the pile is being pushed *down* the model, and it is interesting to note the gap that has formed between the pile and the soil elements, typical of lateral pile behavior in cohesive and dense cohesionless soils. Plots of the force versus confining stress and

displacement were then used to develop the parameters shown in Figure 9, as illustrated in Figure 11.

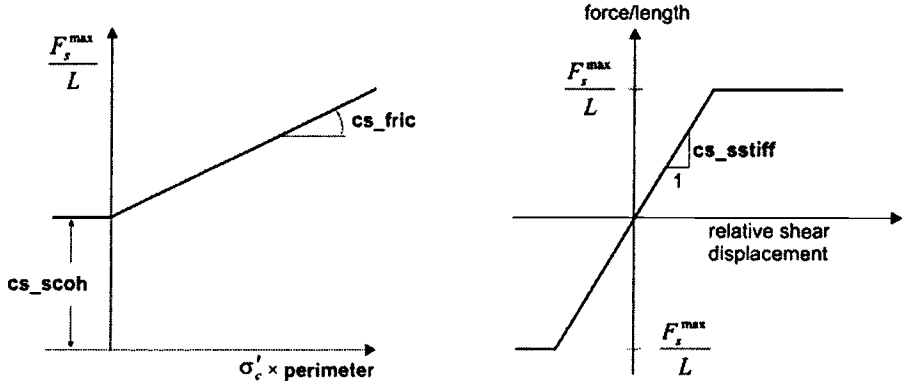

a) Shear strength criterion b) Shear force versus displacement

Figure 8. Graphical illustration of the shear pile interface springs used in FLAC (F_s is the shear force in the spring, σ'_c is the effective confining stress, cs_scoh and cs_fric represent the strength, and cs_sstiff represents the shear spring stiffness). (Itasca 2000).

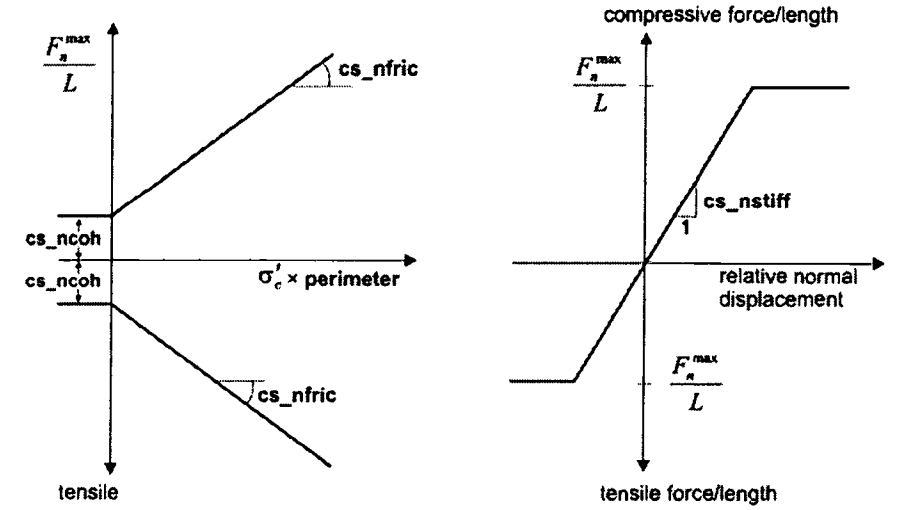

a) Normal strength criterion b) Normal force versus displacement

Figure 9. Graphical illustration of the normal pile interface springs used in FLAC (F_n is the shear force in the spring, σ'_c is the effective confining stress cs_ncoh and cs_nfric represent the strength, and cs_nstiff represents the normal spring stiffness). (Itasca 2000).

The shear spring values were estimated assuming that the shear stiffness was equivalent to the shear modulus of the adjacent soil matrix, and that the shear interface strength was equivalent to a skin friction, as typically estimated in the vertical capacity analysis of piles. For end-bearing piles, the strength of the shear interface spring along the bottom pile element was adjusted to account for the ultimate pile tip resistance.

Validation of the Normal Spring Stiffness and Strength Values

Two of the centrifuge models studied herein included lateral pile load tests conducted within the centrifuge. The results of the cyclic lateral load tests in horizontally layered soils and sloping rock fill were used to validate the above procedures for developing the normal pile interface spring stiffness and strength values. The two lateral load test centrifuge models are shown in Figure 12. The centrifuge models were modeled within FLAC and parametric studies were conducted to evaluate the effect of varying different soil and interface spring values. The results of the parametric study were used to develop modifications to the above procedures for estimating the lateral response of piles using FLAC.

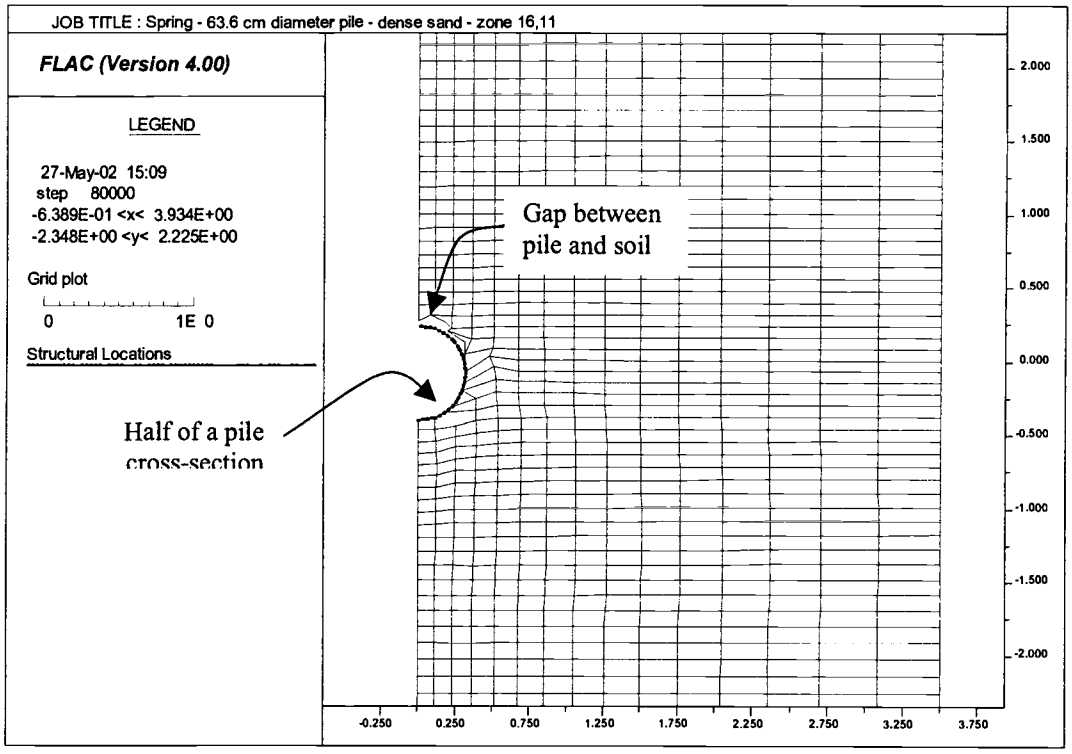

Figure 10. A typical FLAC model used to estimate the normal pile interface spring stiffness and strength values. Because of symmetry, only half of the pile is modeled. The model represents a horizontal plane through the pile at a specific depth.

Sloping Rock Fill

Lateral pile load tests of the piles in sloping rock fill were modeled in FLAC. Sensitivity studies were conducted by varying parameters, such as the soil dilation angle, friction angle and cohesion, and the normal spring stiffness and strength values. The best correlation between the measured moments and deformations for the piles in the sloping rock fill were for a dilation angle of 0, an artificial cohesion of 15 kPa applied to the rock, and a reduction in the downslope spring stiffness by a factor of 10.

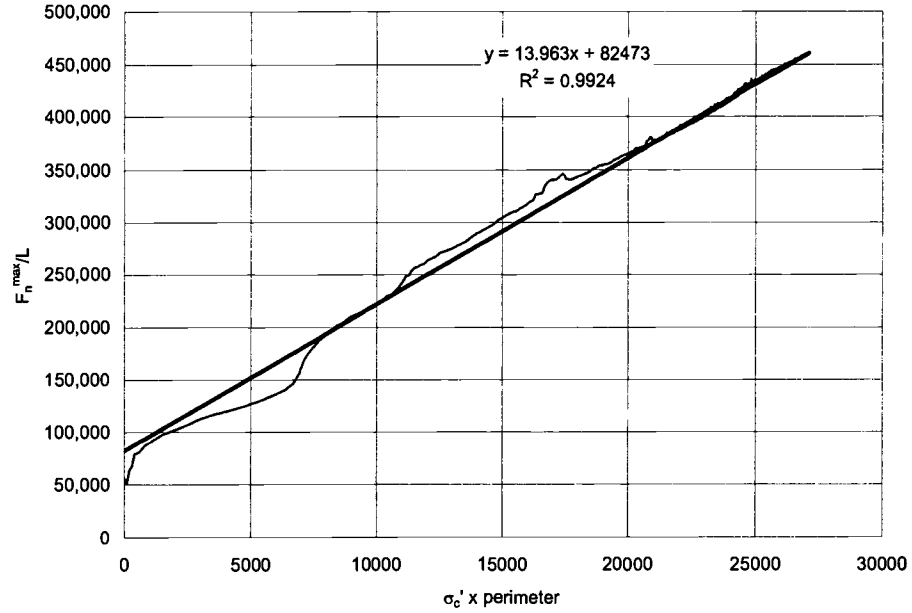

Intercept (cs_ncoh)	**8.45E+04**
Slope	13.8505
cs_nfric	**85.8705** degrees

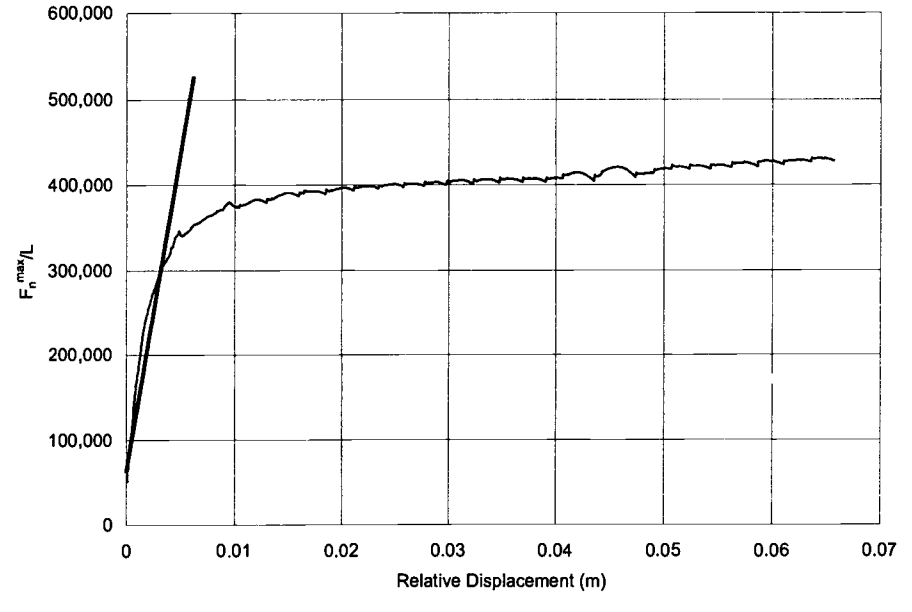

cs_nstiff	**7.50E+07**	slope intercept	6.39E+04

Figure 11. Data from a FLAC analysis to determine the normal pile interface spring stiffness and strength values. These plots are analogous to the plots in Figure 9, and show the best-fit lines to the data, and the resulting FLAC interface spring parameters.

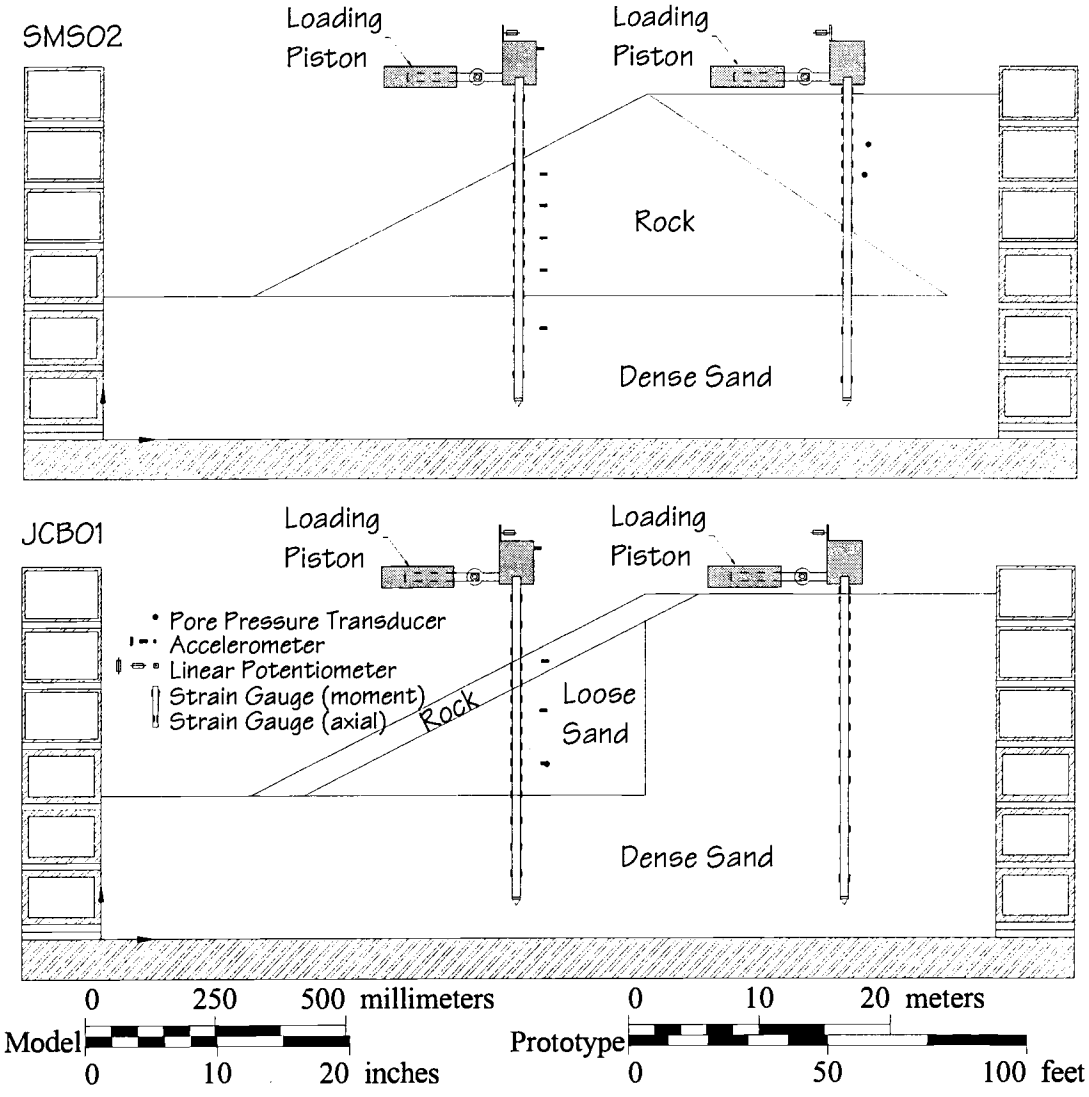

Figure 12. Centrifuge model geometries for lateral pile load tests of models SMS02 and JCB01.

The reduction in the downslope stiffness was anticipated, as there was a decrease in effective confining stress on the downslope side of the pile, and the stiffness of soil is a function of effective confining stress. This decrease in downslope

behavior is also accounted for in the commonly used lateral pile analysis computer program LPILE (Ensoft 1999).

The artificial rock cohesion was an adjustment because FLAC models a continuum, whereas the rock particles behaved as discrete particles. A general rule has been that for a soil to be modeled as a continuum, the individual grain size particles should be on the order of 30 to 40 times less than the dimension of interest (footing, pile, slope, etc.). For the rock dike and piles, the ratio of the median rock size and pile diameter is approximately 2.5. Because of this small ratio, individual rock particle interaction was not accurately modeled using continuum mechanics (i.e. FLAC), therefore an artificial cohesion was used to modify the modeled continuum behavior to match the measured behavior. This pseudo-cohesion can be envisioned as the force required to move individual rock particles over and around each other near and at the ground surface. This increase in lateral resistance in rock fill near the ground surface was also noted by Diaz et al. (1984) from the results of full-scale lateral pile load tests in rock fill at the Port of Los Angeles.

Figure 13 shows a comparison between the measured and predicated bending moments and displacements for the piles in the sloping rock fill for both centrifuge models, using the artificial cohesion and decreased downslope normal spring stiffness. In addition, the figure also shows predictions using LPILE (Ensoft 1999). The LPILE analyses were modified to account for the sloping conditions, but they did not include a pseudo-cohesion in the rock fill. The bending moments were measured in the centrifuge models using calibrated strain gauges, as discussed in Chapter 2. Figure 14

shows the measured and predicted bending moment and displacement profiles from SMS02 and JCB01. Two cases are shown, one using the modifications noted above (reduced downslope stiffness and rock pseudo-cohesion) and the other without the modification factors.

Backland (Horizontally Layered) Soils

The results of the cyclic load tests of the piles in the horizontally layered backfill from the centrifuge models were also modeled in FLAC. The sensitivity analysis indicated that the best correlation between the measured and predicted bending moments and displacements was for the case with no modification. This was expected, as the horizontally layered backfill with sandy soils does not require a modification for sloping conditions or for large particle sizes. Figure 15 shows the results of the analyses using the best-fit values. Figure 16 shows comparisons between the measured and predicted moment and displacement profiles for one load cycle for the piles in the horizontally layered backland for SMS02 and JCB01.

Modeling of the Water (Pore Fluid)

Water located above the ground surface was modeled as a normal pressure acting on the soil surface. The water within the soil was modeled as incompressible, with steady-state, hydrostatic pore pressures and the potential for the generation of excess pore pressures in liquefiable soils. Groundwater flow was not modeled in any of the analyses. Pore pressures were allowed to generate during dynamic loading, but

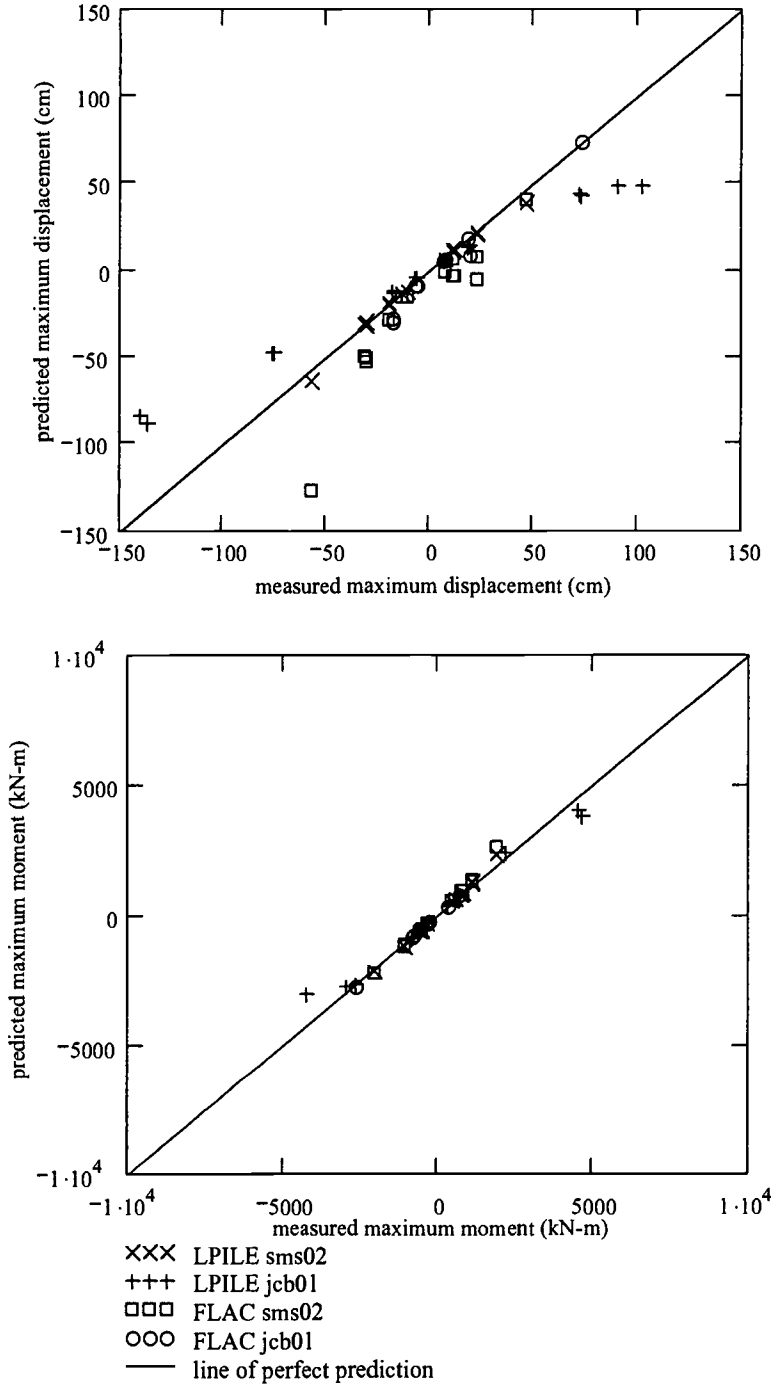

Figure 13. Comparison between the predicted moments and displacements using FLAC and the measured values from the centrifuge models SMS02 and JCB01 for the piles in the sloping rock fill.

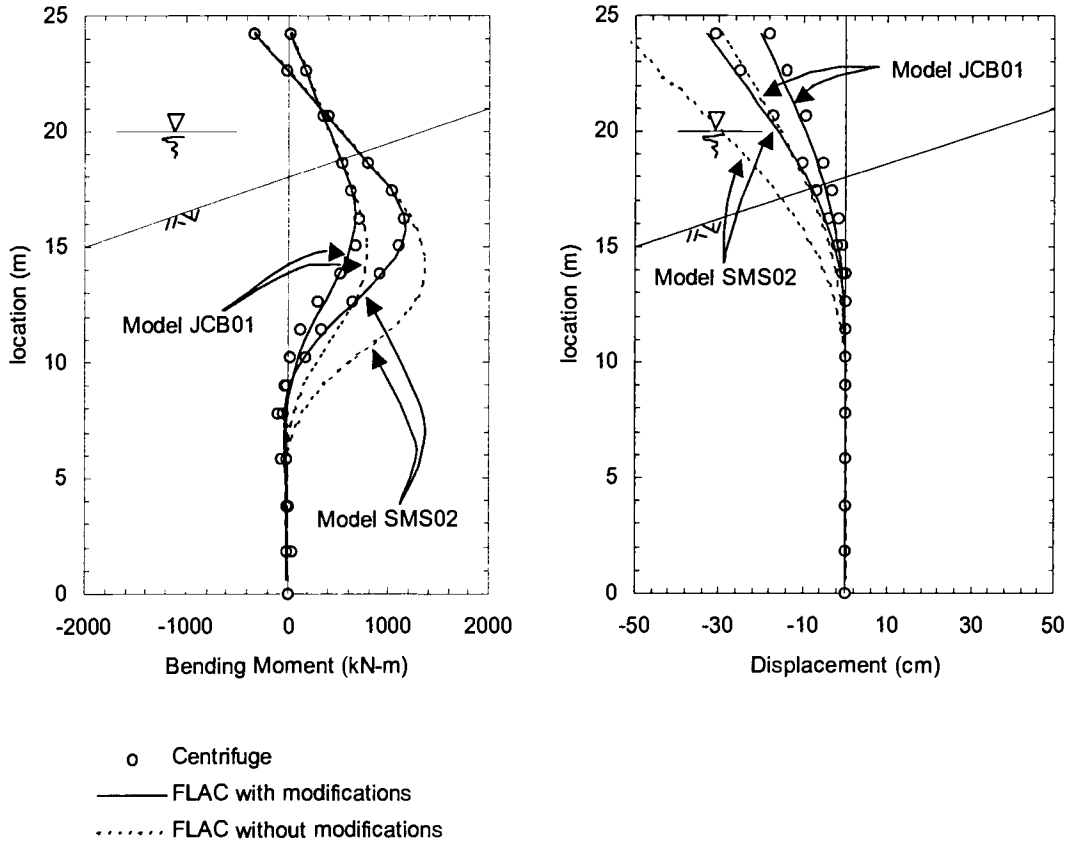

Figure 14. Comparison between the predicted moments and displacements using FLAC and the measured values from centrifuge models for the pile in the sloping rock fill for one cycle of the load sequence.

they were not allowed to dissipate. This simplification was justified since minimal pore pressure dissipation was expected during the relatively short application of earthquake shaking (generally 10 to 30 seconds).

Boundary Conditions

For the static solutions, the bottom boundary was fixed in the horizontal and vertical directions and the lateral boundaries were fixed in the horizontal direction. For

the dynamic solutions the lateral boundaries utilized the free-field option in FLAC that approximated a free field condition. For the FLAC models of the centrifuge tests, the free field boundary conditions were not applied; instead the model container was modeled directly.

Modeling of the Earthquake Motions

The input earthquake motions were recorded accelerograms, and were input at the base of each model as horizontal acceleration time histories. The damping of the earthquake motions for numerical stability utilized the Rayleigh damping option within FLAC. Typically percentages of damping for soil and structural elements were 5 and 1 percent, respectively (Itasca 2000). Unfortunately, Rayleigh damping is frequency dependent, and the damped center frequency had to be estimated. The frequency was estimated by running the model undamped, and monitoring the horizontal and vertical velocities throughout the model. The frequencies of the vertical time histories with the largest magnitude (from a Fast Fourier Transform analysis) were then selected as the center frequency to be damped within the FLAC model. Different damped center frequencies were chosen for the soil and structural elements.

The input time histories were also modified in the frequency domain to remove signal processing artifacts. The low frequency range was filtered using a Butterworth filter to remove the majority of the baseline drift. The low frequency cutoff was visually chosen for each time history to have minimal effect on the time history, while still removing the majority of the baseline drift. However, this did not remove all of

the baseline drift, and a post-processing routine was applied to each of the FLAC models to remove the remaining baseline drift from the model results.

In addition, the high frequencies were also filtered with a Butterworth filter to limit numerical resonance within the FLAC model. The high cutoff frequency was chosen such that the wavelength of the propagating shear wave was on the order of 10 times less than the minimum zone dimension.

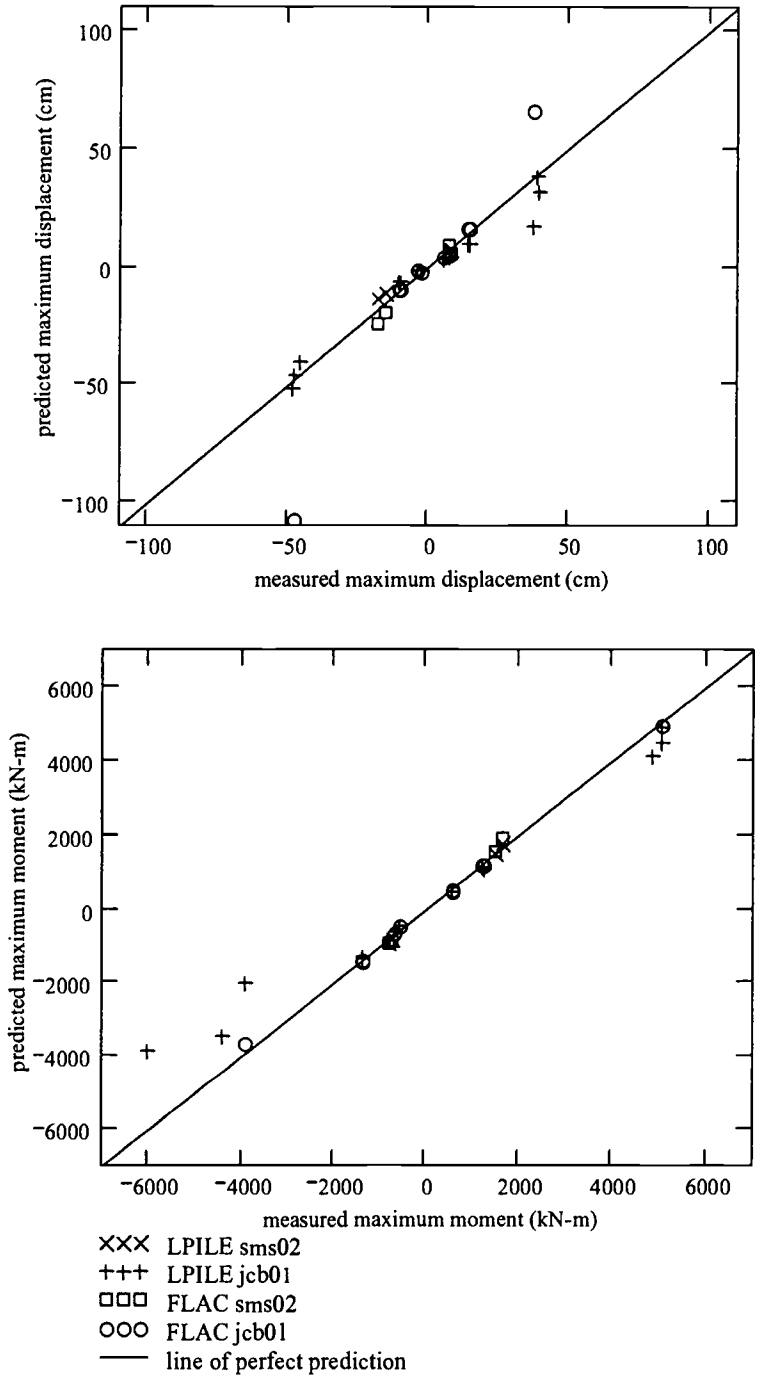

Figure 15. Comparison between the predicted bending moments and displacements using FLAC and the measured values from the centrifuge models SMS02 and JCB01 for the piles in the horizontally layered backland soils.

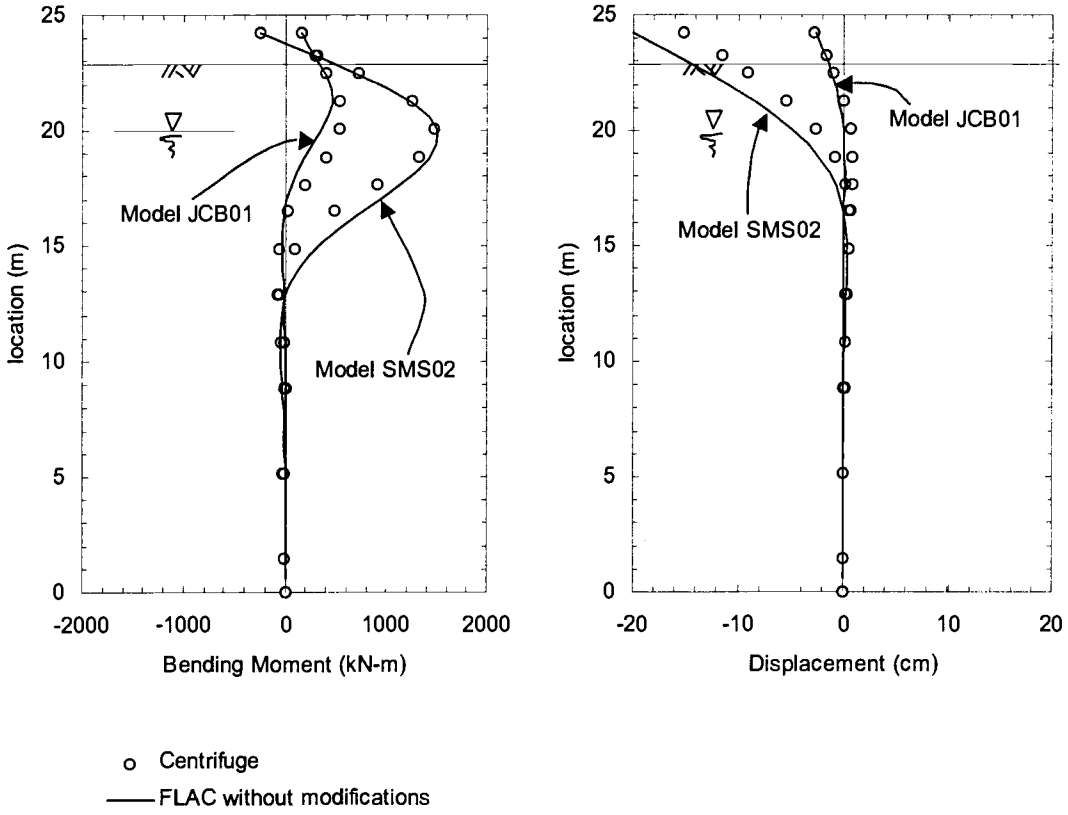

Figure 16. Comparison between the predicted moments and displacements using FLAC and the measured values from the centrifuge models for the pile in the horizontally layered backland for one cycle of the load sequence.

CHAPTER 2 – MANUSCRIPT NO. 1:

THE DYNAMIC CENTRIFUGE MODELING OF PILE-SUPPORTED WHARVES

Nason J. McCullough
Stephen E. Dickenson
Scott M. Schlechter
Jonathon C. Boland

Submitted to the

ASTM Geotechnical Testing Journal

ASTM International
100 Barr Harbor Drive
P.O. Box C700
West Conshohocken, PA 19428-2959

ABSTRACT

Pile-supported wharves are a key intermodal links between waterside and landside traffic at port facilities worldwide. Yet there are numerous difficulties in the design of these complex structures, as they often involve weak soils (liquefiable sands and/or soft clays), non-uniform sloping rock fill, static and dynamic soil-structure interaction, vertical and often batter piles, etc. These difficulties, as well as the limited database of well-instrumented field case histories led to the physical modeling research effort presented herein, to better understand the seismic performance of pile-supported wharves.

Five centrifuge models of general wharf-embankment geometries were seismically tested in the large-scale centrifuge facility at the University of California at Davis. The models included: single-lift, multi-lift and sliver (cut-slope) rock dike configurations; loose liquefiable sand as well as dense sand to model the effect of cohesionless soil improvement; soft clays as well as clays that had been mixed with cement to model the effect of cohesive soil improvement; vertical pile-supported wharves as well as models including batter piles; and vertical single piles placed in the sloping rock fill and in the horizontal backland that were subjected to cyclic lateral loads as well as dynamic earthquake shaking. Each model included nearly 100 instruments, including accelerometers, pore pressure transducers, linear potentiometers, and strain gauges. This paper summarizes the design, construction and testing of these models.

INTRODUCTION

A suite of centrifuge models was tested to evaluate the seismic performance of pile-supported wharf structures. Pile-supported wharf structures (Figure 17) are commonly used to provide the intermodal transition between waterside and landside traffic and commerce. A pile-supported wharf, as discussed herein, refers to the combination of the wharf deck, piles, rock dike, backfill soils, and foundation soils.

The seismic analysis of these structures typically relies on methods that have not been specifically developed for, nor validated for, use in the analysis of pile-supported wharf structures. This is due in part to the limited number of well-instrumented seismic field case histories that can be used to validate these design methods. In fact, to the authors' knowledge, there are only a few field case histories for which there are rough approximations of the ground deformations, ground motions, structural response of the wharf and post-earthquake observation of pile performance. Therefore, the centrifuge models presented herein were conducted to observe the seismic performance of pile-supported wharf structures, and to supplement the current pile-supported wharf seismic performance case history database.

A total of five centrifuge models were tested, with each model being subjected to a suite of earthquake acceleration time histories. The models were heavily instrumented with strain gauges calibrated to monitor pile bending moments, accelerometers to measure accelerations with the soil profile and the response of the structural elements, pore pressure transducers to measure the generation of excess pore

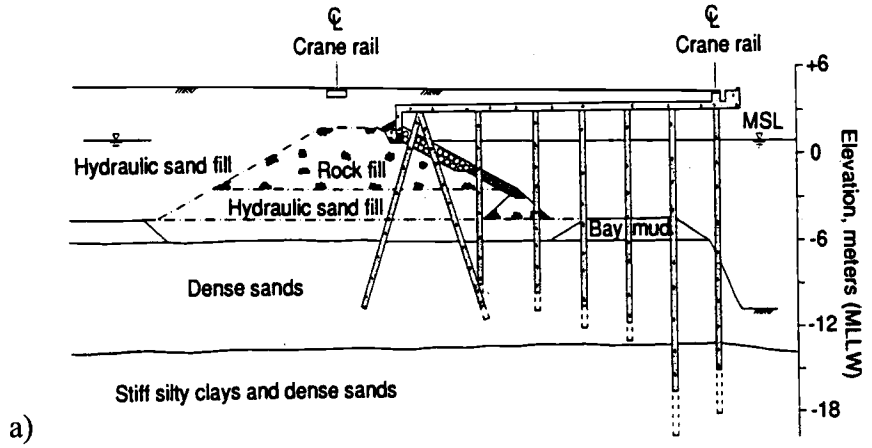

a)

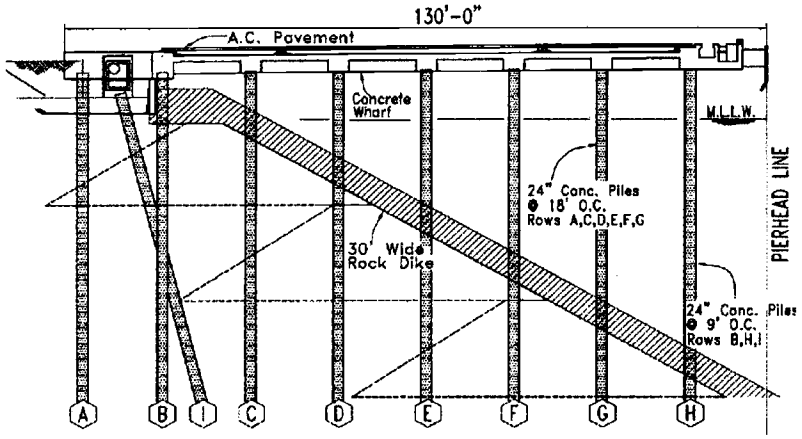

b)

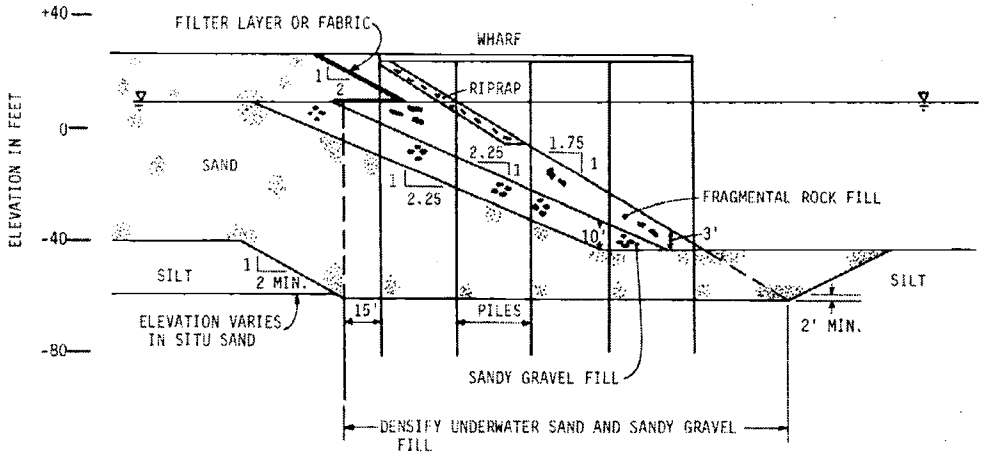

c)

Figure 17. Typical pile-supported wharf structures; a) Port of Oakland, California (Egan et al. 1992 from *Grouting, Soil Improvement and Geosynthetics*, reprinted by permission of ASCE), b) Port of Long Beach, California (Mukhopadhyay 1998 from *Civil Engineering*, reprinted by permission of ASCE, courtesy of Port of Long Beach), and c) Port of Portland, Oregon (Dames and Moore 1984).

pressures within the soil profile, and linear potentiometers to measure vertical and horizontal displacements of the soil surface and the structural elements.

This paper provides a summary of the centrifuge modeling and testing program, model response, and lessons learned during the modeling and testing program. The specifics of each model as well as the complete recorded data set are available in the data reports by McCullough et al. (2000), Schlechter et al. (2000a), Schlechter et al. (2000b), Boland et al. (2001a), and Boland et al. (2001b). These data reports are also accessible at the following website:

http://ccee.oregonstate.edu/geotech/research/index.html.

DESCRIPTION OF THE CENTRIFUGE FACILITY

The testing of all the centrifuge models was conducted at the Center for Geotechnical Modeling, located on the University of California at Davis campus (UC Davis). The centrifuge had a 9 m radius arm and was equipped with a large, one-dimensional shake table driven by two pairs of servo-hydraulic actuators acting in parallel, one pair mounted on either side of the model (Kutter et al. 1994). The centrifuge had a maximum model mass of 2,500 kg, an available bucket area of 4.0 m^2, and a maximum centrifugal acceleration of 50 g at the radius of the model (Wilson 1998). However, at the time of the tests the maximum centrifugal acceleration was approximately 40 g. The shake table was designed to accommodate a 1.7 m long model container and provide input accelerations of up to 15 g. For more information,

Kutter et al. (1991 and 1994) provide a thorough description of the UC Davis centrifuge facility and shake table.

MODEL CONTAINER

The models were constructed in a large flexible shear beam container, designed and built to have a shear modulus profile approximating that of a softened (i.e. liquefied) soil deposit. The nominal inside dimensions of the container were 1720 mm long, 685 mm wide, and 702 mm deep (Figure 18). The container consisted of six hollow aluminum rings separated by 12 mm thick layers of 20 durometer neoprene rubber (Figure 18). The mass of each of the upper three aluminum rings was approximately one-half the mass of each of the lower three rings. The area of the neoprene varied, such that the shear stiffness of the box increased with depth. Rows of vertical shear rods (all-thread rods) were attached to the bottom ends of the container to provide complementary shear stresses along the lateral soil boundaries.

MODEL SCALING

The centrifuge allows for stress conditions in scaled models to represent prototype field stresses. Since the strength and modulus values of soils are a function of stress state, the increase in the confining stress due to centrifugal acceleration leads to a relatively accurate representation of soil behavior at a model scale. It is important to note that centrifugal acceleration is a function of the speed of rotation and the distance from the center of the arm, and since the container and model occupy a range

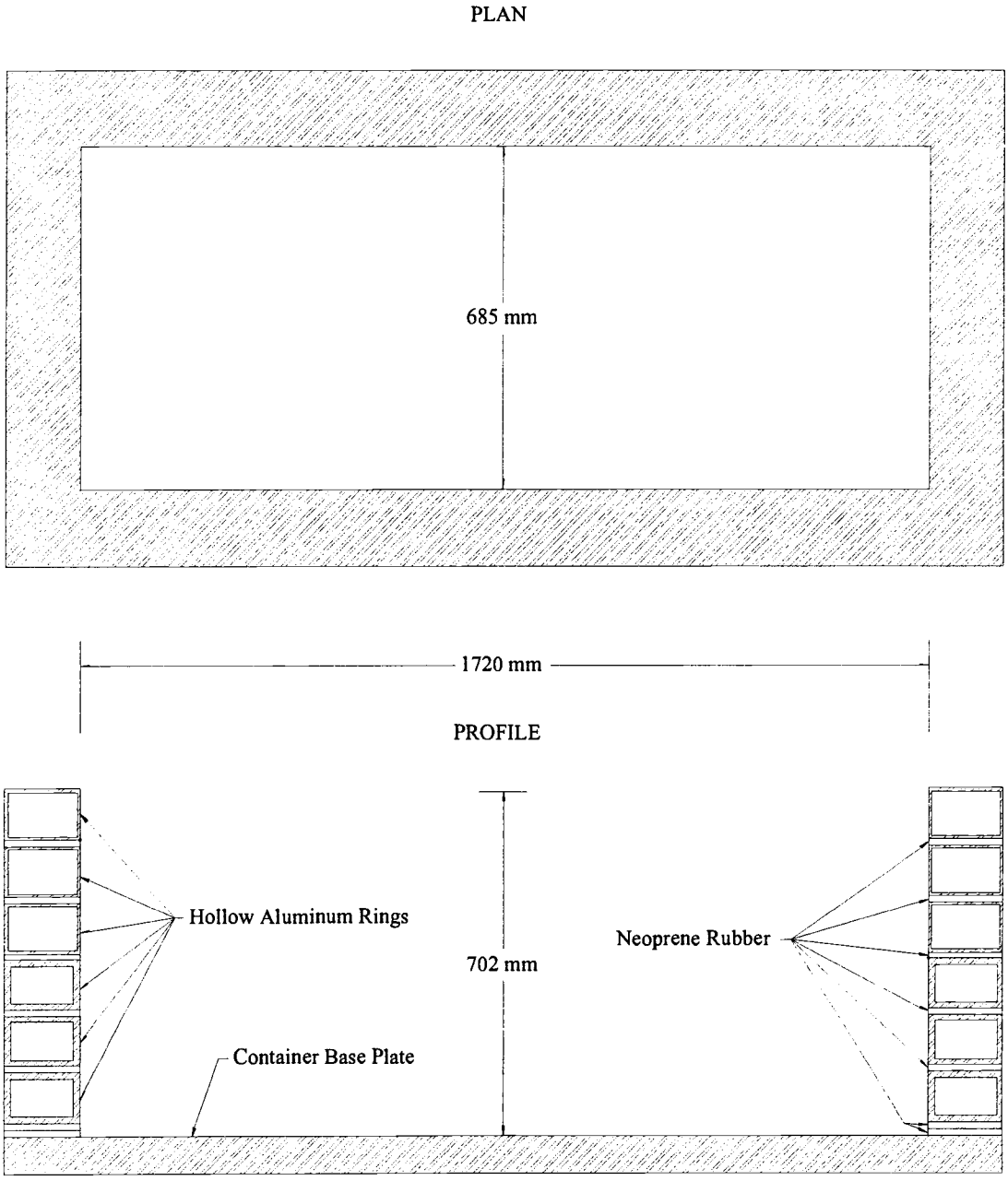

Figure 18. Plan and profile views of the container utilized for the suite of centrifuge models.

of radii, the centrifugal acceleration varies over the depth of the model during testing. This is assumed to be a negligible effect, with the target acceleration presented being the acceleration located at approximately the upper third point of the container. The models presented herein were tested at 40.05 g. With an acceleration of 40 g at the upper third point of the container, the accelerations at the top and bottom of the container were 38.95 g and 42.26 g, respectively.

With a centrifugal acceleration of 40 g, the resulting centrifugal model scaling factor was 40. Centrifuge scaling has been described in detail by numerous other authors (e.g. Kutter 1994, Scott 1991), and therefore is not presented herein for brevity. Due to the centrifugal acceleration being limited to 40 g, and the size of the prototype models to be tested, two of the models were modeled at a 70 percent geometric scale in addition to the centrifuge scaling. Geometric scaling (also called one-g scaling) is described in more detail by Iai (1989) and Scott (1991).

The resulting scale relationships are shown in equations 20 and 21 for the centrifugal and geometric scaling, respectively, and the factors and values for this suite of tests are shown in Table 2.

$$n = \frac{\text{prototype}}{\text{model}} \approx 40 \tag{20}$$

$$\lambda = \frac{\text{prototype}}{\text{model}} \approx 1.43 \tag{21}$$

Table 2. Model scaling factors and values.

	Centrifuge Scale Factors	Centrifuge Scale Values	Geometric Scale Factors	Geometric Scale Values
Acceleration	n^{-1}	0.025	1	1
Velocity	1	1	$\lambda^{1/2}$	1.20
Length	n	40	λ	1.43
Time (Dynamic)	n	40	$\lambda^{1/2}$	1.20
Time (Diffusion)	$n^2(c_v^*)^{-1}$	$1600(c_v^*)^{-1}$	λ if $c_v^* = \lambda$ $\lambda^{0.5}$ if $c_v^* = \lambda^{1.5}$	1.43 if $c_v^* = \lambda$ 1.20 if $c_v^* = \lambda^{1.5}$
Mass Density	1	1	1	1
Mass	n^3	64000	λ^3	2.92
Force	n^2	1600	λ^3	2.92
Stress	1	1	λ	1.43
Pile Stiffness (EI)	n^4	2560000	λ^5	2.92
Moment	n^3	64000	λ^4	4.16

Where $c_v^* = \left(\frac{c_{v\text{-}p}}{c_{v\text{-}m}} \right)$, c_v is the coefficient of consolidation.

PORE FLUID

One inconsistency that arises in both the centrifugal and geometric scaling is the time scale. As shown in Table 2 for dynamic analyses, time is scaled by n and $\lambda^{1/2}$ for centrifugal and geometric scaling, respectively. However, for diffusion (groundwater flow) the scaling factors are a function of the coefficient of consolidation. The coefficient of consolidation, as shown in equation 22, is a function of the viscosity of the pore fluid. Therefore, by adjusting the pore fluid viscosity, the diffusion time scale can be made to equal the dynamic time scale.

$$c_v = \frac{K(1+e)}{\rho_w a_v \mu} \tag{22}$$

where K is the permeability of the soil, e is the void ratio of the soil, ρ_w is the mass density of the fluid, a_v is the coefficient of compressibility, and μ is the kinematic viscosity of the fluid.

This pore fluid scaling was performed for the models presented herein, with the pore fluid viscosity increased by approximately 40 by adding methyl-cellulose to the pore fluid (Kutter 1994). Approximately 1 to 3 percent of the methyl-cellulose by weight was mixed with water to obtain pore fluid viscosities that were on the order of 30 to 40 times that of distilled water at 20 degrees Celsius. Because such a small amount of methyl-cellulose was required, the properties (i.e. density, chemical behavior) of the pore fluid were similar to that of distilled water. Methyl-cellulose is a food derivative, and as such decomposes over time, therefore benzoic acid was also added to the pore fluid at a ratio of 1 percent by weight of methyl-cellulose to limit the decay over the lifespan of the model (approximately 1 month).

DESIGN OF THE MODELS

Geometry

The models were designed to approximate typical pile-supported wharf cross sections of western United States ports. Given the simplifications of the centrifuge models, boundary conditions, and scaling effects, it was not possible to directly model specific structural details inherent to pile-supported wharves. However, the models

were designed and constructed to model geotechnical issues, such as slope deformations, pore pressure generation, seismic site response, and soil-structure interaction of piles and embankment. The models were also constructed to study pile bending moments, however, they were not constructed to study other structural aspects, such as the effect of the wharf stiffness on the model response, pile-wharf deck connection details, the variation in response due to pile degradation, etc.

Five pile-supported wharf models were tested (Table 3). Cross-section profiles and plan views of each model are presented in Figure 19 through Figure 23. All of the models consisted of rock dike configurations retaining backfill soil, with three rows of seven vertical piles supporting a wharf deck. Models SMS02 and JCB01 also included two pairs of batter piles and two single vertical piles that were subjected to cyclic lateral pile load tests (Figure 24). A summary of each model is provided in the following text.

Table 3. Model summary.

Model	Rock Dike	Prototype Scale				
		Water Depth (m)	Rock Dike Height (m)	Transverse Pile Spacing (m)	Longitudinal Pile Spacing (m)	Pile Diameter (mm)
NJM01	Two-lift	16.0	19.5	5.1	6.1	637
NJM02	Two-lift	16.1	20.1	5.1	5.8	546
SMS01	Two-lift	16.1	20.1	5.1	5.8	546
SMS02	Single-lift	12.4	15.2	4.0	4.0	637
JCB01	Sliver (cut-slope)	12.4	15.2	4.0	4.0	637

Model NJM01, the first model tested, was of a typical pile-supported wharf geometry, and included a loose, liquefiable backfill soil, a two-stage rock dike, and an all vertical pile-supported wharf deck.

Model NJM02 included several variations on NJM01, including geometric scaling in addition to the centrifugal scaling. A layer of clay was sandwiched between two layers of dense sand below the rock dikes. The backfill soil was modeled as loose, and the clay (San Francisco Bay Mud) was modeled as being normally to slightly over-consolidated (i.e. OCR ranging from 1.0 to 1.5).

Model SMS01 was identical to NJM02, except that the weak soil layers (clay and liquefiable loose sand) were partially improved to model the effects of soil improvement. The sand was modeled as improved by placing a uniformly dense region. The clay improvement was modeled as columnar walls of cement mixed with clay, laid out on a grid in plan view (Figure 21), similar to patterns of improvement due to deep-soil-cement-mixing (CDSM) that have been conducted at the Port of Oakland.

The design of models NJM02 and SMS01 included a 70 percent geometric scaling, but it should be noted that it is not necessary to apply this factor. If the factor is not applied, these models represent a prototype with a water depth of approximately 11.2 m and a rock dike height of approximately 14.0 m.

SMS02 contained a single lift rock dike, and all of the foundation and backfill soils were dense (improved). JCB01, the final model, consisted of a sliver rock dike configuration in which a thin layer of rock overlaid a slope of loose sand. The backfill

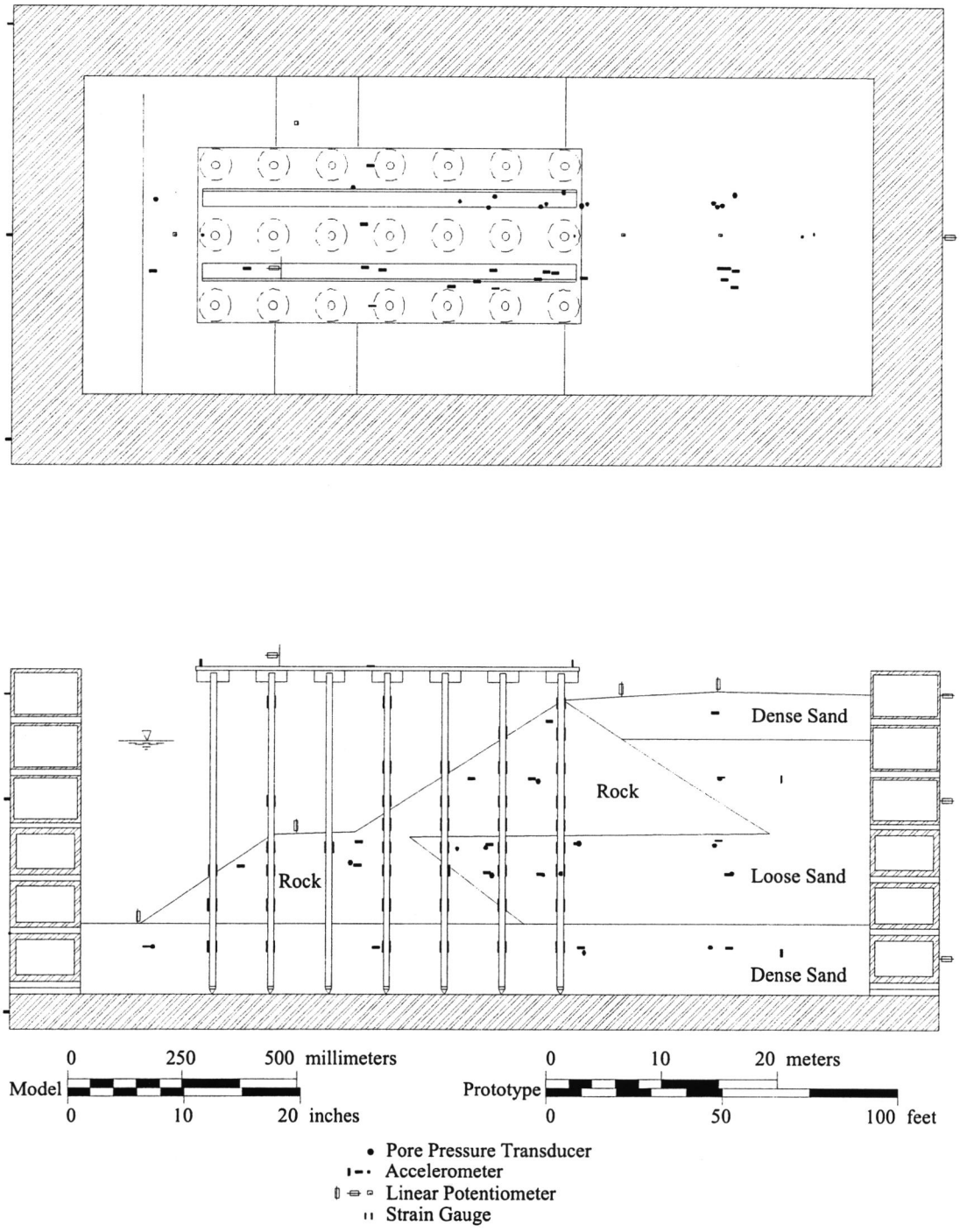

Figure 19. Plan and profile of centrifuge model NJM01.

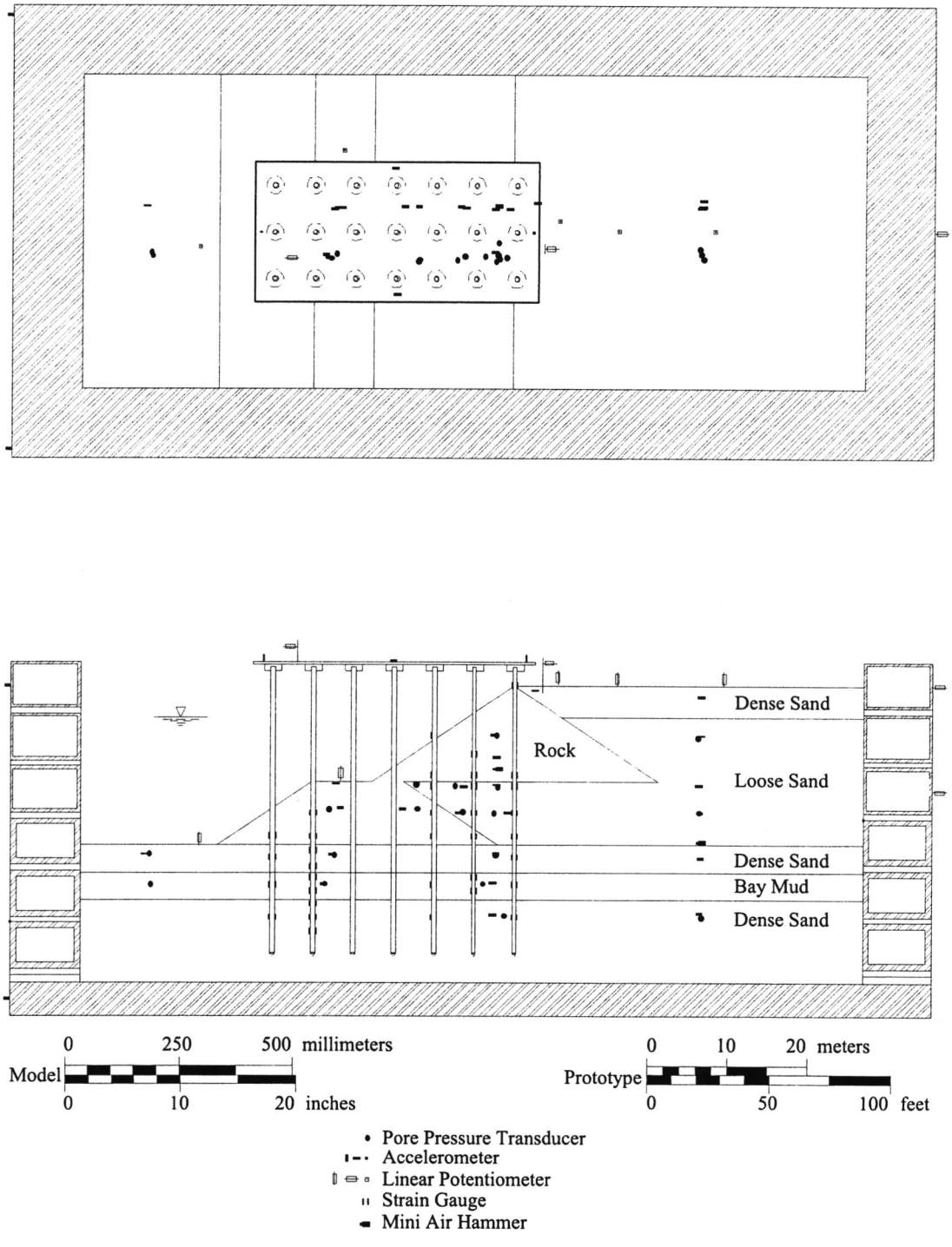

Figure 20. Plan and profile of centrifuge model NJM02.

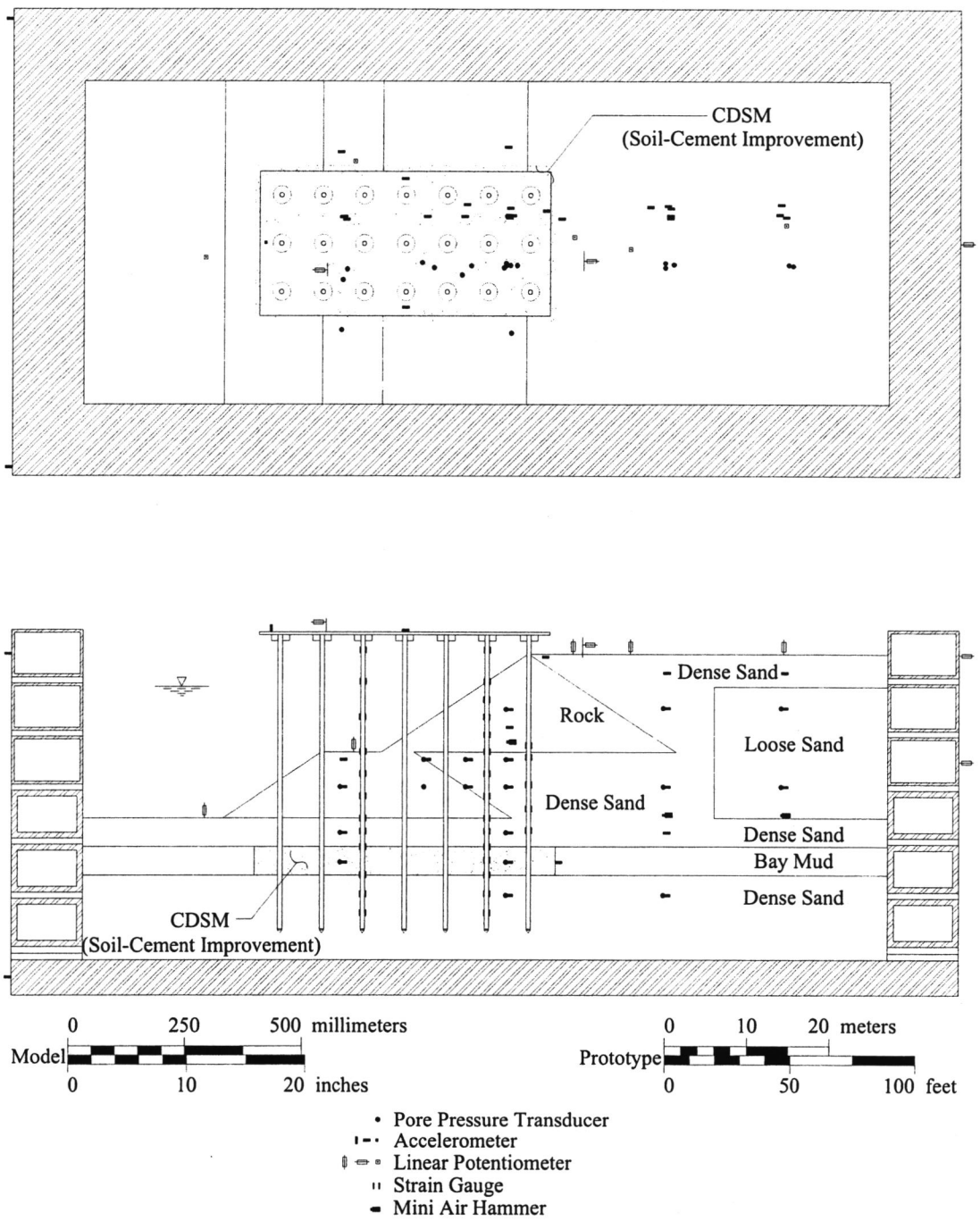

Figure 21. Plan and profile of centrifuge model SMS01.

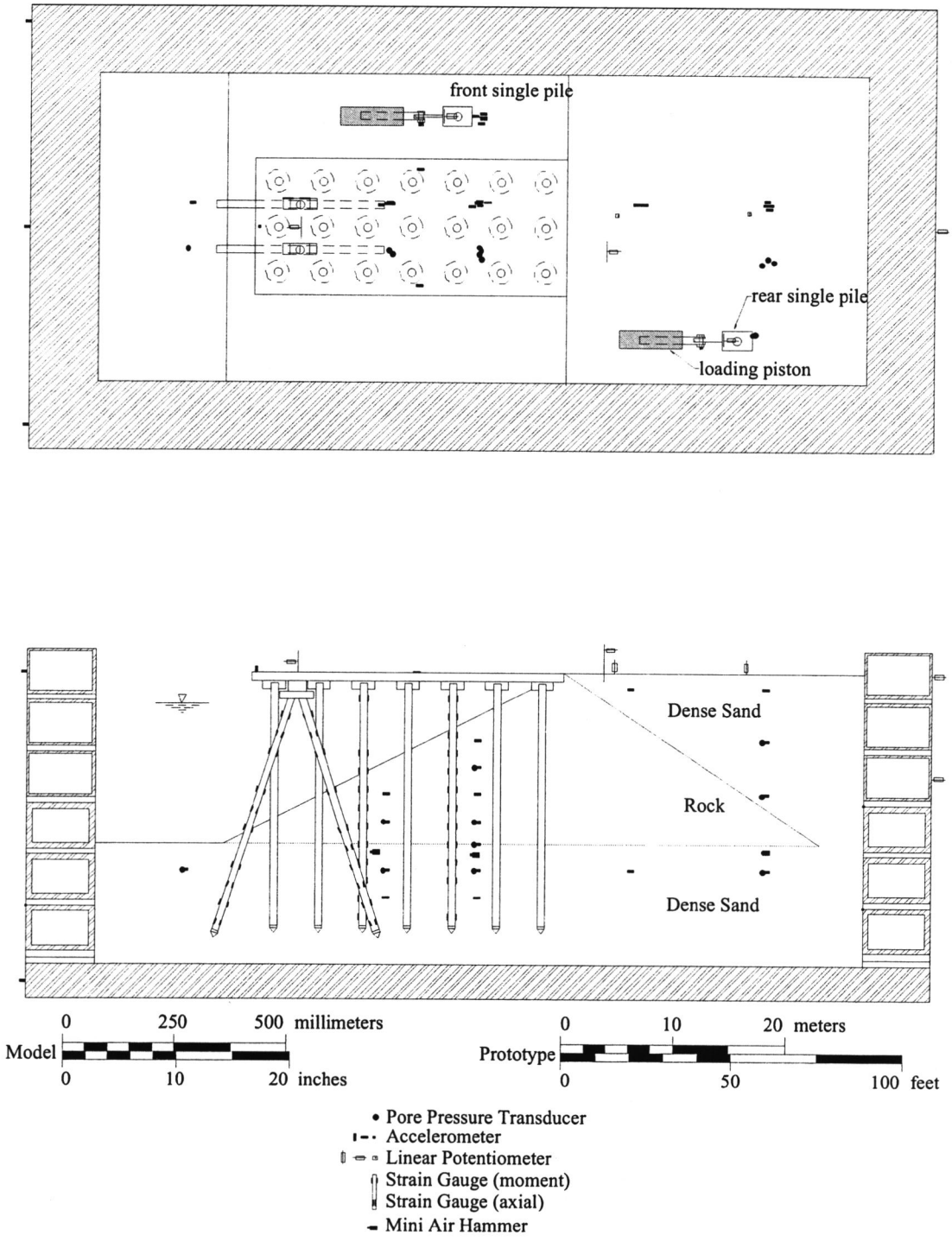

Figure 22. Plan and profile of centrifuge model SMS02.

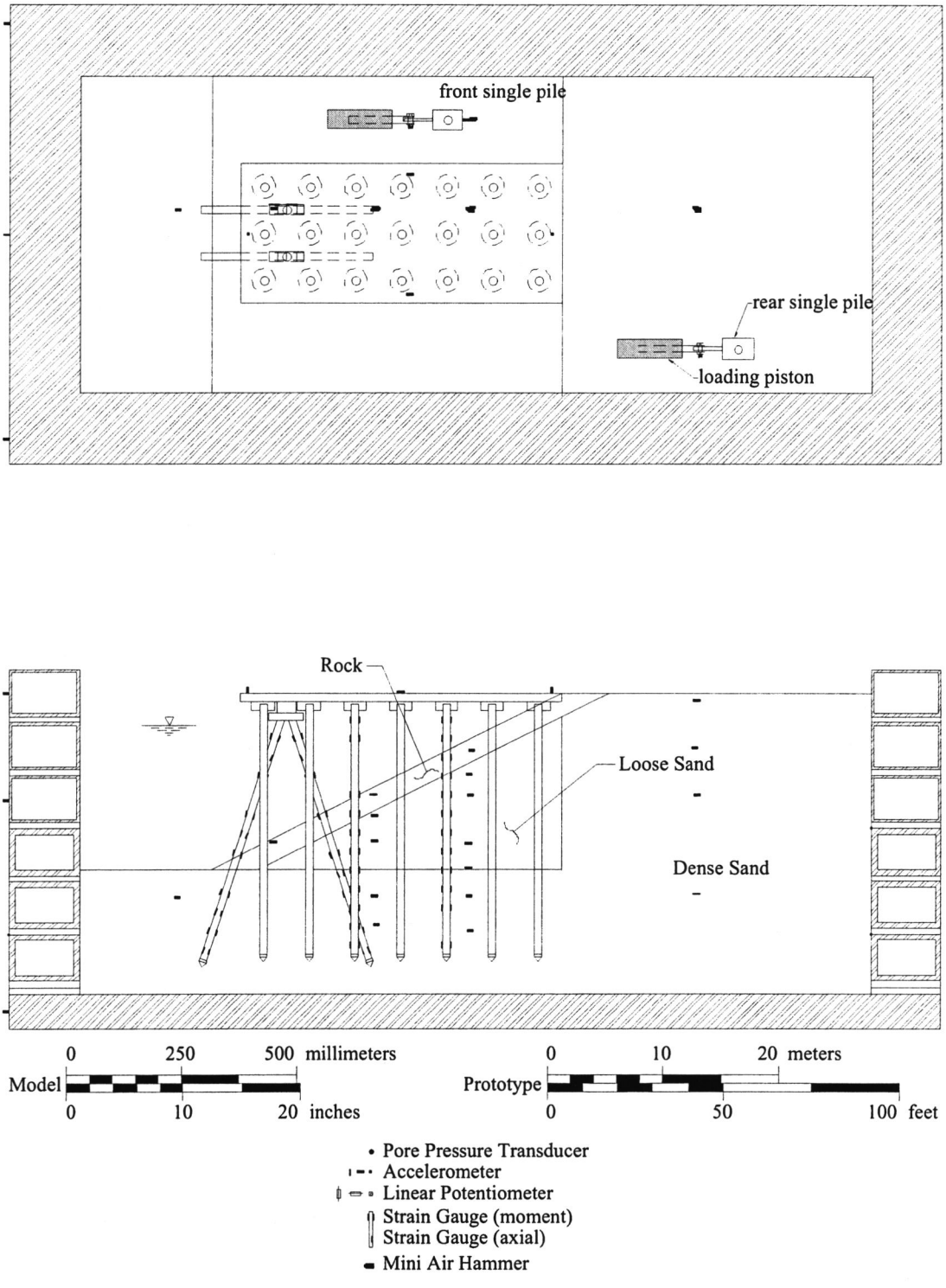

Figure 23. Plan and profile of centrifuge model JCB01.

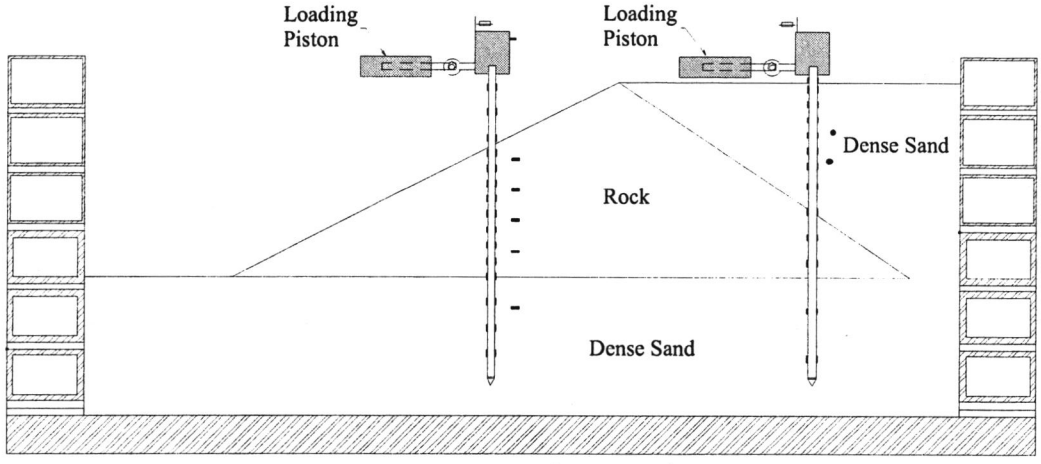

a)

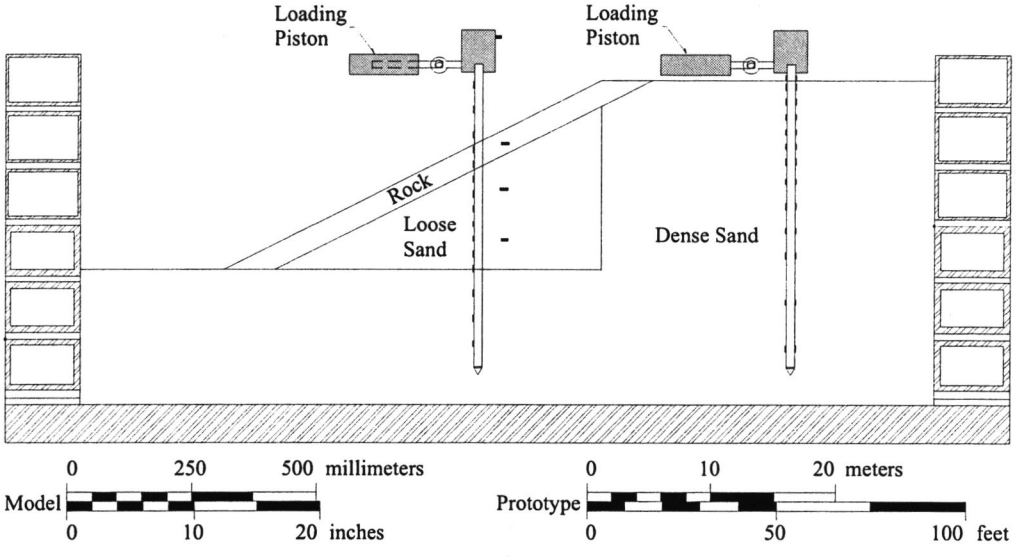

b)

Figure 24. Plan views showing the locations of the single piles in models a) SMS02, and b) JCB01 that were used for the cyclic lateral load tests.

soil behind the wharf and the foundation soils were all dense. Both SMS02 and JCB01 included two sets of batter piles connected to the waterside of the wharf deck. These models also included two single vertical piles, one in the mid-slope of the rock dike, and one in the backland, that were subjected to cyclic lateral load tests, in addition to being monitored during the dynamic shaking.

Structural Elements

The structural elements (piles, pile caps, and wharf deck) within the model were represented by aluminum sections, though the prototype elements are typically reinforced concrete. The target prototype piles were 610 mm octagonal pre-stressed reinforced concrete piles, typical of modern pile-supported wharves in the United States. For this project, the diameter and the elastic modulus of the piles were scaled, though the strength was not scaled due to the difficulty in obtaining a material and section that could scale both the elastic modulus and bending moment capacity. This resulted in the scaled bending moment capacity of the model piles being on the order of 10 times greater than the reinforced concrete prototype piles. The diameters were not scaled exactly, as readily available aluminum tubing was used to represent the piles. Table 4 tabulates the model and prototype properties of the pile elements, as well as the target prototype values.

The target prototype wharf deck was a 1219 mm (4 ft) thick concrete wharf and pavement section. The mass of the target prototype was scaled in the model, but the strength and stiffness of the wharf deck was not scaled. Solid aluminum plate was

used for the wharf deck. The piles were attached to the wharf decks with pile caps that were securely bolted to the piles and wharf deck to provide a fixed-moment connection. The thickness of the wharf deck was such that the tributary load on each pile due to the pile caps and wharf deck would approximate the tributary load due to the target prototype concrete deck. Table 5 tabulates the wharf deck properties for the models.

Table 4. Pile properties for all of the centrifuge models, including the prototype target pile properties.

Pile Properties	Models	Aluminum Tubing		Prototype Target Prestressed Concrete Piles
		Values in Model Scale	Values in Prototype Scale	
Diameter (mm)	NJM01, SMS02, JCB01	15.9	636	610
	NJM02, SMS01	9.53	546	
Wall Thickness (mm)	NJM01, NJM02, SMS01, SMS02, JCB01	0.889	50.8	NA
Moment of Inertia, I (m^4)	NJM01, SMS02, JCB01	1.18×10^{-9}	3.02×10^{-3}	3.78×10^{-4}
	NJM02, SMS01	2.27×10^{-10}	2.42×10^{-3}	
Modulus of Elasticity, E (GPa)	NJM01, NJM02, SMS01, SMS02, JCB01	70	70	30
Stiffness, EI ($Pa\text{-}m^4$)	NJM01, SMS02, JCB01	82.53	2.11×10^{8}	1.15×10^{8}
	NJM02, SMS01	15.90	1.69×10^{8}	
Plastic Moment (N-m)	NJM01, NJM02, SMS01, SMS02, JCB01	28.12	7.5×10^{6}	$6.1\text{-}9.8 \times 10^{5}$

Nevada Sand

The sand used in the models was Nevada Sand. This was relatively fine sand commonly used for centrifuge modeling. The sand was extensively tested for use in the VELACS (Verification of Liquefaction Analyses by Centrifuge Studies), and details on the properties of Nevada Sand can be found in Arulmoli et al. (1991). A summary of the sand is provided in Table 6.

Table 5. Wharf deck properties for all of the centrifuge models, including the prototype target wharf deck properties.

Pile Properties	Models	Model Scale	Prototype Scale	Target Prototype Value
Wharf Deck Thickness (mm)	NJM01, SMS02, JCB01	6.35	255	1219
	NJM02, SMS01	19.1	766	
Wharf Deck Transverse Length (m)	NJM01	0.840	33.7	NA
	NJM02, SMS01	0.622	35.7	
	SMS02, JCB01	0.700	28.1	
Wharf Deck Longitudinal Length (m)	NJM01	0.380	15.2	NA
	NJM02, SMS01	0.305	17.5	
	SMS02, JCB01	0.300	12.0	
Wharf Deck Mass Density (kg/m^3)	NJM01, NJM02, SMS01, SMS02, JCB01	2723	2723	2243
Tributary Mass per Pile (kg) [1)]	NJM01	0.610	39,334	38,102
	NJM02, SMS01	0.196	36,620	
	SMS02, JCB01	0.691	44,557	39,689

1) Includes the wharf deck, pile caps, connection bolts, etc., and is for the vertical model piles only.

Table 6. Summary of Nevada Sand properties.

Classification	Uniform, Fine Sand; SP
Specific Gravity[1)]	2.67
Mean Grain Size, D_{50} (mm)	0.15
Coefficient of Uniformity, C_U	1.6
Maximum dry unit weight (kN/m^3)	16.76
Minimum dry unit weight (kN/m^3)	13.98
Void Ratio at 40% Dr [1)]	0.736
Void Ratio at 60% Dr [1)]	0.661
Angle of internal friction at 40% Dr [1)]	33.0°
Angle of internal friction at 60% Dr [1)]	35.5°

1) Arulmoli et al. (1991) for VELACS Nevada Sand

The rock that was used in the models was imported from Catalina Island off the coast of southern California. This is the same rock that has been used in the construction of the Ports of Long Beach and Los Angeles. Given that the model and prototype strength, modulus, and mass density values of cohesionless soils are generally assumed to be equivalent, it is not common to exactly model the gradation of field material in the centrifuge. However, the rock dikes were influential in the soil-structure interaction with the pile elements, and since the pile elements were scaled, it was necessary to scale the rock particles. However, if the entire rock gradation were scaled, the finer portions of the gradation would alter the groundwater flow behavior of the rock. Therefore, the coarse gradation of the rock was scaled by the scaling factors, while the finer portion of the gradation was not scaled, resulting in a fairly uniformly graded rock. Figure 25 shows the target prototype rock gradation, the target model gradations (the target model gradation for NJM02 and SMS01 include the geometric scaling factor), as well as the actual gradations used in the models.

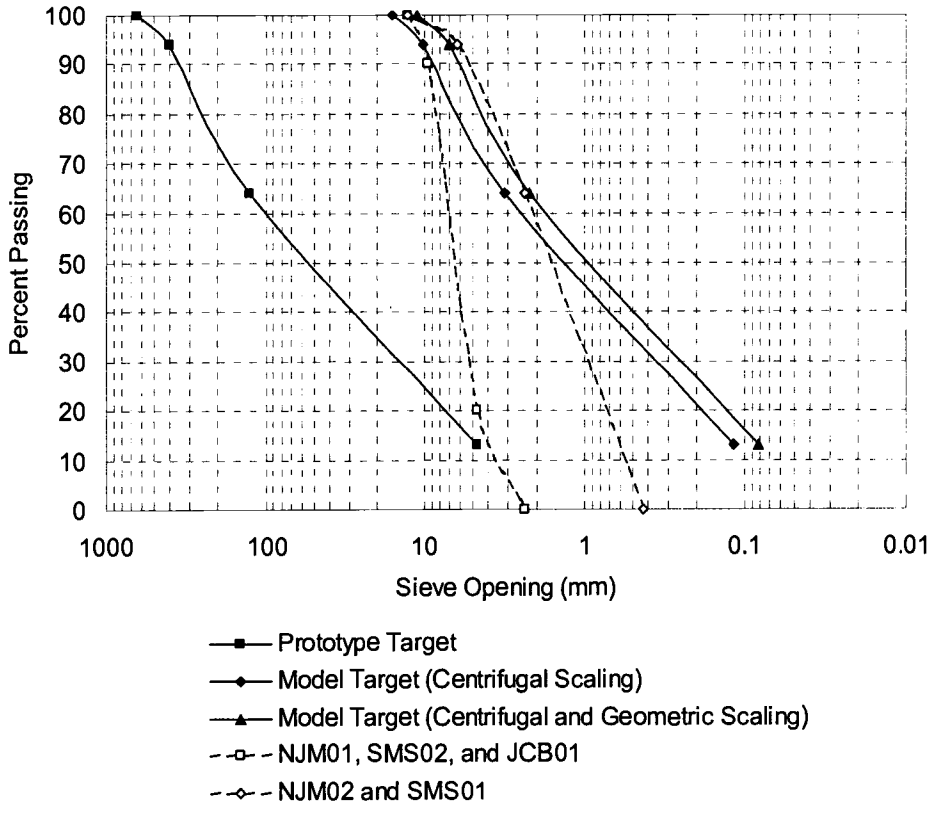

Figure 25. rock gradations used in the models.

The clay used in models NJM02 and SMS01 was remolded San Francisco Bay Mud, a soil well characterized in the technical literature. The clay was consolidated during construction using a large hydraulic press, thus reducing the amount of time required for primary consolidation during the actual centrifuge test. For NJM02, the clay was consolidated to an OCR of 1.5 relative to the dredge line before spinning. After spinning, the OCR of the clay varied from 1.5 beneath the dredge line to 1.0 beneath the rock dike and backland. For SMS01, the clay was consolidated to an OCR

of 1.0 relative to the backland before spinning. After spinning, the OCR of the clay varied from 3.8 beneath the dredge line to 1.0 beneath the backland.

INSTRUMENTATION

Four types of electronic instruments were used to measure and monitor the performance of the models:

1) Accelerometers (ACC) – were used to continually record accelerations during shaking events within the soil profile, on the structure, and on the container. These data were processed to estimate soil amplification, response spectra, and elastic deformations.
2) Pore pressure transducers (PPT) – were used to continually measure the generation and dissipation of excess pore pressures within the soil profile during spin-up, shaking events, and spin-down.
3) Strain gauges (SG) – were wired and calibrated to continually measure the moments in the piles, the data of which were used to estimate pile curvature, shear and displacements, and the applied soil pressure.
4) Linear potentiometers (LP) – were used to measure displacements of the wharf deck, soil surfaces, and the container.

Figure 19 through Figure 23 show the general locations of all instruments that were placed within the models (note that not all instruments were recorded during the testing sequence). The location of all instruments was measured both before and after the test sequence.

The orientation of the instrumentation was carefully noted during construction to insure a datum direction that was maintained upon data reduction. All of the recorded data were corrected so that a positive response occurred in the positive axis direction. In addition, the PPTs were oriented perpendicular to the direction of shaking to minimize measurement of the *sloshing* of the pore water within the saturated soil column.

The strain gauges were calibrated to measure moments by subjecting the piles to a known moment and measuring the voltage output in a controlled laboratory setting prior to the centrifuge testing. The strain gauges consisted of two stacked gauges oriented perpendicular to each other. The strain gauges were placed in pairs on the exterior of the piles, completing a full strain gauge bridge at each gauge elevation. The strain gauge wires were fed internally through the length of the pile, exiting at the top. To accomplish this, holes were drilled on each side of the pile, located above each set of gauges and on the axis opposite the direction of shaking (and bending), thereby minimizing any effects the holes may have had on the overall bending behavior of the piles.

After the strain gauges were mounted and coated (following manufacturer recommendations), a three step sealing process was undertaken: 1) a microcrystaline wax was heated and used to coat the interior and exterior of the pile, 2) oversize plastic pile tips were inserted into the pile toes, and 3) clear heat shrink-wrap was placed on the exterior of the piles. This three step process assured that the strain gauges would be protected from the fluid and the abrasive action of the rock and soil.

The linear potentiometers within the model referenced the top ring of the box, therefore absolute displacements were the difference of the linear potentiometer within the model and the linear potentiometer measuring the displacement at the top ring of the box.

MODEL CONSTRUCTION

Model construction followed a sequence by which each soil layer starting from the bottom was placed, interspersed with the placement of the instrumentation and structural elements at their design elevations. The container and soil were weighed at various intervals to validate the density of the placed soil. The following sections describe specific aspects of the model construction process.

Soil Placement

The sand was placed dry using an air pluviation technique. Two pluviators were calibrated to place the sand at various relative densities. The calibrations were a function of drop height and flow rate. By adjusting these parameters it was possible to obtain the design densities. Calibration checks were made during placement of the sand by weighing sand pluviated into containers of known volume, and adjustments where made to the pluviation process as necessary to provide the design relative densities.

The clay was mixed with water into a slurry using a ribbon mixer at a water content of 137 percent. For NJM02, three equal sublayers of clay were placed, while

for SMS01, two equal sublayers of clay were placed. For each sublayer, the clay slurry was sandwiched between layers of filter paper to increase the rate of consolidation. After placement of each sublayer the clay was consolidated using a hydraulic press. Water contents were taken during placement and after testing to estimate the void ratio of the saturated clay. In addition, Torvane and pocket penetrometer tests were conducted on the clay to provide estimates of the undrained shear strength. After the test sequence, for NJM02 the undrained strength as measured with the Torvane varied from 12.4 kPa beneath the dredge line to 29.2 kPa beneath the rock dike and backland. For SMS01 the undrained strength was uniformly 29.2 kPa across the model.

For SMS02 the improved clay was placed by excavating the unimproved clay after consolidation, following the grid pattern outlined in Figure 21, and replacing the unimproved clay with the soil-cement slurry, which was then allowed to cure. Approximately 40 percent of the clay within the improved zone was replaced with the soil-cement mixture. SMS01 was tested at 7 and 8 days after placement of the improved clay. The average unconfined compressive strength of the improved clay at 7 days was 917 kPa, with a maximum of 1118 kPa and a minimum of 637 kPa.

The rock had a target dry density of 1600 kg/m^3, and was placed by manually dropping it from a height of approximately 30 cm and gently tamping it in 5 cm thick layers. Checks on the calibration were made during construction by weighing the amount of rock placed within known volumes.

During placement of the soil layers, indicator markers were placed within the model to assist in examining the model behavior. The indicators consisted of thin

layers of black sand (Nevada sand that was dyed black with India ink) placed on horizontal layers and vertical columns throughout the profile. The horizontal markers were used to aid in visualizing vertical displacements, while the vertical columns were used to aid in visualizing horizontal displacements during model dissection.

In addition, miniature air hammers were placed within models NJM02, SMS01, SMS02, and JCB01. The air hammers were used to generate shear waves in flight, which were measured by the accelerometer arrays. The recorded shear waves were used to estimate the in-situ shear wave velocities. A detailed description of the miniature air hammers can be found in Arulnathan et al. (2000).

The in-situ soil properties for each model are tabulated in Table 7.

Table 7. In-situ soil properties.

Model	Loose Sand			Dense Sand			Rock		Clay	
	D_r (%)	ρ_{dry} (kg/m^3)	n (%)	D_r (%)	ρ_{dry} (kg/m^3)	n (%)	ρ_{dry} (kg/m^3)	n (%)	ρ_{dry} (kg/m^3)	n (%)
NJM01	39	1519	43	82	1662	39	1682	38	–	–
NJM02	45	1538	43	85	1673	39	1735	35	942	64
SMS01	35	1507	44	70	1620	40	1650	39	1017	62
SMS02	–	–	–	70	1620	40	1611	40	–	–
JCB01	40	1522	43	74	1633	40	1611	40	–	–

where: D_r is the relative density, ρ_{dry} is the dry mass density, and n is the porosity of the soil

Placement of the Piles and Wharf Deck

In all of the models, the piles were placed in the model after the soil layers had been placed up to the dredge line, and prior to the rock dike placement. Extreme care was taken to keep the piles within their design location and alignment through the use of a template system. The piles were installed to their design elevation using a vibrator and when necessary a rubber mallet. Care was taken to ensure that the strain gauges were in alignment with the container. The batter piles and single piles in SMS02 and JCB01 were installed in a similar manner. The wharf deck was removed after the piles were placed to allow better access during placement of the subsequent sand and rock layers, and was then placed back on the piles after saturation was complete.

Saturation

After the soil layers and piles had been placed within the model, the model was saturated with the pore fluid. The saturation process consisted of: 1) sealing the container with a lid; 2) creating a vacuum within the model container to remove the majority of the air from the container and soil voids; 3) flooding the container and soil voids with carbon dioxide to displace the majority of the remaining air; 4) creating a vacuum within the container to remove the carbon dioxide, leaving only an insignificant amount of air in the container; 5) pulling the pore fluid through a de-airing system and slowly allowing it to saturate the model, starting at the bottom of the container; 6) allowing the fluid level to reach equilibrium at the design elevation; and 7) releasing the vacuum and removing the container lid.

MODEL TESTING

Each model was subjected to a series of input motions. Initially small motions (less than 0.05 g peak prototype acceleration) were applied to verify that the shake table, data acquisition, and instrumentation were responding correctly. After the small motions, larger motions were input (peak prototype accelerations greater than 0.1 g). The larger motions consisted of two recorded acceleration time histories scaled to different levels. The two motions were the Loma Prieta earthquake motion recorded at the Oakland Outer Harbor, and the Northridge earthquake motion recorded at Rinaldi station (Figure 26).

During the testing sequence, shear wave velocities were introduced into the model using a shear hammer mounted on the base of the container for NJM01, and using the miniature air hammers for NJM02, SMS01, SMS02, and JCB01. The shear waves were recorded using the accelerometer profiles, allowing for an estimation of the shear wave velocities of the soil between earthquake motions.

SMS02 and JCB01 also included the lateral pile load tests conducted on the single piles in the backland and the rock dike slope. These tests were conducted before the earthquake tests, and consisted of cyclically loading the piles using a hydraulic ram for between 2 and 8 cycles.

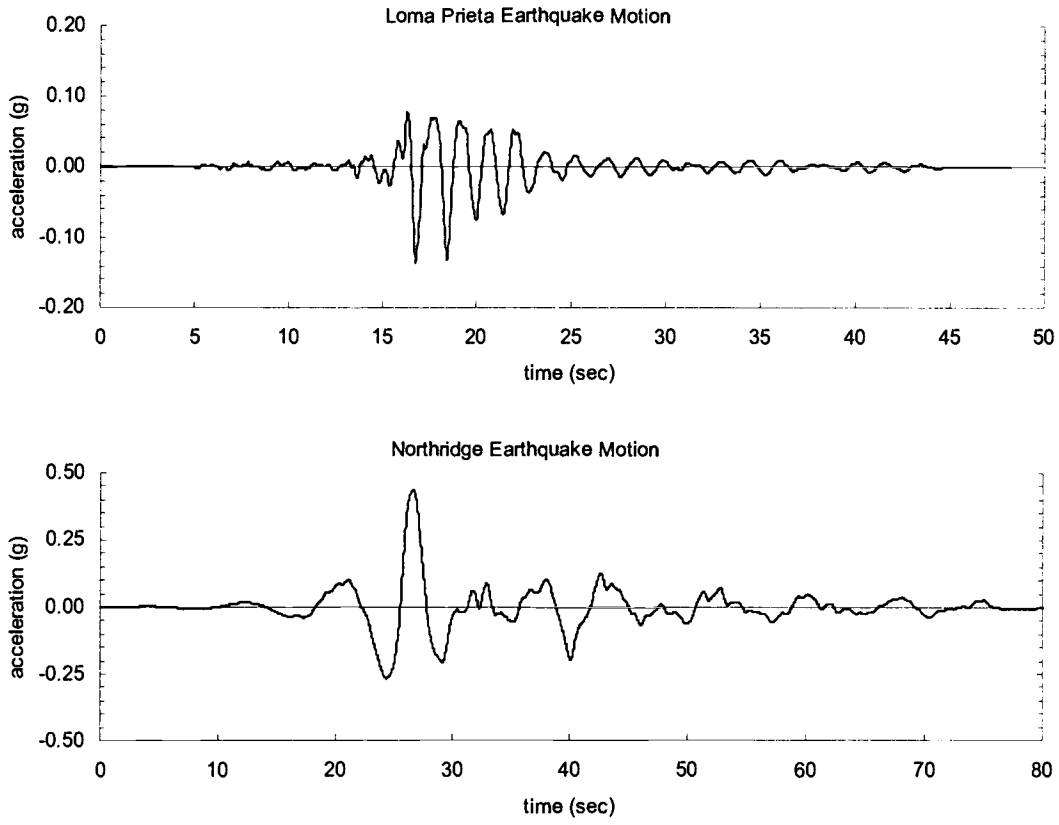

Figure 26. Un-scaled input acceleration time histories.

TEST RESULTS

The observed model response during the testing of the five centrifuge models appears to predict a seismic behavior consistent with the few available field case histories. This is illustrated in Figure 27, showing the relationship between the peak ground acceleration measured just beneath the ground surface in the backland for the models and the permanent lateral displacement of the wharf deck. Note that a series of input motions was applied to each model, therefore the deformations and model

response during successive input motions were recorded on models altered by the previous input motions. Also included in the figure are the results of three field case histories, the Port of Los Angeles during the 1994 Northridge Earthquake (Muraleetharan et al. 1995), the Port of Oakland during the 1989 Loma Prieta Earthquake (Egan et al. 1992, Singh et al. 2001), and the Port of Kobe during the 1995 Hyogoken-Nambu Earthquake (Iai 1998). Though the geometries of these case histories vary from the centrifuge models, they have aspects that make them similar in many ways. The specific case from the Port of Oakland included batter piles, a multi-lift rock dike, bay mud, and liquefiable backfill, making this model similar to NJM01, NJM02 and SMS02. The Port of Los Angeles case contained a sliver (cut-slope) rock dike, liquefiable sands, and batter piles, making this model most similar to JCB01. The Port of Kobe location consisted of a single lift rock dike, and piles installed through liquefiable sands and clays, and a caisson wall behind the pile-supported wharf as the primary method of earth retention, instead of a large rock dike.

Patterns of deformation as measured in the centrifuge appear to be reasonable, as seen for models NJM02 and SMS01 in Figure 28, Figure 29, and Figure 30, showing ground cracks behind the wharf deck, gapping between the piles and rock dike, and liquefaction induced vertical settlement in the backland, respectively. The settlement shown in Figure 30 for SMS01 is approximately 13 mm model scale. The procedure by Ishihara and Yoshimine (1992) was used to estimate the settlement, assuming the full thickness of the loose, saturated sand liquefies, a vertical settlement of 13 mm was predicated, in agreement with the measured value.

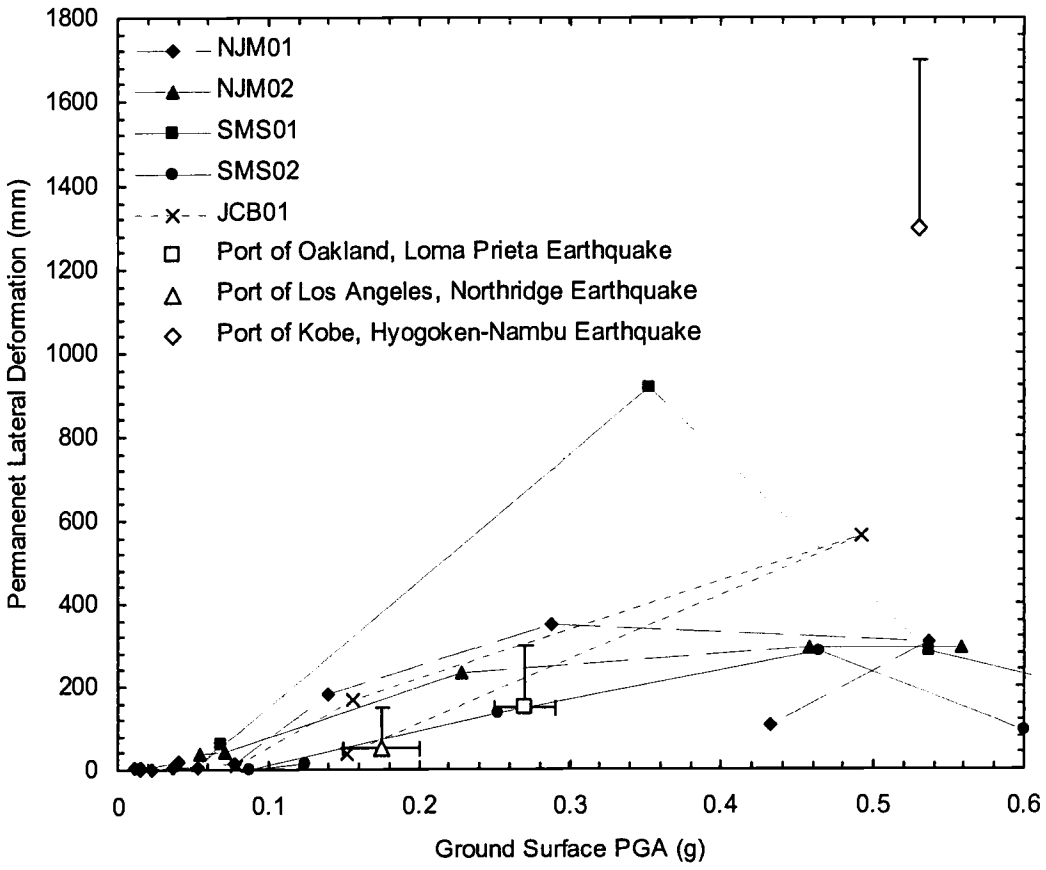

Figure 27. Measured and observed permanent lateral wharf deformation for various levels of shaking. The error bars represent the range of observed and/or estimated values.

Figure 28. NJM02 post-test ground cracks and separation between the piles and soils.

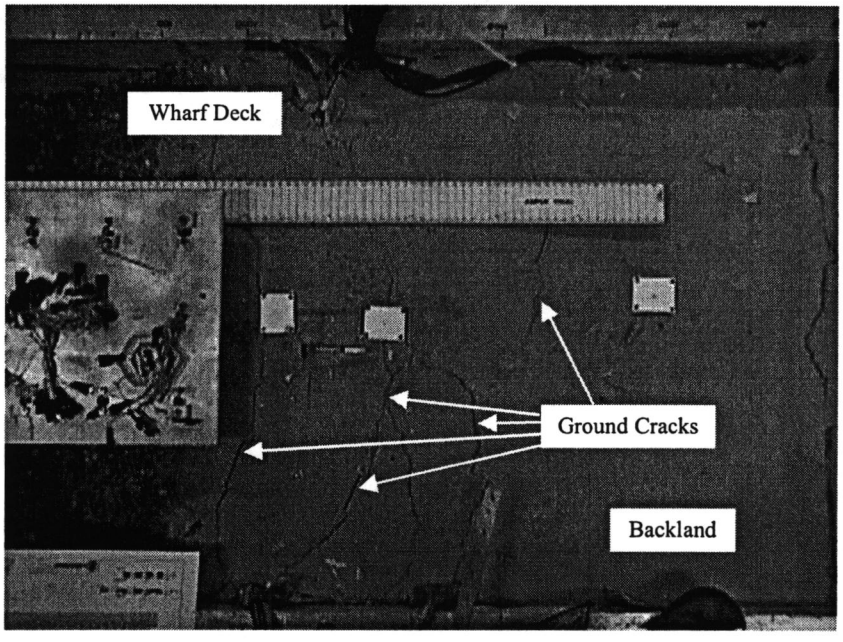

Figure 29. Post-test ground cracks in SMS01 due to lateral slope movement.

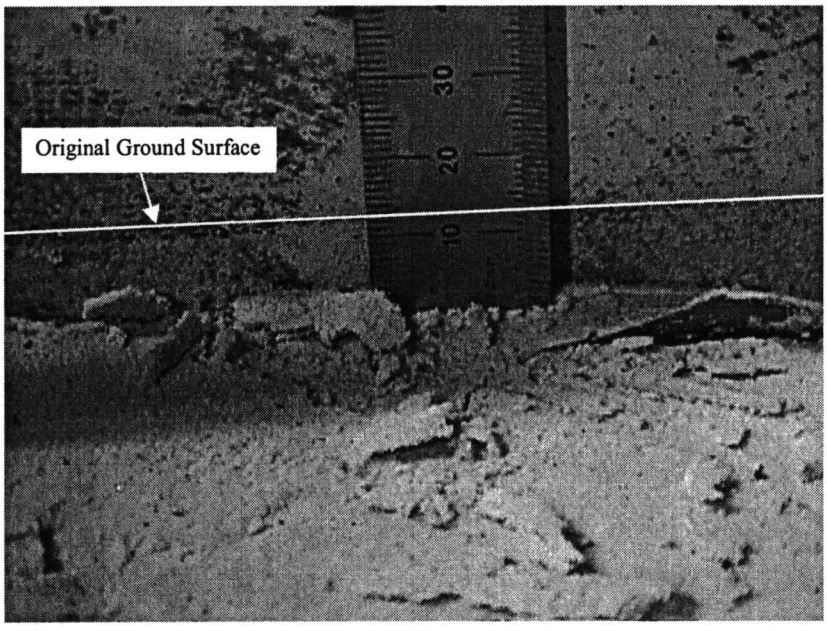

Figure 30. Post-test ground surface settlement in the backland of SMS01 due to liquefaction.

Given the complexity of the tested models, the authors would like to highlight several issues regarding the design and testing of these centrifuge models, which may be applicable to researchers designing and testing centrifuge models similar to those presented in this paper:

1) The method of sealing the strain gauges noted above and running the wires inside the piles resulted in none of the strain gauges failing due to water infiltration. Several of the piles were also utilized in more than one centrifuge model, highlighting their durability. By running the

wires inside the piles, the wires were less susceptible to damage during installation. In addition, the combination of the shrink wrap and beeswax, along with the standard strain gauge sealing process provide a water tight barrier. However, there were failures of the wiring and data collection system to which the piles were connected.

2) The number of strain gauges that were chosen per pile was generally based on the data to be obtained. The design of the strain gauge layout was such that the measured moments could be used to back calculate pile displacements and the applied soil pressures. The applied soil pressure is back calculated by double differentiating the moment data. This requires a minimum of three strain gauges per soil layer, if one point of applied soil pressure is to be calculated. The displacements, however, are calculated by double integrating the moment data, and only require strain gauge spacing close enough to provide an accurate moment profile. This is generally accomplished by having a minimum of one strain gauge located in the middle of the layer and one strain gauge located at each layer interface. Based on these requirements, the piles presented herein generally had a minimum of three strain gauges per soil layer. However, some redundancy was required, as there were some failures of the wiring and data collection system. In addition, there was a limited number of recordable data channels, resulting in not all of the strain gauges being recorded during each test.

3) One of the critical aspects of this research was the quantification of permanent lateral displacements. However, it was only possible to measure the displacements at select points at the ground surface. Exact measurements of instrument locations were also made before and after the test sequence. However, since each model was subjected to multiple earthquake shakes, it was not possible to determine the deformation profiles for any one specific shake during the test sequence. It is recommended that only one large shake be conducted if displacement profiles are of primary interest. However, if site/structure response is of primary interest, multiple shakes are entirely valid. Another difficulty in conducting multiple large shakes is that each shake produces excess pore pressures resulting in incremental soil densification. To accurately examine the response of the ensuing shakes, an estimation of the soil densification of the previous shake was required. This was not a trivial issue, and should be addressed when designing seismic centrifuge models.

ACKNOWLEDGEMENTS

The authors would like to gratefully acknowledge staff of the centrifuge facility at UC Davis, who helped many long days, nights, and weekends in constructing and testing these models, and the assistance from Manfred Deitrich and Andy Brickman at Oregon State University.

This research effort was supported by grant no. CMS-9702744 from the National Science Foundation, grant no. SA2394JB from the Pacific Earthquake Engineering Research Center, and included additional industry support from the Port of Oakland, Port of Long Beach, URS Corp., and Hayward Baker, Inc. The support from these agencies and companies is greatly appreciated.

REFERENCES

Arulnathan, R., Boulanger, R.W., Kutter, B.L., Sluis, B. 2000. "A New Tool for Vs Measurements in Model Tests." *ASTM Geotechnical Testing Journal.* Vol. 23, Issue 4. pp 444-452.

Arulmoli, K., Muraleetharan, K.K., Hossain, M.M., and Fruth, L.S. 1992. *VELACS: Verification of Liquefaction Analyses by Centrifuge Studies Laboratory Testing Program Soil Data Report.* Prepared for: National Science Foundation. The Earth Technology Corporation. Project No. 90-0562. Irvine, CA.

Boland, C.B., Schlechter, S.M., McCullough, N.M., Dickenson, S.E., Kutter, B.L., and Wilson, D.W. 2001a. *Data Report: Pile-Supported Wharf Centrifuge Model (SMS02).* Geotechnical Engineering Group, Department of Civil, Construction and Environmental Engineering. Oregon State University.

Boland, C.B., Schlechter, S.M., McCullough, N.M., Dickenson, S.E., Kutter, B.L., and Wilson, D.W. 2001b. *Data Report: Pile-Supported Wharf Centrifuge Model (JCB01).* Geotechnical Engineering Group, Department of Civil, Construction and Environmental Engineering. Oregon State University.

Dames and Moore. 1984. *Geotechnical Studies for the Port of Portland Terminal 2 Rehabilitation.* Prepared for the Port of Portland.

Egan, J.A., Hayden, R.F., Scheibel, L.L., Otus, M., and Serventi, G.M. 1992. "Seismic Repair at Seventh Street Marine Terminal." Proceedings of the conference *Grouting, Soil Improvement, and Geosynthetics.* ASCE Geotechnical Special Publication No. 30, Volume 2. New Orleans, Louisiana. February 25-28.

Iai, S. 1989. "Similitude for Shaking Table Tests on Soil-Structure-Fluid Model in 1g Gravitation Field." *Soils and Foundations.* Vol. 29, No. 1. March. pp. 118.

Ishihara, K., and Yoshimine, M. 1992. "Evaluation of Settlements in Sand Deposits Following Liquefaction During Earthquakes." *Soils and Foundations*. Vol. 32, No. 1. pp. 29-44.

Kutter, B.L., Idriss, I.M., Kohnke, T., Lakeland, J., Li, X.S., Sluis, W., Zeng, X., Tauscher, R., Goto, Y., and Kubodera, I. 1994. "Design of a Large Earthquake Simulator at UC Davis." Proceedings, *Centrifuge 94*. Lueng, Lee, and Tan, Eds. Balkema, Rotterdam. pp.169-175.

Kutter, B.L., Li, X.S., Sluis, W., and Cheney, J.A. 1991. "Performance and Instrumentation of the Large Centrifuge at Davis." Proceedings, *Centrifuge 91*. Ko and Mclean, Eds. Balkema, Rotterdam. pp. 19-26.

McCullough, N.J., Schlechter, S.M., Dickenson, S.E., Kutter, B.L., and Wilson, D.W., 2000. *Data Report: Pile-Supported Wharf Centrifuge Model (NJM01)*. Geotechnical Engineering Group, Department of Civil, Construction and Environmental Engineering. Oregon State University.

Mukhopadhyay, G. 1998. "Preparing for Pier A." *Civil Engineering*. ASCE. August. pp 36-39.

Muraleetharan, K.K., Thiessen, D.A., Jagannath, S.V., and Arulmoli, K. 1995. "Performance of Port Facilities During the Northridge Earthquake." Proceedings of the *Third International Conference on Recent Advances in Geotechnical Earthquake Engineering and Soil Dynamics*. Vol III. St. Louis, Missouri. April 2-7.

Schlechter, S.M., McCullough, N.J., Dickenson, S.E., Kutter, B.L., and Wilson, D.W. 2000a. *Data Report: Pile-Supported Wharf Centrifuge Model (NJM02)*. Geotechnical Engineering Group, Department of Civil, Construction and Environmental Engineering. Oregon State University.

Schlechter, S.M., McCullough, N.J., Dickenson, S.E., Kutter, B.L., and Wilson, D.W. (2000b). *Data Report: Pile-Supported Wharf Centrifuge Model (SMS01)*. Geotechnical Engineering Group, Department of Civil, Construction and Environmental Engineering. Oregon State University.

Scott, R.F. 1991. "Modeling of Earth Structures." *Proc., Port of Los Angeles Seismic Workshop*.

Singh, J.P., Tabatabaie, M., and French, J.B. 2001. "Geotechnical and Ground Motion Issues in Seismic Vulnerability Assessment of Existing Wharf Structures." *Proceedings of the ASCE Ports 2001 Conference*. Norfolk, Virginia, April 29-May 2.

Wilson, D.W. 1998. *Soil-Pile-Superstructure Interaction in Liquefying Sand and Soft Clay*. Ph.D. Dissertation. University of California. Davis, CA. September.

CHAPTER 3 – MANUSCRIPT NO. 2:

THE SEISMIC PERFORMANCE OF PILE-SUPPORTED WHARVES

Nason J. McCullough
Stephen E. Dickenson

Submitted to the

ASCE Journal of Waterway, Port, Coastal, and Ocean Engineering

ASCE Publications
1801 Alexander Bell Dr.
Reston, VA 20191

ABSTRACT

The seismic behavior of pile-supported wharves involves complex soil-structure-interaction. Observed seismic behavior from field case histories has indicated that structural damage of pile-supported wharves has primarily been due to permanent ground deformations. This clearly shows that the seismic performance of pile-supported wharves is a soil-structure interaction problem. However, there are few well-documented seismic field case histories of pile-supported wharves that include site-specific data on ground motions, ground and pile deformations, and pile performance. Given the limited number of well-documented case histories, a centrifuge modeling study was undertaken to supplement the seismic field case histories of pile-supported wharves with model case histories.

Several key issues arose from the case history examination: 1) Batter piles were noted to perform poorly during earthquakes, but the poor performance of batter piles was mainly due to permanent soil deformations. The case histories also showed that batter piles performed satisfactorily when permanent ground deformations were limited; 2) The primary cause of permanent ground deformations was generally due to with soil liquefaction; 3) Given the dynamic loading and the flexibility of pile-supported wharves, permanent deformations should be anticipated during high levels of seismic shaking, even for geotechnically and structurally competent geometries; and 4) Wharf piles tended to reduce slope deformations, however, maximum pile bending moments below grade (i.e. due to deep-seated soil deformation) were often as large or larger than the maximum pile bending moments at the pile/deck connection.

INTRODUCTION

Pile-supported wharves (Figure 31) are complex soil-structure interaction systems, and as discussed herein refer to the system of piles, wharf deck, rock dike, foundation and backfill soils. There are three well-documented seismic case histories of pile-supported wharf failures presented herein; 1) Port of Oakland during the 1989 Loma Prieta Earthquake, 2) Port of Los Angeles during the 1994 Northridge Earthquake, and 3) Port of Kobe during the 1995 Hyogoken-Nambu Earthquake. There are numerous less well-documented case histories, but due to the limited quantifiable information, only general observations from these case histories are of interest.

Given the limited number of seismic field case histories, a centrifuge model study was conducted to supplement these cases with a suite of model case histories. Five centrifuge models of pile-supported wharves were dynamically tested. The models were well-instrumented and provided valuable information of the seismic performance and behavior of pile-supported wharves.

This paper presents a summary of the field and model case histories, and highlights several key issues regarding the seismic performance of pile-supported wharves.

FIELD CASE HISTORY SUMMARY

There are a limited number of field case histories documenting the seismic performance of pile-supported wharves at levels of shaking of engineering interest.

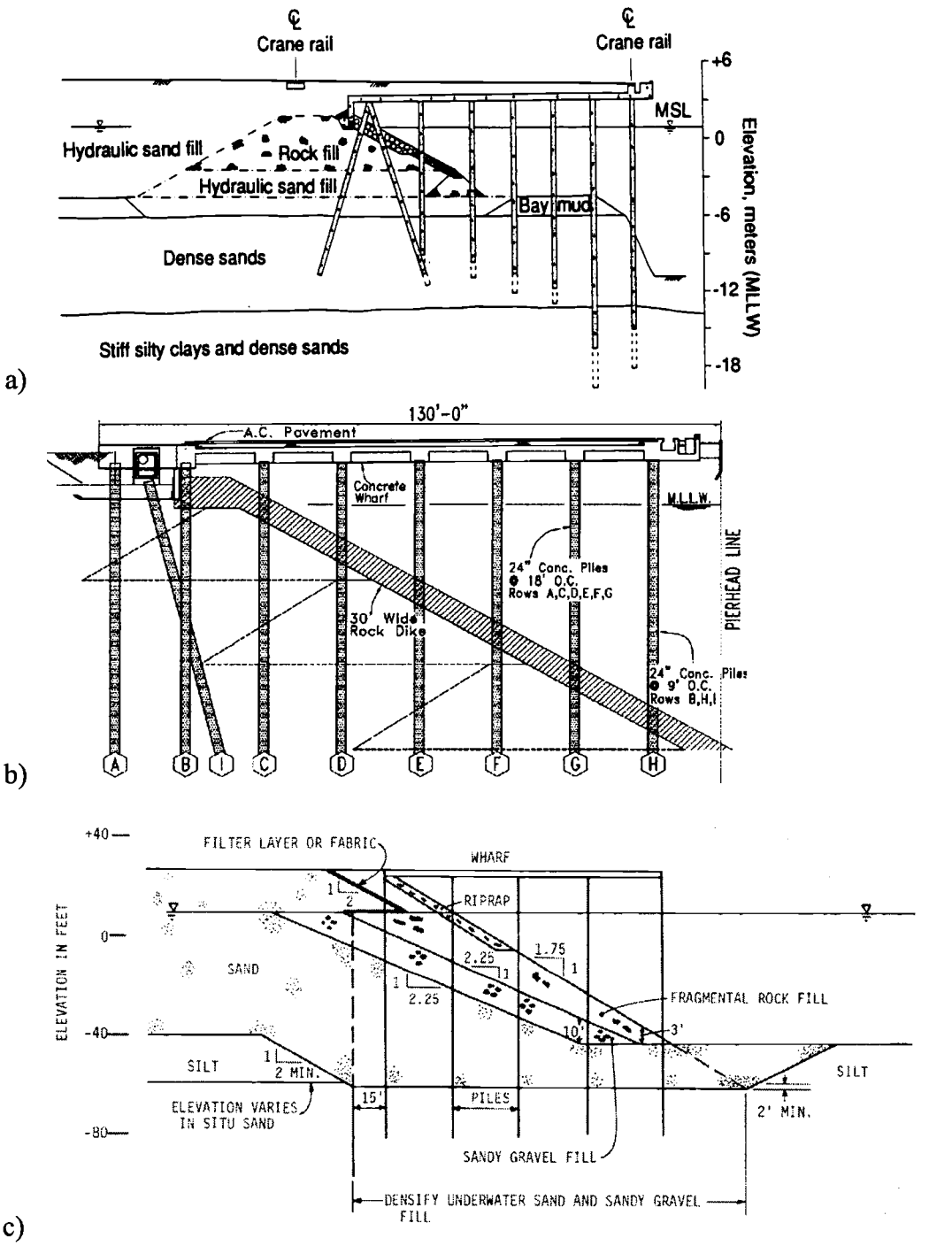

Figure 31. Typical pile-supported wharf structures; a) Port of Oakland, California (Egan et al. 1992 from *Grouting, Soil Improvement and Geosynthetics*, reprinted by permission of ASCE), b) Port of Long Beach, California (Mukhopadhyay 1998 from *Civil Engineering*, reprinted by permission of ASCE, courtesy of Port of Long Beach), and c) Port of Portland, Oregon (Dames and Moore 1984).

Furthermore, the majority of the field case histories lack instrumentation, with the seismic performance typically estimated based on noted structural failures and deformations estimated from ground crack measurements. Few sites had been accurately surveyed prior to the earthquakes, and few sites contained ground motion recording. However, there are general lessons to be learned from the available case histories.

In general, pile-supported wharves which were damaged during earthquakes were also noted to have sustained moderate to high large levels of permanent ground deformation. Several cases of damage to pile-supported wharves in conjunction with moderate to large permanent ground deformations include; Anchorage during the 1964 Alaska Earthquake, Port of Oakland during the 1989 Loma Prieta Earthquake, Port of San Fernando during the 1990 Philippines Earthquake, Port of Los Angeles during the 1994 Northridge Earthquake, Port of Kobe during the 1995 Hyogoken-Nambu Earthquake, Petkim petrochemical facility during the 1999 Turkey Earthquake, and the Port of Kandla during the 2001 India Earthquake These case histories are documented by: Iai (1998), Werner (1998), PIANC (2001), EERI (1991a), EERI (1991b), EQE (1990), EERI (2000), EERI (2002).

In general, the above case histories indicated a *threshold* peak ground acceleration (PGA) value for various levels of damage. For instance, pile-supported wharf structures subjected to PGA values less than 0.1 g typically suffered none to negligible damage, structures subjected to PGA values ranging from approximately 0.1 to 0.15 g suffered minor damage, structures subjected to PGA values ranging from

0.2 to 0.25 g generally suffered moderate damage, and structures subjected to PGA values greater than approximately 0.35 g suffered severe damage.

Three well-documented case histories illustrate the poor seismic performance of pile-supported wharves subjected to moderate to large ground deformations. The Seventh Street Terminal (Figure 31a) at the Port of Oakland during the 1989 Loma Prieta Earthquake suffered significant damage due to permanent ground deformations. The earthquake had a moment magnitude of 6.9 and a PGA at the port of approximately 0.25 to 0.29 g. Seventh Street Terminal consisted of six rows of vertical piles, and one row of landside batter piles, installed through a single lift rock dike, retaining and supported on loose sandy fill. Significant liquefaction of the loose fill was noted at the site, causing permanent lateral ground deformations on the order of 15 to 30 cm (Egan et al. 1992, Singh et al. 2001). Approximately 75 percent of the batter piles and between 3 and 20 percent of the vertical piles failed at the pile/deck connection (Singh et al. 2001). The failures noted were generally complete separation and shear failure of the connection (Figure 32). In addition, pile integrity testing conducted eleven years after the earthquake indicated pile damage at depth near the interface between soil layers in many of the piles (Oyenuga et al. 2001), likely due to the permanent ground deformations incurred during the earthquake.

Another well-documented case history is the Port of Los Angeles during the 1994 Northridge Earthquake. The Northridge Earthquake had a moment magnitude of 6.7 and a maximum PGA of approximately 0.15 to 0.20 g at the port. Approximately 5 to 15 cm of permanent lateral deformations were reported (Buslov et al. 1996,

Figure 32. Port of Oakland damaged batter pile during the 1989 Loma Prieta Earthquake.

Muraleetharan et al. 1995) for Berths 121, 126, and 126/0. Berths 121 and 126 consisted of six rows of vertical piles constructed over a rock dike retaining loose sandy fill. Berth 126/0 consisted of seven rows of vertical piles and one row of landside batter piles constructed over a sliver (cut-slope) rock dike. Berth 121 and 126 experienced the upper bound deformations (approximately 15 cm), due to liquefaction of the loose sandy fill, while Berth 126/0 experienced the lower bound deformations (approximately 5 cm). Berths 121 and 126 suffered extensive damage, with approximately 80 percent of the piles damaged, whereas approximately 40 percent of

the piles at Berth 126/0 were damaged. However, the damage to Berths 121 and 126 was limited mainly to hairline cracks, while the damage to the batter piles in Berth 126/0 included significant concrete spalling and separation between the piles and deck (Buslov et al. 1996). Therefore, even though larger deformations and more damage was noted for Berths 121 and 126, the damage was less critical, whereas the damage to the batter piles at Berth 126/0, which was subjected to less permanent ground deformation, was much more significant.

The last well-documented case history is Takahama Wharf at the Port of Kobe during the 1995 Hyogoken-Nambu Earthquake. The Hyogoken-Nambu Earthquake had a magnitude of 7.2 and an approximate PGA of 0.53 g at the port. The wharf consisted of a pile-supported wharf constructed through rock fill, with stacked concrete blocks located behind the wharf to retain the backfill soils (Figure 33). The wharf deck was supported by three rows of 700 mm diameter steel pipe piles. Permanent ground deformations were measured between 1.3 and 1.7 meters (Figure 34). In addition to the pile/deck connection failures, there were several noted buckling failures at depth, near soil interfaces (Figure 33). Figure 35 shows the extracted piles after the earthquake. This case history highlights the necessity to account for the possibility of large moments at depth during design.

There are also several interesting cases where liquefaction was observed adjacent to the pile-supported wharves, yet there was little or no permanent ground deformation, and there was no noted damage to the pile-supported wharf. This was noted at the Port of Limon during the 1991 Costa Rica Earthquake (EERI 1991b), the

Port of Seattle during the 2001 Nisqually Earthquake, and the Port of Kandla during the 2001 India Earthquake (EERI 2002). These cases illustrate that permanent ground deformations are a requisite for liquefaction-induced structural damage.

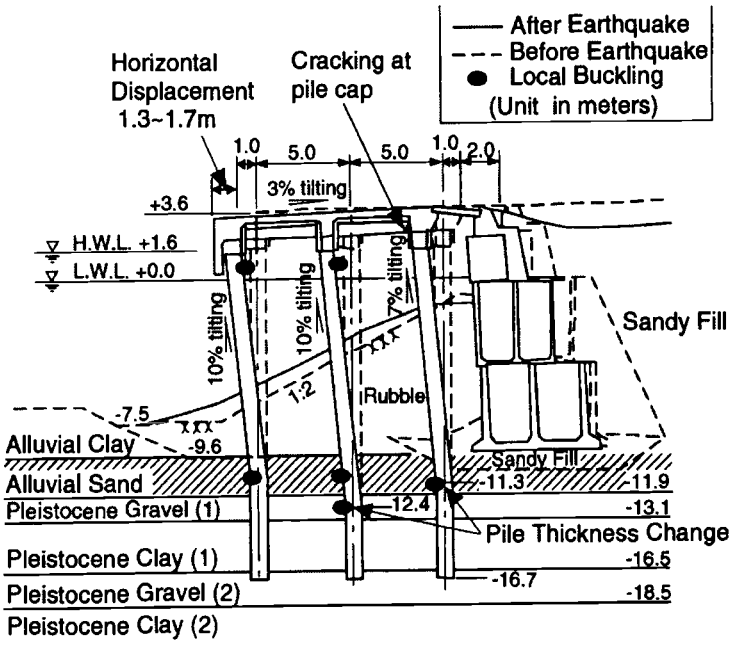

Figure 33. Port of Kobe Takahama Wharf damaged during the 1995 Hyogoken-Nambu Earthquake (Iai 1998 from *Geotechnical Earthquake Engineering and Soil Dynamic III*, reprinted by permission of ASCE).

There is an interesting case history during the 2001 India Earthquake, in which the Port of Navlakhi sustained permanent ground deformations due to shear straining in a soft clay layer of 30 to 45 cm, yet no structural damage was noted at the pile-supported wharf (EERI 2002). However, the field investigation was limited to brief above ground observations; unobservable structural damage could have occurred within the soil profile or beneath the wharf deck.

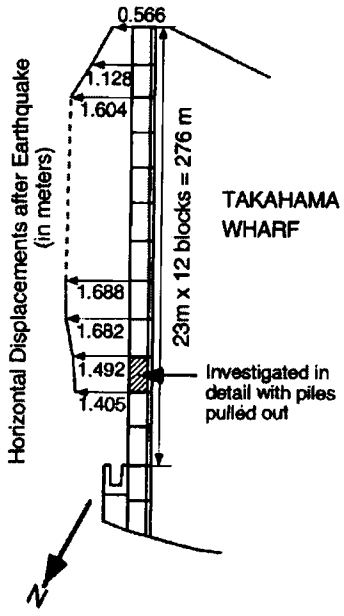

Figure 34. Permanent lateral deformations Takahama Wharf at the Port of Kobe measured following the 1995 Hyogoken-Nambu Earthquake (Iai 1998 from *Geotechnical Earthquake Engineering and Soil Dynamic III*, reprinted by permission of ASCE).

Even though batter piles have been noted to perform badly during earthquakes, there are several case histories illustrating acceptable performance. For example, Berths 24, through 26 and 60 through 62 at the Port of Oakland during the 1989 Loma Prieta Earthquake showed no observable structural damage, hypothesized to be due to the negligible permanent lateral deformations. However, due to the much greater stiffness of batter piles, in comparison to vertical piles, they are much more susceptible to damage. As noted for Berth 121, 126, and 126/0 at the Port of Los Angeles, even though the wharf with all vertical piles was subjected to larger ground deformations, and suffered a greater percentage of noted damage, the adjacent batter pile wharf suffered much more devastating damage. The vertical piles mainly suffered

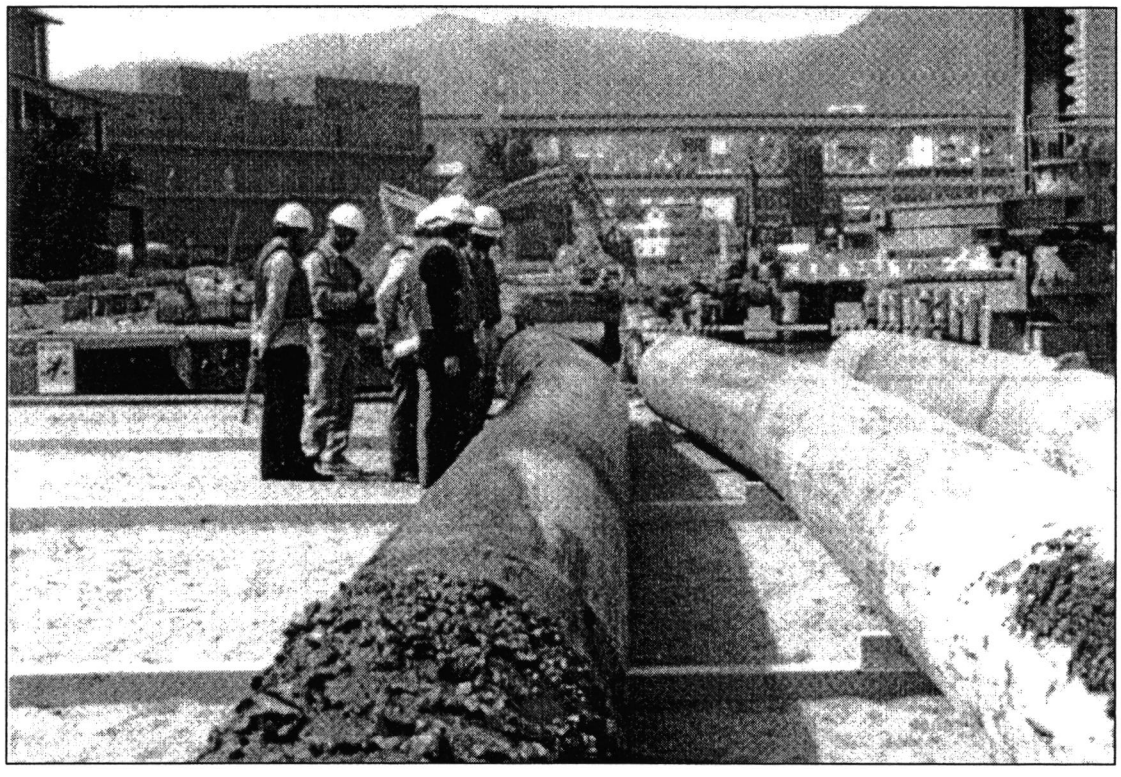

Figure 35. Port of Kobe Takahama Wharf damaged during the 1995 Hyogoken-Nambu Earthquake piles extracted from the wharf for inspection. The top of the piles are at the bottom of the photo (Iai 2003).

hairline and slightly larger cracks, relatively easily repaired with epoxy, while the batter piles suffered significant concrete spalling and separation from the wharf deck, requiring much more costly and time consuming repairs.

Based on the above seismic field case histories, there are two key issues relating to the seismic performance of pile-supported wharves:

1) The vast majority of noted structural damage to pile-supported wharves has been due to permanent ground deformations. The magnitude of the deformations appears to be a function of the liquefaction of adjacent

soils. In addition, pile damage was typically a function of the pile-supported wharf flexibility. More flexible (all vertical pile) wharves generally performed better, with damage more easily repaired. Less flexible (batter pile) wharves have generally suffered more devastating damage, such as complete shear failure of the pile/deck connection.

2) There is limited specific information regarding the seismic performance of pile-supported wharves. Very few of the structures had accelerometers located within the vicinity of the wharf, and very few of the wharves contained survey data prior to the respective earthquakes. In the vast majority of the cases, the post-seismic deformation of the wharves was estimated based on the mapping of ground cracks. There is also very limited data on the performance of piles beneath the ground surface; there could be many failures at depth that have not been noted.

MODEL CASE HISTORIES

Given the limited number of well-characterized field case histories, a research program was conducted to supplement the database of seismic case histories with a suite of model case histories. This research program utilized centrifuge models of typical pile-supported wharf geometries subjected to a suite of earthquake acceleration time histories, with the performance monitored through the use of approximately 100 instruments per test.

Five centrifuge models were tested as part of the research program. The models were constructed and tested at the centrifuge facility at the University of California at Davis Center for Geotechnical Modeling. A summary of the five models in provided in Table 8, and cross-sections of the models are presented in Figure 36 through Figure 40.

Table 8. Centrifuge model summary.

Model	Rock Dike	Prototype Scale				
		Water Depth (m)	Rock Dike Height (m)	Transverse Pile Spacing (m)	Longitudinal Pile Spacing (m)	Pile Diameter (mm)
NJM01	Two-lift	16.0	19.5	5.1	6.1	637
NJM02	Two-lift	16.1	20.1	5.1	5.8	546
SMS01	Two-lift	16.1	20.1	5.1	5.8	546
SMS02	Single-lift	12.4	15.2	4.0	4.0	637
JCB01	Sliver	12.4	15.2	4.0	4.0	637

Model NJM01 consisted of a typical pile-supported wharf with all vertical piles, installed through a multi-lift rock dike retaining a loose, liquefiable backfill soil. Model NJM02 was a smaller scale model, and included a layer of clay (San Francisco Bay Mud) at depth, as well as loose, liquefiable backfill soils. Model SMS01 modeled the improved case of NJM02, where a portion of the loose sand was placed dense, and a portion of the clay was improved with cement. Model SMS02 contained a single-lift rock dike, and the wharf structure included a pair of batter piles, and sands that had were placed dense to model soil improvement. Model JCB01 utilized the same wharf

and pile structure as SMS02, but modeled a sliver (cut-slope) rock fill section, underlain by loose, liquefiable sands, with the backland being dense sand. Models SMS02 and JCB01, though they contained the batter piles, had the option to disconnect the batter piles from the wharf deck to compare the behavior of the pile-supported wharf with and without batter piles.

Specifics concerning model fabrication and centrifuge testing are contained in the following reports: McCullough et al. (2000), Schlechter et al. (2000a), Schlechter et al. (2000b), Boland et al. (2001a), and Boland et al. (2001b).

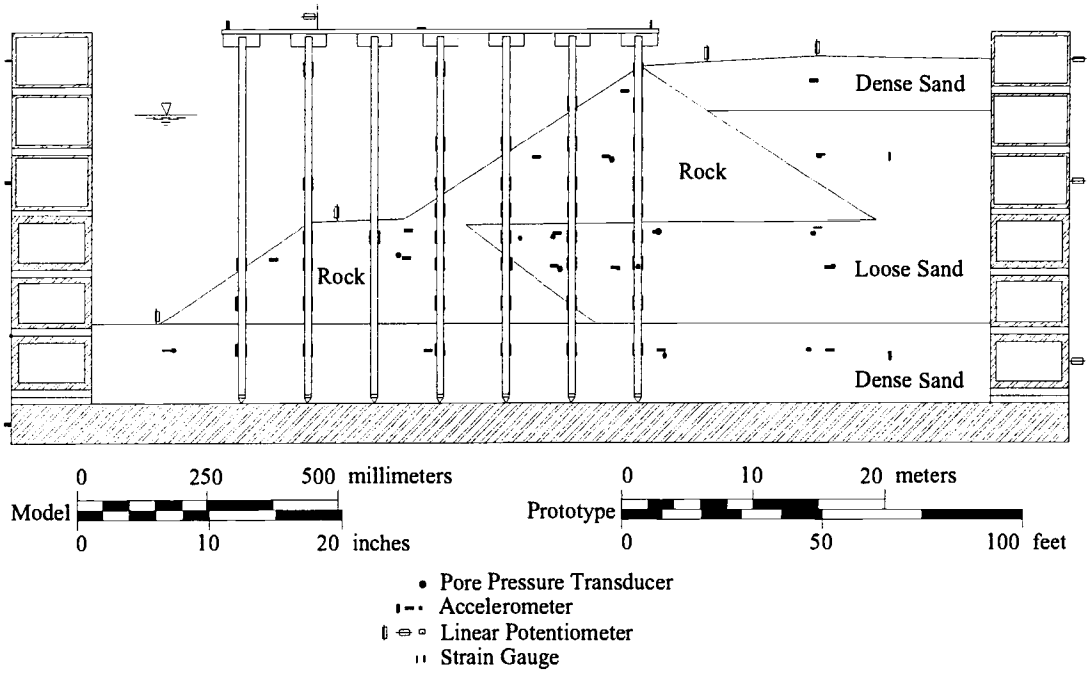

Figure 36. Centrifuge model NJM01.

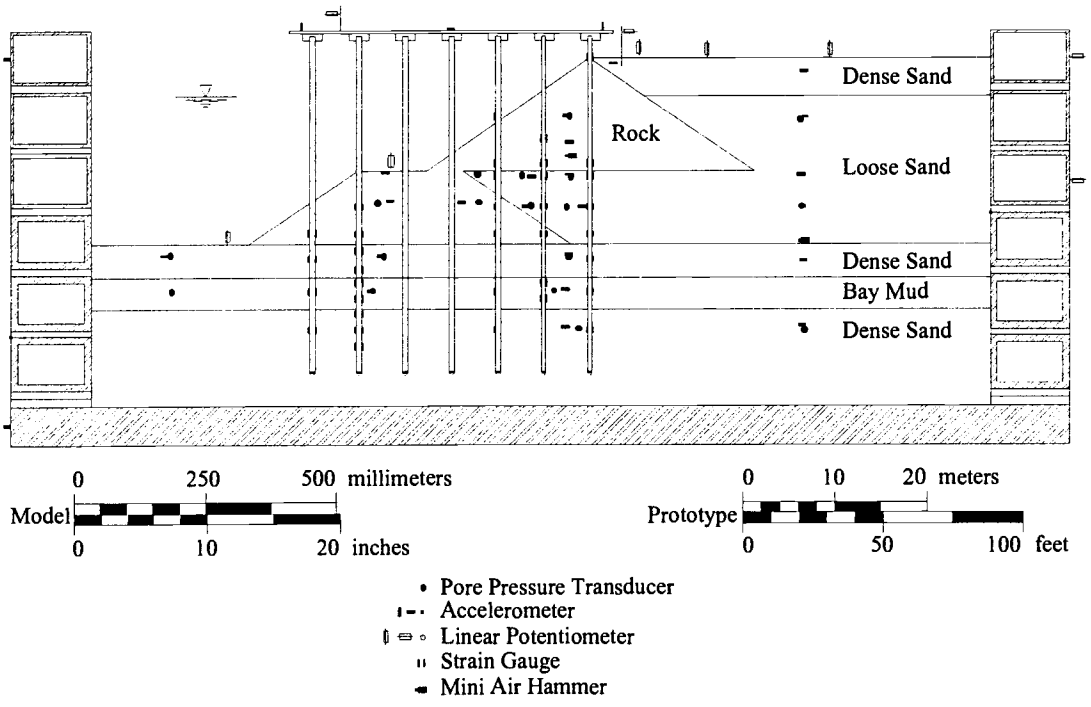

Figure 37. Centrifuge model NJM02.

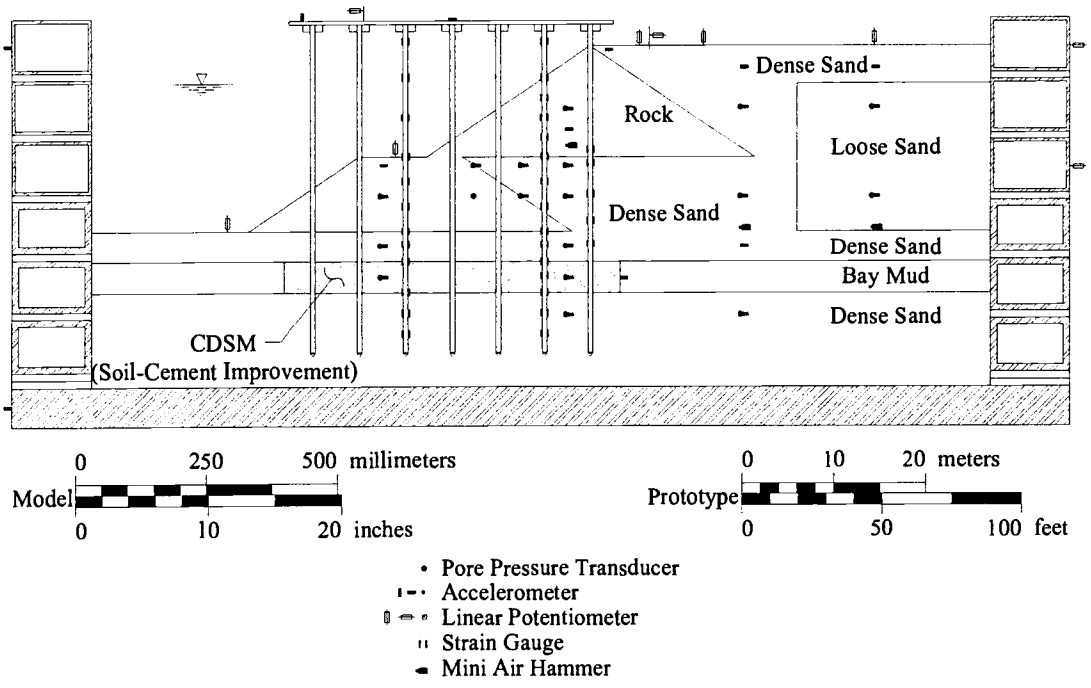

Figure 38. Centrifuge model SMS01.

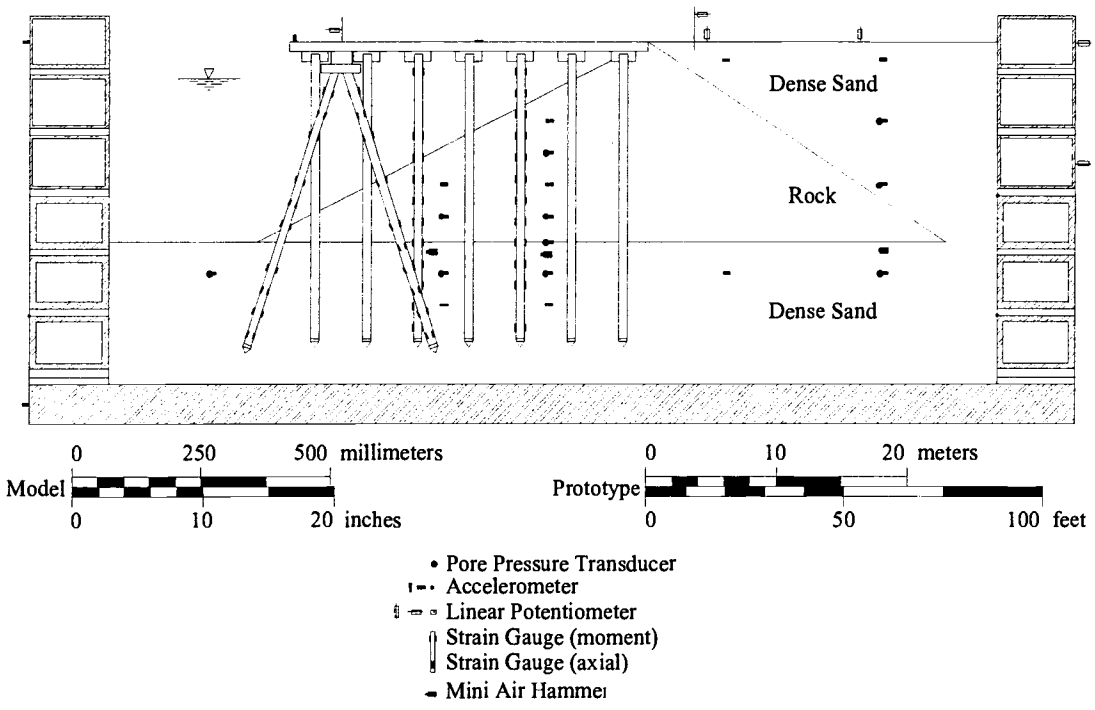

Figure 39. Centrifuge model SMS02.

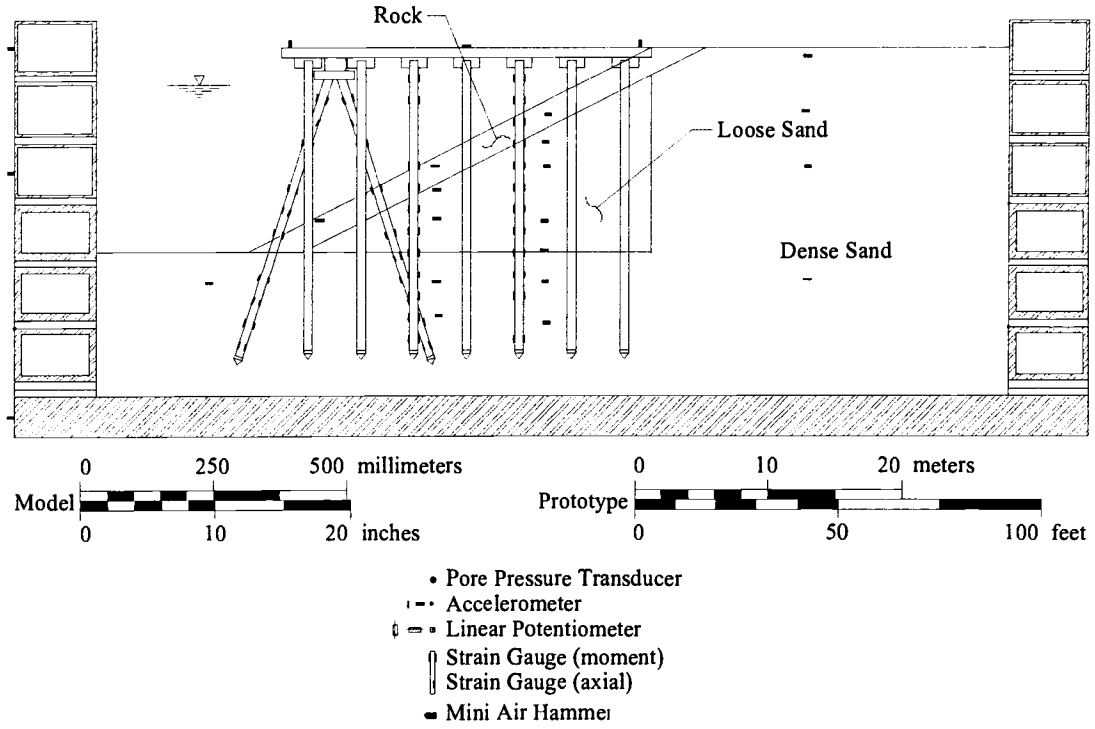

Figure 40. Centrifuge model JCB01.

GENERAL PERFORMANCE OF PILE-SUPPORTED WHARVES

Plots were developed illustrating the general seismic performance of field and model case histories on the seismic performance of pile-supported wharves. Figure 41 relates the peak ground surface acceleration in the backland to the permanent wharf displacement. In most cases, the horizontal deformation of the wharf deck was approximately equal to the horizontal deformation of the soil immediately behind the wharf deck. The backland peak ground acceleration and the permanent wharf displacement were typically the only information available from field case histories, and by plotting this information for all field and model case histories, the applicability of the model case histories was evaluated. Shown on the figure are the three field case histories of seismic wharf performance for which quantitative values were noted, the Port of Oakland during the 1989 Loma Prieta Earthquake, the Port of Los Angeles during the 1994 Northridge Earthquake, and the Port of Kobe (Takahama Wharf) during the 1995 Hyogoken-Nambu Earthquake. In general, the model case history data were in agreement with the field case histories. The case histories also indicate a relationship between seismic slope stability and performance, as can be noted by the decreasing deformations with increasing factors of safety. The one exception is model SMS01, which included a relatively large amount of soil improvement, but resulted in a relatively large amount of deformation.

It is interesting to note that even for relatively stable wharves (factors of safety greater than 2.0), when subjected to high levels of shaking (greater than 0.4 to 0.5 g), deformations on the order of 200 mm or more are expected. As a note, the design level

of shaking for many western United States ports is greater than 0.4 g. This highlights that pile-supported wharves are flexible systems, and some deformations should be anticipated at high levels of shaking, even for stable geometries. Ground treatment is often employed in the field to reduce (however not eliminate) the magnitude of expected soil deformations.

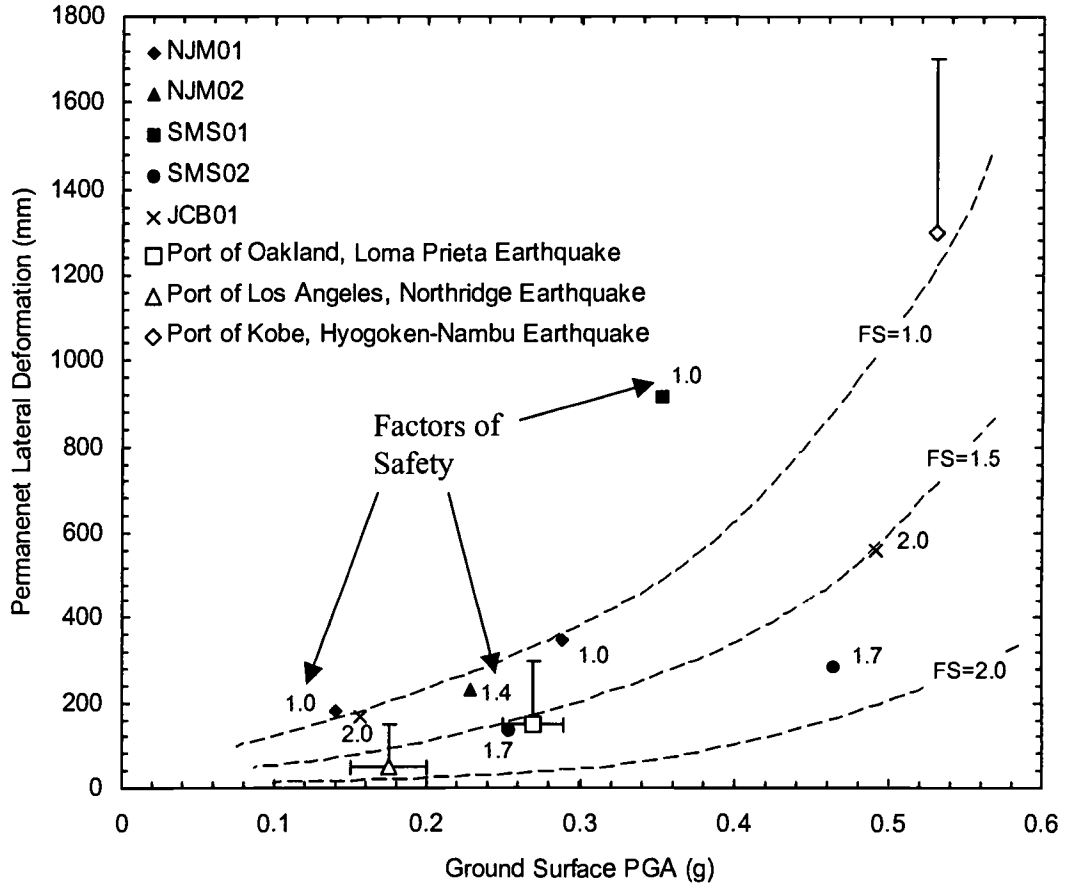

Figure 41. Relationship between the ground surface peak ground acceleration in the backland and the permanent lateral deformation of the wharf deck.

Figure 42 through Figure 46 illustrate the performance of the various pile-supported wharf geometries by plotting the maximum cyclic and residual bending moments in the piles from one earthquake test for each centrifuge model. These figures illustrate the general patterns of model behavior. Large bending moments are indicative of concentrated loads, and are typically located near the failure plane(s) and/or soil interfaces. For model NJM01, the failure occurred through the loose sand and the connection between the upper and lower rock dikes. Model NJM02 showed similar behavior, though there were indications of failure through the clay. Model SMS01 indicated that even with a substantial amount of soil improvement (of both the loose sand and clay) large moments still developed. This was in part due to the stronger earthquake motion, but also the concentration of the failure plane at depth, at the interface between the CDSM and the dense sand (it should be noted that the CDSM in the model did not penetrate into the underlying dense sand). Model SMS02 indicated relatively small moments, as this was the most stable geometry modeled. Model JCB01 indicated that the loose, liquefied sand pushed on the piles, which were effectively pinned in the dense sand foundation.

The models appeared to fail through the weak soils (soft clays and/or liquefied sands), with the largest moments developing at interfaces, such as the loose/dense sand interfaces of models NJM01, NJM02, and JCB01, or the CDSM/dense sand interface of model SMS01. It was also apparent from the models for the potential of large bending moments to develop at depth. These moments were due to the global (in)stability of the dike and seismic soil response. This is illustrated in Figure 47,

showing the relationships between the pile bending moments and the peak backland ground surface accelerations. The moments have been normalized for comparison between the models by multiplying the moment times the pile diameter and dividing by the elastic modulus and moment of inertia of the pile. The plotted moments for each model were the largest recorded moments of all the piles for each test. Larger peak backland ground accelerations resulted in more liquefaction, resulting in lower slope stability factors of safety. It is indicated in Figure 47a that the moments at the top of the piles (near the pile/deck connection) were a function of the post-seismic factor of safety. However, this relationship was not readily apparent for the moments at depth (Figure 47b). The seismic factor of safety is plotted adjacent to the symbols, which were calculated using traditional slope stability analysis methods, and included the effect of the centrifuge measured excess pore pressures and the beneficial effects of the piles. The bending moments plotted for the field case histories were the plastic moment capacities of noted pile failures, however, since the piles failed, the induced moments may have been larger than the plastic moment capacity.

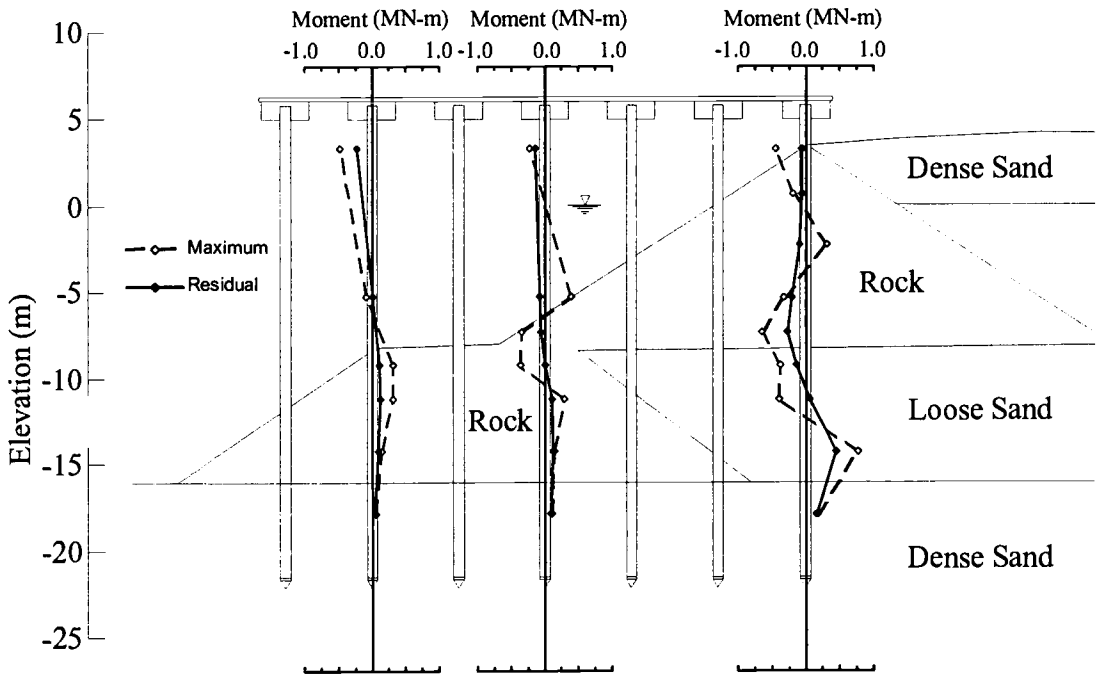

Figure 42. Maximum cyclic and residual moments for three piles for centrifuge model NJM01. The input PGA and the backland ground surface PGA values were 0.15 g and 0.14 g, respectively. The input motion was the 1989 Loma Prieta motion recorded at the Port of Oakland Outer Harbor. The permanent lateral wharf deformation was 182 mm.

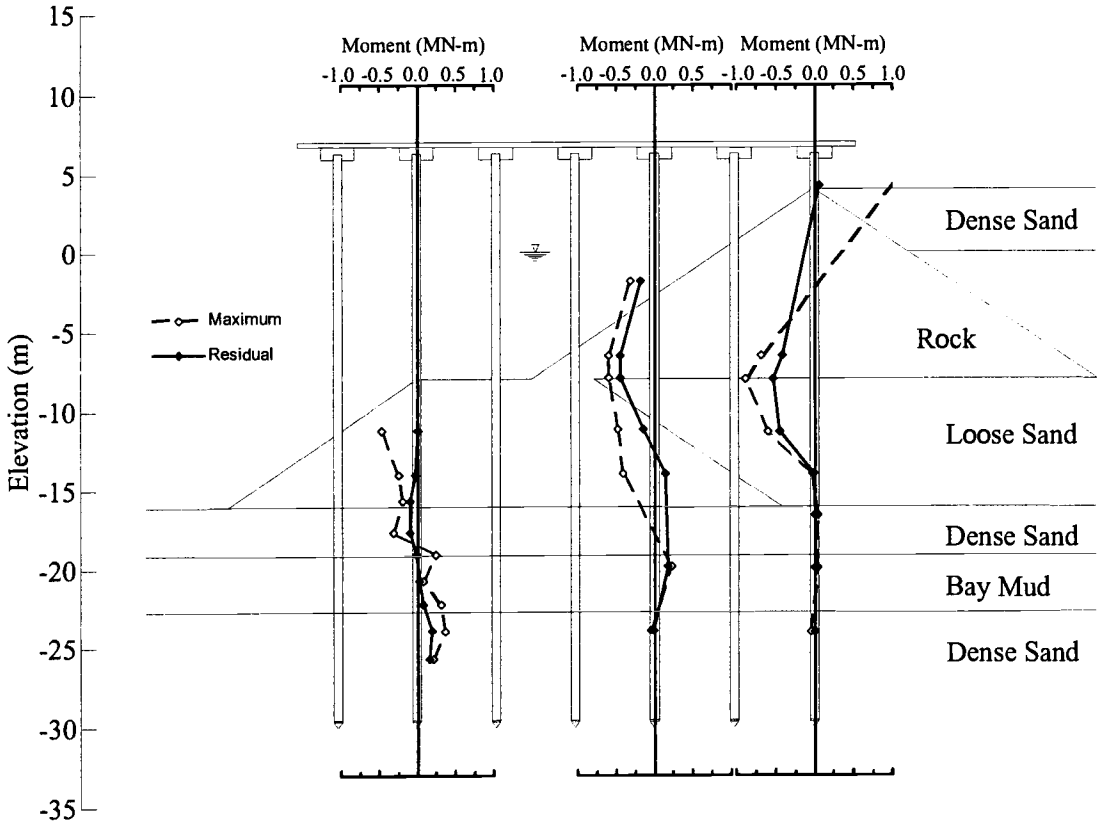

Figure 43. Maximum cyclic and residual moments for three piles for centrifuge model NJM02. The input PGA and the backland ground surface PGA values were 0.17 g and 0.23 g, respectively. The input motion was the 1989 Loma Prieta motion recorded at the Port of Oakland Outer Harbor. The permanent lateral wharf deformation was 231 mm.

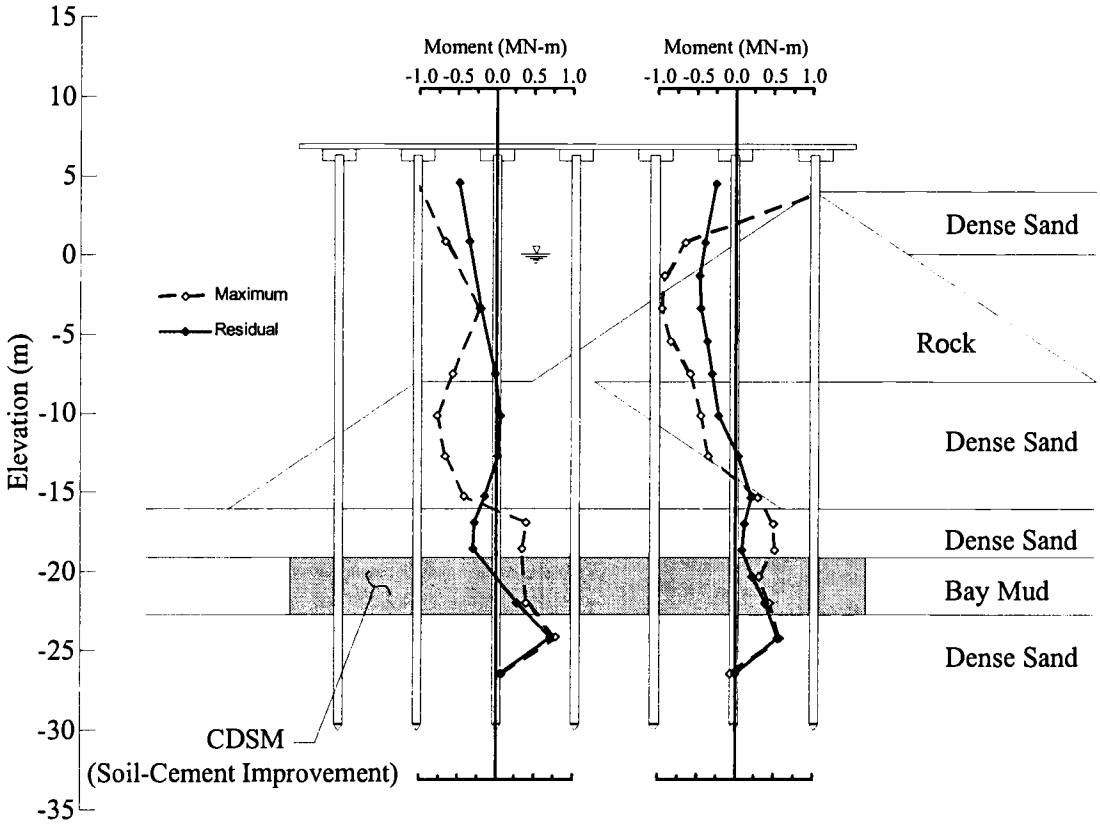

Figure 44. Maximum cyclic and residual moments for two piles for centrifuge model SMS01. The input PGA and the backland ground surface PGA values were 0.42 g and 0.35 g, respectively. The input motion was the 1989 Loma Prieta motion recorded at the Port of Oakland Outer Harbor. The permanent lateral wharf deformation was 916 mm.

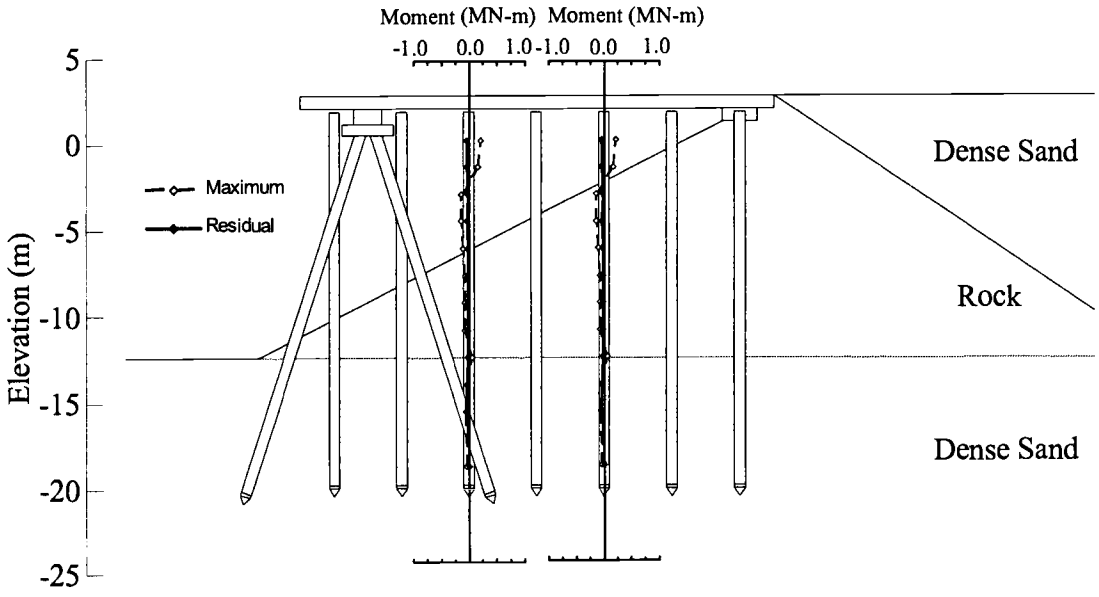

Figure 45. Maximum cyclic and residual moments for two piles for centrifuge model SMS02. The input PGA and the backland ground surface PGA values were 0.19 g and 0.25 g, respectively. The input motion was the 1989 Loma Prieta motion recorded at the Port of Oakland Outer Harbor. The permanent lateral wharf deformation was 136 mm.

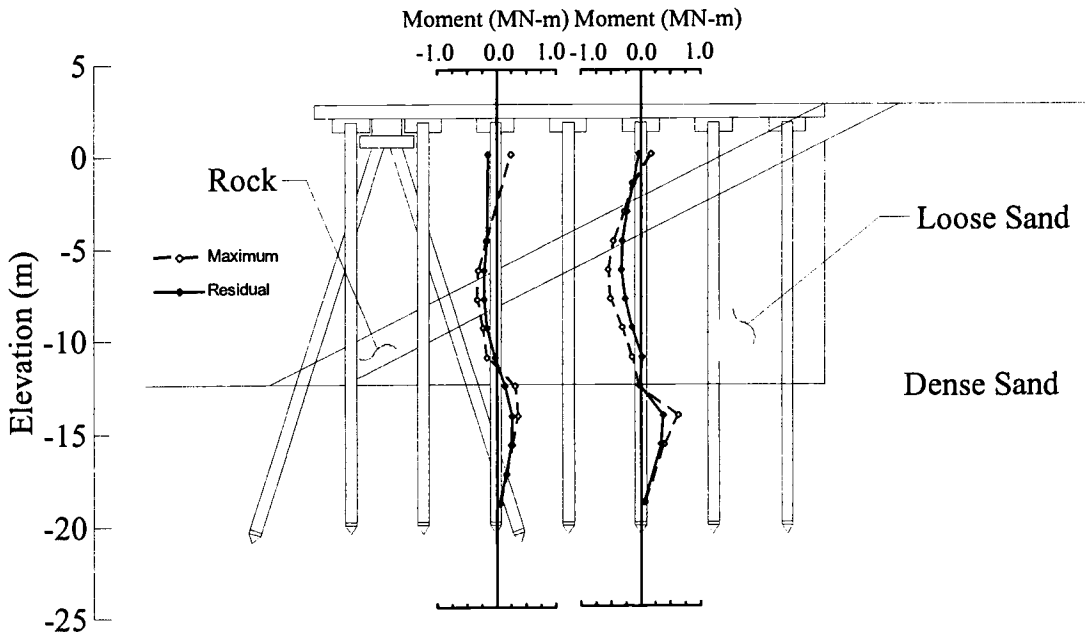

Figure 46. Maximum cyclic and residual moments for two piles for centrifuge model JCB01. The input PGA and the backland ground surface PGA values were 0.15 g and 0.16 g, respectively. The input motion was the 1989 Loma Prieta motion recorded at the Port of Oakland Outer Harbor. The permanent lateral wharf deformation was 169 mm.

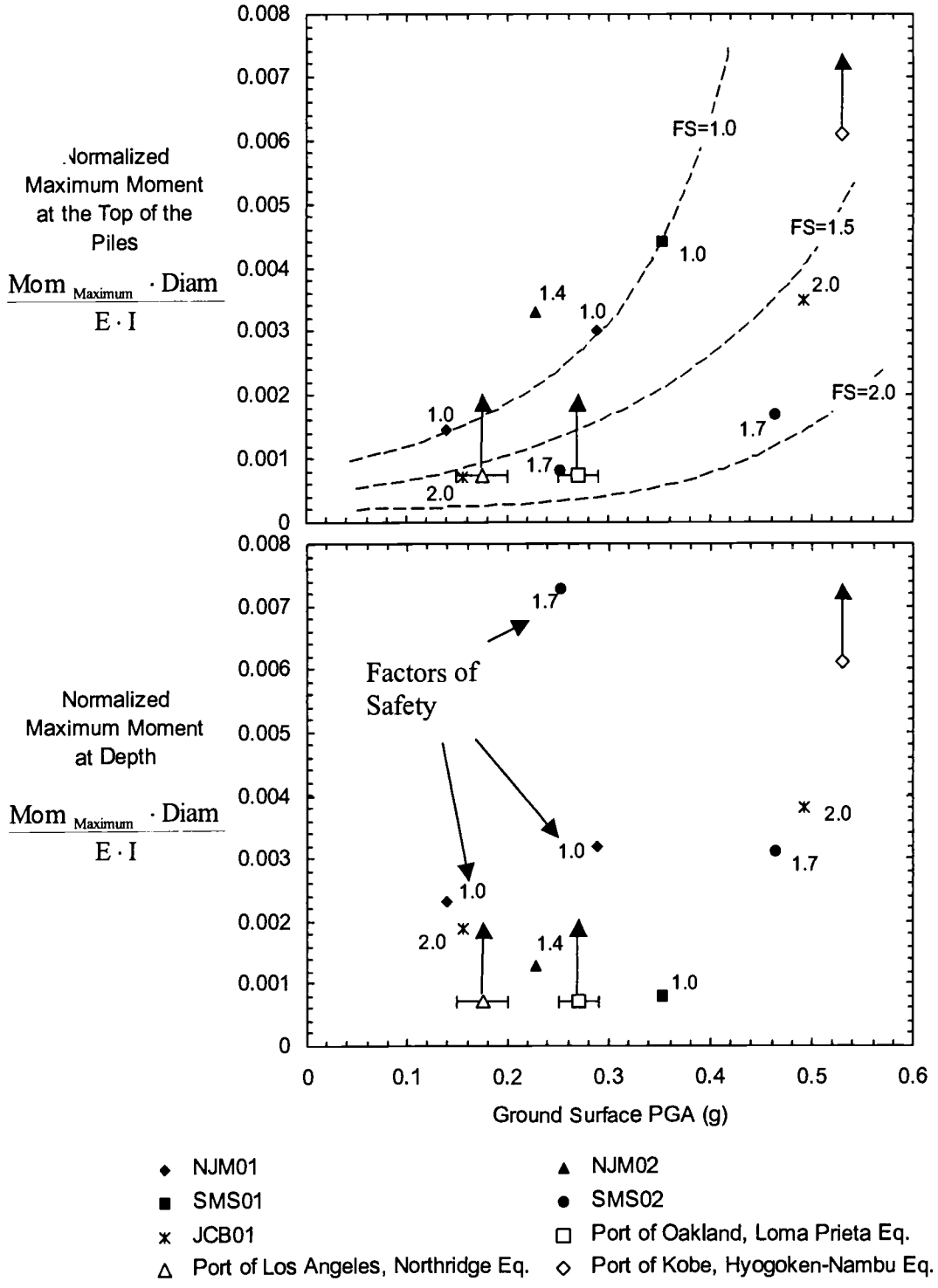

Figure 47. Relationship between the peak ground surface acceleration and the maximum dynamic pile bending moments adjacent to the pile/deck connection and at depth.

The moments at depth were plotted against the permanent lateral wharf deformations in Figure 48, indicating that the residual moments at depth were a function of global (in)stability (deep-seated failure planes). Only the largest moment in the piles was plotted for each model. The case history deformations represent the average and maximum observed deformations. Though there is scatter in the data, and there does not appear to be a relationship with the post-seismic factor of safety, there is a definite trend between the residual moments at depth and the permanent lateral wharf deformations.

The analysis of pile-supported wharves is often accomplished in one of two ways: 1) the structure is modeled using a structural engineering analysis method (i.e. SAP2000, ADINA, etc.), with the soil modeled as a set of springs below the ground surface, or 2) the soil is modeled using a geotechnical analysis method (i.e. Newmark sliding block, FLAC, DYSAC2, etc.), with the structure either not included, or modeled very simply as linear elements. For method 1, the simplified soil model does not allow for the prediction of global soil movements, therefore, large moments at depth are not predicted. For method 2, global soil movements can be predicted, but due to simplified structural element modeling, the structural performance is not accurately captured. It is possible to force the soil displacements estimated using method 2 onto the structure in method 1, but this uncoupled approach often does not include the structural elements during the method 2 analysis, therefore the forced displacements are often too large. Figure 49 illustrates the importance of both methods, by relating a moment ratio (the moments at the top of the pile divided by the

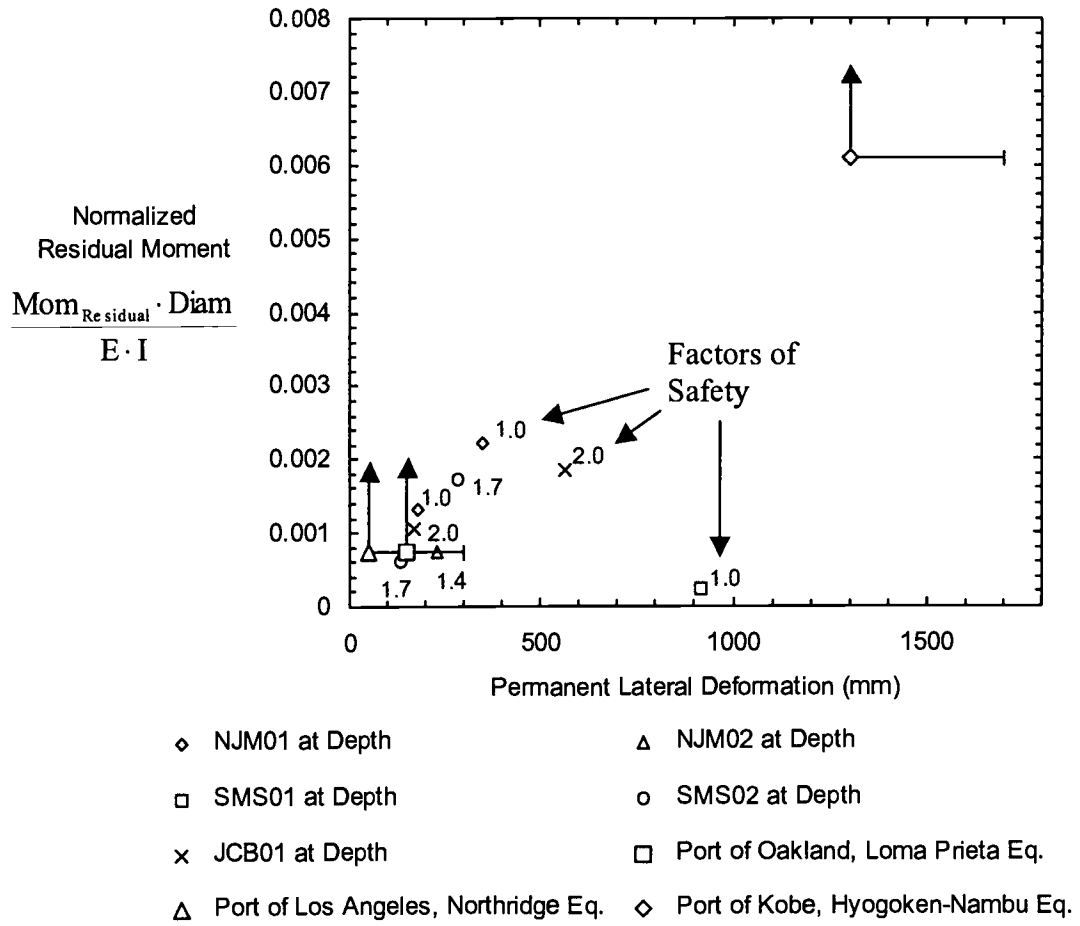

Figure 48. The normalized residual moment recorded at depth, plotted against the permanent lateral deformation of the wharf deck.

moments at depth) to the measured ground surface peak ground accelerations in the centrifuge models. This figure illustrates that the moments at depth and at the top of the piles (adjacent to the pile/deck connection) are often approximately equal to the moments at depth. This relationship is heavily dependent on the global soil behavior of the pile-supported wharf, as more stable rock dike geometry will lead to smaller moments at depth. However, as the level of ground shaking increases, larger permanent soil deformations should be expected, as should larger moments at depth.

SUMMARY

Pile-supported wharves are a very complex geotechnical and structural interaction problem. The damaging failures that have occurred were often structural; due to geotechnical instability. The documented field case histories, as well as a suite of model case histories, were presented, illustrating the seismic behavior of pile-supported wharves. Plots relating the seismic performance of pile-supported wharves to measurable and/or predictable quantities (i.e. permanent lateral deformations, peak

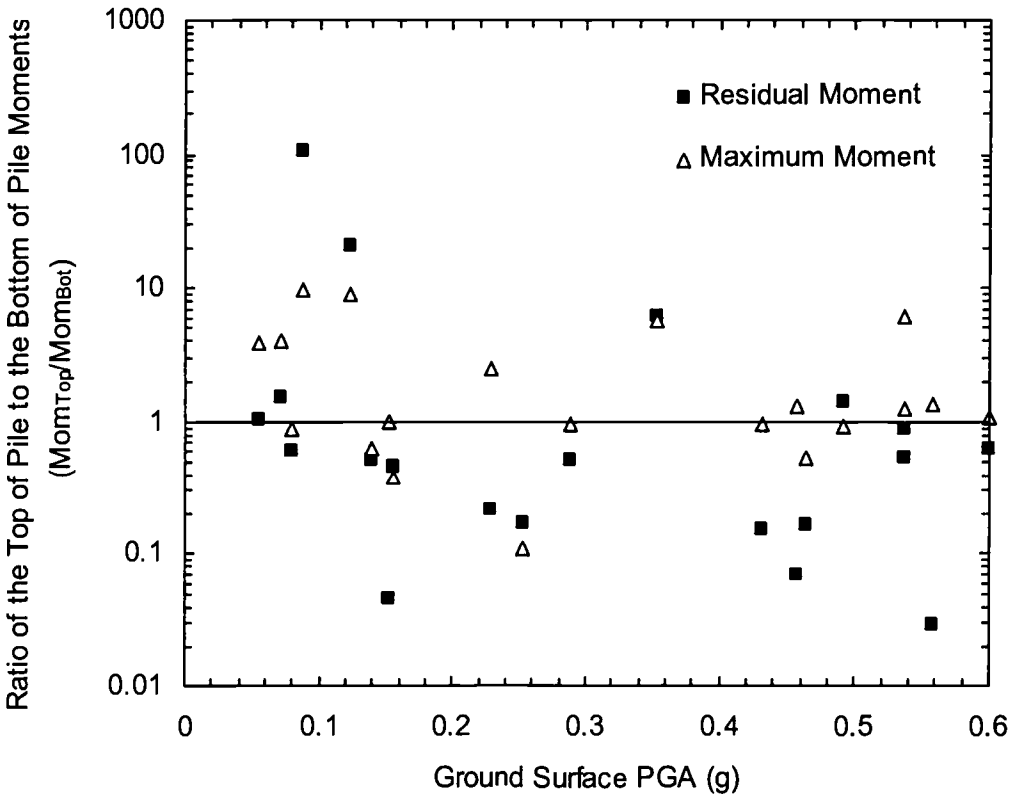

Figure 49. Ratio of the pile bending moments recorded adjacent to the pile/deck connection to the maximum pile moments recorded at depth, plotted against the peak ground surface acceleration in the backland.

ground surface accelerations) were presented to aid in advancing the seismic analysis and design of pile-supported wharves. Some key lessons to be gleaned from the case histories are:

1) Pile-supported wharf damage was generally a function of permanent ground deformation. Generally, larger ground deformations resulted in greater damage. However, the amount and severity of the damage was also a function of the system stiffness. Stiffer, batter pile-supported wharves generally performed poorer than all vertical pile supported wharves when subjected to the same amount of deformation. In addition, batter pile damage was generally much more severe than damage to vertical piles subjected to the same level of shaking, due to their greater stiffness.

2) Moderate to large ground deformations were generally due to the liquefaction of adjacent soils. Mitigation of the liquefaction hazards adjacent to pile-supported wharf structures appears to be a worthwhile endeavor to limit permanent ground deformations.

3) Given the dynamic loading and flexibility of pile-supported wharves, small to moderate permanent deformations should be anticipated in regions of high seismicity, even for geotechncially and structurally component geometries. Peak ground accelerations of 0.4 g and greater are typical design levels for ports in Japan and the western United

States, and based on the study presented herein, deformations on the order of 200 mm or greater should be anticipated during a design event of this magnitude.

4) The maximum cyclic bending moments at the pile/deck connections appeared to be related to the peak ground surface acceleration (Figure 47a). However, the bending moments at depth (Figure 47b) appeared to be a function of permanent ground deformation, and not the peak ground surface acceleration.

5) The moments at depth were often as large or larger than the moments at the pile/deck connection (Figure 49). This was more typical of geometries that were less geotechnically stable, as larger deformations due to the liquefaction of adjacent soils generally occurred. Geometries that were more geotechnically stable generally resulted in moments at the pile/deck connection that are larger than the moments at depth.

ACKNOWLEDGEMENTS

The authors would like to gratefully acknowledge the staff of the centrifuge facility at UC Davis, who helped many long days, nights, and weekends in constructing and testing these models, and the assistance from Manfred Deitrich and Andy Brickman at Oregon State University.

This research effort was supported by grant no. CMS-9702744 from the National Science Foundation, grant no. SA2394JB from the Pacific Earthquake

Engineering Research Center, and included additional industry support from the Port of Oakland, Port of Long Beach, URS Corp, and Hayward Baker, Inc. The support from these agencies and companies is greatly appreciated.

REFERENCES

Boland, C.B., Schlechter, S.M., McCullough, N.M., Dickenson, S.E., Kutter, B.L., and Wilson, D.W. 2001a. *Data Report: Pile-Supported Wharf Centrifuge Model (SMS02)*. Geotechnical Engineering Group, Department of Civil, Construction and Environmental Engineering. Oregon State University.

Boland, C.B., Schlechter, S.M., McCullough, N.M., Dickenson, S.E., Kutter, B.L., and Wilson, D.W. 2001b. *Data Report: Pile-Supported Wharf Centrifuge Model (JCB01)*. Geotechnical Engineering Group, Department of Civil, Construction and Environmental Engineering. Oregon State University.

Buslov, V.M., Rowghani, M., Weismair, M. 1996. "Evaluating Earthquake Damage to Concrete Wharves." *Concrete International*. August. pp 50-54

EERI (Earthquake Engineering Research Institute). 1991a. "Philippines Earthquake Reconnaissance Report." *Earthquake Spectra*. EERI. Supplement A to Vol. 7. October.

EERI (Earthquake Engineering Research Institute). 1991b. "Costa Rica Earthquake of April 22, 1991 Reconnaissance Report." *Earthquake Spectra*. EERI. Supplement B to Vol. 7. October.

EERI (Earthquake Engineering Research Institute). 2000. "Kocaeli, Turkey, Earthquake of August 17, 1999 Reconnaissance Report." *Earthquake Spectra*. EERI. Supplement A to Vol. 16. December.

EERI (Earthquake Engineering Research Institute). 2002. "Bhuj, India Earthquake of January 26, 2001 Reconnaissance Report." *Earthquake Spectra*. EERI. Supplement A to Vol. 18. July.

Egan, J.A., Hayden, R.F., Scheibel, L.L., Otus, M., and Serventi, G.M. 1992. "Seismic Repair at Seventh Street Marine Terminal." Proceedings of the conference *Grouting, Soil Improvement, and Geosynthetics*. ASCE Geotechnical Special Publication No. 30, Volume 2. New Orleans, Louisiana. February 25-28.

EQE. 1990. *The July 16, 1990 Philippines Earthquake.* EQE Engineering, San Francisco, CA. August.

Iai, S. 1998. "Seismic Analysis and Performance of Retaining Structures." Proceedings of the conference *Geotechnical Earthquake Engineering and Soil Dynamics III.* ASCE Geotechnical Special Publication No. 75. Edited by P. Dakoulas, M. Yegian, and R.D. Holtz. Volume 2. pp 1020-1044.

Iai, S. 2003. Personal communication.

McCullough, N.J., Schlechter, S.M., Dickenson, S.E., Kutter, B.L., and Wilson, D.W., 2000. *Data Report: Pile-Supported Wharf Centrifuge Model (NJM01).* Geotechnical Engineering Group, Department of Civil, Construction and Environmental Engineering. Oregon State University.

Muraleetharan, K.K., Thiessen, D.A., Jagannath, S.V., and Arulmoli, K. 1995. "Performance of Port Facilities During the Northridge Earthquake." Proceedings of the *Third International Conference on Recent Advances in Geotechnical Earthquake Engineering and Soil Dynamics.* Vol III. St. Louis, Missouri. April 2-7.

Oyenuga, D., Abe, S., Sedarat, H., Krimotat, A., Salah-Mars, S., Ogunfunmi, K. 2001. "Analysis of Existing Piles with Missing Data in Seismic Retrofit Design at the Port of Oakland." *Proceedings of the ASCE Ports 2001 Conference.* Norfolk, Virginia, April 29-May 2.

PIANC (International Navigation Association). 2001. *Seismic Design Guidelines for Port Structures.* International Navigation Association Working Group No. 34. A.A. Balkema.

Schlechter, S.M., McCullough, N.J., Dickenson, S.E., Kutter, B.L., and Wilson, D.W. 2000a. *Data Report: Pile-Supported Wharf Centrifuge Model (NJM02).* Geotechnical Engineering Group, Department of Civil, Construction and Environmental Engineering. Oregon State University.

Schlechter, S.M., McCullough, N.J., Dickenson, S.E., Kutter, B.L., and Wilson, D.W. (2000b). *Data Report: Pile-Supported Wharf Centrifuge Model (SMS01).* Geotechnical Engineering Group, Department of Civil, Construction and Environmental Engineering. Oregon State University.

Singh, J.P., Tabatabaie, M., and French, J.B. 2001. "Geotechnical and Ground Motion Issues in Seismic Vulnerability Assessment of Existing Wharf Structures." *Proceedings of the ASCE Ports 2001 Conference.* Norfolk, Virginia, April 29-May 2.

Werner, S.D. (Editor). 1998. *Seismic Guidelines for Ports*. ASCE Technical Council on Lifeline Earthquake Engineering. Monograph No. 12. March 1998. ASCE, Reston, VA.

CHAPTER 4 – MANUSCRIPT NO. 3:

THE SEISMIC ANALYSIS OF PILE-SUPPORTED STRUCTURES ON SLOPES

Nason J. McCullough
Stephen E. Dickenson

Submitted to the

ASCE Journal of Geotechnical and GeoEnvironmental Engineering

ASCE Publications
1801 Alexander Bell Dr.
Reston, VA 20191

ABSTRACT

This paper addresses the seismic analysis of pile-supported wharves, typical waterfront structures at western United States ports. However, many aspects of the study presented herein are not specific to pile-supported wharves, and can be readily applied to the seismic analysis of pile-supported structures on slopes (i.e. bridge abutments, pile-supported buildings near open faces, etc.). The seismic performance of pile-supported wharves has generally been good, however, there are noted failures during recent earthquakes. These failures often occurred during levels of shaking that were much less than the design level earthquake motions, and highlight the need to better understand the dynamic soil-structure interaction problem of piles in slopes.

Results are presented from a study to validate two deformation-based analysis methods, a two-dimensional, effective stress numerical model (FLAC), and a simple, straightforward procedure based on the rigid, sliding block concept (Newmark). The validations were completed using seismic case histories. The results indicate that the practice-oriented sliding block model is able to relatively accurately predict deformations, provided that the analysis method accounts for excess pore pressure generation and the stabilizing effect of the piles in the slope. The advanced numerical procedure utilized a relatively simple pore pressure generation constitutive model that predicted deformations and acceleration quite well, pore pressures were somewhat well predicted, though maximum dynamic and residual moments were not well predicted. The numerical procedure is advantageous compared to the sliding block method, as the pattern of deformations are predicted, a complete time history analysis

is performed, the full soil-structure interaction problem is modeled, and estimations of structural performance are provided.

INTRODUCTION

Pile-supported wharves (Figure 50) provide an important intermodal link between waterside and landside traffic. Pile-supported wharves, as discussed herein, refer to the system of piles supporting a wharf deck installed through a sloping rock dike and into native soils. This pile-wharf-dike system has also been referred to as a marginal wharf. In some instances the construction of the pile-supported wharf utilized a cut-slope, in which existing soil was excavated, however, the majority of pile-supported wharf construction has involved reclaimed land, in which a perimeter rock dike was utilized to retain backfill soil.

It has been extensively documented in seismic field case histories that pile-supported wharf damage has been noted primarily in cases where moderate to significant permanent ground deformations were observed (Werner 1998, PIANC 2001). In addition, much of the damage has occurred during levels of shaking that were much less than current design level motions. This highlights the necessity for seismic analysis methods capable of reliably predicting permanent ground deformations. Two common analysis methods are often utilized for the prediction of permanent ground deformations:

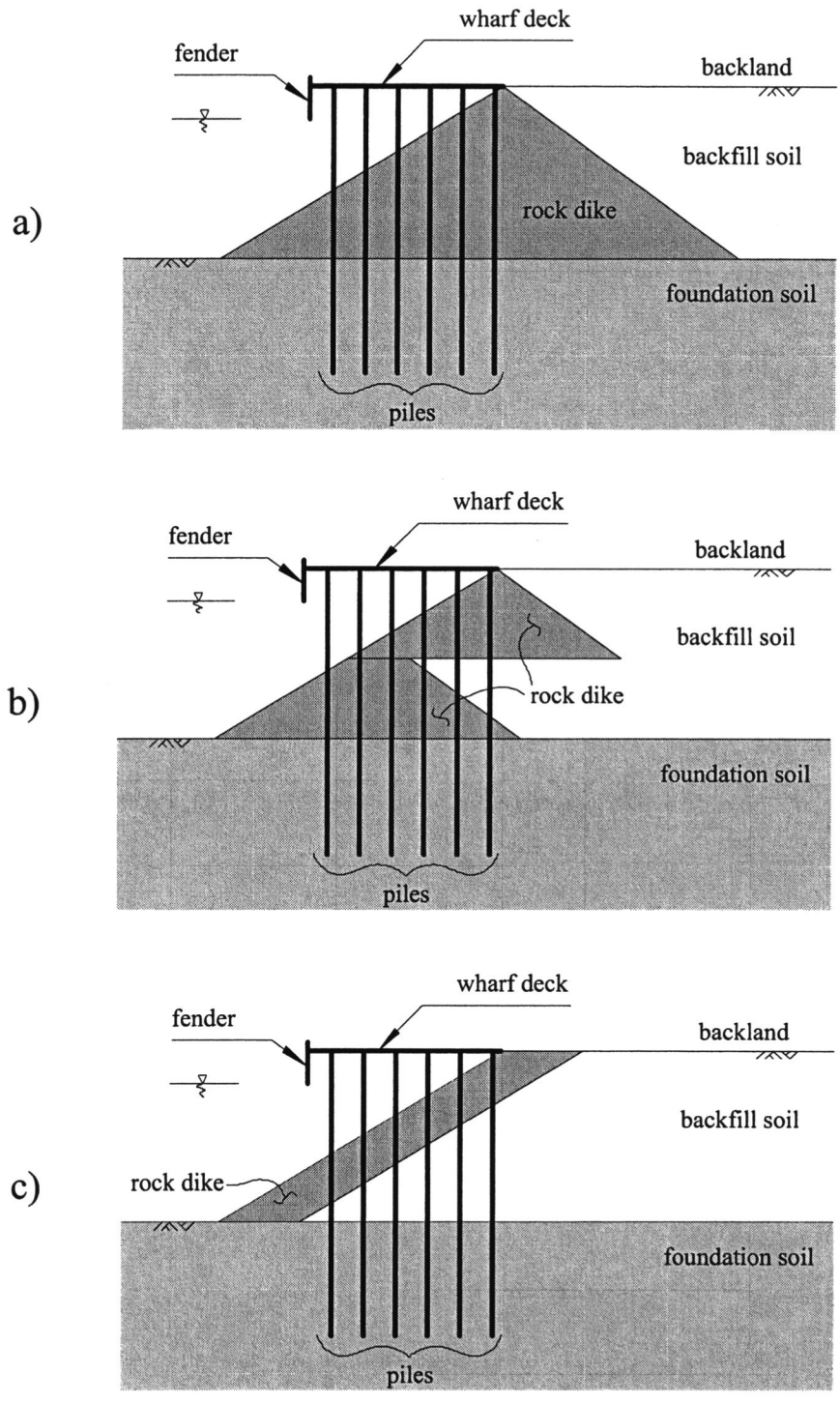

Figure 50. Typical Pile-Supported Wharf Geometries; a) single lift, b) multi-lift, and c) sliver (cut-slope) rock dike configurations.

1) The rigid, sliding block (Newmark) procedure. Slope stability and a yield acceleration are estimated using limit-equilibrium methods. The portions of the design acceleration time histories exceeding the yield acceleration are double-integrated to obtain an estimate of permanent slope deformations. The sliding block method can be modified to include the effect of soil degradation (i.e. excess pore pressure generation and strain softening) and the beneficial effect of piles in the slope.

2) Numerical models. These models are capable of representing the full soil continuum and modeling in the time domain. In addition, they are often capable of modeling structural elements and soil-structure interaction, and liquefaction and the generation of excess pore pressures.

However, given the limited number of case histories documenting the dynamic response of pile-supported wharves, and the limited information available from the documented case histories, these methods of analysis have not been rigorously validated.

This paper presents the results of an applied research effort conducted to compare performance predictions using the above analysis methods and the observed performance of field case histories and physical models. The physical models consisted of a suite of well-instrumented pile-supported wharf centrifuge models tested to supplement the limited field case history database (McCullough and

Dickenson 2003a, 2003b). In addition, key issues regarding the seismic performance-based analysis of pile-supported wharves are presented.

METHODS OF ANALYSIS

Two geotechnical methods for estimating the seismic performance of slopes are presented herein; 1) the rigid, sliding block method, and 2) a numerical analysis method. The procedures followed for each method are described below.

Rigid, sliding block method

The rigid, sliding block analyses followed the work of Newmark (1965), and were based on simple limit equilibrium stability analysis. The first step required an estimation of the critical, or yield, acceleration of the specific slope. The yield acceleration was the acceleration required to bring the slope stability factor of safety to unity. The second step involved the integration of an acceleration time history. When the ground motion acceleration exceeds the critical acceleration (a_{crit}, a_y, k_y) the *block* is assumed to move downslope. The *block* represents the failure mass as a rigid body. By double integrating the area of the acceleration time history exceeding the critical acceleration, the relative displacement of the block can be estimated. A more in-depth description of the sliding block method can be found in Kramer (1996), Wilson and Keefer (1985), Jibson (1993), or Hynes-Griffin and Franklin (1984).

The primary limitations of the sliding block method are: 1) the soil, particularly in the liquefiable zones, is not a rigid material, as assumed by the method;

2) the method is dependent on the acceleration time histories used as input, often with orders of magnitude variations due only to the characteristics of the acceleration time histories (even when scaled to equivalent peak accelerations); 3) the pattern of slope deformations is not predicted; 4) a single mode of failure has to be assumed to calculate the critical acceleration; and 5) the forces/displacements applied from the soil to the pile elements are not readily computed.

However, the sliding block method does have its advantages, such as: 1) characteristics of the earthquake motions are captured (e.g. duration, frequency content, etc.) as representative design acceleration time histories are used; 2) the interaction of the piles and the soil can somewhat be accounted for, if only in a simplified manner, either as a resisting shear force or a pseudo-cohesion in the soils; 3) soil degradation can be accounted for as an equivalent shear strength for liquefied soils and post-cyclic reduction in strength for soft clays; and 4) deformations are predicted, which are often directly related to a target performance criteria.

Soil strength degradation affects both cohesive and cohesionless soils. For cohesive soils, degradation during cyclic loading typically results in a 10 to 30 percent decrease in undrained shear strength (Makdisi and Seed 1978, Rau and Sitar 1998). However, Kulhawy and Mayne (1990) noted that there is also approximately a 10 percent increase in undrained strength for each order of magnitude increase in loading strain rate. Earthquake loading typically induces a strain rate that is several orders of magnitude greater than typical laboratory tests. It is important to note that the strength degradation occurs mainly after several to many cycles of shaking, and may therefore

affect the post-cyclic strength behavior, whereas the loading rate strength increase occurs only during the cyclic loading. For estimating permanent slope deformations during an earthquake, it is recommended that the analysis include an inertial earthquake loading (i.e. seismic coefficient), an increase in shear strength of cohesive soils due to strain rate effects, and if the earthquake is of sufficient duration and contains a number of stress/strain cycles, a reduction in strength and stiffness due to cyclic strain degradation.

Loose, saturated, sandy soils also exhibit strength degradation during cyclic loading due to the collapse of the soil skeleton, and the generation of excess pore pressures. For soils exhibiting full liquefaction (excess pore pressure ratios of 1.0), the liquefied soil strength is expressed as a function of the pre-earthquake corrected SPT blowcount (Seed and Harder 1990), and as a function of the initial effective overburden stress (Baziar et al. 1992, Ishihara 1993, Stark and Mesri 1992, Olson and Stark 2002). If full liquefaction is not reached, an estimate of an equivalent friction angle (ϕ'_{eq}) can be determined using the following relationship (Ebeling and Morrison 1992):

$$\phi'_{eq} = tan^{-1}\left[(1 - r_u)tan(\phi')\right] \tag{23}$$

where ϕ' is the effective angle of internal friction for the soil and r_u is the excess pore pressure ratio.

In the analyses presented herein the limit-equilibrium slope stability program UTEXAS3 (Wright 1992) was utilized for estimating the yield coefficient. The cyclic

shear strength of the cohesive soils was assumed to be the same as the undrained static shear strength (the reduction in strength due to degradation was assumed to negate the increase in strength to the loading rate). The piles were included in the analyses as reinforcement elements. The strength of the piles was estimated using the method proposed by Broms (1964). The ultimate resistance of the soil as determined from Broms (1964) was applied as a reinforcement element shear resistance. The maximum shear resistance was determined to be the minimum value as determined assuming short pile or long pile behavior, as the short pile behavior is based on the soil capacity and the long pile method is based on the pile capacity, the minimum of which was assumed to be the actual capacity. The procedure was as follows:

1) The critical failure surface was estimated using an acceleration coefficient for which the factor of safety against slope stability was unity, without the pile elements.
2) The critical failure surface was then used to estimate the ultimate resistance from the piles using the assumptions noted above.
3) The ultimate resistance was then included in the same analysis as step 1, however the pile elements were now included, and a new critical failure surface was determined using an acceleration for which the factor of safety against slope stability was unity.
4) Steps 2 and 3 were then repeated until there was negligible difference in failure surface locations.

The resulting acceleration value determined in step 3 was then used as the yield acceleration, and the portion of the acceleration time histories exceeding the yield acceleration were double integrated to provide an estimate of the permanent slope deformation.

Finite-difference numerical analyses

The numerical modeling utilized the computer program FLAC (Itasca 2000). FLAC (Fast Lagrangian Analysis of Continua) is a two-dimensional finite-difference computer program developed for the modeling of geo-mechanical problems, and is especially well suited for the analysis of unstable problems (such as the liquefaction induced slope deformation of embankments). The validation and use of FLAC for the seismic modeling of port structures has been documented by Roth et al. (1992), McCullough et al. (2001), McCullough (2003), and McCullough and Dickenson (1998). The constitutive model utilized in the numerical analysis was based on a Mohr-Coulomb constitutive model in which the soil strength was defined by the typical Mohr-Coulomb failure parameters (cohesion and angle of internal friction), the volumetric strain behavior was defined by a dilation angle, and the elastic behavior was defined by the shear and bulk modulus of the soil. In addition, the constitutive model included a plastic flow rule to model plastic soil behavior. A complete description of the constitutive model can be found in Itasca (2000).

The low-strain shear modulus (G_o) and bulk modulus (K) modulus values for cohesionless soils were defined by Equations 24 and 25, respectively. K_2 and m were

constants determined either from published correlations or developed from curve fitting, ν was Poisson's ratio, P_a was atmospheric pressure, and σ'_c is the effective confining stress. However, if shear wave velocities (V_s) were measured, then the low-strain shear modulus values were estimated using Equation 26 using the total soil density (ρ_{total}).

$$G_0 = P_a \cdot K_2 \left(\frac{\sigma'_c}{P_a} \right)^m \tag{24}$$

$$K = \frac{2G_o(1+\nu)}{3(1-2\nu)} \tag{25}$$

$$G_o = V_s^{\,2} \cdot \rho_{total} \tag{26}$$

For cohesive soils, the undrained elastic modulus (E_u) was estimated from the plasticity index, overconsolidation ratio, and the undrained shear strength (Duncan and Buchignani 1976, USACE 1983). The low-strain shear modulus was then estimated using Equation 27, and an assumed undrained Poisson's ratio (ν_u).

$$G_0 = \frac{E_u}{2(1+\nu_u)} \tag{27}$$

The basic Mohr-Coulomb model was also modified to account for the cyclic generation of excess pore pressures using the cyclic stress approach (Martin et al.

1975, Seed et al. 1976, and Seed 1979), in which a damage parameter was related to the excess pore pressure following the work of Annaki and Lee (1977). The implementation of this procedure in a constitutive model was originally adapted for FLAC by Roth et al. (1991) for the seismic analysis of Pleasant Valley Dam. The procedure was as follows:

1) Estimate the soil cyclic resistance using laboratory test data or empirically estimate using the liquefaction evaluation curve recommended by Youd et al. (1997). The pore pressure generation scheme then used a simplified cyclic resistance curve (Figure 51) to define the liquefaction resistance of the soil.
2) The large overburden stress and initial static shear stress corrections (Harder and Boulanger 1997) were applied, if applicable.
3) For each stress cycle noted during the analysis, an incremental number of cycles to liquefaction was calculated using Figure 51.
4) The excess pore pressure ratio (r_u) was then related to a damage parameter (D), as the inverse of the summation of the incremental number of cycles to liquefaction (N):

$$r_u = D = \sum \frac{1}{N} \tag{28}$$

5) As the excess pore pressure increased, the effective stress in the soil decreased, leading to a decrease in cohesionless soil strength.

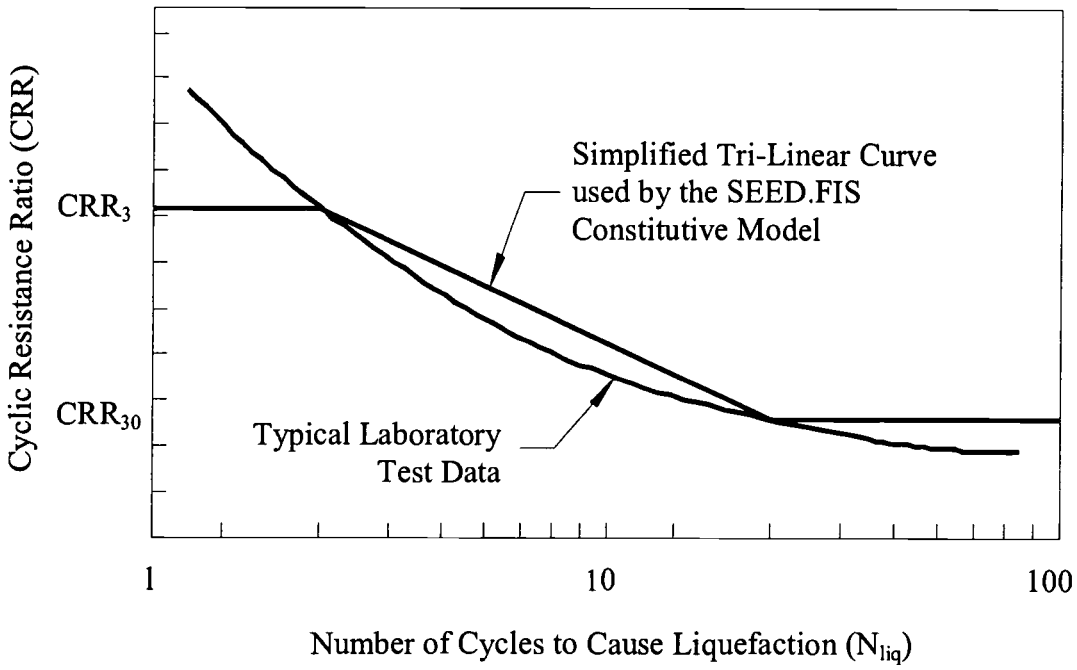

Figure 51. Simplified cyclic strength curve.

Dawson et al. (2001) provide an in-depth overview of a constitutive model that is essentially identical to the one described above. The numerical model included the effect of pore pressure generation, but pore pressure dissipation was not modeled. Liquefied soil strengths were modeled, using the recommendations of Stark and Mesri (1992). Ground surface settlements due to the consolidation of liquefied soils were modeled using a post-processing routine implementing the recommendations of Ishihara and Yoshimine (1992).

The interaction of the piles and soil was modeled with SSI springs. The SSI springs had a strength (represented by a *cohesion* and a *friction angle*) and a stiffness. The properties of the SSI springs in the normal direction were determined using a

model of the piles in plan view, at several different depths (stress states). The cross-section of the piles was pushed into the soil and the soil-structure response was used to estimate the spring stiffness and strength, following a procedure outlined by Itasca (2000). The SSI springs in the shear direction were estimated assuming that the shear stiffness was approximated by the shear modulus of the soil and the shear strength was estimated using estimates of skin friction commonly conducted for vertical pile capacity analysis.

Water located above the ground surface was modeled as an equivalent pressure acting on the soil surface, while fluid within the soil was modeled as hydrostatic (seepage forces were not modeled). Groundwater flow was not modeled.

The seismic boundary conditions for the field case history consisted of a free-field boundary condition, as implemented in the numerical model. The seismic damping in the models utilized the Raleigh damping option. For all of the models the percentage damping was chosen as 5 percent, based on typical soil behavior. The damped center frequency was determined by observing the undamped model behavior.

RESULTS OF THE SLIDING BLOCK VALIDATION STUDY

The rigid, sliding block procedure outlined above was used to predict the seismic performance of the pile-supported wharf centrifuge models. Each centrifuge model was tested with a suite of earthquake motions, but only the first large earthquake motion (greater than 0.1 g) was used for the validation study, as each subsequent test introduced additional uncertainty in geometry and soil properties. The

centrifuge models are shown in Figure 52 through Figure 56. The results of the validation study are summarized in Table 9 and presented in Figure 57.

In Figure 57, the plotted centrifuge displacements were the permanent horizontal displacements at the ground surface immediately adjacent to the wharf deck. The arrows represent predictions of deformations that are of infinite magnitude. The open symbols represent analyses that did not include the effect of the piles, while the solid symbols represent analysis that included the effect of the piles. The analyses utilized the mean plus one standard deviation excess pore pressure ratio for each soil layer that was recorded in the centrifuge models. The vertical error bars represent the range of predictions using the various recorded acceleration time histories. The horizontal error bars represent the range of the measured deformations between the wharf deck and the backland soil immediately adjacent to the wharf deck.

For several centrifuge models (JCB01 without piles, SMS01 with and without piles), the post-earthquake factor of safety was less than 1.0, resulting in infinite displacements by sliding block procedures. These values are illustrated with arrows on the top of the figure. The analysis utilized all of the earthquake acceleration time histories that were recorded within the approximate failure mass. This included between 7 and 14 time histories for each test. The range of predicted values, due to the use of the different acceleration time histories, is illustrated by the vertical error bars on the figure.

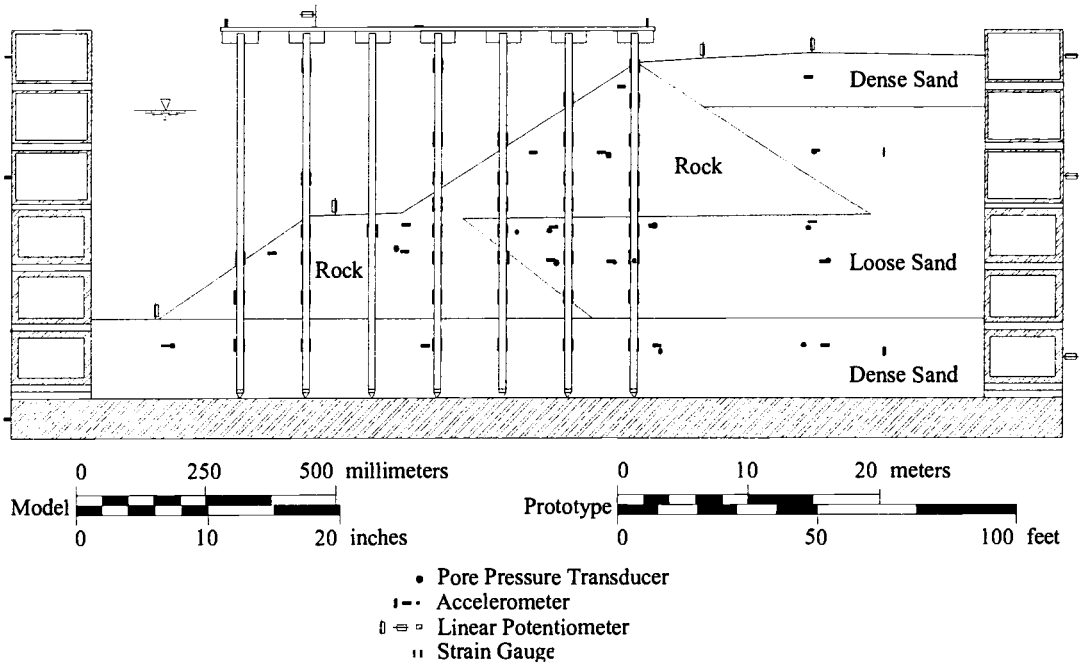

Figure 52. Centrifuge model NJM01.

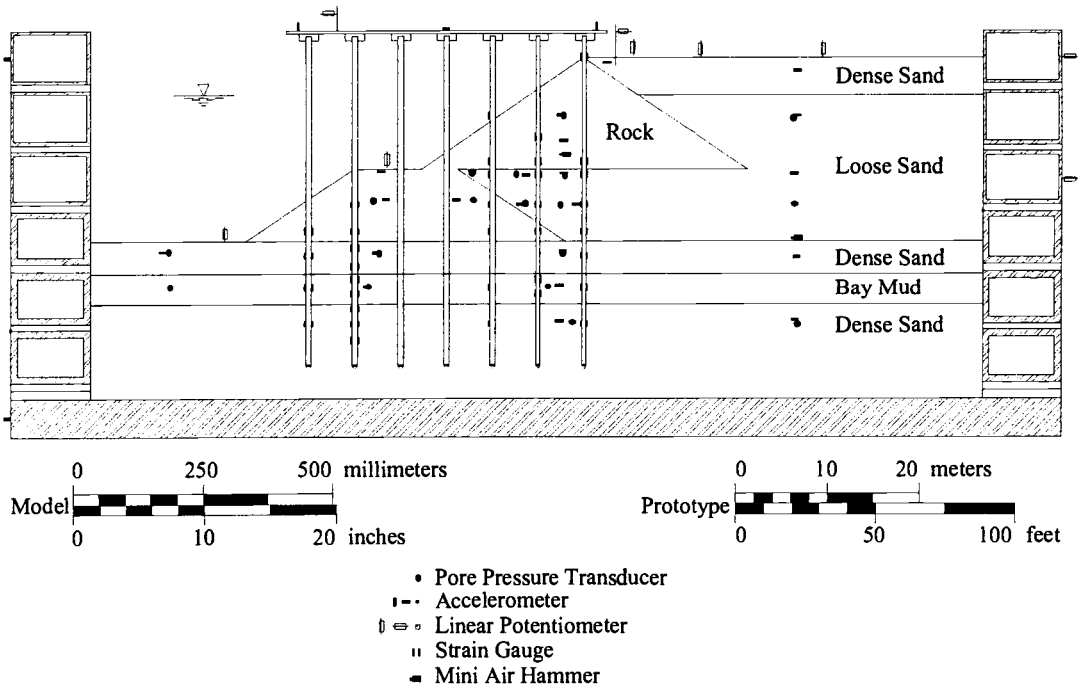

Figure 53. Centrifuge model NJM02.

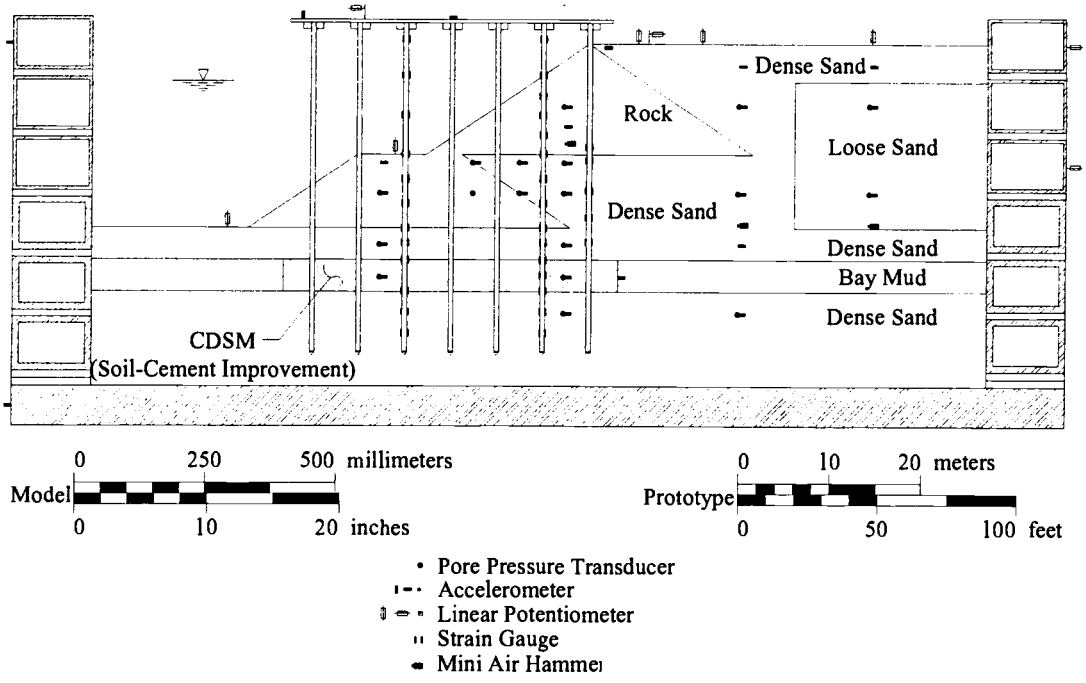

Figure 54. Centrifuge model SMS01.

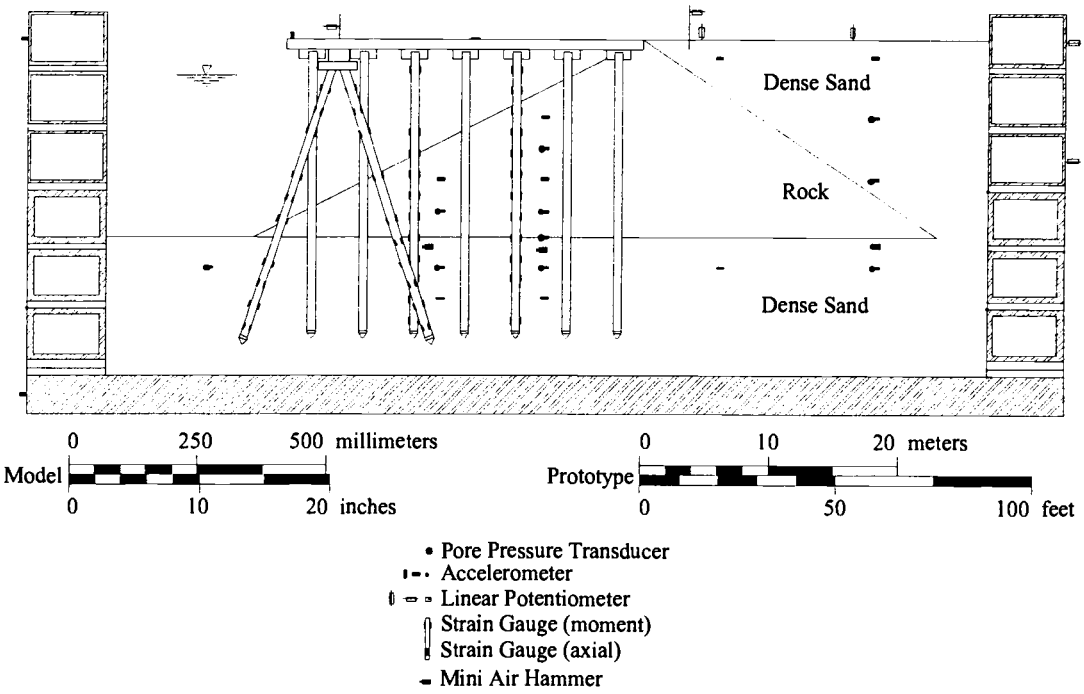

Figure 55. Centrifuge model SMS02.

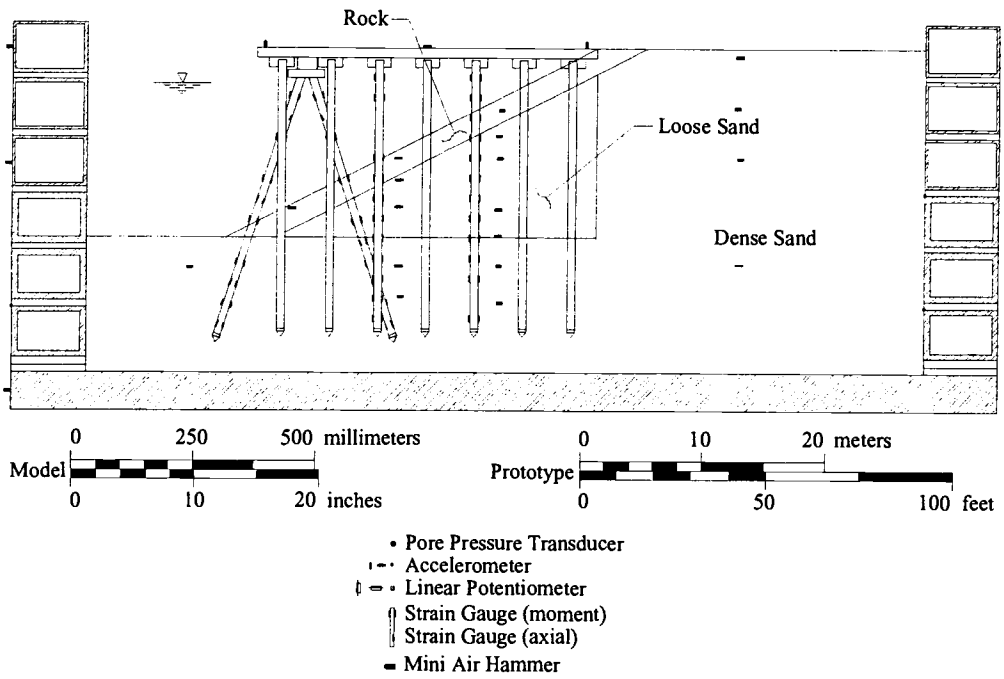

Figure 56. Centrifuge model JCB01.

The validation study shows that a reasonable prediction of deformations was made using the rigid, sliding block method, if modifications were made to account for the degradation of soil strength and the stabilizing effect of the piles. In general, the deformations were over-predicted when the effect of the piles is neglected, and the deformations were under-predicted when the effect of the piles is incorporated in the analyses. In addition, the best predictions were obtained when the mean plus one standard deviation pore pressure measured in the soil layers was utilized.

Table 9. Parameters used in the rigid, sliding block analyses, and results of the validation study.

Centrifuge Model [1]	Excess Pore Pressure Ratio, r_u (%) [2]		Failure Plane	Included Pile Elements? [3]	Factor of Safety [4]	Yield Acceleration (g) [5]	Average Calculated Deformation (mm) [5], [6]
	Loose Sand	Dense Sand					
NJM01 (182 mm)	80	24	Circular	No	1.21	0.05	201
				Yes	1.30	0.06	95
			Non-Circular	No	0.81	n/a	n/a
				Yes	0.85	n/a	n/a
NJM02 (228 mm)	52	21	Circular	No	1.31	0.06	236
				Yes	1.50	0.08	126
			Non-Circular	No	1.26	0.05	426
				Yes	1.44	0.07	199
SMS01 (848 mm)	100	70	Circular	No	0.85	n/a	n/a
				Yes	1.00	n/a	n/a
			Non-Circular	No	0.79	n/a	n/a
				Yes	0.95	n/a	n/a
SMS02 (113 mm)	no loose sand	58	Circular	No	1.38	0.07	137
				Yes	1.71	0.10	30
			Non-Circular	No	1.19	0.05	248
				Yes	1.68	0.10	39
JCB01 (110 mm)	94	37	Circular	No	< 0.5	n/a	n/a
				Yes	2.17	0.12	7
			Non-Circular	No	< 0.5	n/a	n/a
				Yes	2.30	0.09	33

Notes:

1) The values in parenthesis represent the measured horizontal deformation of the wharf deck in the centrifuge models.
2) The excess pore pressure was the mean plus one standard deviation, as measured for each soil layer in the centrifuge model.
3) The pile elements were modeled as reinforcement elements in UTEXAS3.
4) The factor of safety was for a seismic coefficient of 0.0.
5) n/a represents the case were the factor of safety was less than 1.0, therefore the yield acceleration and displacements were not estimated.
6) The average deformation was the average calculated value using the all of the acceleration time histories that were located within the failure mass.

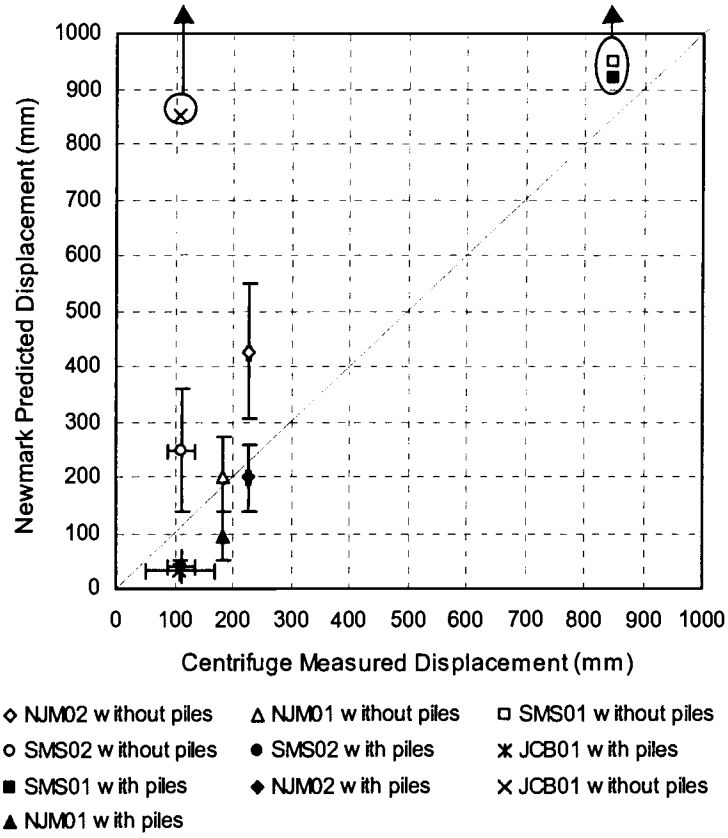

Figure 57. Results of the rigid, sliding block validation study.

The difficulty in using the rigid, sliding block method in practice lies in accurately estimating the pore pressure generation and obtaining representative acceleration time histories. These are usually not known, as they were in these validation studies. However, even when these values are known (as they were this validation study), there was still a significant range in the calculated displacements. Therefore, great care should be taken when interpreting the results of rigid, sliding block analyses when used to estimate permanent lateral deformations.

RESULTS OF THE NUMERICAL MODEL VALIDATION STUDY

Lateral Pile Behavior in Sloping Rock Fill

An initial validation was conducted to estimate the lateral response of piles in sloping rock fill. The measured performance of two centrifuge models (Figure 58) was used to validate the static lateral pile response modeling capabilities of the numerical model. The results of the study indicated that the rock fill acts as individual particles, while the numerical model represents the rock as a continuum. The continuum assumption for soils is generally valid when the particle dimensions are on the order of 30 to 40 times less than the dimension of interest (for this case the pile diameter). For the rock fill, individual rock particles were approximately 3 times smaller than the pile diameter, clearly indicating that the rock fill was not a continuum in relation to the piles. In order to account for the particle interaction effects, the best comparison between the numerical model analyses and the measured lateral pile response was obtained when a *pseudo-cohesion* was used for the rock fill. The pseudo-cohesion accounted for the individual rock particle/pile interaction in a simplified manner that was not accurately captured using the continuum model directly. The best fit for these models was found using a pseudo-cohesion of 15 kPa. In addition, it was found that the downslope normal spring stiffness was approximately a factor 10 less than the upslope stiffness. The predicted and measured responses for one load cycle are shown in Figure 59, comparing the results using the noted modifications.

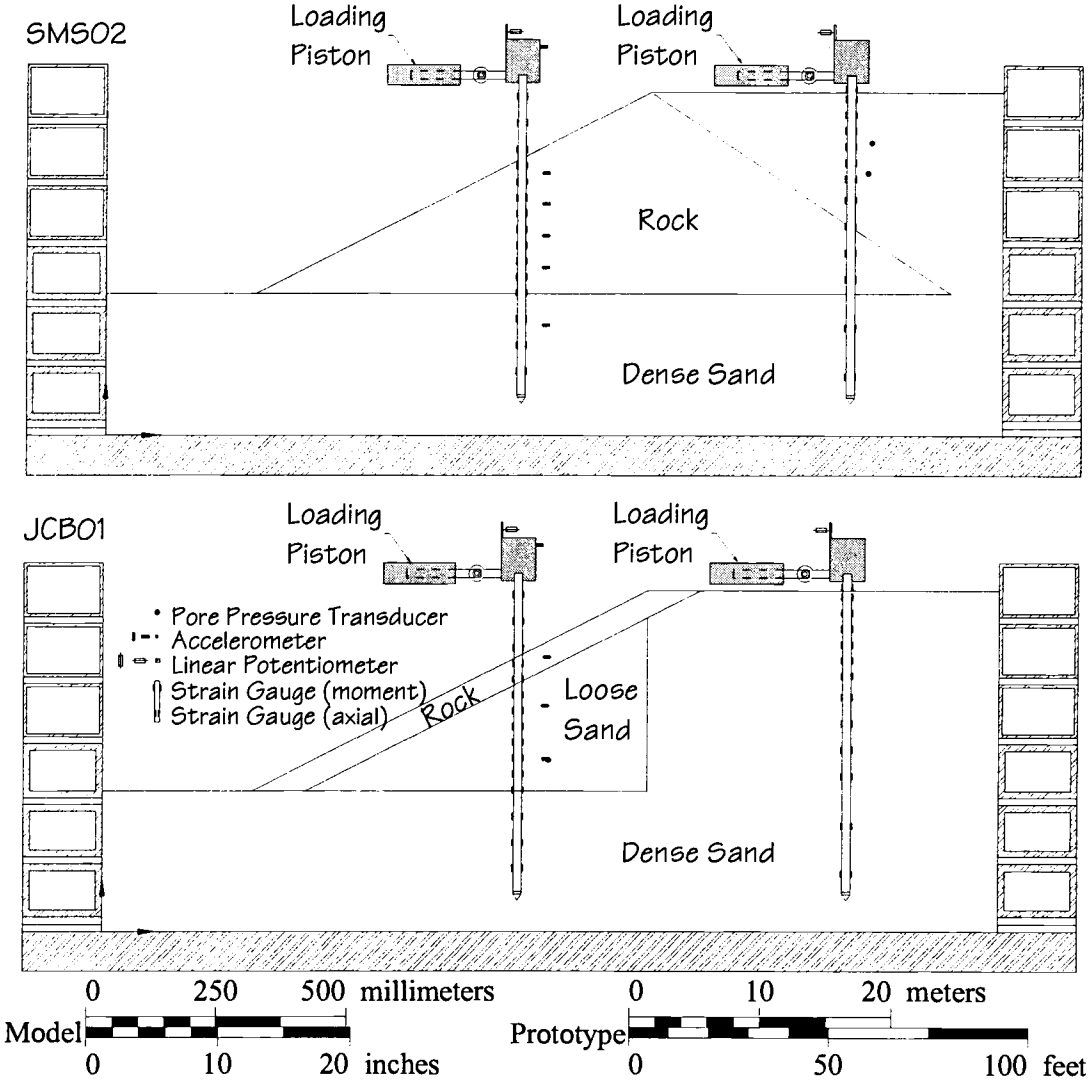

Figure 58. Centrifuge Model Geometries for Lateral Pile Load Tests.

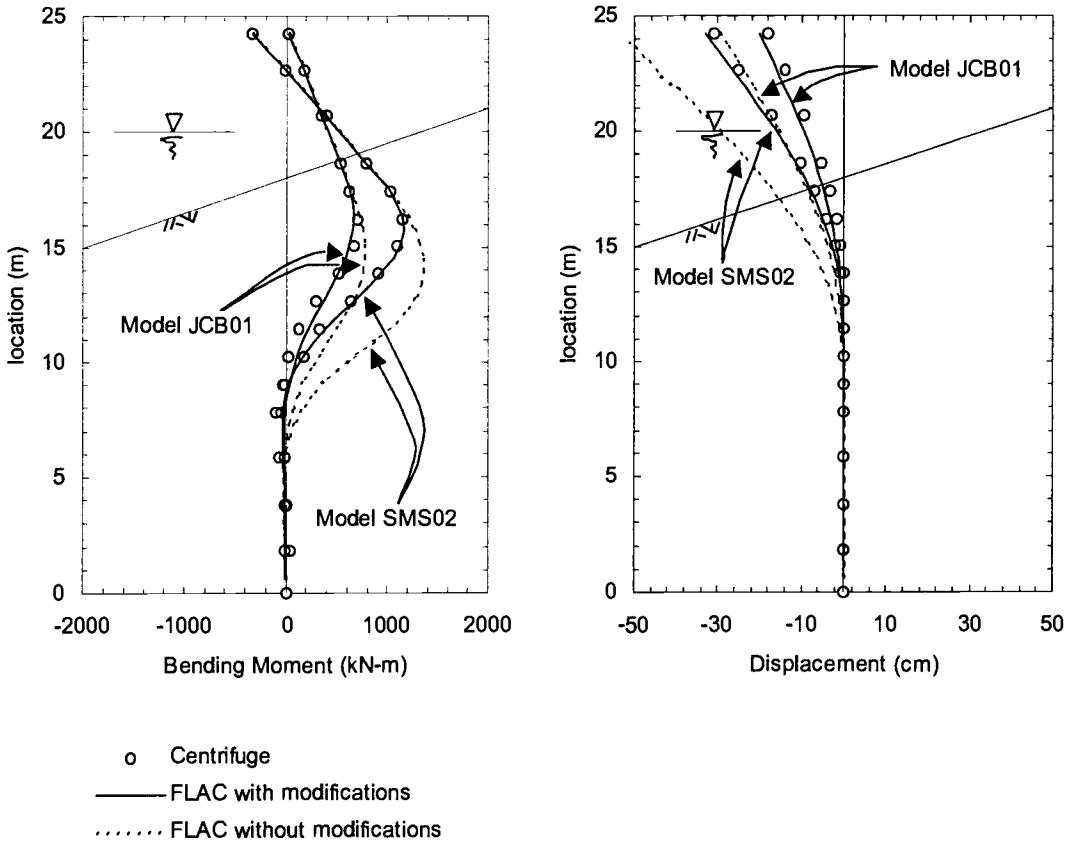

Figure 59. Comparison between the predicted moments and displacements for the pile in the sloping rock fill.

Port of Oakland

The seismic performance of the Seventh Street Terminal (Berths 35 through 38) pile-supported wharf at the Port of Oakland during the 1989 Loma Prieta Earthquake was estimated using the numerical model. Field observations indicated permanent ground surface lateral displacement of the rock dike on the order of 15 to 30 cm, with approximately 13 to 30 cm of settlement (Egan et al. 1992, Singh et al.

2001). In addition, the majority of the batter piles and approximately 20 percent of the vertical piles failed at the pile/deck connection (Singh et al. 2001). It was also noted by Singh et al. (2001) and Oeynuga (2001) that many of the vertical piles probably failed at the approximate interface between the Bay Mud/hydraulic fill and the dense sand, based on the results of pile integrity testing. These failures were likely due to pinning of the piles in the dense sands while lateral forces due to permanent ground deformations pushed on the upper portions of the piles in the rock fill.

Berth 38 was modeled with the design geometry shown in Figure 60 and numerical model grid, soil layers, and structural elements shown in Figure 61. The soil and structural properties used in the model are shown in Table 10 and Table 11, respectively. The structural strengths and stiffness values presented in the table are the full values; while the values used in the numerical analyses were divided by the pile spacing (2.1 m for the outboard crane rail pile and 3.7 m for the remaining vertical and batter piles) to account for the longitudinal pile spacing. In addition, the shear springs at the tip of each pile was increased to account for end bearing of the piles.

The nearest recorded acceleration time history was recorded at the ground surface approximately 1.5 kilometers from Berth 38 at the Port of Oakland Outer Harbor Wharf. The two horizontal components of the recorded motions were vectorally combined to produce a motion perpendicular to Berth 38. The combined motion was deconvolved to the base of the numerical model (El. –21 m) using SHAKE91 (Idriss and Sun 1992). The input motion is shown in Figure 62.

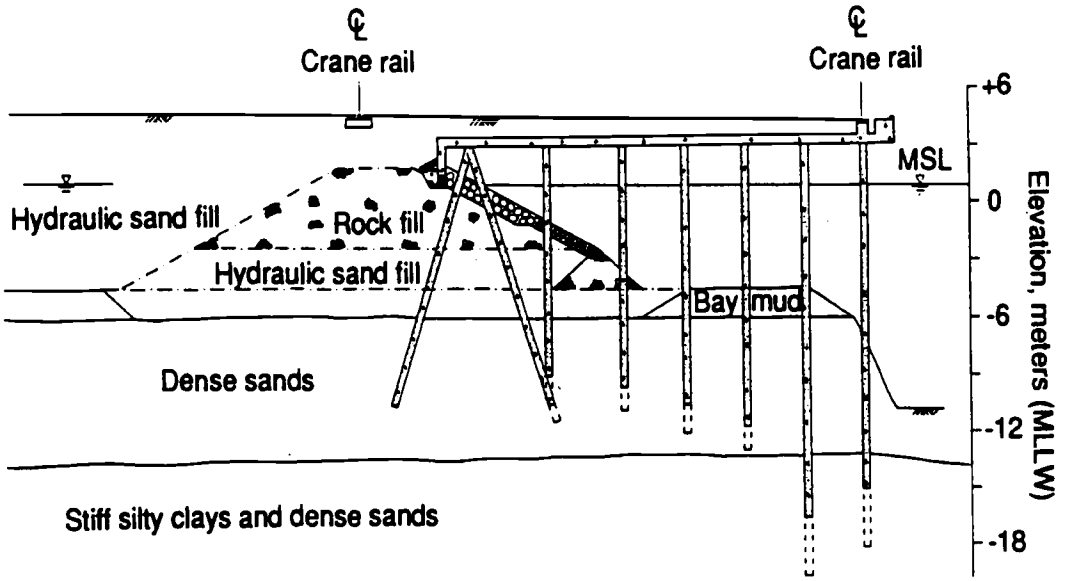

Figure 60. Pile-supported wharf at the Port of Oakland Seventh Street Terminal, prior to the 1989 Loma Prieta Earthquake (Egan et al. 1992 from *Grouting, Soil Improvement and Geosynthetics*, reprinted by permission of ASCE).

Table 10. Soil properties used in the FLAC validation of the Port of Oakland seismic case history.

Soil Layer	Dry Mass Density (kg/m^3)	Porosity (%)	Angle of Internal Friction (deg)	Cohesion (kPa)	Shear Wave Velocity (m/sec)	Drained Poisson's Ratio
1. Pavement Section and Ballast	1958	20	45	0	666	0.20
2. Rock Fill	1737	35	42	10	262	0.20
3. Hydraulically Placed Sand	1443	44	30	0	198	0.35
4. Bay Mud Clay	979	60	0	38	152	0.35
5. Dense Sand	1752	34	40	0	351	0.30
6. Stiff Clay and Dense Sands	1701	40	30	12	243	0.35

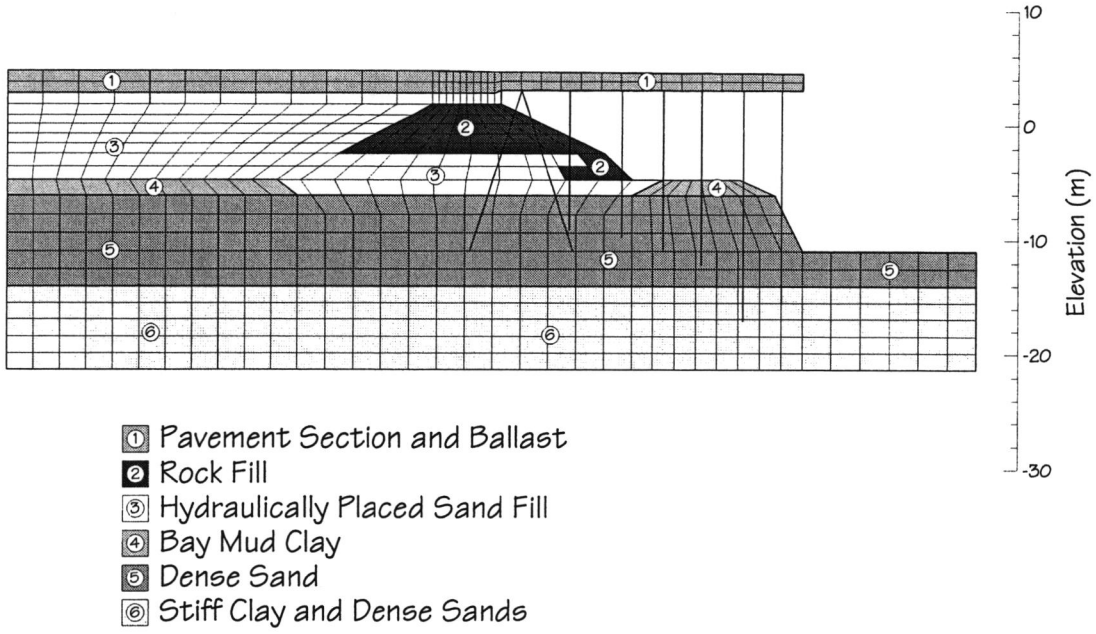

Figure 61. Geometry, grid and structural elements that were used in the numerical model of the Port of Oakland Seventh Street Terminal, Berth 38.

The results of the numerical analysis are illustrated graphically in Figure 63. The analysis predicted a horizontal displacement of the rock dike at the ground surface of 27 cm and a vertical settlement of 22 cm, both in agreement with the observed values of 15 to 30 cm and 13 to 30 cm, respectively. In addition, FLAC predicted plastic hinge development at the top of the all the piles (at the location of the first structural node below the wharf deck). In addition, plastic hinge development at depth was predicted (Figure 63) at the Bay Mud/hydraulic fill and dense sand interfaces.

Table 11. Structural properties used in the FLAC validation of the Port of Oakland seismic case history.

	Vertical and Batter Piles	Wharf Deck
Width (m)	0.41	unit width
Height (m)	0.41	0.46
Modulus of Elasticity (GPa)	30.44	30.44
Mass Density (kg/m^3)	2422	2422
Plastic Moment, top 2.4 m of piles (kN-m)	81	–
Plastic Moment, bottom of piles (kN-m)	164	–

SSI Pile Spring Properties		Normal Springs	Shear Springs
Stiffness (MPa)	Rock	958	287
	Dense Sand	192	287
	Hydraulic Fill	88.6	287
	Bay Mud	83.8	287
Cohesion (kPa)	Rock	4788	0
	Dense Sand	584	0
	Hydraulic Fill	411	0
	Bay Mud	9241	17
Friction Angle (deg)	Rock	89.4	25
	Dense Sand	81.2	25
	Hydraulic Fill	80.0	20
	Bay Mud	89.2	0

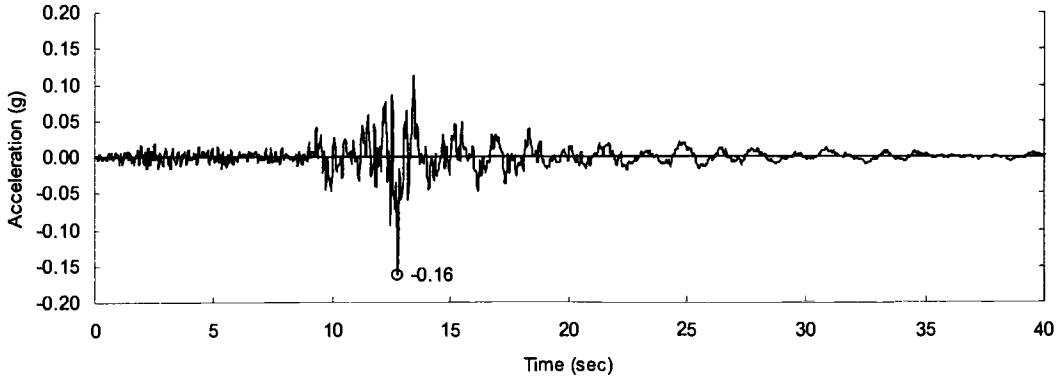

Figure 62. Input acceleration time history for the numerical model (El. –21m).

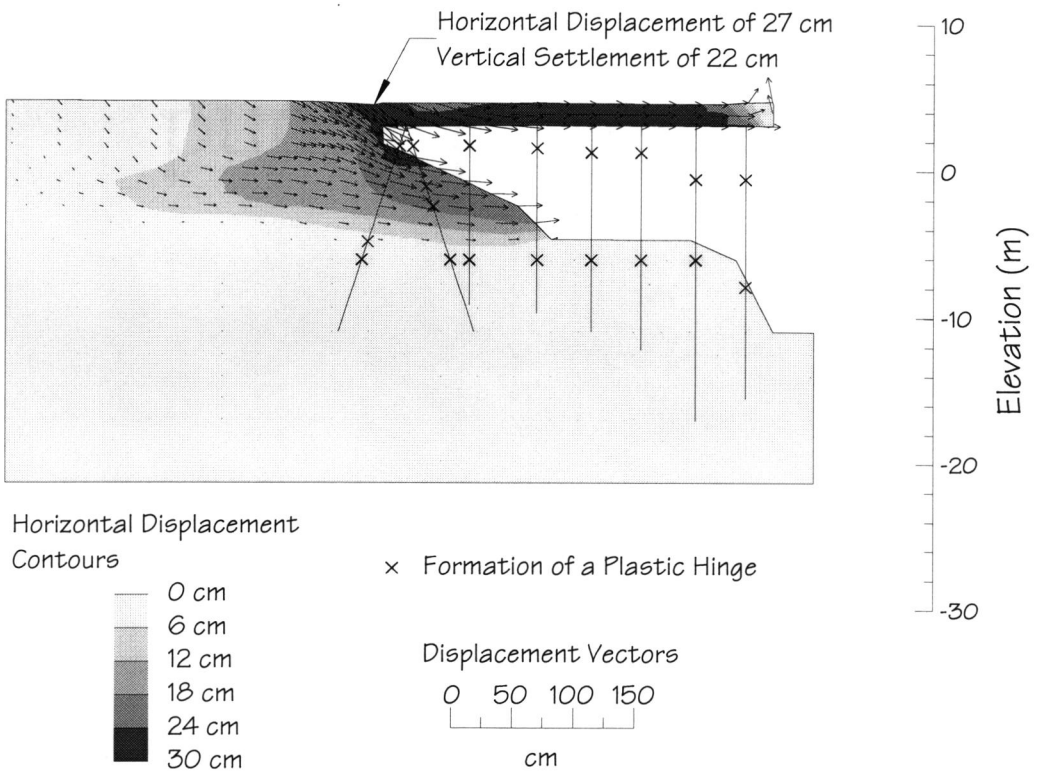

Figure 63. Numerical model predicted performance of Berth 38, Seventh Street Terminal, Port of Oakland during the 1989 Loma Prieta Earthquake.

Centrifuge Models

Each of the centrifuge models validated in the rigid, sliding block study were modeled utilizing the numerical modeling procedures outlined above. A description of the centrifuge models can be found in McCullough and Dickenson (2003a). The cohesionless and cohesive soil properties are shown in Table 12 and Table 13, respectively. The sand utilized in the models was Nevada Sand. Density measurements were taken during placement of the sand, and were related to the porosity, static

strength, and cyclic strength, using the results of the laboratory tests for the VELACS study (Arulmoli et al. 1992). The rock strengths were estimated based on rock fill strengths published in the literature using the measured densities and porosities (Leps 1970, Marachi et al. 1972). The Bay Mud clay density and porosity were estimated based on water content tests of saturated samples of the clay, and the strength values were estimated based on the results of Torvane and Pocket Penetrometer tests in the clay, as well as the undrained strength ratio for the clay. For SMS01, approximately 40 percent of the clay was replaced with the cement-improved clay mixture within the improved region. Samples of the cement-improved clay were taken, and estimates of strength were based on unconfined compression tests of the samples, tested at the same number of cured days.

The modulus values of the cohesionless soils were calculated based on in-situ shear-wave velocity tests. A miniature air hammer (Arulnathan et al. 2000) was used to generate shear waves within the centrifuge models, which were recorded by the vertical accelerometer arrays. Low strain shear modulus values were then back-calculated from the shear wave velocities. A best-fit line was developed for the shear wave velocity profiles, with estimated K_2 and m (Equation 24) values of 840 and 0.58 for the sands, respectively. The density of the sands did not statistically affect the best-fit correlations. Best fit K_2 and m values of 1817 and 0.51 were estimated for the rock, respectively.

Table 12. Cohesionless soil properties for the centrifuge models.

Model	Relative Density (%)	Dry Mass Density (kg/m3)	Porosity (%)	Effective Angle of Internal Friction (deg)	Dilation Angle (deg)	CRR_3	CRR_{30}
Loose Sand							
NJM01	39	1519	43.4	33.0	6.6	0.19	0.023
NJM02	45	1538	42.8	33.7	9.0	0.24	0.050
SMS01	35	1507	43.8	32.6	4.9	0.16	0.005
JCB01	40	1522	43.3	33.2	7.0	0.20	0.028
Dense Sand							
NJM01	82	1662	39.11	37.91	24.3	0.51	0.22
NJM02	85	1673	38.78	38.25	25.5	0.53	0.23
SMS01	70	1620	40.37	36.55	19.3	0.42	0.16
SMS02	70	1620	40.37	36.55	19.3	0.42	0.16
JCB01	74	1633	40.0	37.0	21.0	0.45	0.18
Rock							
NJM01	-	1682	37.7	45.0	15.0	-	-
NJM02	-	1762	34.7	45.0	15.0	-	-
SMS01	-	1650	38.9	45.0	15.0	-	-
SMS02	-	1611	40.3	45.0	15.0	-	-
JCB01	-	1611	40.3	45.0	15.0	-	-

Table 13. Cohesive soil properties for the centrifuge models.

Model	Dry Mass Density (kg/m3)	Porosity (%)	Undrained shear strength (kPa)		Cement improved clay unconfined compressive strength (kPa)
			Beneath dredge line	Beneath backland	
Bay Mud clay					
NJM02	942	64.4	12.4	29.2	-
SMS01	1017	61.6	29.2	29.2	917

The undrained elastic modulus ratio (E_u/s_u) was estimated as 450 for the Bay Mud clay. Since the utilized constitutive model did not include cyclic modulus reduction, the modulus values of all the soils were reduced by 20 percent during the dynamic analyses to partially represent dynamic modulus reduction of the soils. Twenty percent represents the average reduction based on the average cyclic shear strain measured in the numerical model.

Two sizes of piles were used in the centrifuge models. The following properties are reported in prototype units. Models NJM01, SMS02 and JCB01 used aluminum tubing that was 64 cm diameter and 3.6 cm wall thickness, while NJM02 and SMS01 used aluminum tubing that was 54 cm diameter and 3.6 cm wall thickness. The modulus of elasticity of the aluminum was 70 GPa. The plastic moment of the piles was 7.5 MN-m and 48.7 MN-m for the 54 cm and 64 cm diameter piles, respectively. The SSI interaction springs were calculated for each model, at approximately 1 to 2 m intervals along the length of the piles. The SSI interaction springs values are not presented herein due to the large volume of data and necessary brevity.

The results of the validation study are summarized in Figure 64. It can be seen from the figure that the maximum and residual moments were generally not very well predicted. The R^2 correlation coefficient for the maximum and residual moments were 0.22 and 0.16, respectively. The pore pressures and accelerations were somewhat well predicted, with R^2 correlation coefficients of 0.58 and 0.60, respectively. The displacements were very well predicted, with an R^2 correlation coefficient of 0.89. It

should be noted that numerous additional analyses were conducted to evaluate the effect of various modeling parameters (e.g. soil-pile interaction spring stiffness and strength, numerical model damping, changes in shear modulus as a function of pore pressure generation and cyclic strain, etc.). The presented validation study results were for the analyses that best fit the measured centrifuge performance.

The poor prediction of the moments is not well understood. The numerical models accounted for the rock particle behavior, as well as the difference in upslope and downslope stiffness. It was anticipated that the residual moments would be fairly well predicted if the displacements were well predicted, as the residual moments are a function of global soil movement. It was also anticipated that the maximum moments would be fairly well predicted if the accelerations were well predicted, as the maximum moments are a function of the shear wave propagation and the inertial loading of the wharf deck. However, the displacements and accelerations were well predicted, yet the moments were generally poorly predicted.

The accelerations predicted by FLAC were generally larger than those measured in the centrifuge, and this is anticipated to be due to the lack of a strain-based modulus reduction for the constitutive model, and the simplified method of damping that was used in the models.

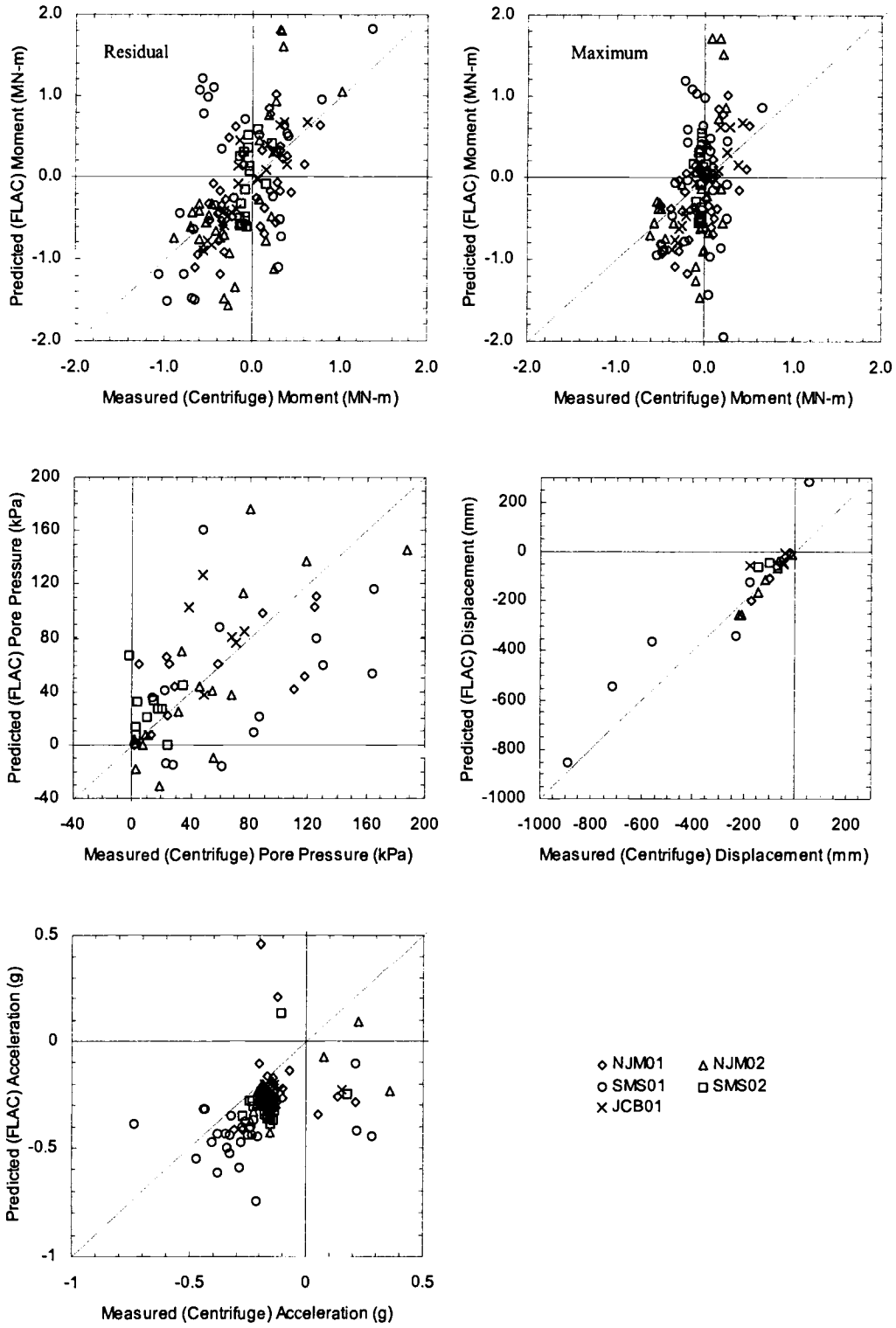

Figure 64. Results of the FLAC validation study using the centrifuge model test data.

Figure 65 shows the centrifuge measured and numerical model predicted residual moments for centrifuge model SMS01. It can be seen that the numerical model largely over-predicted the moments at the soil interfaces, especially for pile number 2. It is interesting to note the large bending moments that developed at depth within the piles were approximately of the same magnitude as the moments at the top of the piles. Even though the numerical model tended to over-predict the moments at depth, a conservative prediction was still obtained, whereas analysis methods that only model the soil as a set of springs attached to the piles would not have predicted the large moments at depth.

DISCUSSION

Several topical lessons were learned during the analysis efforts presented herein, including:

1) Representative permanent seismically induced deformations of pile-supported wharves can be predicted using the rigid, sliding block method of analysis, if modifications are made by including the effect of the pile elements, and pore pressure generation is accounted for. However, even when pore pressure generation and input acceleration time histories were known, the predictions still contained much variation.

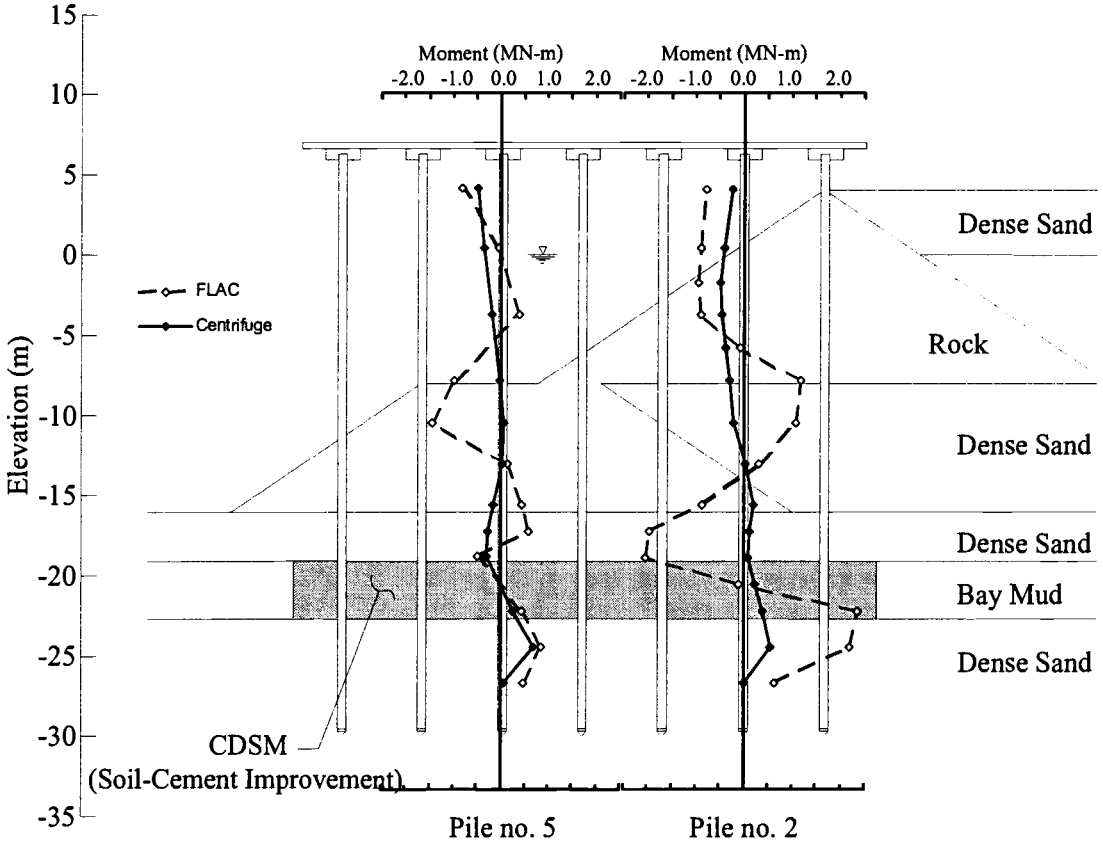

Figure 65. Comparison between the Centrifuge measured and FLAC predicted residual moments in piles number 2 and 5 for centrifuge model SMS01.

2) Cyclic lateral behavior of piles in sloping rock fill can be fairly well modeled using a continuum numerical model if the difference between upslope and downslope SSI spring stiffness is accounted for. In addition, it appears necessary to include a pseudo-cohesion for the rock fill to account for the individual rock particle interaction with the pile elements.

3) Advanced numerical models can be used to predict seismically-induced permanent deformations, accelerations, and excess pore pressure generation relatively well. This appears to be true even though a relatively simple Mohr-Coulomb constitutive model was used in conjunction with a simplified stress-based pore pressure generation model to represent dynamic pore pressure generation. However, even when the displacements, pore pressures and accelerations were fairly well predicted, both the maximum cyclic and residual moments were largely over predicted.

4) It is clear that large moments develop at depth when there is even moderate soil displacement, due to global behavior of the rock dike and adjacent soils. These moments are only-predicted through the use of analysis methods that have the capability to model the global soil system.

SUMMARY

The dynamic performance of pile-supported wharves represent a complex geotechnical and structural interaction problem. The failures that occurred were often structural, yet the structural failures were often due to geotechnical failures (slope instability, liquefaction, etc.). The performance-based design of pile-supported wharves requires a clear understanding of the seismic geotechnical performance. However, due to the lack of seismic field case histories, and the limited amount of the

data from the case histories, most of the analysis methods for estimating the geotechnical performance have undergone limited validation. This paper presented the results of a research effort to validate two types of geotechnical seismic performance analysis methods; 1) a simplified rigid, sliding block, and 2) an advanced numerical model. The methods were validated using field case histories and a suite of seismic pile-supported wharf centrifuge models. The results of the validation study indicated that the seismically-induced deformations were fairly well predicted if pore pressure generation and the effects of the piles was modeled, if even in a simplified manner. However, based on the results of this research effort, it appears as though pile bending moments are not very well predicted. Future efforts are recommended to better understand the dynamic bending behavior of piles in sloping rock fill.

The results of these analysis and validations indicate the necessity of model validation. A lack of validation can lead to a poor understanding of the uncertainty involved in seismic analyses, and an over-confidence in the analysis results. The analysis results presented are not only applicable to pile-supported wharves, but also to other pile-supported structures near open slopes (i.e. bridge abutments, railroad trestles, pile-supported buildings near open faces, etc.).

ACKNOWLEDGEMENTS

The authors would like to gratefully acknowledge Scott Schlecther and Jonathan Boland for the tremendous amount of work put into constructing and testing these models, as well as the staff of the centrifuge facility at UC Davis, who helped

many long days, nights, and weekends in constructing and testing these models, and the assistance from Manfred Deitrich and Andy Brickman at Oregon State University.

This research effort was supported by grant no. CMS-9702744 from the National Science Foundation, grant no. SA2394JB from the Pacific Earthquake Engineering Research Center, and included additional industry support from the Port of Oakland, Port of Long Beach, URS Corp, and Hayward Baker, Inc. The support from these agencies and firms is greatly appreciated.

REFERENCES

Arulmoli, K., Muraleetharan, K.K., Hossain, M.M., and Fruth, L.S. 1992. *VELACS: Verification of Liquefaction Analyses by Centrifuge Studies Laboratory Testing Program Soil Data Report.* Prepared for: National Science Foundation. The Earth Technology Corporation. Project No. 90-0562. Irvine, CA. Baziar, M.H., Dobry, R., and Elgamel, A.W.M. 1992. "Engineering Evaluation of Permanent Ground Deformations Due to Seismically-Induced Liquefaction." *Technical Report NCEER-92-0007.* National Center for Earthquake Engineering Research. State University of New York, Buffalo, NY.

Arulnathan, R., Boulanger, R.W., Kutter, B.L., Sluis, B. 2000. "A New Tool for Vs Measurements in Model Tests." *ASTM Geotechnical Testing Journal.* Vol. 23, Issue 4. pp 444-452.

Broms, B.B. 1964. "Lateral Resistance of Piles in Cohesionless Soils." *Journal of the Soil Mechanics and Foundations Division.* American Society of Civil Engineers. Vol 90, No. SM3, May, 1964. pp 123-157

Dawson, E.M., Roth, W.H., Nesarajah, S., and Davis, C.A. 2001. "A Practice Oriented Pore-Pressure Generation Model." Proceedings of the *2nd FLAC Symposium*, Lyon, France. A.A. Balkema Publishing, Rotterdam, Netherlands.

Duncan, J.M. and Buchignani, A.L. 1976. *An Engineering Manual for Slope Stability Studies.* Department of Civil Engineering, University of California, Berkeley. 94 pp.

Erickson, B.P., Ferritto, J., Hebert, D.C., and Werner, S.D. 1998. "Chapter 5: Seismic Design and Analysis." In *Seismic Guidelines for Ports*. Edited by S.D. Werner. ASCE-TCLEE Monograph No. 12. American Society of Civil Engineers, Reston, VA. March.

Hynes-Griffin, M.E., and A.G. Franklin. 1984. "Rationalizing the Seismic Coefficient Method," U.S. Army Corps of Engineers Waterways Experiment Station. *Miscellaneous Paper GL-84-13*. Vicksburg, MS. 21 p.

Ishihara, K. 1993. "Liquefaction and Flow Failure During Earthquakes." *Geotechnique*. Vol. 43, No. 3. pp. 351-415.

Ishihara, K., and Yoshimine, M. 1992. "Evaluation of Settlements in Sand Deposits Following Liquefaction During Earthquakes." *Soils and Foundations*. Japanese Society of Soil Mechanics and Foundation Engineering. Vol. 32, No. 1. Pp. 173-188.

Itasca. 2000. *FLAC version 4.0 User's Manual*. Itasca Consulting Group, Minneapolis, MN.

Jibson, R.W. 1993. "Predicting Earthquake-Induced Landslide Displacements Using Newmark's Sliding Block Analysis." *Transportation Research Record, No. 1411-Earthquake-Induced Ground Failure Hazards*. Transportation Research Board. National Research Council. Washington, D.C. pp. 9-17.

Kramer, S.L. 1996. *Geotechnical Earthquake Engineering*. Prentice Hall, Upper Saddle River, NJ. 653 pp.

Kulhawy, F.H., and Mayne, P.W. 1990. *Manual on Estimating Soil Properties for Foundation Design*. Final Report, Project 1493-6, EL-6800, Electric Power Research Institute, Palo Alto, CA.

Leps, T.M. 1970. "Review of Shearing Strength of Rockfill." *Journal of the Soil Mechanics and Foundations Division*. ASCE. Vol. 96, No. SM4. pp. 1159-1170.

Makdisi, F.I. and Seed, H.B. 1978. "Simplified Procedure for Estimating Dam and Embankment Earthquake-Induced Deformations." *Journal of the Geotechnical Engineering Division*. ASCE. Vol. 104, No. GT7. pp. 849-867.

Marachi, N.D., Chan, C.K., and Seed, H.B. 1972. "Evaluation of Properties of Rockfill Materials." *Journal of the Soil Mechanics and Foundations Division*. ASCE. Vol. 98, No. SM1. pp. 95-114.

McCullough, N.J. and Dickenson, S.E. 1998. "Estimation of Seismically induced Lateral Deformations for Anchored Sheetpile Bulkheads." Proceedings of the *Geotechnical Earthquake Engineering and Soil Dynamics III* conference, Seattle WA. P. Dakoulas, M. Yegian, and R.D. Holts (eds.). Geotechnical Special Publication No. 75. American Society of Civil Engineers, Reston, VA. pp 1095-1106.

McCullough, N.J. and Dickenson, S.E. 2003a. "The Seismic Performance of Pile-Supported Wharves." Submitted for publication in the *ASCE Journal of Waterway, Port, Coastal and Ocean Engineering.* American Society of Civil Engineers.

McCullough, N.J. and Dickenson, S.E. 2003b. "The Dynamic Centrifuge Modeling of Pile-Supported Wharves." Submitted for publication in the *ASTM Geotechnical Testing Journal.* American Society for Testing and Materials.

McCullough, N.J., Dickenson, S.E., and Pizzimenti, P.B. 2001. "The Seismic Modeling of Sheet Pile Bulkheads for Waterfront Applications." Proceedings of the *2nd FLAC Symposium*, Lyon, France. A.A. Balkema Publishing, Rotterdam, Netherlands.

Olson, S.M. and Stark, T.D. 2002. "Liquefied strength ratio from liquefaction flow failure case histories." *Canadian Geotechnical Journal.* National Research Council, Canada. Vol. 39, No. 3. pp. 629-647.

PIANC (International Navigation Association). 2001. *Seismic Design Guidelines for Port Structures.* International Navigation Association Working Group No. 34. A.A. Balkema.

Rau, G.A. and Sitar, N. 1998. "Post-Cyclic Response of Holocene Bay Mud from San Francisco." Proceedings of the *Geotechnical Earthquake Engineering and Soil Dynamics III* conference, Seattle WA. P. Dakoulas, M. Yegian, and R.D. Holts (eds.). Geotechnical Special Publication No. 75. American Society of Civil Engineers, Reston, VA. pp 246-257.

Roth, W.H., Bureau, G., Brodt, G. 1991. "Pleasant Valley Dam: An Approach to Quantifying the Effect of Foundation Liquefaction." *Proceedings of the 17th International Congress on Large Dams.* Vienna, Austria. pp. 1199-1223.

Roth, W.H., Fong, H., and de Rubertis, C. 1992. "Batter Piles and the Seismic Performance of Pile-Supported Wharves." *Proceedings of the '92 Ports Conference.* American Society of Civil Engineers. Seattle, WA, July 20-22, 1992. pp 336-349.

Seed, R.B. and Harder, L.F. 1990. "SPT-Based Analysis of Cyclic Pore Pressure Generation and Undrained Residual Strength." Proceedings of the *H.Bolton Seed Memorial Symposium*. J.M. Duncan (ed.). University of California, Berkeley. Vol. 2. pp 351-376.

Serventi, J. 2003. "Port of Oakland: Lessons Learned from the Loma Prieta Earthquake." Presented at the seminar on the *Geotechnical Engineering for Waterfront Structures*. Sponsored by the Seattle Section Geotechnical Group of American Society of Civil Engineers, Seattle, WA. March 15, 2003.

Stark, T.D. and Mesri, G. 1992. "Undrained Shear Strength of Sands for Stability Analysis." *Journal of Geotechnical Engineering*. ASCE. Vol. 118, No. 11. pp. 1727-1747.

USACE. 1983. *Soils and Geology Procedures for Foundation Design of Buildings and Other Structures (Except Hydraulic Structures)*. United State Army Corps of Engineers. Technical Manual TM 5-818-1.

Werner, S.D. (Editor). 1998. *Seismic Guidelines for Ports*. ASCE Technical Council on Lifeline Earthquake Engineering. Monograph No. 12. March 1998. ASCE, Reston, VA.

Wilson, R.C. and D.K. Keefer. 1985. "Predicting Area Limits of Earthquake-Induced Landsliding," *Evaluating Earthquake Hazards in the Los Angeles Region*. J.I. Ziony (ed.). USGS Professional Paper 1360. Reston, VA. pp. 317-345.

Wright, S.G., 1992. *UTEXAS3, A Computer Program for Slope Stability Calculations*. Austin, Texas. May, 1990, revised July 1991 and 1992.

CHAPTER 5 – SUMMARY AND CONCLUSIONS

Pile-supported wharves subjected to moderate to low levels of shaking have generally performed well during past earthquakes. However, cases of poor performance have been noted and were generally attributed to the poor performance of adjacent soils (soft clays and/or liquefiable sands), resulting in permanent lateral embankment deformations. Given that the analysis of pile-supported wharves involves complex soil-structure-interaction, and that permanent lateral deformations control the seismic behavior, it is a necessity that the seismic performance of pile-supported wharves be clearly understood during design. In addition, the complex behavior necessitates the use of validated analysis methods. The use of non-validated analysis methods may provide an unreasonable level of confidence during the design process.

This dissertation presented the results of a research effort aimed at better understanding the seismic performance of and the geotechnical analysis methods for pile-supported wharves. There were a limited number of documented seismic field case histories for pile-supported wharves, and very few of the case histories were documented in adequate detail to allow for validation studies. Given the paucity of field case histories, five heavily instrumented centrifuge models of pile-supported wharves were constructed and dynamically tested. These model case histories were used to supplement the case history database, and provide a better understanding of the seismic performance of pile-supported wharves.

An examination of the seismic case histories highlighted several key issues:

1) Batter piles have generally performed poorly during earthquakes, when subjected to moderate to large soil deformations. However, batter piles subjected to smaller permanent soil displacements were noted to have performed much better, though the damage was generally more devastating due to their larger stiffness in comparison to vertical piles.
2) The majority of the structural pile-supported wharf failures were due to permanent lateral soil deformations, which were often due to the liquefaction of adjacent soils. Pile-supported wharves constructed in and adjacent to competent soils have generally performed satisfactorily during earthquakes, highlighting the benefit of soil improvement for weak soils within the vicinity of pile-supported wharves.
3) The centrifuge models highlighted that even competent pile-supported wharf geometries (factors of safety against slope stability greater than 1.5) should anticipate moderate amounts of permanent lateral deformations (20 cm or greater) during high levels of shaking (0.4 g or greater).
4) The maximum cyclic pile bending moments near the pile/deck connection appear to be a function of the level of ground shaking, as the primary forces on the piles are due to the cyclic inertial loading of the wharf deck.
5) The residual pile bending moments at depth appear to be a function of the permanent lateral deformation of the embankment. The larger the

permanent lateral deformations, the larger the moments at depth. Therefore, pile failures at depth are anticipated for pile-supported wharves that have been subjected to moderately large levels of permanent lateral deformations.

6) There are a limited number of noted pile failures at depth from post-earthquake reconnaissance investigations; however, this is likely due to the inability to visually observe these failures.

7) The model case histories highlighted that bending moments that developed at depth were equal to or even greater than the moments near the pile/deck connection. This highlights the need for analysis and design methods to adequately account for the seismic performance of the entire pile-supported wharf system.

With a database of well-documented/instrumented case histories on the seismic performance of pile-supported wharves it was possible to validate the methods of analysis typically used for predicting the geotechnical seismic performance of pile-supported wharves. Two methods that are often used to predict permanent lateral deformations of embankments (including pile-supported wharves) include: 1) limit equilibrium slope stability analysis coupled with rigid, sliding block analysis, and 2) finite-difference/element numerical analysis methods. The validation process involved using these methods of analysis to predict the seismic case history performance. In using the rigid, sliding block method, the seismic degradation of soils due to cyclic shearing and pore pressure generation were accounted for, along with the additional

resistance provided by the pile elements. There was a relatively good comparison between the permanent lateral displacements predicted using the rigid, sliding block method and the values measured in the case histories, though there was substantial scatter in the data. Much of the scatter was due to the assumption of a rigid block, requiring only a single input acceleration time history. In actuality, the failure mass is not rigid, therefore the acceleration time history changes as it propagates through the failure mass. The measured variations in the input acceleration time histories resulted upwards of 200 percent variations in the predicted displacements. Full results of the rigid, sliding block analyses are presented in Appendix A.

The finite-difference computer program FLAC was also used as a comparison to the measured case history performances. The numerical model utilized an effective stress, pore pressure generation constitutive model that allowed for seismic pore pressure generation in the loose, saturated sandy soils. In addition, the pile and wharf deck structural elements were modeled directly, and a complete time history analysis was conducted. Prior to modeling the full pile-supported wharf geometries, a validation was conducted to evaluate the ability of the numerical model to represent the lateral pile behavior in sloping rock fill. This validation study highlighted a key aspect of modeling rock particles having a diameter on the same order of magnitude as the pile element diameter. When the ratio of the pile diameter to the rock diameter is less than approximately 30 to 40, the rock particles behave more as discrete particles and less as a continuum. FLAC is a continuum model, therefore adjustments were made to the modeling to account for the rock particle interaction. A parametric study

revealed that FLAC best predicted the lateral pile response when the downslope soil-structure-interaction springs had a stiffness approximately 10 times less than the upslope springs, and when the rock continuum was modeled with a pseudo-cohesion, to account for the individual rock particle interaction. For this study, a pseudo-cohesion of 15 kPa provided the best predictions.

The results of the lateral pile response where then used in modeling the full pile-supported wharf system. The results of the FLAC predictions, in comparison to the case histories, indicated that the deformations, pore pressures, and accelerations were fairly well predicted. However, the bending moments within the pile elements were poorly, though generally conservatively, predicted. At this time it is not fully understood why the moments were poorly predicted, when predictions of the variables related to the permanent soil deformations were fairly well predicted (i.e. deformations, pore pressures, and accelerations). Full results of the FLAC analyses of the centrifuge models are presented in B.

The research presented was specifically for pile-supported wharves, yet there are other similar structures that could directly benefit from the results of this research. This includes pile-supported structures near a sloping waterfront, such as; bridge abutments, railroad trestles, and building supported on piles adjacent to body of water. In addition, the lessons learned regarding the numerical modeling of discrete particles could be applied towards many analyses in which the diameter of the individual soil particles is on the order of the nominal dimension of the structure being analyzed.

CHAPTER 6 – RECOMMENDATIONS FOR FUTURE RESEARCH

The research results presented herein provided a base for future research. Recommendations for future research of pile-supported wharves include:

1) Provide better field case histories. This includes re-examination of existing case histories to include as-built drawings, pre- and post-earthquake survey data, integrity testing or removal of piles to note failures at depth. In addition, aspects of existing pile-supported wharves in seismically active regions should be documented, including as-built drawings, above grade and bathymetric surveys, and the installation of instrumentation (such as accelerometers, pore pressure transducers and potentially strain gauges to be triggered by seismic events).

2) A more complete evaluation of existing case histories. One complete case history (Port of Oakland Seventh Street Terminal) was used as a validation in this research project. Validation of other case histories, noting both failures and non-failures would greatly increase the understanding of the seismic performance and analysis of pile-supported wharves. These include Takahama Wharf in Kobe, Japan during the 1995 Hygoken-Nambu Earthquake, the Berth 81 at the Port of San Francisco, and the Howard Terminal and Berths 22-24 at the Port of Oakland during the 1989 Loma Prieta Earthquake, and Berths

121-126 and 126/0 at the Port of Los Angeles during the 1994 Northridge Earthquake.

3) Batter piles have performed poorly in some instances during past earthquakes, but there are also instances were batter piles performed satisfactorily. A study utilizing the seismic performance at the Port of Oakland and the centrifuge models that contained batter piles could be conducted to better understand the seismic performance of batter piles.

4) A study examining the advantages and disadvantages of soil improvement. Soil improvement can improve the seismic resistance to liquefaction, and decrease potential deformations. However, as noted for centrifuge model SMS02 presented within, the improved clay at depth forced a failure plane along a much narrower shear zone, concentrating forces in the piles, resulting in large bending moments. It would also be beneficial to study and develop guidelines regarding the extent of soil improvement necessary to limit deformations. In addition, a study on the concurrent use of complimentary methods of ground treatment (e.g. soil densification and CDSM) would be of value.

5) The centrifuge models could be used to analyze the incremental benefit of soil densification. Each centrifuge model was subjected to a series of earthquake motions, with each moderate to large motion generating excess pore pressures, densifying of the potentially liquefiable soils. A careful examination of the shear wave velocities that were measured

between each shake could be used to estimate the level of densification that occurred during the previous shake. A comparison could then be made between the level of densification and the seismic performance of the wharves.

6) Investigate the discrete particle interaction. Full-scale lateral pile load tests in rock fill, in comparison to the centrifuge lateral pile load tests, may aid in understanding this behavior. In addition, p-y correction factors could be developed to aid in traditional lateral analysis of piles in rock fill.

In addition, an exorbitant amount of data was collected from each of the centrifuge models. These data could be used to examine such issues such as:

1) The variations in site response at a waterfront embankment, examining how the ground surface seismic response varies from the backland, along the embankment slope, to the dredge line.
2) The effect of liquefaction on ground surface response.
3) The effect of soil improvement on ground surface response.
4) P-y curves could be back-calculated from the centrifuge data for the various soil types, including rock, dense sand, loose sand, and liquefied sand. In addition the degradation of the p-y curves during cyclic pore pressure generation could be examined.

BIBLIOGRAPHY

Abdoun, T., Dobry, R., and O'Rourke, T.D. 1997. "Centrifuge and Numerical Modeling of Soil-Pile Interaction During Earthquake Induced Soil Liquefaction and Lateral Spreading." *Proc., ASCE Geo-Institute Session on the Observation and Modeling in Numerical Analysis and Model Tests in Dynamic Soil-Structure Interaction Problems during the Geo-Logan '97 Conference.* Logan, Utah. ASCE Geo-Institute, Geotechnical Special Publication No. 64.

Arulanandan, KK., and Scott, R.F. (Eds.). 1993. *Proceedings of the International Conference on the Verification of Numerical Procedures for the Analysis of Soil Liquefaction Problems.* Davis, California. October 17-20, 1993. A.A. Balkema, Brookfield.

Arulmoli, K., Muraleetharan, K.K., Hossain, M.M., and Fruth, L.S. 1992. *VELACS: Verification of Liquefaction Analyses by Centrifuge Studies Laboratory Testing Program Soil Data Report.* Prepared for: National Science Foundation. The Earth Technology Corporation. Project No. 90-0562. Irvine, CA.

Arulnathan, R., Boulanger, R.W., Kutter, B.L., Sluis, B. 2000. "A New Tool for Vs Measurements in Model Tests." *ASTM Geotechnical Testing Journal.* Vol. 23, Issue 4. pp 444-452.

Baziar, M.H., Dobry, R., and Elgamel, A.W.M. 1992. "Engineering Evaluation of Permanent Ground Deformations Due to Seismically-Induced Liquefaction." *Technical Report NCEER-92-0007.* National Center for Earthquake Engineering Research. State University of New York, Buffalo, NY.

Boland, C.B., Schlechter, S.M., McCullough, N.M., Dickenson, S.E., Kutter, B.L., and Wilson, D.W. 2001a. *Data Report: Pile-Supported Wharf Centrifuge Model (SMS02).* Geotechnical Engineering Group, Department of Civil, Construction and Environmental Engineering. Oregon State University.

Boland, C.B., Schlechter, S.M., McCullough, N.M., Dickenson, S.E., Kutter, B.L., and Wilson, D.W. 2001b. *Data Report: Pile-Supported Wharf Centrifuge Model (JCB01).* Geotechnical Engineering Group, Department of Civil, Construction and Environmental Engineering. Oregon State University.

Broms, B.B. 1964. "Lateral Resistance of Piles in Cohesionless Soils." *Journal of the Soil Mechanics and Foundations Division.* American Society of Civil Engineers. Vol 90, No. SM3, May, 1964. pp 123-157

Buslov, V.M., Rowghani, M., Weismair, M. 1996. "Evaluating Earthquake Damage to Concrete Wharves." *Concrete International*. August. pp 50-54

Castro, G. 1975. "Liquefaction and Cyclic Mobility of Sands." *Journal of the Geotechnical Engineering Division*. ASCE. Vol. 101, No. GT6. pp 551-569.

Curras, C.J., Boulanger, R.W., Kutter, B.L., Wilson, D.W. 2001. "Dynamic Experiments and Analyses of a Pile-Group-Supported Structure." *Journal of Geotechnical and Geoenvironmental Engineering*. ASCE. Vol. 127, No. 7. July. pp 585-596.

Dames and Moore. 1984. *Geotechnical Studies for the Port of Portland Terminal 2 Rehabilitation*. Prepared for the Port of Portland.

Dawson, E.M., Roth, W.H., Nesarajah, S., and Davis, C.A. 2001. "A Practice Oriented Pore-Pressure Generation Model." Proceedings of the *2nd FLAC Symposium*, Lyon, France. A.A. Balkema Publishing, Rotterdam, Netherlands.

Diaz, G.M., Patton, B.W., Armstrong, G.L., and Joolazadeh, M. 1984. "Lateral Load Tests of Piles in Sloping Rock Fill." Proceedings of a Symposium on the *Analysis and Design of Pile Foundations*. ASCE National Convention, San Francisco, California. October 1-5.

Duncan, J.M. and Buchignani, A.L. 1976. *An Engineering Manual for Slope Stability Studies*. Department of Civil Engineering, University of California, Berkeley. 94 pp.

EERI (Earthquake Engineering Research Institute). 1991a. "Philippines Earthquake Reconnaissance Report." *Earthquake Spectra*. EERI. Supplement A to Vol. 7. October.

EERI (Earthquake Engineering Research Institute). 1991b. "Costa Rica Earthquake of April 22, 1991 Reconnaissance Report." *Earthquake Spectra*. EERI. Supplement B to Vol. 7. October.

EERI (Earthquake Engineering Research Institute). 2000. "Kocaeli, Turkey, Earthquake of August 17, 1999 Reconnaissance Report." *Earthquake Spectra*. EERI. Supplement A to Vol. 16. December.

EERI (Earthquake Engineering Research Institute). 2002. "Bhuj, India Earthquake of January 26, 2001 Reconnaissance Report." *Earthquake Spectra*. EERI. Supplement A to Vol. 18. July.

Egan, J.A., Hayden, R.F., Scheibel, L.L., Otus, M., and Serventi, G.M. 1992. "Seismic Repair at Seventh Street Marine Terminal." Proceedings of the conference *Grouting, Soil Improvement, and Geosynthetics*. ASCE Geotechnical Special Publication No. 30, Volume 2. New Orleans, Louisiana. February 25-28.

Ensoft. 1999. *LPILE version 3.0 User's Manual*. Ensoft, Inc. Austin, Texas.

EQE. 1990. *The July 16, 1990 Philippines Earthquake*. EQE Engineering, San Francisco, CA. August.

Erickson, B.P., Ferritto, J., Hebert, D.C., and Werner, S.D. 1998. "Chapter 5: Seismic Design and Analysis." In *Seismic Guidelines for Ports*. Edited by S.D. Werner. ASCE-TCLEE Monograph No. 12. American Society of Civil Engineers, Reston, VA. March.

Finn, W.D.L., Pickering, D.J., and Bransby, P.L. 1971. "Sand Liquefaction in Triaxial and Simple Shear Tests." *Journal of the Soil Mechanics and Foundations Division*. ASCE. Vol. 97, No. SM4. pp 639-659.

Goh, S.H., and Orourke, T.D. 1999. "Limit State Model for Soil-Pile Interaction During Lateral Spreading." Proc., Seventh International U.S.-Japan Workshop on Earthquake Resistant Design of Lifeline Facilities and Countermeasures Against Soil Liquefaction. Seattle, Washington. O'Rourke, Bardet, and Hamada (Eds.). MCEER Technical Report, MCEER-99-0019. Buffalo, New York. pp 237-260.

Harder, L. F., Jr., and Boulanger, R. W. 1997. "Application of K_σ and K_α correction factors." *Proc., NCEER Workshop on Evaluation of Liquefaction Resistance of Soils*. National Center for Earthquake Engineering Research, State Univ. of New York at Buffalo. pp 167–190.

Hynes-Griffin, M.E., and A.G. Franklin. 1984. "Rationalizing the Seismic Coefficient Method," U.S. Army Corps of Engineers Waterways Experiment Station. *Miscellaneous Paper GL-84-13*. Vicksburg, MS. 21 p.

Iai, S. 1989. "Similitude for Shaking Table Tests on Soil-Structure-Fluid Model in 1g Gravitation Field." *Soils and Foundations*. Vol. 29, No. 1. March. pp. 118.

Iai, S. 1998. "Seismic Analysis and Performance of Retaining Structures." Proceedings of the conference *Geotechnical Earthquake Engineering and Soil Dynamics III*. ASCE Geotechnical Special Publication No. 75. Edited by P. Dakoulas, M. Yegian, and R.D. Holtz. Volume 2. pp 1020-1044.

Iai, S. 2003. Personal communication.

Inel, S., Roth, W.H., and de Rubertis, C. 1993. "Nonlinear Dynamic Effective-Stress Analysis of Two Case Histories." Proc., Third International Conference on Case Histories in Geotechnical Engineering. St. Louis, Missouri, USA. June 1-4, 1993. Paper No. 14.14. pp. 1735-1741.

Ishihara, K. 1993. "Liquefaction and Flow Failure During Earthquakes." *Geotechnique*. Vol. 43, No. 3. pp. 351-415.

Ishihara, K., and Yoshimine, M. 1992. "Evaluation of Settlements in Sand Deposits Following Liquefaction During Earthquakes." *Soils and Foundations*. Vol. 32, No. 1. pp. 29-44.

Itasca. 2000. *FLAC version 4.0 User's Manual*. Itasca Consulting Group, Minneapolis, MN.

Jibson, R.W. 1993. "Predicting Earthquake-Induced Landslide Displacements Using Newmark's Sliding Block Analysis." *Transportation Research Record, No. 1411-Earthquake-Induced Ground Failure Hazards*. Transportation Research Board. National Research Council. Washington, D.C. pp. 9-17.

Ko, H-Y., Atkkinson, R.H., and Goble, G.C. 1984. *Centrifuge Testing of Model Piles and Pile Groups*. U.S. Department of Transportation, Federal Highway Administration. Report No. FHWA/RD-84/002. Final Report, November 1984. Vols. I-III.

Kramer, S.L. 1996. *Geotechnical Earthquake Engineering*. Prentice Hall, Upper Saddle River, NJ. 653 pp.

Kulhawy, F.H., and Mayne, P.W. 1990. *Manual on Estimating Soil Properties for Foundation Design*. Final Report, Project 1493-6, EL-6800, Electric Power Research Institute, Palo Alto, CA.

Kutter, B.L., Idriss, I.M., Kohnke, T., Lakeland, J., Li, X.S., Sluis, W., Zeng, X., Tauscher, R., Goto, Y., and Kubodera, I. 1994. "Design of a Large Earthquake Simulator at UC Davis." Proceedings, *Centrifuge 94*. Lueng, Lee, and Tan, Eds. Balkema, Rotterdam. pp.169-175.

Kutter, B.L., Li, X.S., Sluis, W., and Cheney, J.A. 1991. "Performance and Instrumentation of the Large Centrifuge at Davis." Proceedings, *Centrifuge 91*. Ko and Mclean, Eds. Balkema, Rotterdam. pp. 19-26.

Leps, T.M. 1970. "Review of Shearing Strength of Rockfill." *Journal of the Soil Mechanics and Foundations Division*. ASCE. Vol. 96, No. SM4. pp. 1159-1170.

Makdisi, F.I. and Seed, H.B. 1978. "Simplified Procedure for Estimating Dam and Embankment Earthquake-Induced Deformations." *Journal of the Geotechnical Engineering Division*. ASCE. Vol. 104, No. GT7. pp. 849-867.

Marachi, N.D., Chan, C.K., and Seed, H.B. 1972. "Evaluation of Properties of Rockfill Materials." *Journal of the Soil Mechanics and Foundations Division*. ASCE. Vol. 98, No. SM1. pp. 95-114.

Martin, G.R., Finn, W.D.L., and Seed, H.B. 1975. "Fundamentals of Liquefaction Under Cyclic Loading." *Journal of the Geotechnical Engineering Division*. ASCE. Vol. 101, No. GT5. May. pp 423-438.

McCullough, N.J. 1998. *The Seismic Vulnerability of Sheet Pile Walls*. A thesis submitted to Oregon State University in partial fulfillment of the degree of Master of Science. Oregon State University, Corvallis, Oregon. pp. 127.

McCullough, N.J. and Dickenson, S.E. 1998. "Estimation of Seismically induced Lateral Deformations for Anchored Sheetpile Bulkheads." Proceedings of the *Geotechnical Earthquake Engineering and Soil Dynamics III* conference, Seattle WA. P. Dakoulas, M. Yegian, and R.D. Holts (eds.). Geotechnical Special Publication No. 75. American Society of Civil Engineers, Reston, VA. pp 1095-1106.

McCullough, N.J. and Dickenson, S.E. 2003a. "The Seismic Performance of Pile-Supported Wharves." Submitted for publication in the *ASCE Journal of Waterway, Port, Coastal and Ocean Engineering*. American Society of Civil Engineers.

McCullough, N.J. and Dickenson, S.E. 2003b. "The Dynamic Centrifuge Modeling of Pile-Supported Wharves." Submitted for publication in the *ASTM Geotechnical Testing Journal*. American Society for Testing and Materials.

McCullough, N.J., Dickenson, S.E., and Pizzimenti, P.B. 2001. "The Seismic Modeling of Sheet Pile Bulkheads for Waterfront Applications." Proceedings of the *2nd FLAC Symposium*, Lyon, France. A.A. Balkema Publishing, Rotterdam, Netherlands.

McCullough, N.J., Schlechter, S.M., Dickenson, S.E., Kutter, B.L., and Wilson, D.W., 2000. *Data Report: Pile-Supported Wharf Centrifuge Model (NJM01)*. Geotechnical Engineering Group, Department of Civil, Construction and Environmental Engineering. Oregon State University.

Mukhopadhyay, G. 1998. "Preparing for Pier A." *Civil Engineering*. ASCE. August. pp 36-39.

Muraleetharan, K.K., Arulmoli, K., Wittkop, R.C., and Foxworthy, J.E. 1997. "Use of Centrifuge and Numerical Modeling in Design of Pier 400 at the Port of Los Angeles." *Transportation Research Record – Centrifuge Modeling, Intelligent Geotechnical Systems, and Reliability-Based Design.* National Research Council, National Academy Press. Washington, D.C.

Muraleetharan, K.K., Thiessen, D.A., Jagannath, S.V., and Arulmoli, K. 1995. "Performance of Port Facilities During the Northridge Earthquake." Proceedings of the *Third International Conference on Recent Advances in Geotechnical Earthquake Engineering and Soil Dynamics.* Vol III. St. Louis, Missouri. April 2-7.

Olson, S.M. and Stark, T.D. 2002. "Liquefied strength ratio from liquefaction flow failure case histories." *Canadian Geotechnical Journal.* National Research Council, Canada. Vol. 39, No. 3. pp. 629-647.

Oyenuga, D., Abe, S., Sedarat, H., Krimotat, A., Salah-Mars, S., Ogunfunmi, K. 2001. "Analysis of Existing Piles with Missing Data in Seismic Retrofit Design at the Port of Oakland." *Proceedings of the ASCE Ports 2001 Conference.* Norfolk, Virginia, April 29-May 2.

PIANC (International Navigation Association). 2001. *Seismic Design Guidelines for Port Structures.* International Navigation Association Working Group No. 34. A.A. Balkema.

Rau, G.A. and Sitar, N. 1998. "Post-Cyclic Response of Holocene Bay Mud from San Francisco." Proceedings of the *Geotechnical Earthquake Engineering and Soil Dynamics III* conference, Seattle WA. P. Dakoulas, M. Yegian, and R.D. Holts (eds.). Geotechnical Special Publication No. 75. American Society of Civil Engineers, Reston, VA. pp 246-257.

Roth, W.H., Scott, R.F., and Cundall, P.A. 1986. "Nonlinear Dynamic Analysis of a Centrifuge Model Embankment." *Proceedings of the 3rd U.S. National Conference on Earthquake Engineering.* August 24-28, Charleston, South Carolina. Vol. I, pp. 505-516.

Roth, W.H., Bureau, G., Brodt, G. 1991. "Pleasant Valley Dam: An Approach to Quantifying the Effect of Foundation Liquefaction." *Proceedings of the 17th International Congress on Large Dams.* Vienna, Austria. pp. 1199-1223.

Roth, W.H., Dawson, E, Mehrain, M., and Sayegh, A. 2003. "Analyzing the Seismic Performance of Wharves, Part 1: Structural Engineering Approach." *Proceedings of TCLEE 2003: 6th U.S. Conference and Workshop on Lifeline Earthquake Engineering.* ASCE. To be held in Long Beach, California, August 10-13, 2003.

Roth, W.H. and Dawson, E. 2003. "Analyzing the Seismic Performance of Wharves, Part 2: SSI Analysis with Non-Linear, Effective-Stress Soil Models." *Proceedings of TCLEE 2003: 6th U.S. Conference and Workshop on Lifeline Earthquake Engineering.* ASCE. To be held in Long Beach, California, August 10-13, 2003.

Roth, W.H., Fong, H., and de Rubertis, C. 1992. "Batter Piles and the Seismic Performance of Pile-Supported Wharves." *Proceedings of the '92 Ports Conference.* American Society of Civil Engineers. Seattle, WA, July 20-22, 1992. pp 336-349.

Schlechter, S.M., McCullough, N.J., Dickenson, S.E., Kutter, B.L., and Wilson, D.W. 2000b. *Data Report: Pile-Supported Wharf Centrifuge Model (SMS01).* Geotechnical Engineering Group, Department of Civil, Construction and Environmental Engineering. Oregon State University.

Schlechter, S.M., McCullough, N.J., Dickenson, S.E., Kutter, B.L., and Wilson, D.W. 2000a. *Data Report: Pile-Supported Wharf Centrifuge Model (NJM02).* Geotechnical Engineering Group, Department of Civil, Construction and Environmental Engineering. Oregon State University.

Scott, R.F. 1991. "Modeling of Earth Structures." *Proc., Port of Los Angeles Seismic Workshop.*

Scott, R.F., Hushmand, B., and Rashidi, H. 1993. "Model No. 3 Primary Test Description and Test Results." Proceedings of the *International Conference on the Verification of Numerical Procedures for the Analysis of Soil Liquefaction Problems.* K. Arulanandan and R.F. Scott (Eds). Volume I. Davis, California. Balkema Publishers, Rotterdam. pp 435-462.

Seed, H. B., Tokimatsu, K., Harder, L. F., and Chung, R. M. 1985. "The Influence of SPT Procedures in Soil Liquefaction Resistance Evaluations." *Journal of Geotechnical Engineering.* ASCE, Vol. 111, No. 12. pp 1425-1445.

Seed, H.B. 1979. "Soil Liquefaction and Cyclic Mobility Evaluation for Level Ground During Earthquakes." *Journal of the Geotechnical Engineering Division.* ASCE. Vol. 105, No. GT2. pp 201-255.

Seed, H.B., Martin, P.P, and Lysmer, J. 1976. "Pore-Pressure Changes During Soil Liquefaction." *Journal of the Geotechnical Engineering Division*. ASCE. Vol. 102, No. GT4. April. pp 323-345.

Seed, H.G., and Peacock, W.H. 1971. "Test Procedures for Measuring Soil Liquefaction Characteristics." *Journal of the Soil Mechanics and Foundations Division*. ASCE. Vol. 97, No. SM8. pp 1099-1119.

Seed, R.B. and Harder, L.F. 1990. "SPT-Based Analysis of Cyclic Pore Pressure Generation and Undrained Residual Strength." Proceedings of the *H.Bolton Seed Memorial Symposium*. J.M. Duncan (ed.). University of California, Berkeley. Vol. 2. pp 351-376.

Serventi, J. 2003. "Port of Oakland: Lessons Learned from the Loma Prieta Earthquake." Presented at the seminar on the *Geotechnical Engineering for Waterfront Structures*. Sponsored by the Seattle Section Geotechnical Group of American Society of Civil Engineers, Seattle, WA. March 15, 2003.

Singh, J.P., Tabatabaie, M., and French, J.B. 2001. "Geotechnical and Ground Motion Issues in Seismic Vulnerability Assessment of Existing Wharf Structures." *Proceedings of the ASCE Ports 2001 Conference*. Norfolk, Virginia, April 29-May 2.

Stark, T.D. and Mesri, G. 1992. "Undrained Shear Strength of Sands for Stability Analysis." *Journal of Geotechnical Engineering*. ASCE. Vol. 118, No. 11. pp. 1727-1747.

USACE. 1983. *Soils and Geology Procedures for Foundation Design of Buildings and Other Structures (Except Hydraulic Structures)*. United State Army Corps of Engineers. Technical Manual TM 5-818-1.

Werner, S.D. (Editor). 1998. *Seismic Guidelines for Ports*. ASCE Technical Council on Lifeline Earthquake Engineering. Monograph No. 12. March 1998. ASCE, Reston, VA.

Wilson, D.W. 1998. *Soil-Pile-Superstructure Interaction in Liquefying Sand and Soft Clay*. Ph.D. Dissertation. University of California. Davis, CA. September.

Wilson, R.C. and D.K. Keefer. 1985. "Predicting Area Limits of Earthquake-Induced Landsliding," *Evaluating Earthquake Hazards in the Los Angeles Region*. J.I. Ziony (ed.). USGS Professional Paper 1360. Reston, VA. pp. 317-345.

Wright, S.G., 1992. *UTEXAS3, A Computer Program for Slope Stability Calculations*. Austin, Texas. May, 1990, revised July 1991 and 1992.

Youd, Y.L., Idriss, I.M., Andrus, R.D., Arango, I., Castro, G., Christian, J.T., Dobry, R., Finn, W.D.L., Harder, L.F Jr., Hynes, M.E., Ishihara, K., Doester, J.P., Liao, S.S.C., Marcuson, W.F. III., Martin, G.R., Mitchell, J.K., Moriwaki, Y., Power, M.S., Roberston, P.K., Seed, R.B., Sotkkoe, K.H. II. 2001. "Liquefaction Resistance of Soils: Summary Report From the 1996 NCEER and 1998 NCEER/NSF Workshops on Evaluation of Liquefaction Resistance of Soils." *Journal of Geotechnical and Geoenvironmental Engineering.* ASCE, Vol. 127, No. 10. pp 817-833.

APPENDICES

APPENDIX A

RESULTS OF THE LIMIT EQUILIBRIUM SLOPE STABILITY ANALYSES AND THE NEWMARK RIGID, SLIDING BLOCK ANALYSES

The limit-equilibrium slope stability analyses utilized Spencer's method of analysis, as implemented in the computer program UTEXAS3 (Wright 1992). Factors of safety (FoS) are provided as well as the estimated yield accelerations. The yield accelerations were not calculated for the static analyses, and the analyses were the static factor of safety was less than unity, as this represents a statically unstable geometry.

Permanent slope deformations were estimated using the rigid, sliding block procedure outlined by Newmark (1965). The displacements were estimated using all of the acceleration time histories that were recorded by the accelerometers in the failure plane for each of the centrifuge models. The mean and standard deviation of the estimated displacements is provided in the table. The following six cases were analyzed for each of the five centrifuge models:

Cases:

1 & 2: Static analyses, circular and non-circular failure plane searches.

3 & 4: Seismic analyses, circular and non-circular failure plane searches, mean excess pore pressure ratio, as measured in the representative centrifuge model, was used to calculate reduced soil strengths as:

$$\phi'_{eq} = tan^{-1}\left[(1 - r_u)tan(\phi')\right]$$

5 & 6: Seismic analyses, circular and non-circular failure plane searches, mean plus one standard deviation excess pore pressure ratio, as measured in the representative centrifuge model, was used to calculate reduced soil strengths.

7 & 8: The same as 1 & 2, except that the effect of the pile elements was included as a pseudo-cohesion in the soil layers through which the failure plane passed. The pseudo-cohesion was estimated following the method outlined in Manuscript No. 3.

9 & 10: The same as 3 & 4, except that the effect of the pile elements was included as a pseudo-cohesion in the soil layers through which the failure plane passed. The pseudo-cohesion was estimated following the method outlined in Manuscript No. 3.

11 & 12: The same as 5 & 6, except that the effect of the pile elements was included as a pseudo-cohesion in the soil layers through which the failure plane passed. The pseudo-cohesion was estimated following the method outlined in Manuscript No. 3.

13 & 14: The same as 1 & 2, except that the effect of the pile elements was included as reinforcement elements, as implemented in the UTEXAS3 computer program.

15 & 16: The same as 3 & 4, except that the effect of the pile elements was included as reinforcement elements, as implemented in the UTEXAS3 computer program.

17 & 18: The same as 5 & 6, except that the effect of the pile elements was included as reinforcement elements, as implemented in the UTEXAS3 computer program.

Model	Case	Failure Plane	Piles?	Excess PP Ratio, r_u		Static FoS	Yield Acc (g)	Newmark Disp. (mm)	
				Loose Sand	Dense Sand			Mean	Std. Dev.
NJM01	1	Circular	no	0.00	0.00	*1.474*	-	-	-
NJM01	2	NonCircular	no	0.00	0.00	1.880	-	-	-
NJM01	3	Circular	no	0.60	0.24	1.661	0.175	0.0	0.1
NJM01	4	NonCircular	no	0.60	0.24	1.545	0.095	9.0	6.9
NJM01	5	Circular	no	0.80	0.24	1.208	0.045	201.4	70.8
NJM01	6	NonCircular	no	0.80	0.24	0.810	-	-	-
NJM01	7	Circular	as COH	0.00	0.00	2.066	-	-	-
NJM01	8	NonCircular	as COH	0.00	0.00	2.030	-	-	-
NJM01	9	Circular	as COH	0.60	0.24	1.892	0.223	0.0	0.0
NJM01	10	NonCircular	as COH	0.60	0.24	1.690	0.127	0.3	0.8
NJM01	11	Circular	as COH	0.80	0.24	1.401	0.105	3.6	3.5
NJM01	12	NonCircular	as COH	0.80	0.24	1.107	0.021	595.8	123.1
NJM01	13	Circular	as REIN	0.00	0.00	2.168	-	-	-
NJM01	14	NonCircular	as REIN	0.00	0.00	2.355	-	-	-
NJM01	15	Circular	as REIN	0.60	0.24	1.778	0.174	0.0	0.1
NJM01	16	NonCircular	as REIN	0.60	0.24	1.554	0.094	9.5	7.1
NJM01	17	Circular	as REIN	0.80	0.24	1.297	0.060	94.5	42.9
NJM01	18	NonCircular	as REIN	0.80	0.24	0.851	-	-	-
NJM02	1	Circular	no	0.00	0.00	1.642	-	-	-
NJM02	2	NonCircular	no	0.00	0.00	1.557	-	-	-
NJM02	3	Circular	no	0.42	0.21, 0.07	1.364	0.074	167.1	49.6
NJM02	4	NonCircular	no	0.42	0.21, 0.07	1.370	0.065	225.5	67.0
NJM02	5	Circular	no	0.52	0.21, 0.07	1.314	0.064	236.1	70.2
NJM02	6	NonCircular	no	0.52	0.21, 0.07	1.256	0.047	425.8	121.7
NJM02	7	Circular	as COH	0.00	0.00	1.781	-	-	-
NJM02	8	NonCircular	as COH	0.00	0.00	1.730	-	-	-
NJM02	9	Circular	as COH	0.42	0.21, 0.07	1.500	0.100	64.6	21.1
NJM02	10	NonCircular	as COH	0.42	0.21, 0.07	1.427	0.088	101.5	30.5
NJM02	11	Circular	as COH	0.52	0.21, 0.07	1.449	0.090	94.3	28.5
NJM02	12	NonCircular	as COH	0.52	0.21, 0.07	1.424	0.075	161.4	47.9
NJM02	13	Circular	as REIN	0.00	0.00	1.969	-	-	-
NJM02	14	NonCircular	as REIN	0.00	0.00	1.853	-	-	-
NJM02	15	Circular	as REIN	0.42	0.21, 0.07	1.602	0.101	64.6	21.1

Model	Case	Failure Plane	Piles?	Excess PP Ratio, r_u		Static FoS	Yield Acc (g)	Newmark Disp. (mm)	
				Loose Sand	Dense Sand			Mean	Std. Dev.
NJM02	16	NonCircular	as REIN	0.42	0.21, 0.07	1.557	0.092	87.6	26.7
NJM02	17	Circular	as REIN	0.52	0.21, 0.07	1.503	0.082	126.1	37.6
NJM02	18	NonCircular	as REIN	0.52	0.21, 0.07	1.437	0.069	198.8	59.0
SMS01	1	Circular	no	0.00	0.00	2.081	-	-	-
SMS01	2	NonCircular	no	0.00	0.00	2.031	-	-	-
SMS01	3	Circular	no	1.00	0.47	1.365	0.068	689.8	438.2
SMS01	4	NonCircular	no	1.00	0.47	1.331	0.061	819.0	469.4
SMS01	5	Circular	no	1.00	0.70	0.850	-	-	-
SMS01	6	NonCircular	no	1.00	0.70	0.786	-	-	-
SMS01	7	Circular	as COH	0.00	0.00	2.421	-	-	-
SMS01	8	NonCircular	as COH	0.00	0.00	2.375	-	-	-
SMS01	9	Circular	as COH	1.00	0.47	1.549	0.101	310.2	270.5
SMS01	10	NonCircular	as COH	1.00	0.47	1.510	0.101	310.2	270.5
SMS01	11	Circular	as COH	1.00	0.70	-	-	-	-
SMS01	12	NonCircular	as COH	1.00	0.70	-	-	-	-
SMS01	13	Circular	as REIN	0.00	0.00	2.792	-	-	-
SMS01	14	NonCircular	as REIN	0.00	0.00	2.776	-	-	-
SMS01	15	Circular	as REIN	1.00	0.47	1.669	0.098	332.3	284.3
SMS01	16	NonCircular	as REIN	1.00	0.47	1.619	0.095	350.2	283.3
SMS01	17	Circular	as REIN	1.00	0.70	0.997	-	-	-
SMS01	18	NonCircular	as REIN	1.00	0.70	0.951	-	-	-
SMS02	1	Circular	no	-	0.00	2.140	-	-	-
SMS02	2	NonCircular	no	-	0.00	1.946	-	-	-
SMS02	3	Circular	no	-	0.27	1.891	0.165	0.2	0.5
SMS02	4	NonCircular	no	-	0.27	1.684	0.129	6.2	9.3
SMS02	5	Circular	no	-	0.58	1.382	0.067	136.8	70.2
SMS02	6	NonCircular	no	-	0.58	1.186	0.050	248.4	110.4
SMS02	7	Circular	as COH	-	0.00	3.236	-	-	-
SMS02	8	NonCircular	as COH	-	0.00	3.332	-	-	-
SMS02	9	Circular	as COH	-	0.27	2.893	0.349	0.0	0.0
SMS02	10	NonCircular	as COH	-	0.27	3.002	0.409	0.0	0.0
SMS02	11	Circular	as COH	-	0.58	2.230	0.206	0.0	0.0
SMS02	12	NonCircular	as COH	-	0.58	2.475	0.282	0.0	0.0
SMS02	13	Circular	as REIN	-	0.00	3.443	-	-	-
SMS02	14	NonCircular	as REIN	-	0.00	3.515	-	-	-
SMS02	15	Circular	as REIN	-	0.27	2.585	0.292	0.0	0.0
SMS02	16	NonCircular	as REIN	-	0.27	2.593	0.320	0.0	0.0
SMS02	17	Circular	as REIN	-	0.58	1.709	0.102	30.1	24.9
SMS02	18	NonCircular	as REIN	-	0.58	1.679	0.097	38.6	29.0

Model	Case	Failure Plane	Piles?	Excess PP Ratio, r_u		Static FoS	Yield Acc (g)	Newmark Disp. (mm)	
				Loose Sand	Dense Sand			Mean	Std. Dev.
JCB01	1	Circular	no	0.00	0.00		-	-	-
JCB01	2	NonCircular	no	0.00	0.00	1.403	-	-	-
JCB01	3	Circular	no	0.70	0.30	0.521	-	-	-
JCB01	4	NonCircular	no	0.70	0.30	0.587	-	-	-
JCB01	5	Circular	no	0.94	0.37		-	-	-
JCB01	6	NonCircular	no	0.94	0.37		-	-	-
JCB01	7	Circular	as COH	0.00	0.00		-	-	-
JCB01	8	NonCircular	as COH	0.00	0.00		-	-	-
JCB01	9	Circular	as COH	0.70	0.30	3.307	0.500	0.0	0.0
JCB01	10	NonCircular	as COH	0.70	0.30				
JCB01	11	Circular	as COH	0.94	0.37				
JCB01	12	NonCircular	as COH	0.94	0.37				
JCB01	13	Circular	as REIN	0.00	0.00	3.504	-	-	-
JCB01	14	NonCircular	as REIN	0.00	0.00	4.606	-	-	-
JCB01	15	Circular	as REIN	0.70	0.30	2.452	0.153	0.1	0.3
JCB01	16	NonCircular	as REIN	0.70	0.30	2.007	0.097	22.2	11.8
JCB01	17	Circular	as REIN	0.94	0.37	2.165	0.115	7.1	4.7
JCB01	18	NonCircular	as REIN	0.94	0.37	2.302	0.090	33.0	17.5

NJM01 – CASES 1 AND 2

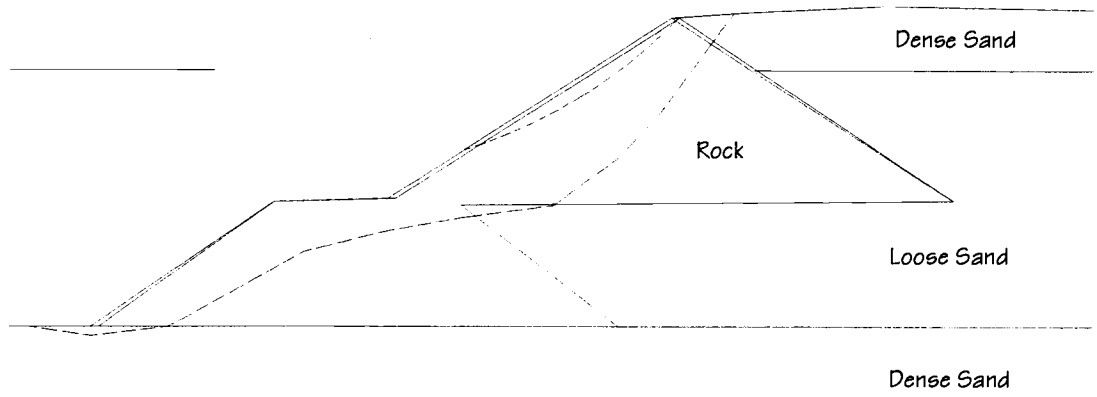

NJM01 – CASES 3 AND 4

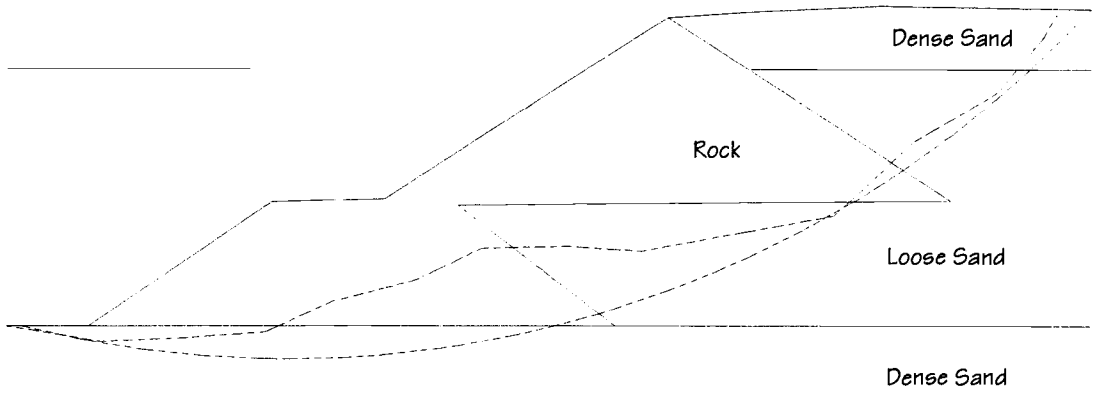

NJM01 – CASES 5 AND 6

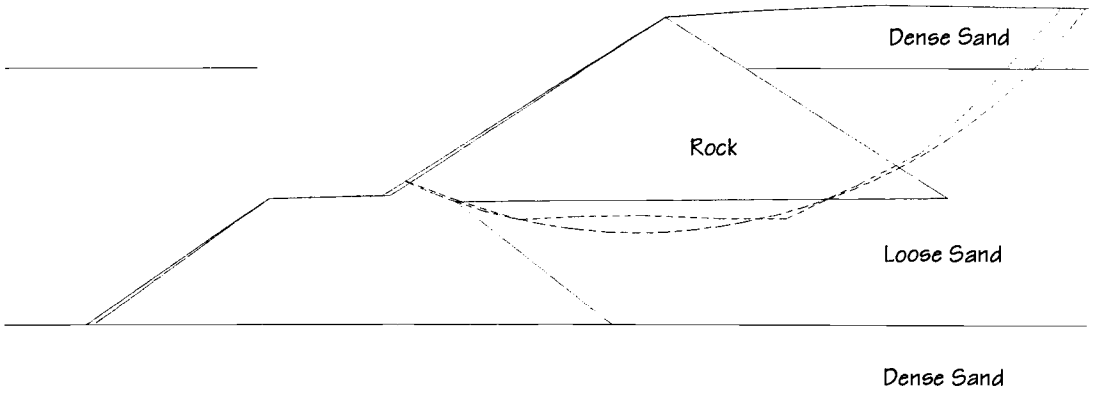

NJM01 – CASES 7 AND 8

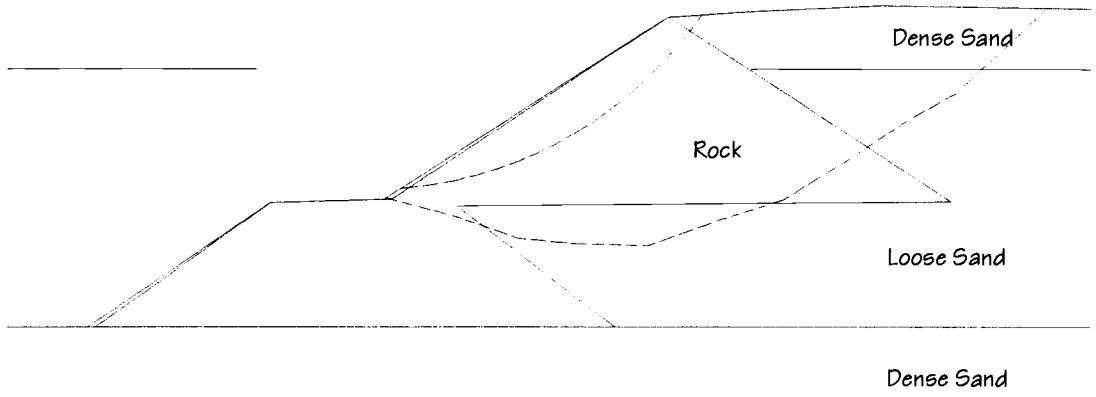

NJM01 – CASES 9 AND 10

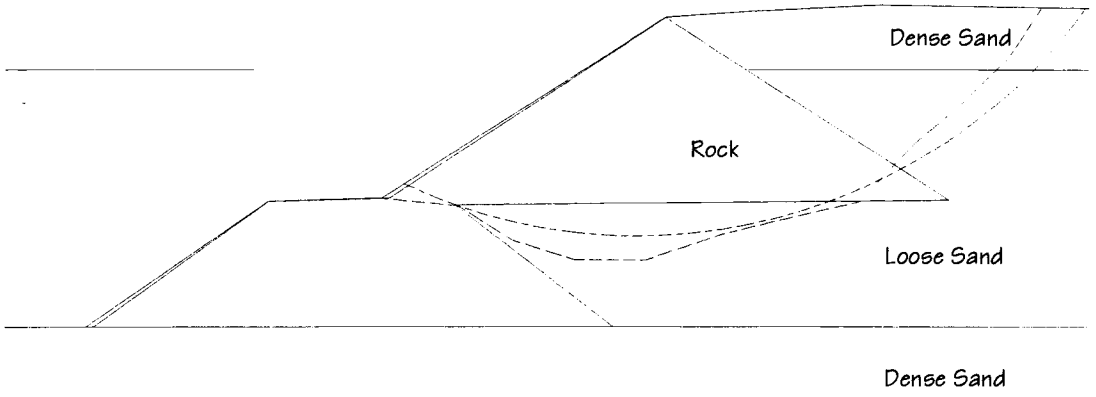

NJM01 – CASES 11 AND 12

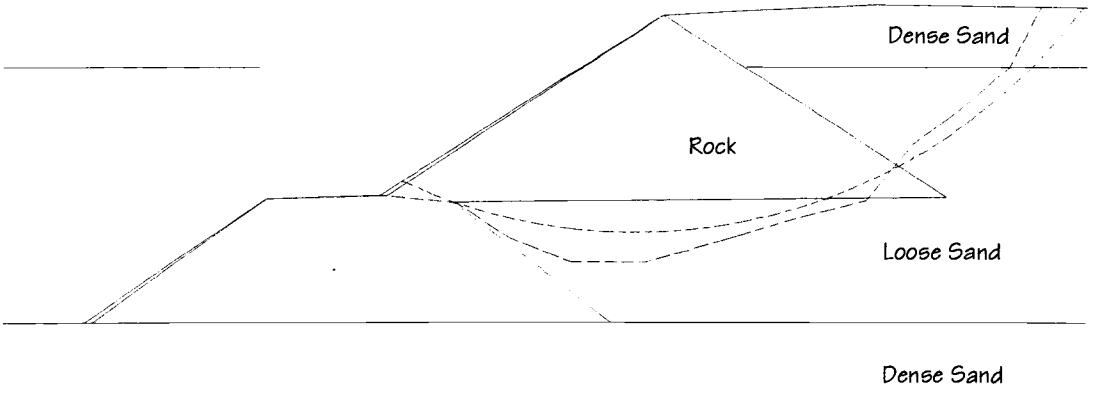

NJM01 – CASES 13 AND 14

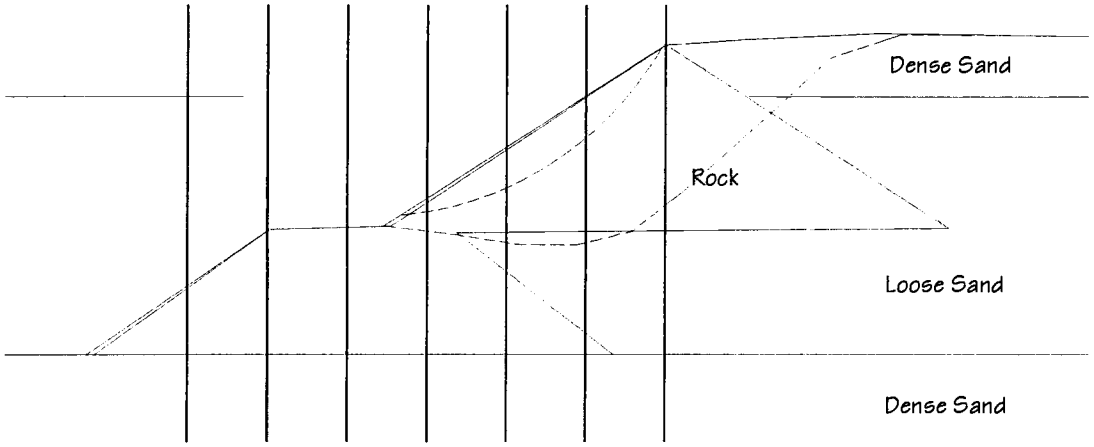

NJM01 – CASES 15 AND 16

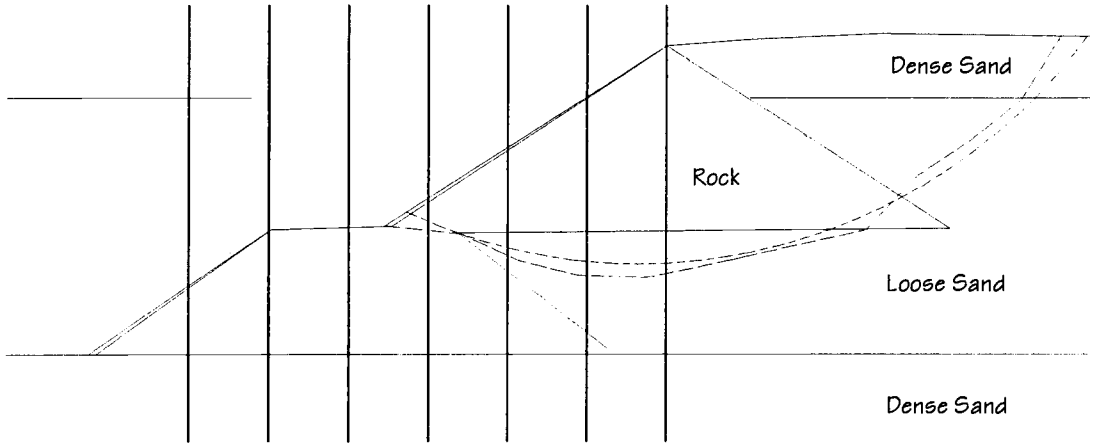

NJM01 – CASES 17 AND 18

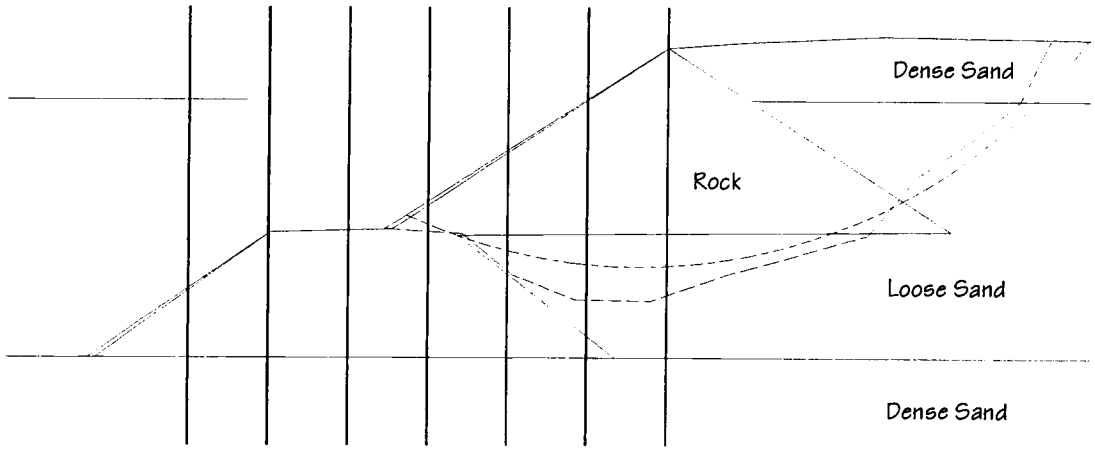

NJM02 – CASES 1 AND 2

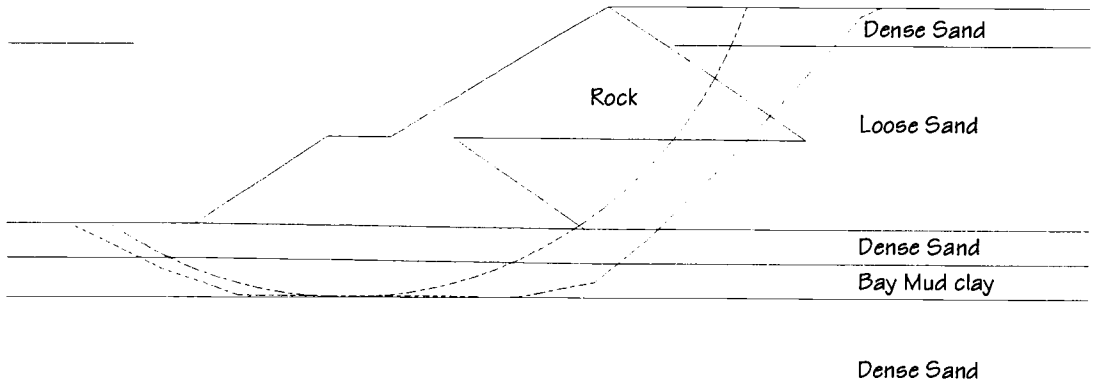

NJM02 – CASES 3 AND 4

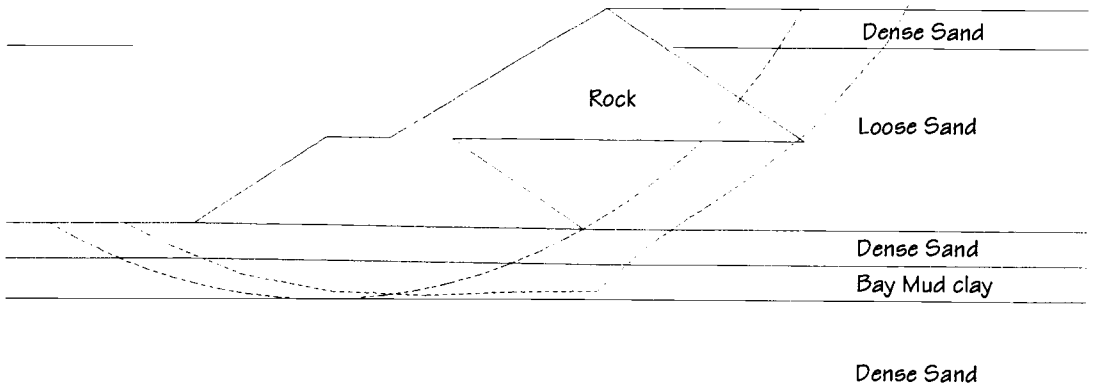

NJM02 – CASES 5 AND 6

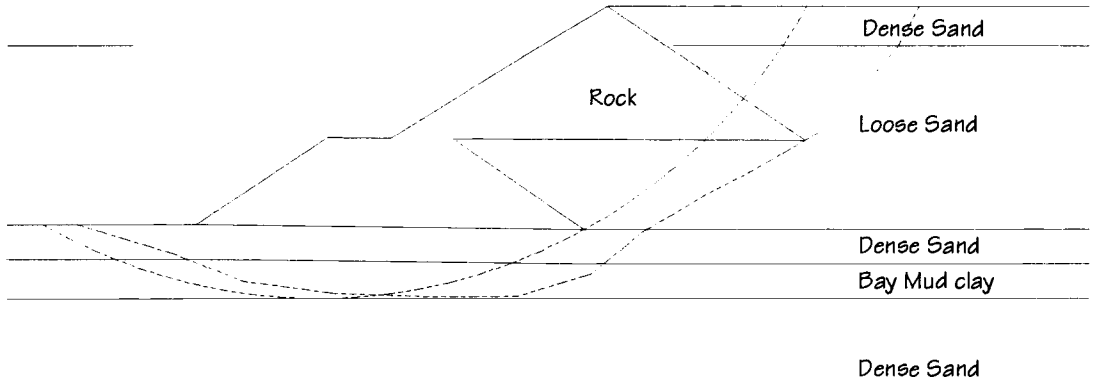

NJM02 – CASES 7 AND 8

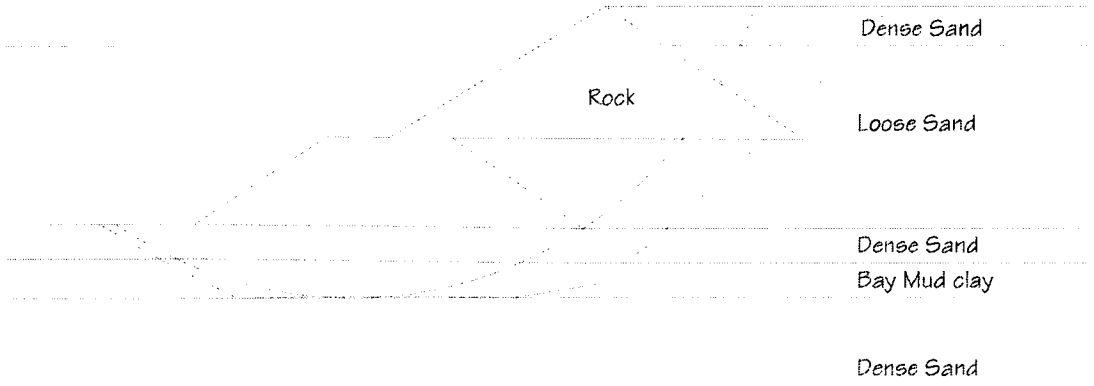

NJM02 – CASES 9 AND 10

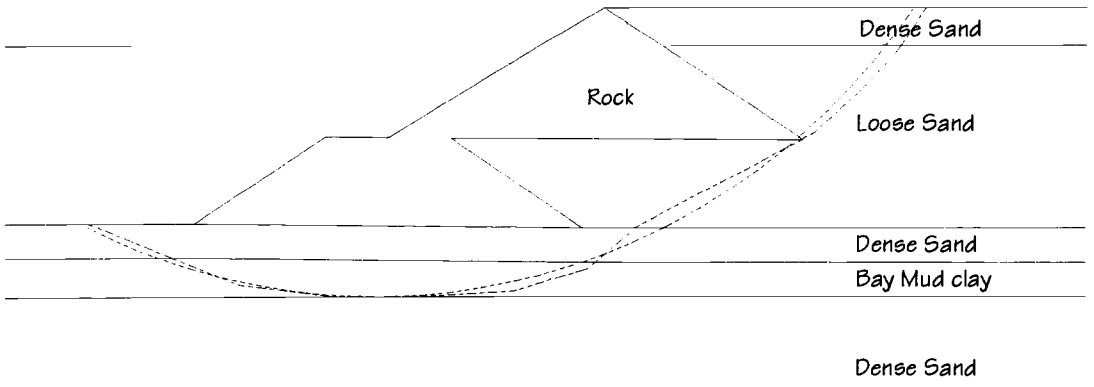

NJM02 – CASES 11 AND 12

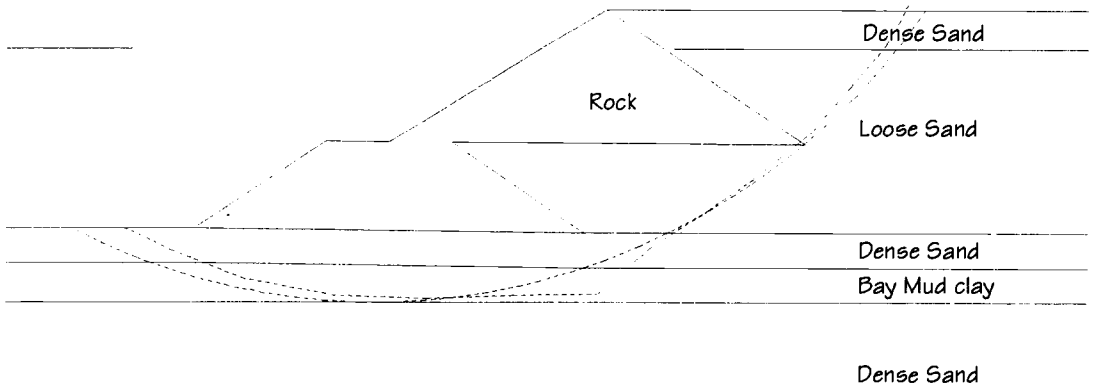

NJM02 – CASES 13 AND 14

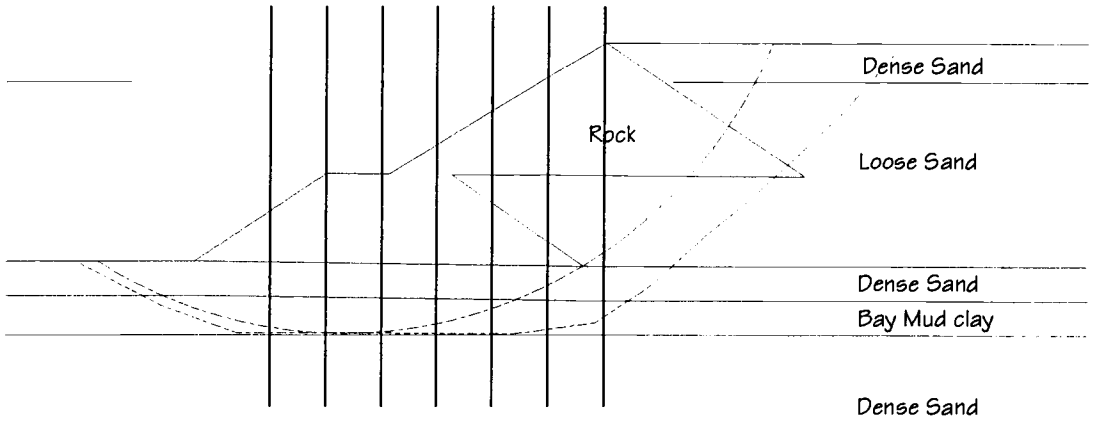

NJM02 – CASES 15 AND 16

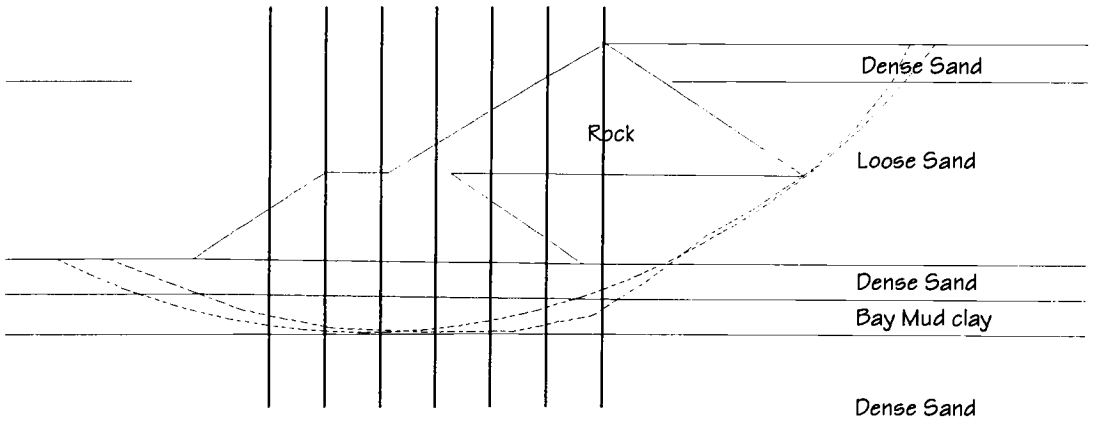

NJM02 – CASES 17 AND 18

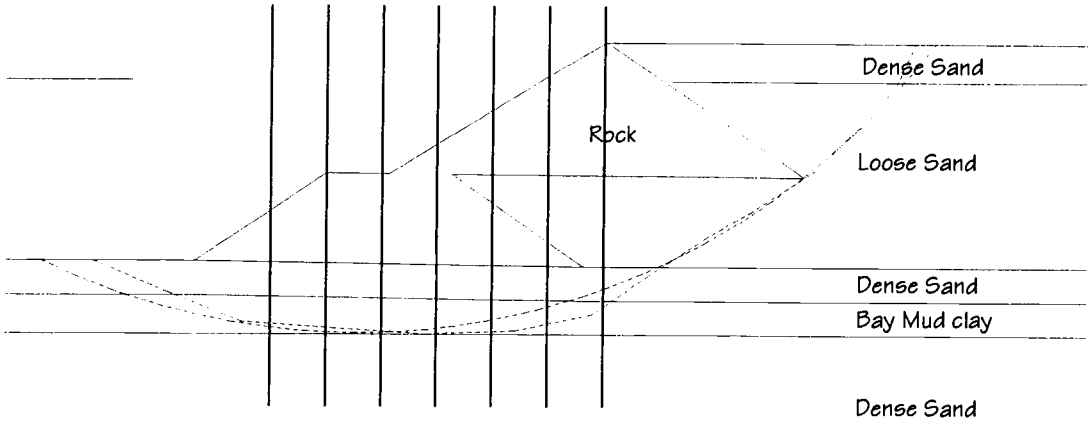

SMS01 – CASES 1 AND 2

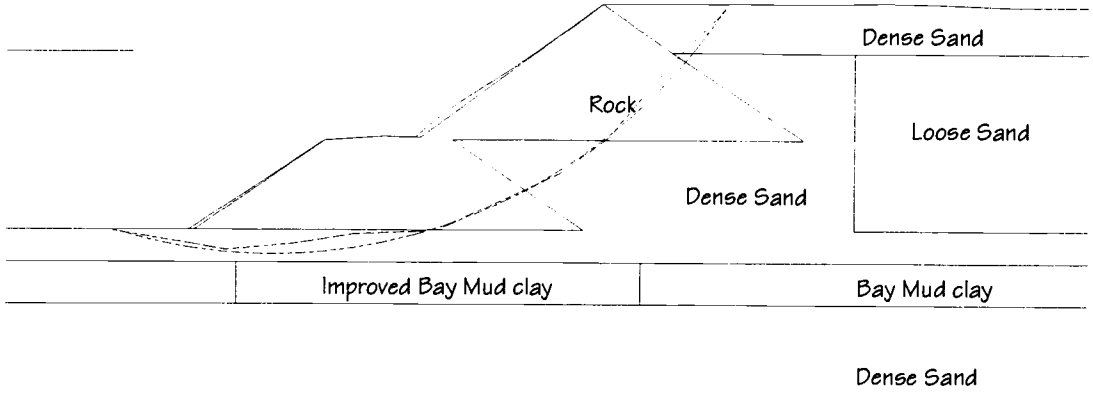

SMS01 – CASES 3 AND 4

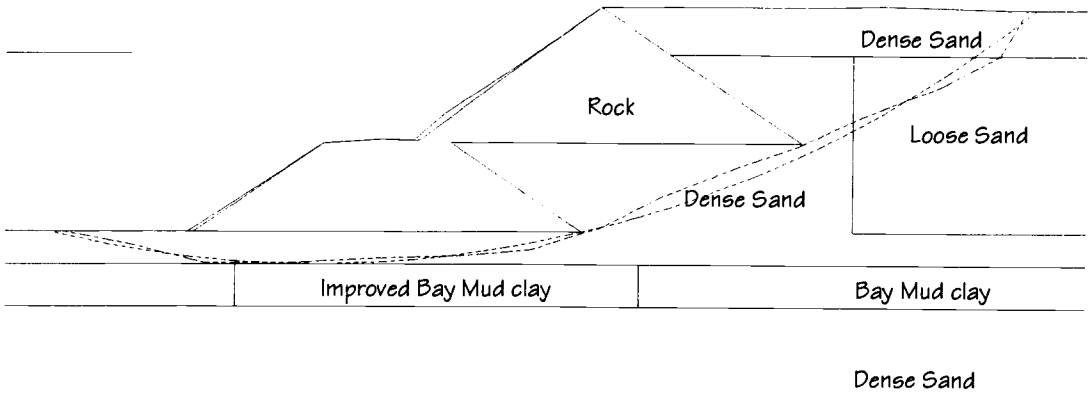

SMS01 – CASES 5 AND 6

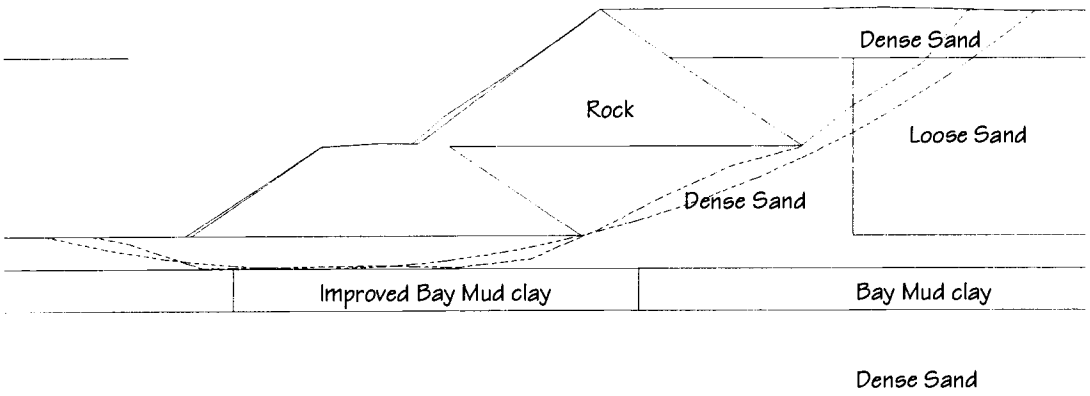

SMS01 – CASES 7 AND 8

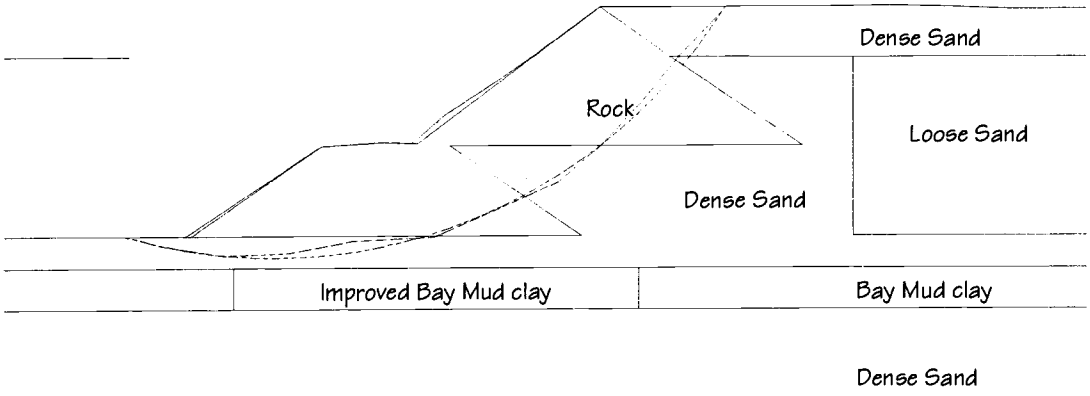

SMS01 – CASES 9 AND 10

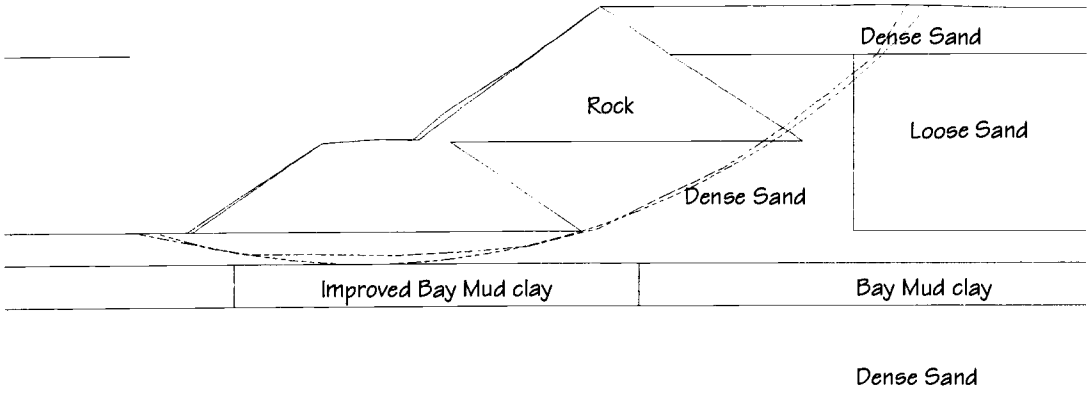

SMS01 – CASES 11 AND 12

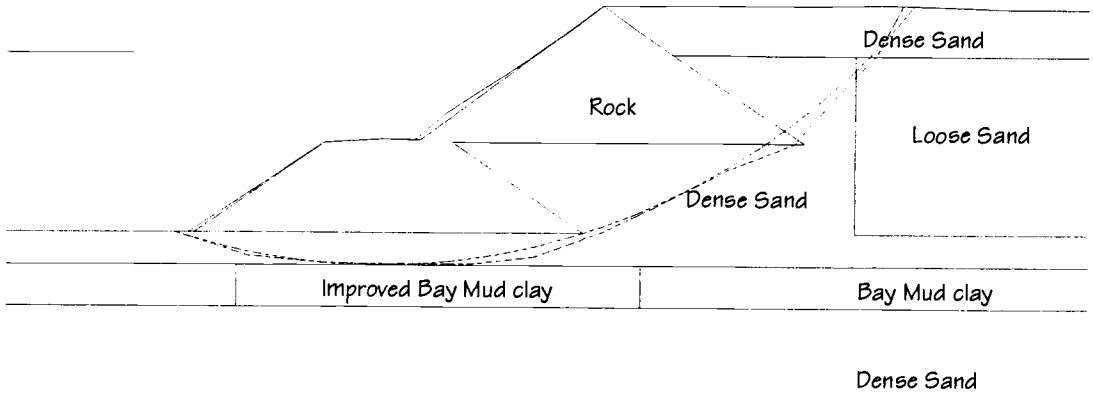

SMS01 – CASES 13 AND 14

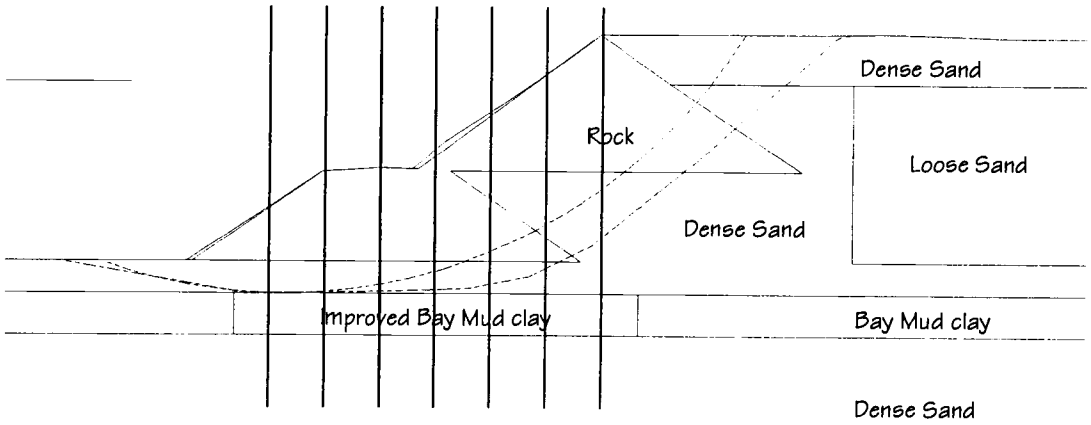

SMS01 – CASES 15 AND 16

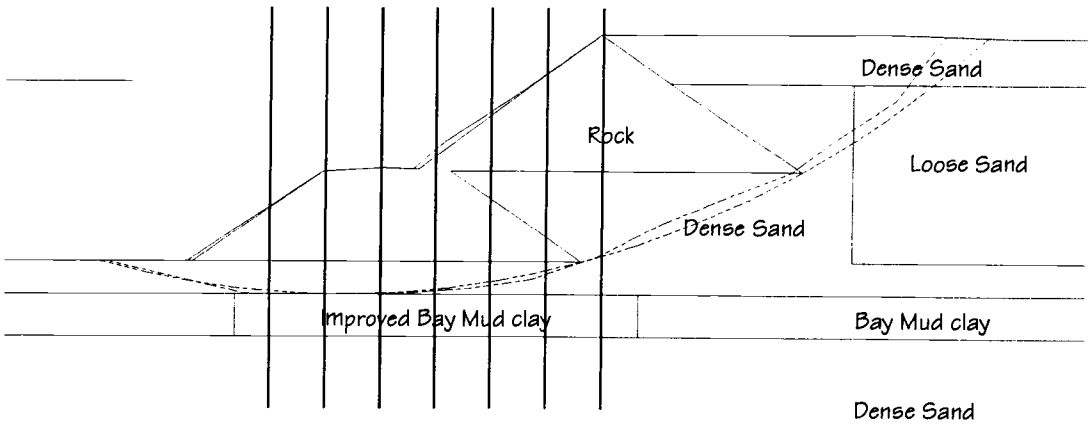

SMS01 – CASES 17 AND 18

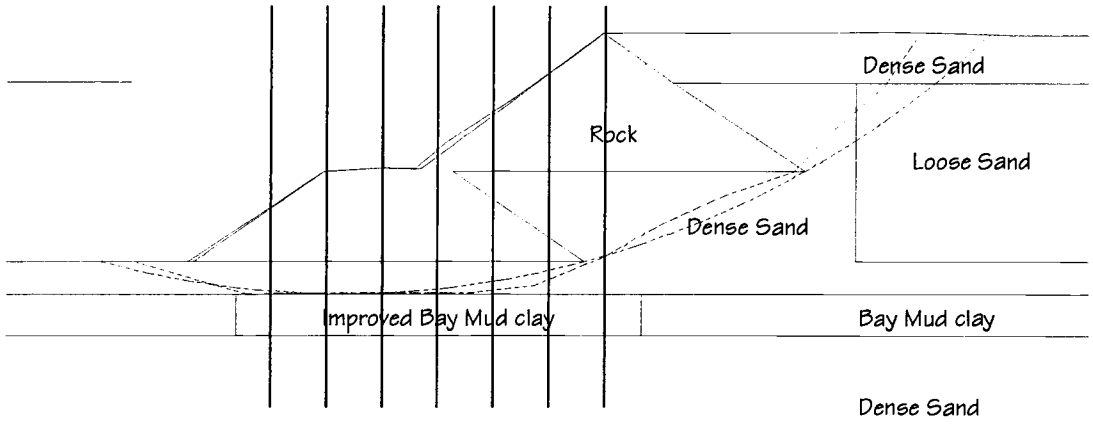

SMS02 – CASES 1 AND 2

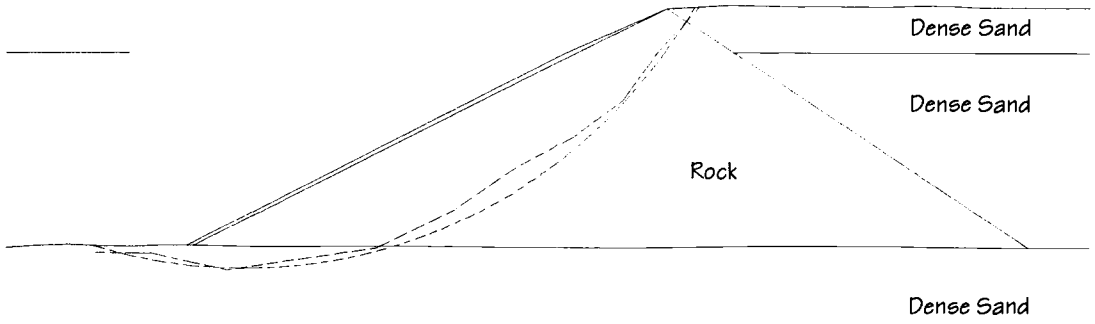

SMS02 – CASES 3 AND 4

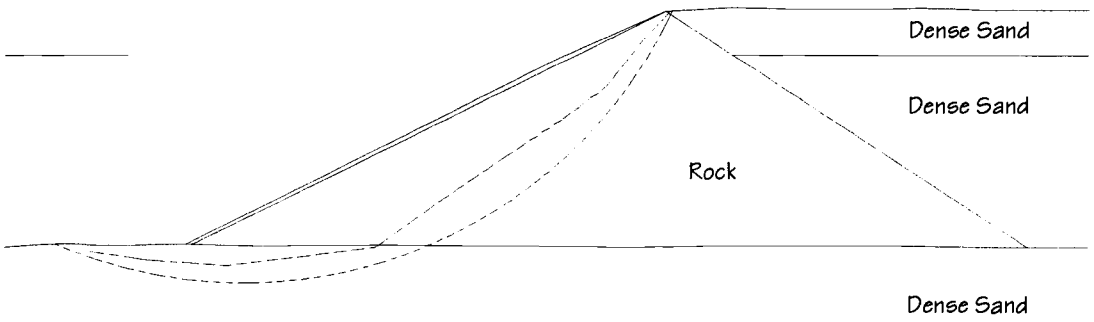

SMS02 – CASES 5 AND 6

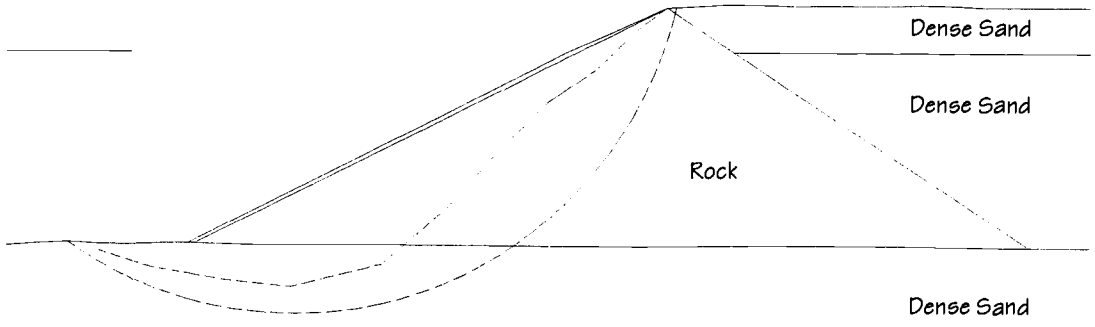

SMS02 – CASES 7 AND 8

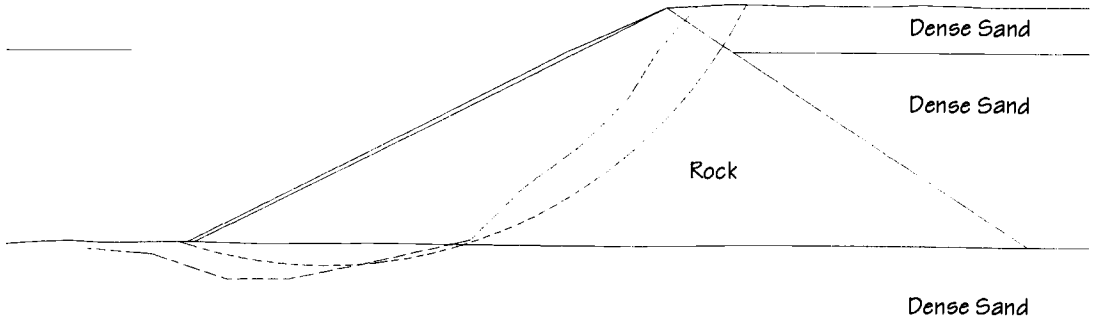

SMS02 – CASES 9 AND 10

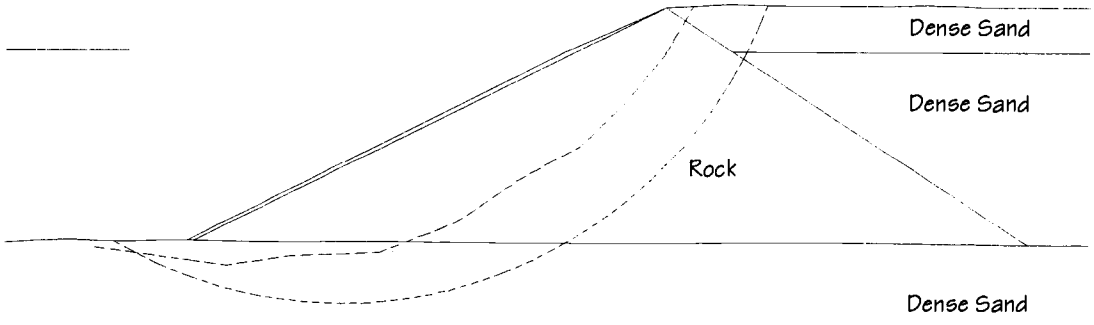

SMS02 – CASES 11 AND 12

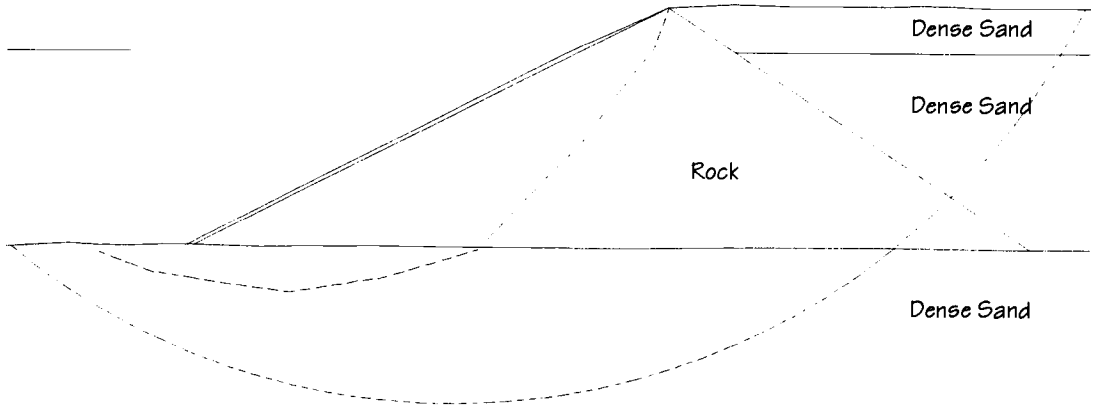

SMS02 – CASES 13 AND 14

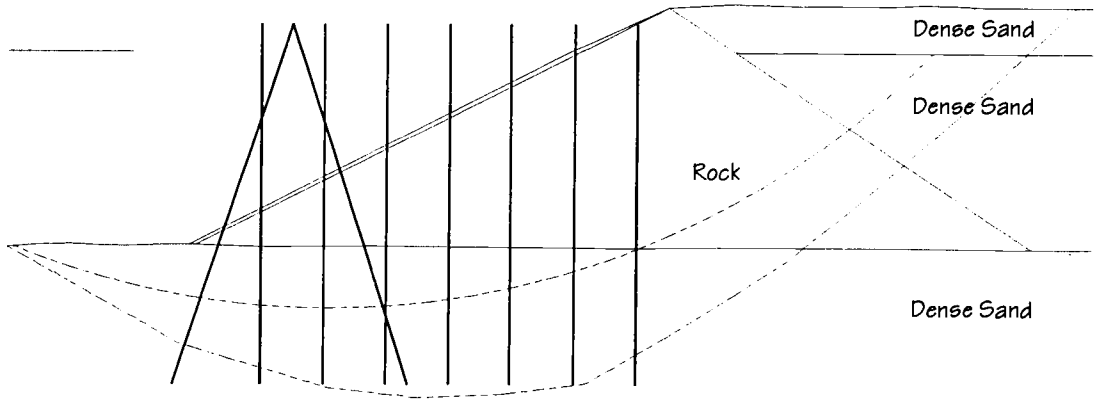

SMS02 – CASES 15 AND 16

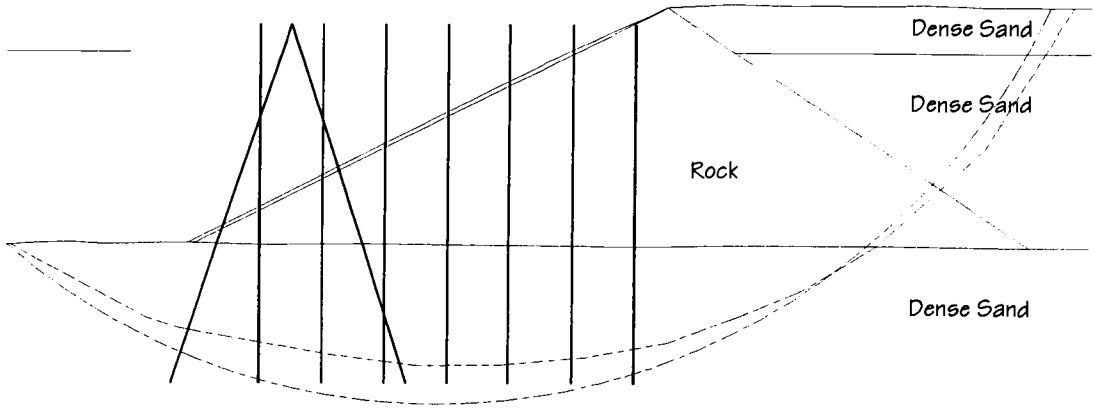

SMS02 – CASES 17 AND 18

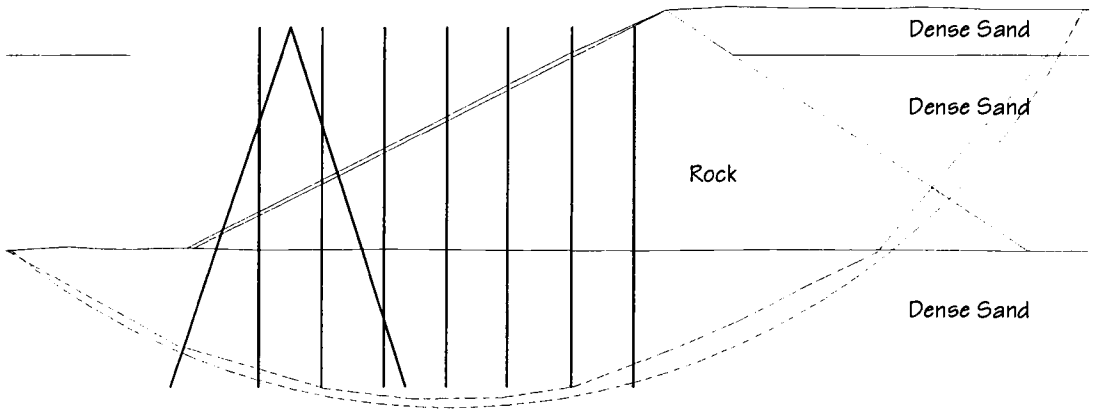

JCB01 – CASES 1 AND 2

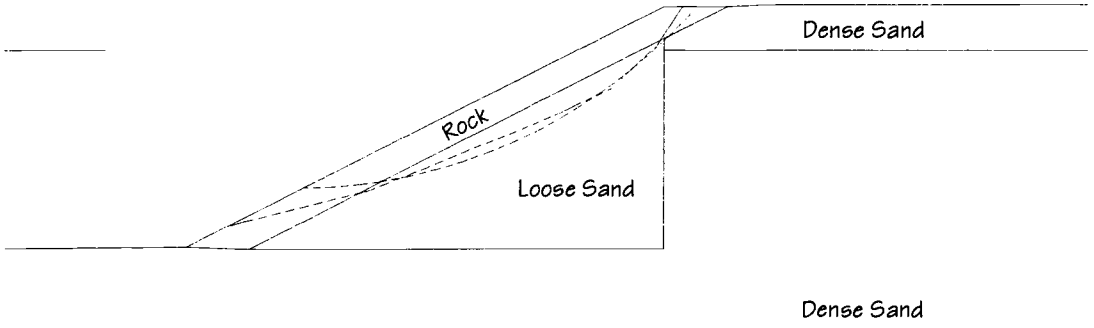

JCB01 – CASES 3 AND 4

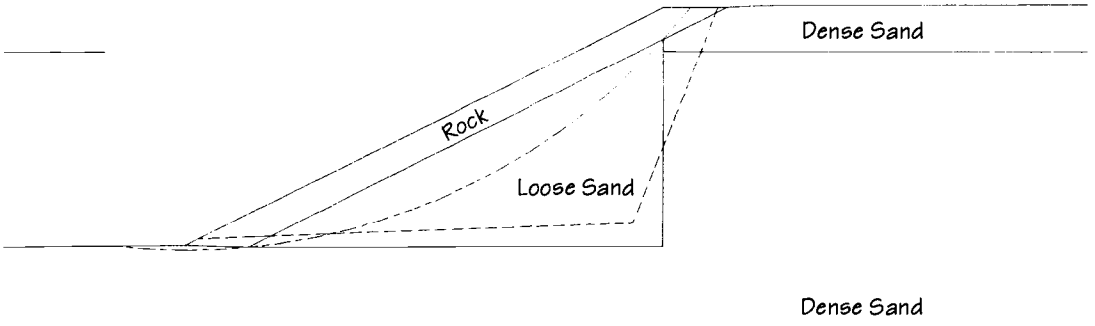

JCB01 – CASE 9

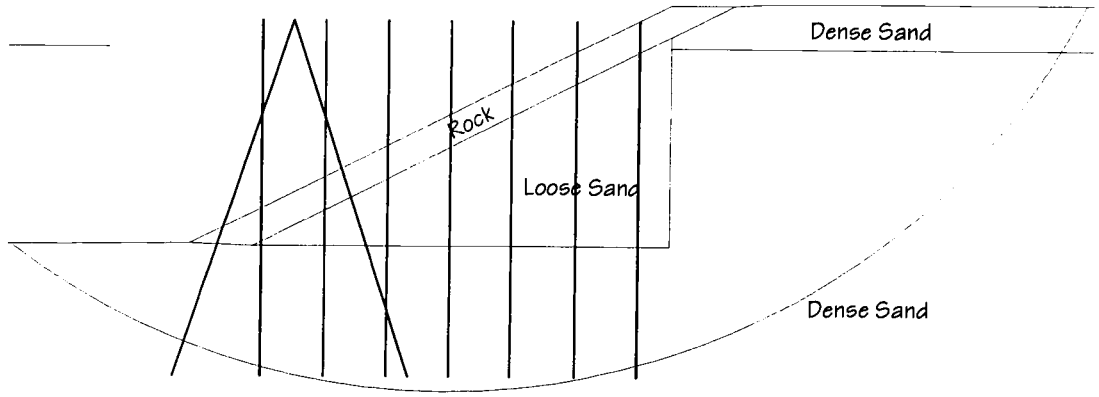

JCB01 – CASES 13 AND 14

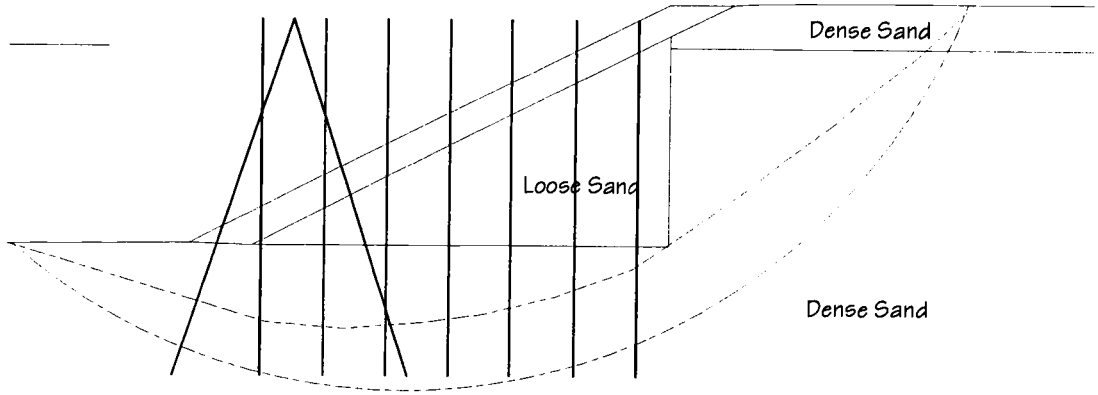

JCB01 – CASES 15 AND 16

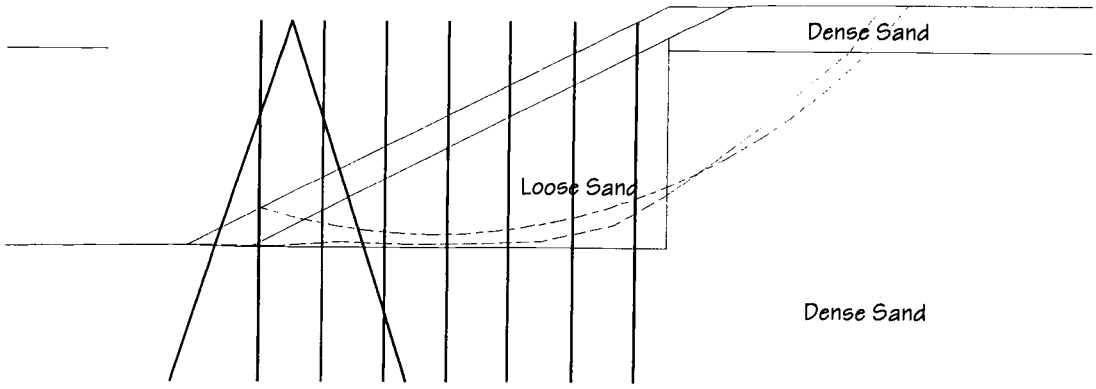

JCB01 – CASES 17 AND 18

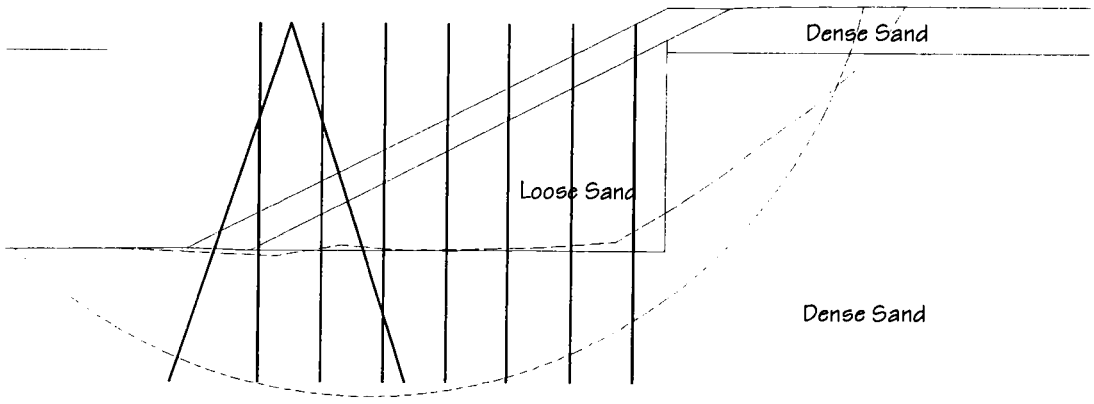

APPENDIX B

NUMERICAL MODEL PREDICTIONS OF THE CENTRIFUGE MODEL PERFORMANCE

The computer program FLAC was used for the dynamic numerical modeling. The following figures graphically illustrate the results of the analyses of the centrifuge models, as presented in Manuscript No. 3.

The model included the container as structural elements, and modeled the soil as a continuum. The units on the figures are metric: meters for locations and displacements and N-m for bending moments. Potentially liquefiable zones were modeled using the SEED.FIS constitutive model (see Chapter 1).

NJM01 – MESH, SOIL LAYERS AND STRUCTURAL ELEMENTS

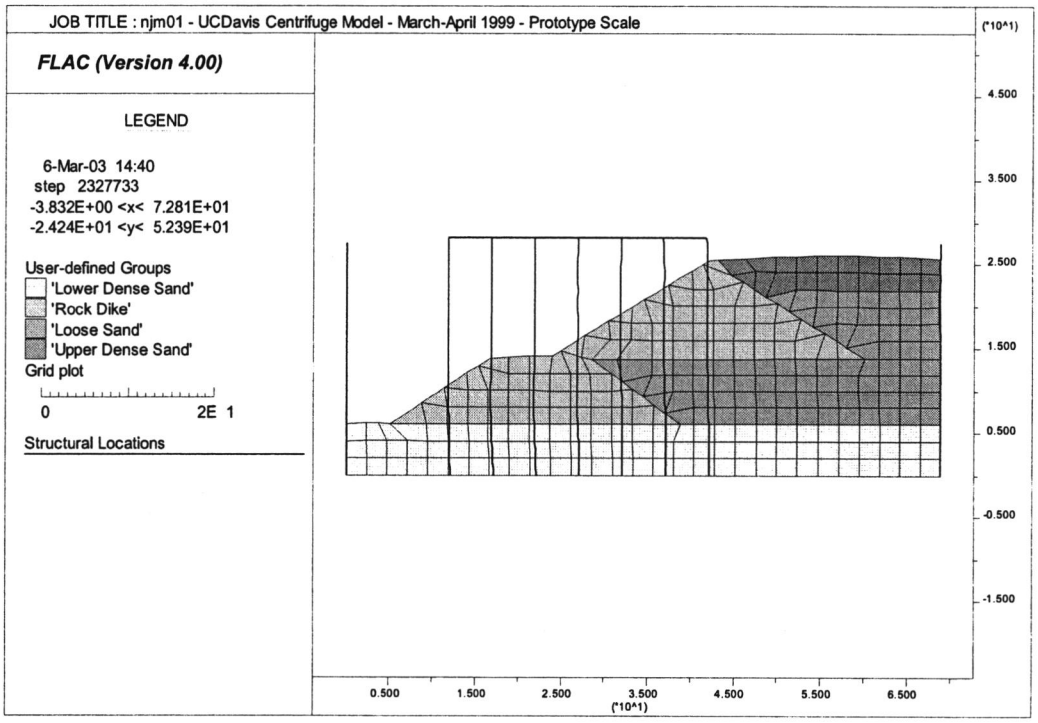

NJM01 – DISPLACEMENT VECTORS

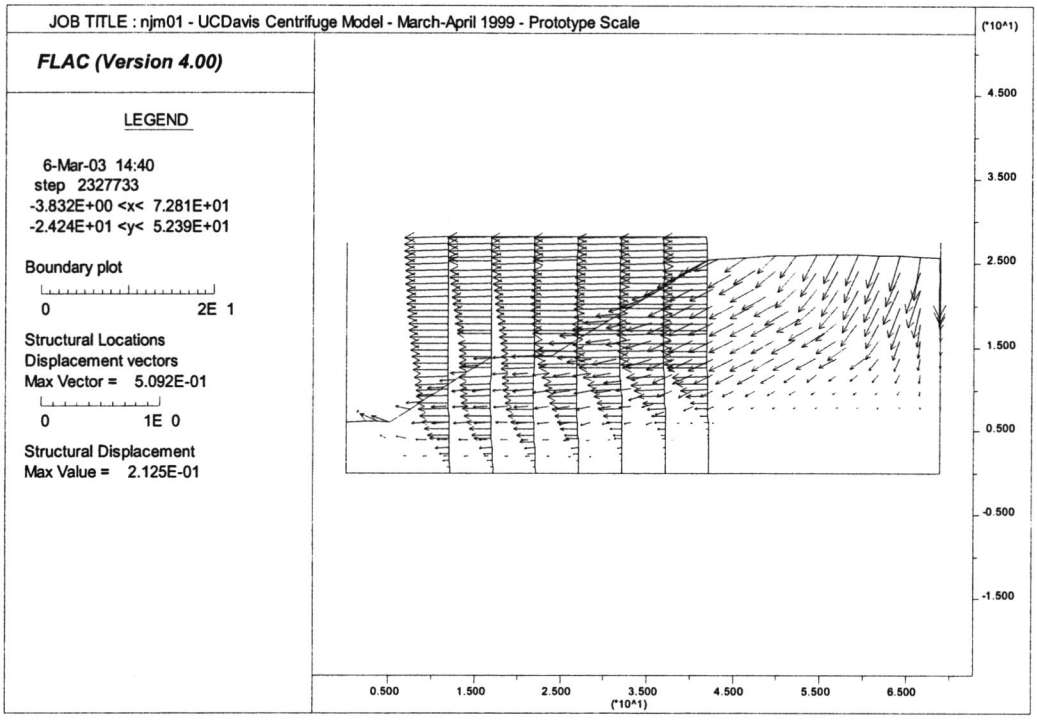

NJM01 – PILE BENDING MOMENTS

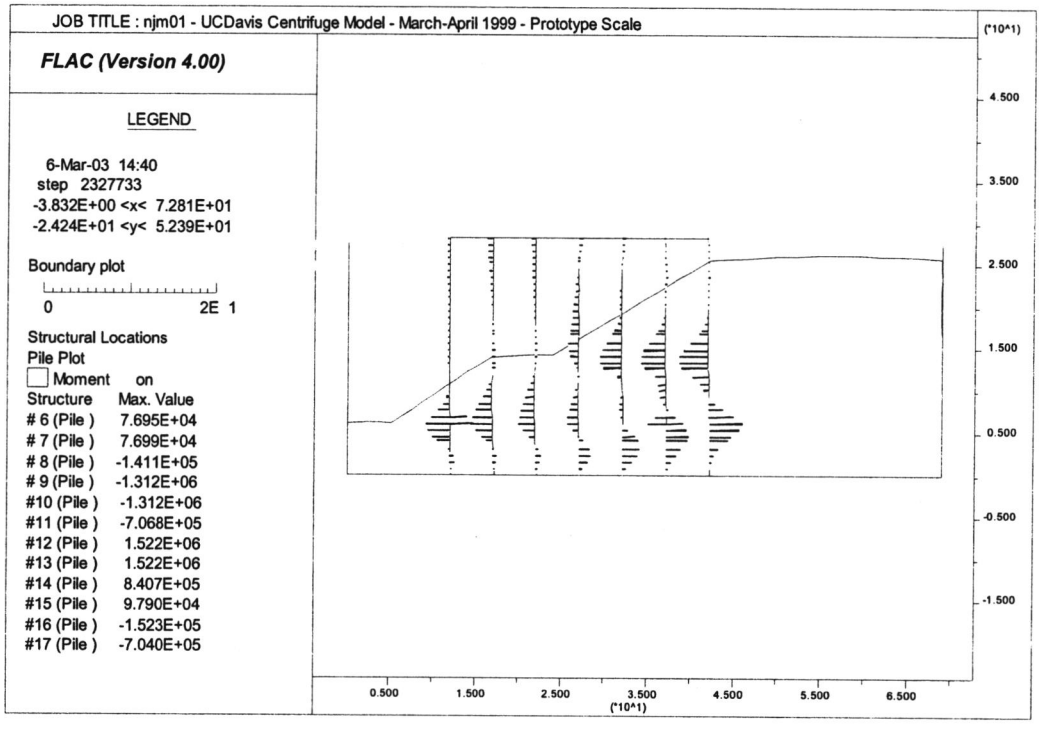

NJM01 – EXCESS PORE PRESSURE GENERATION

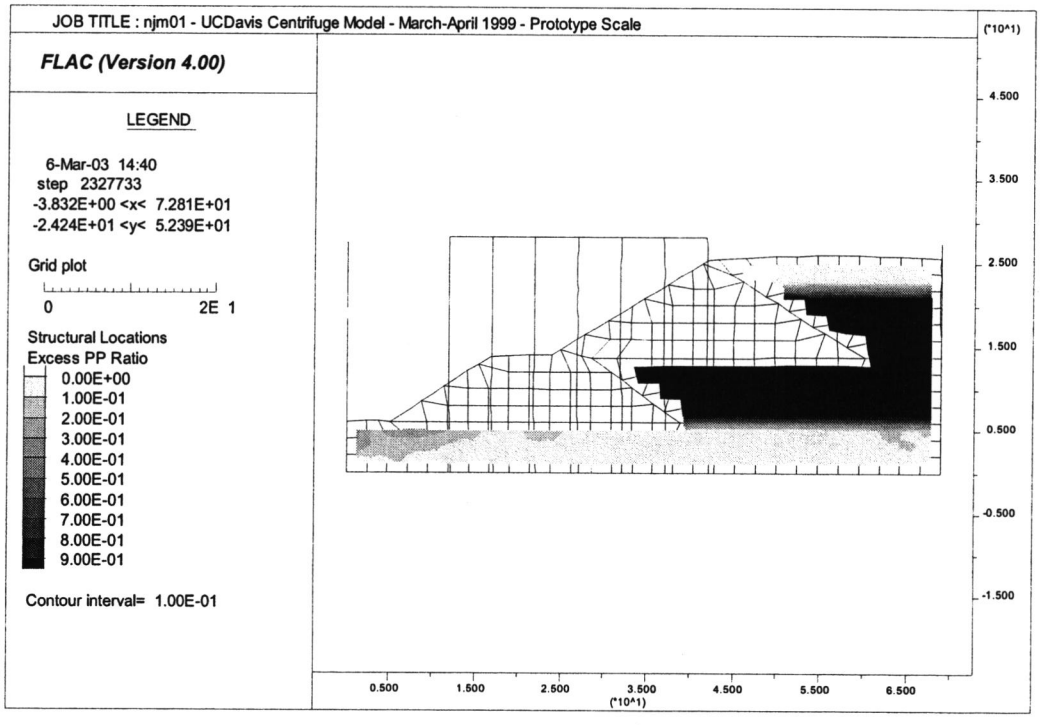

NJM02 – MESH, SOIL LAYERS AND STRUCTURAL ELEMENTS

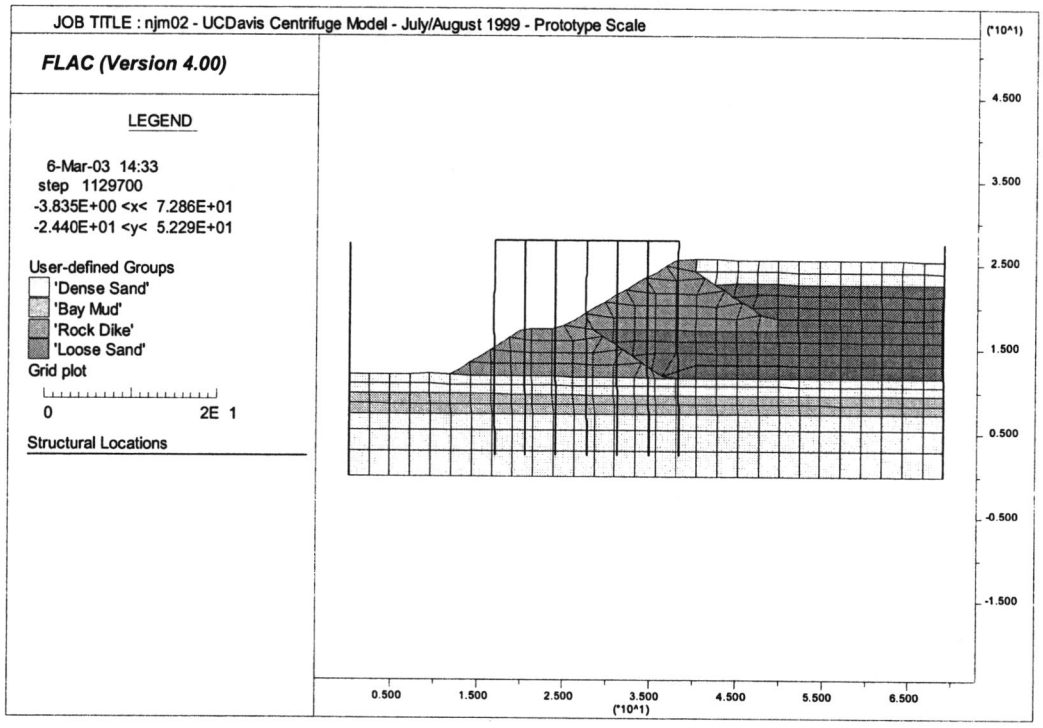

NJM02 – DISPLACEMENT VECTORS

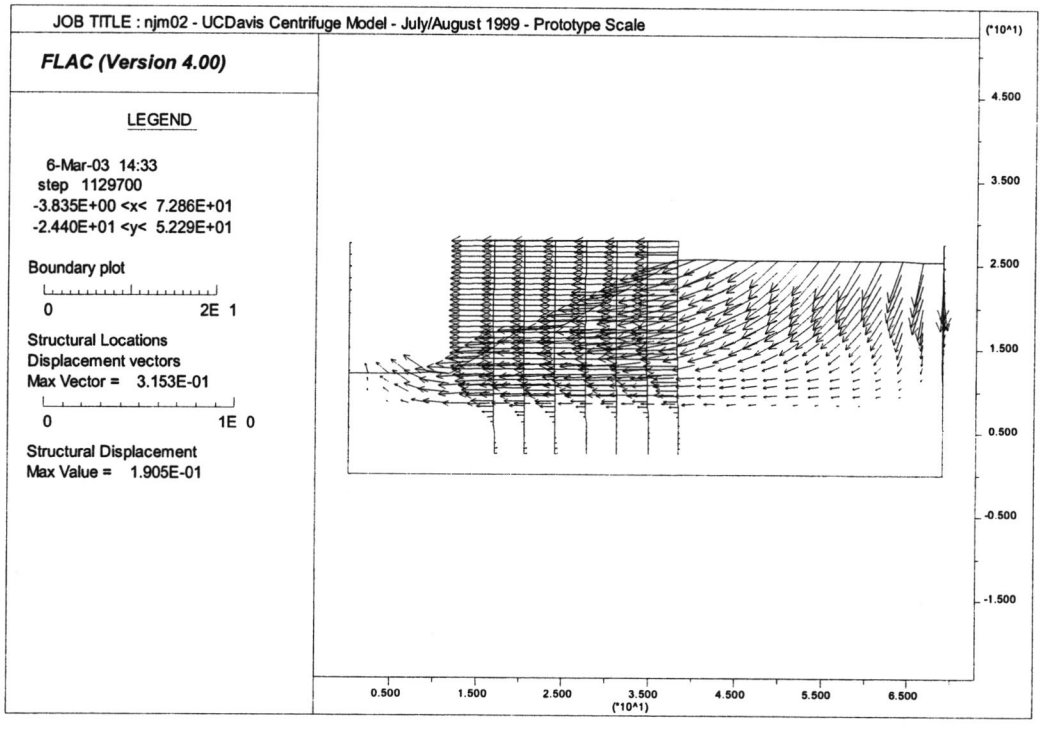

NJM02 – PILE BENDING MOMENTS

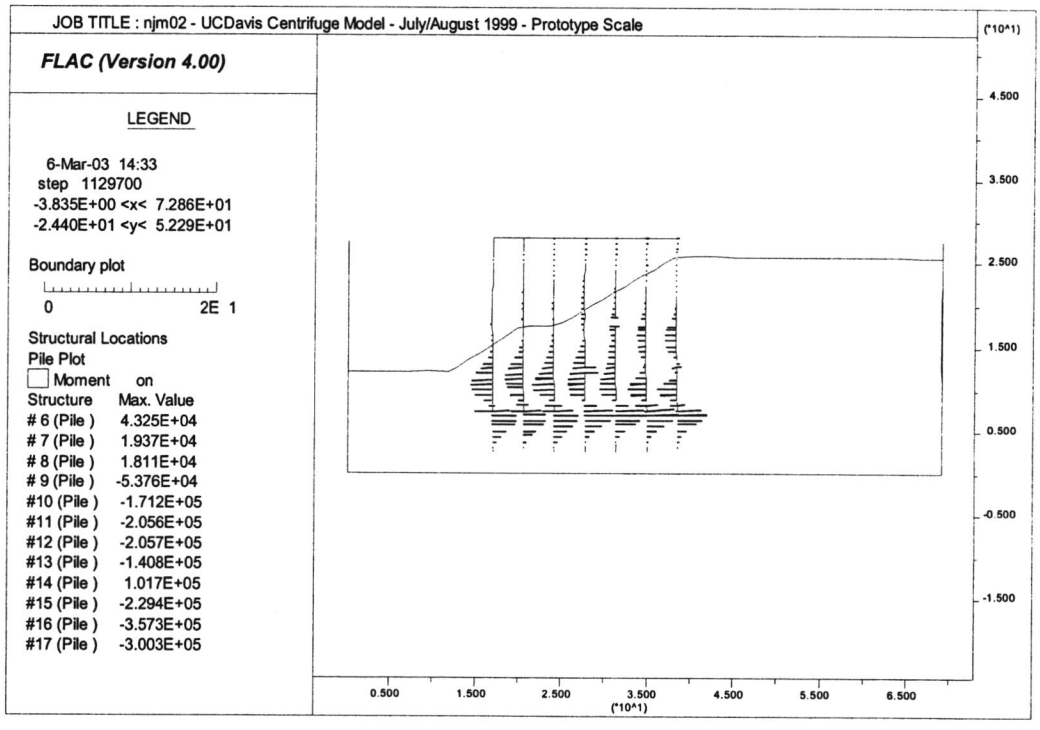

NJM02 – EXCESS PORE PRESSURE GENERATION

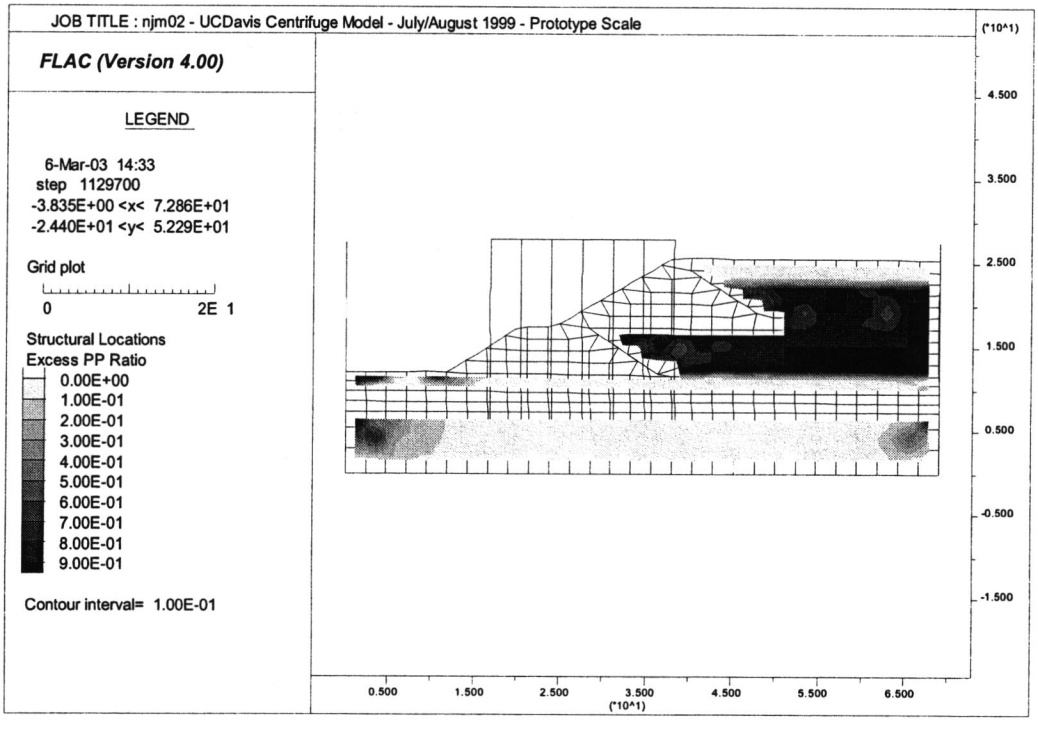

SMS01 – MESH, SOIL LAYERS AND STRUCTURAL ELEMENTS

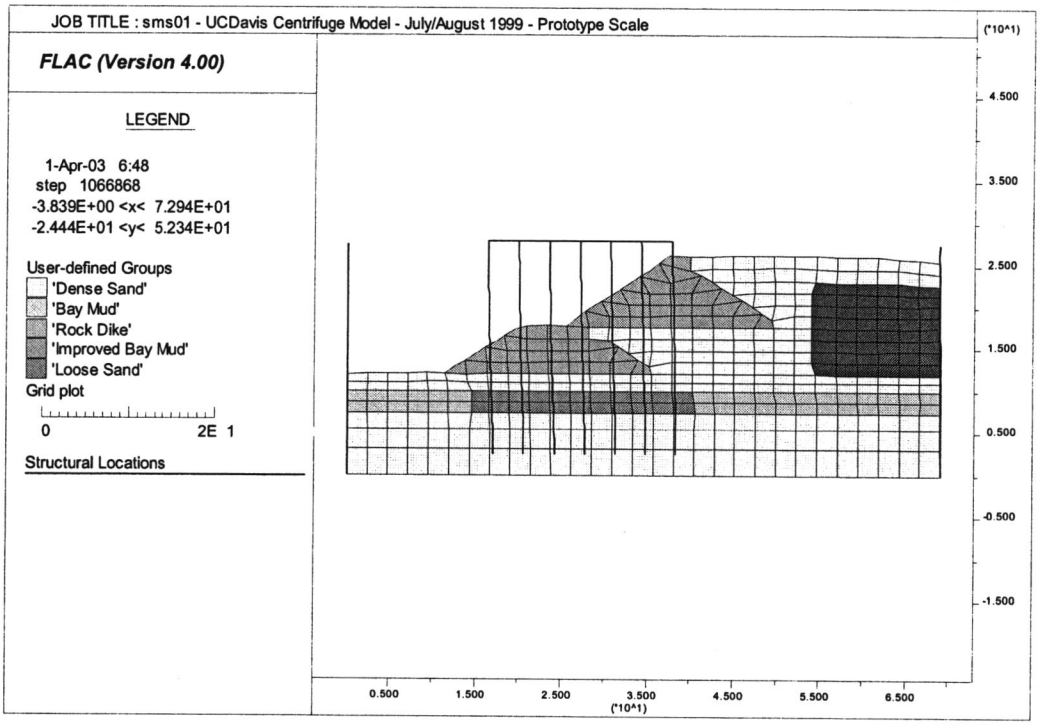

SMS01 – DISPLACEMENT VECTORS

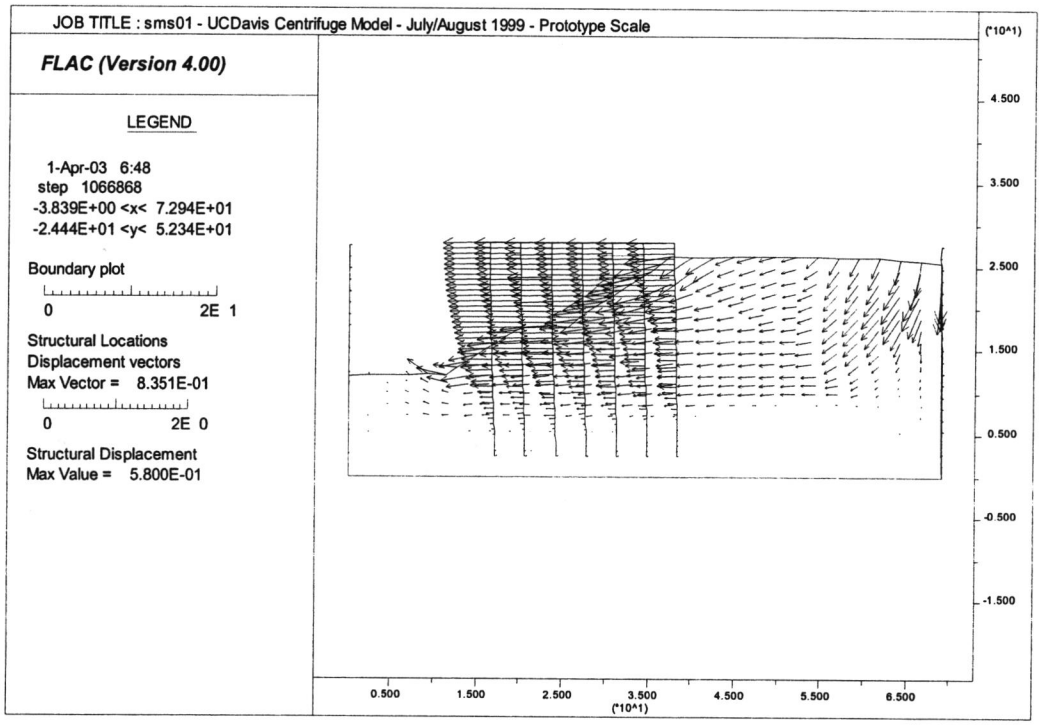

SMS01 – PILE BENDING MOMENTS

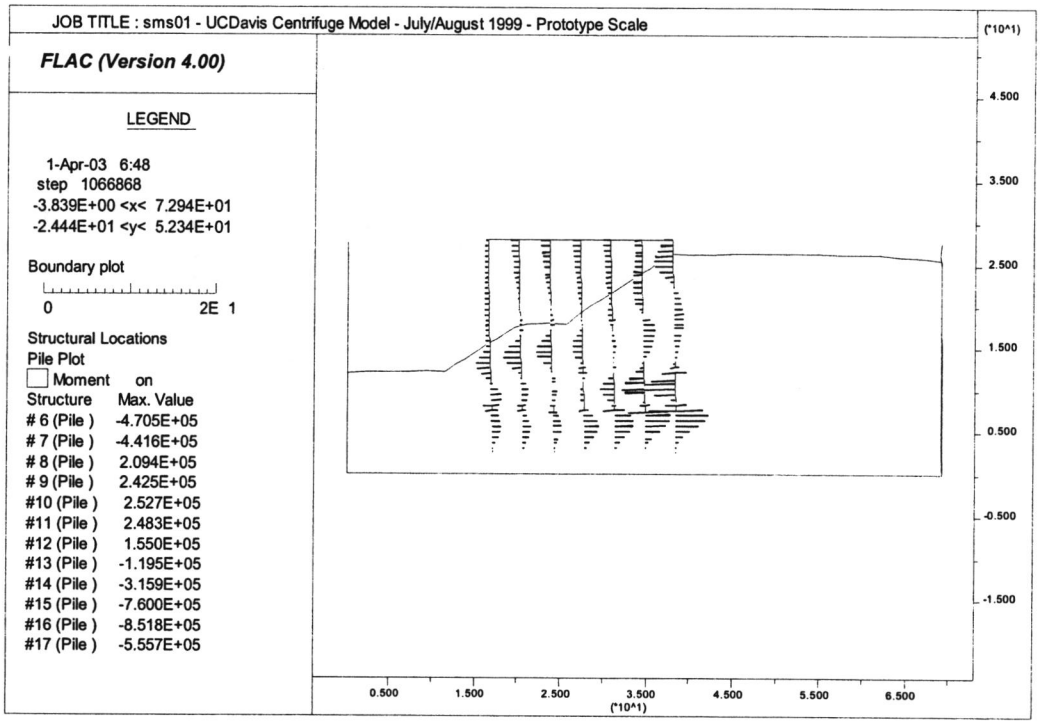

SMS01 – EXCESS PORE PRESSURE GENERATION

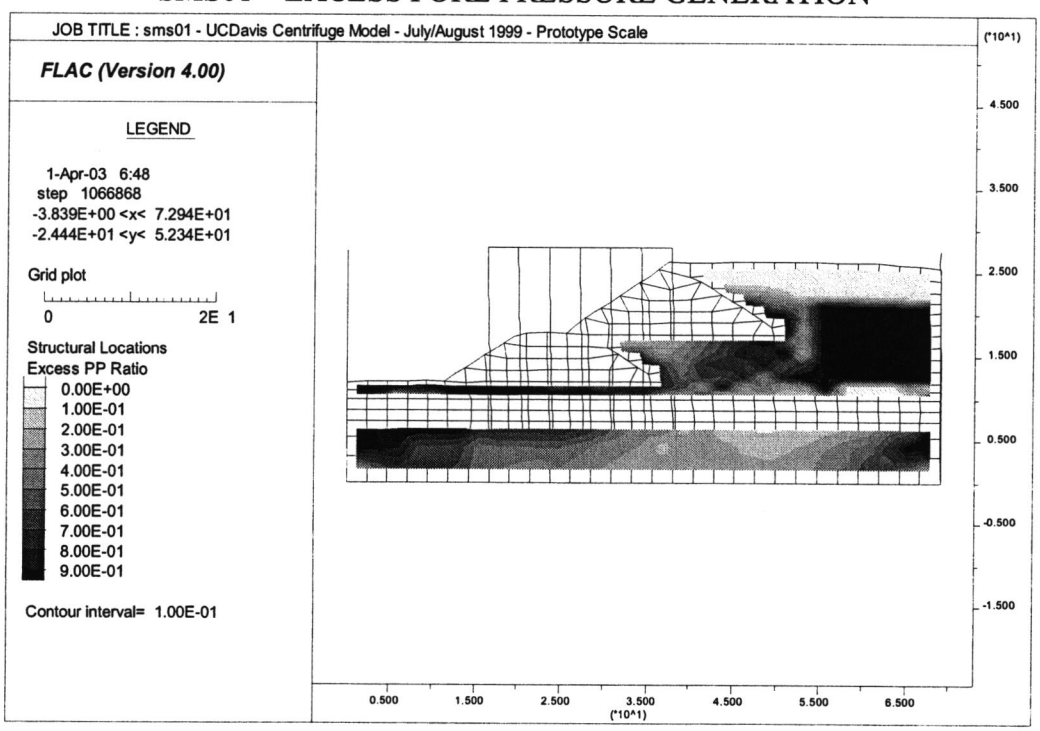

SMS02 – MESH, SOIL LAYERS AND STRUCTURAL ELEMENTS

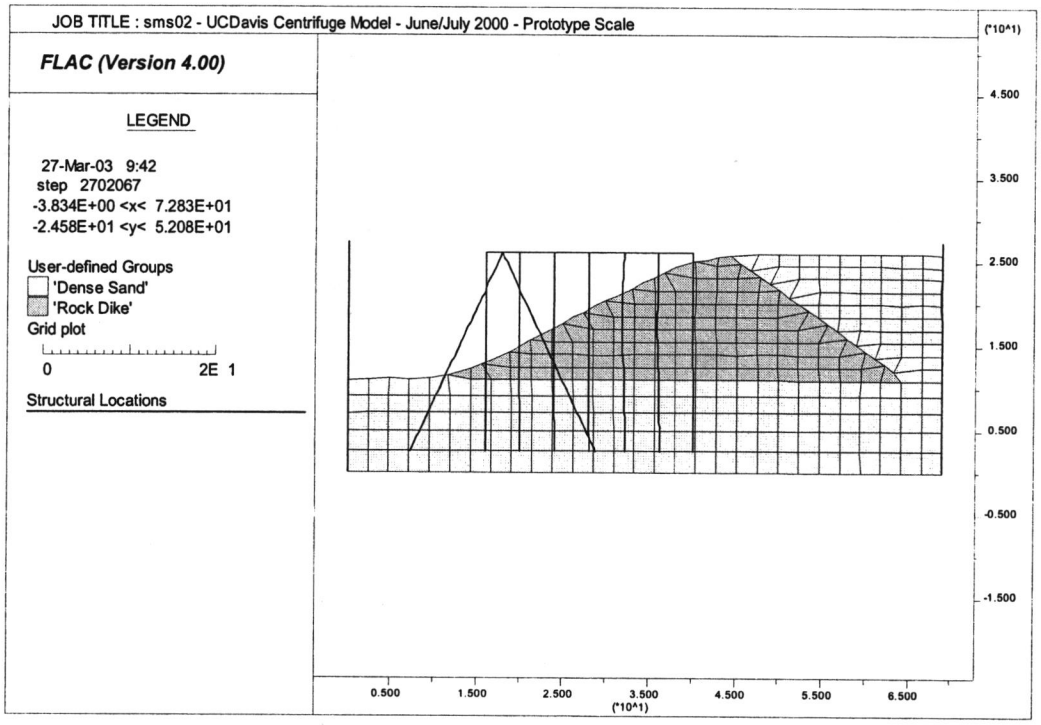

SMS02 – DISPLACEMENT VECTORS

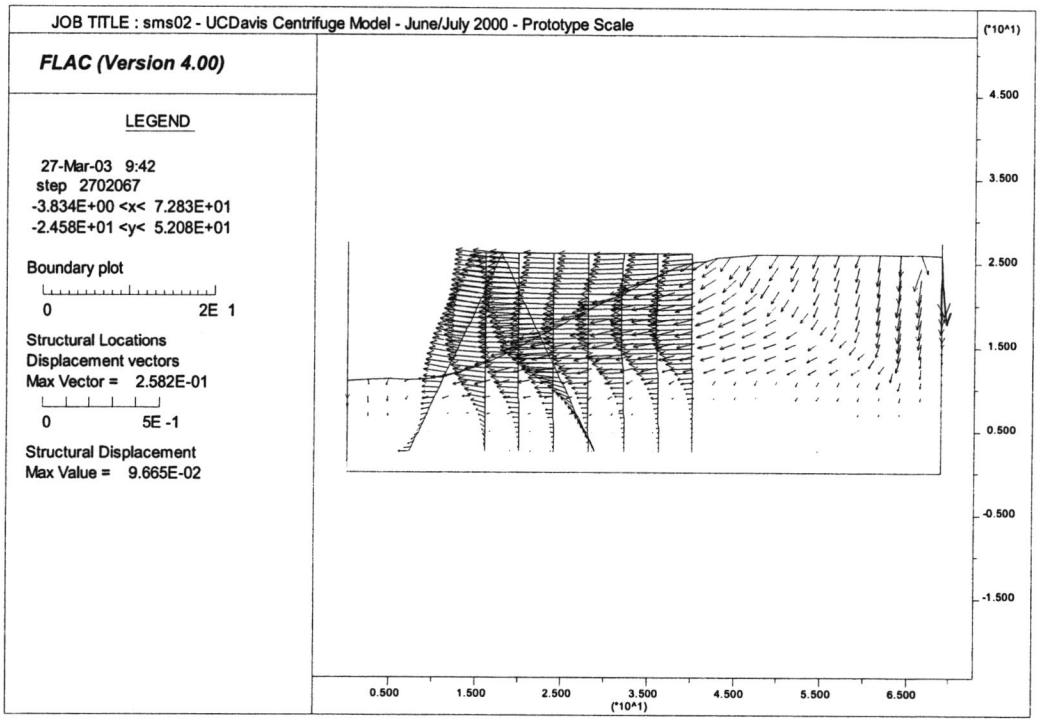

SMS02 – PILE BENDING MOMENTS

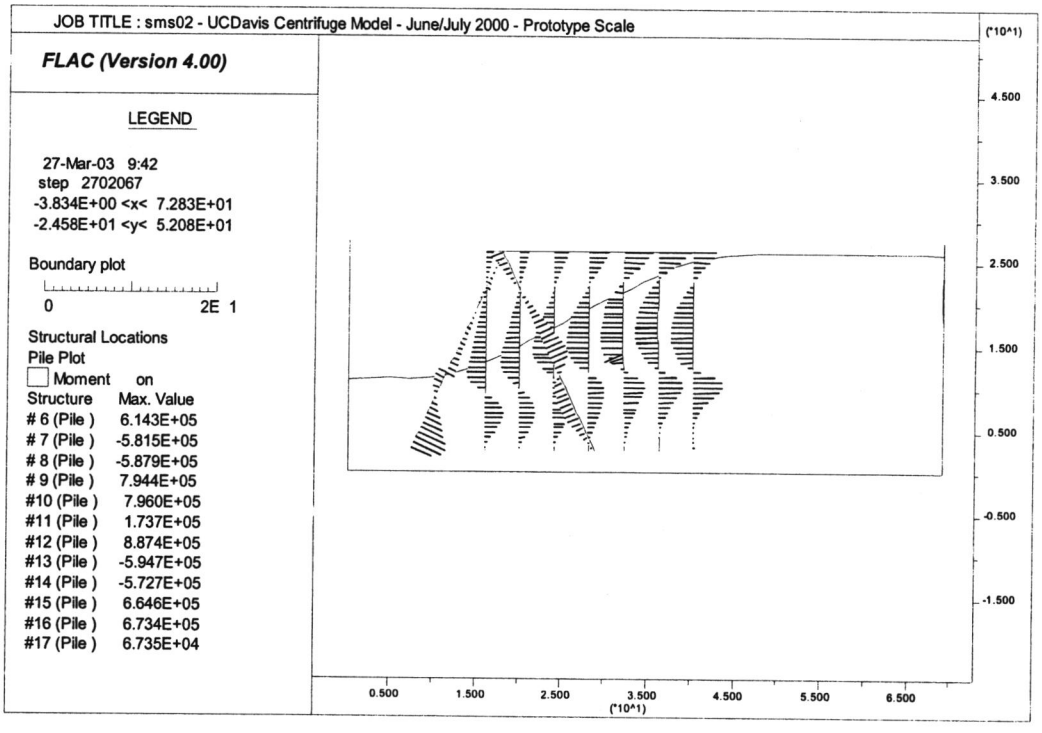

SMS02 – EXCESS PORE PRESSURE GENERATION

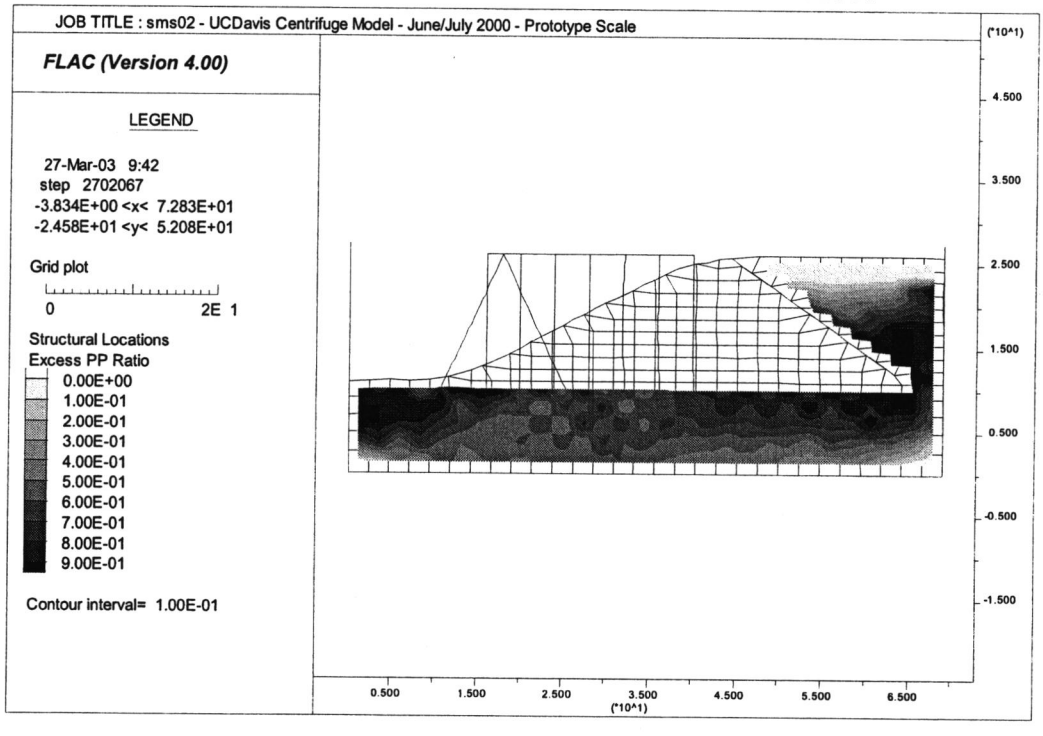

JCB01 – MESH, SOIL LAYERS AND STRUCTURAL ELEMENTS

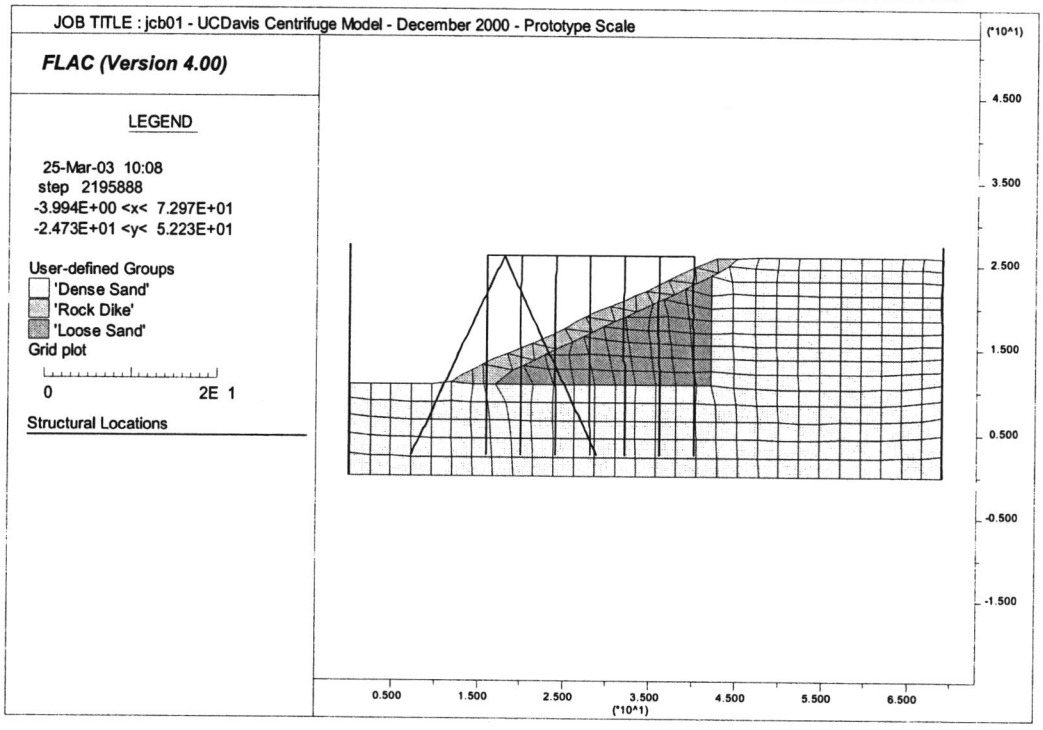

JCB01 – DISPLACEMENT VECTORS

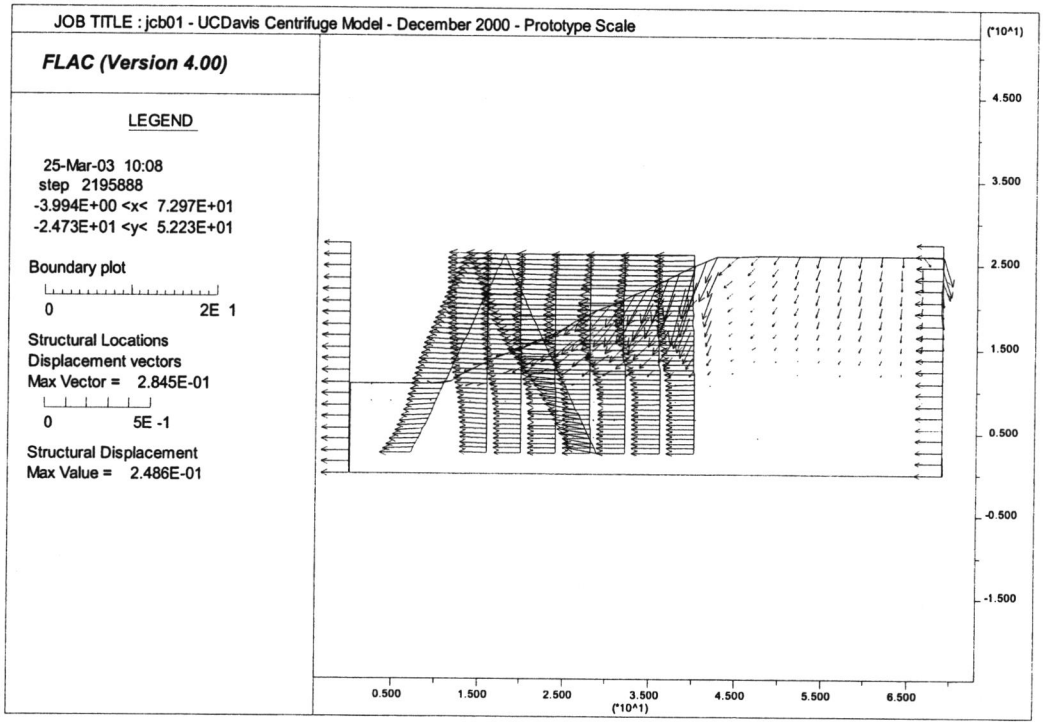

JCB01 – PILE BENDING MOMENTS

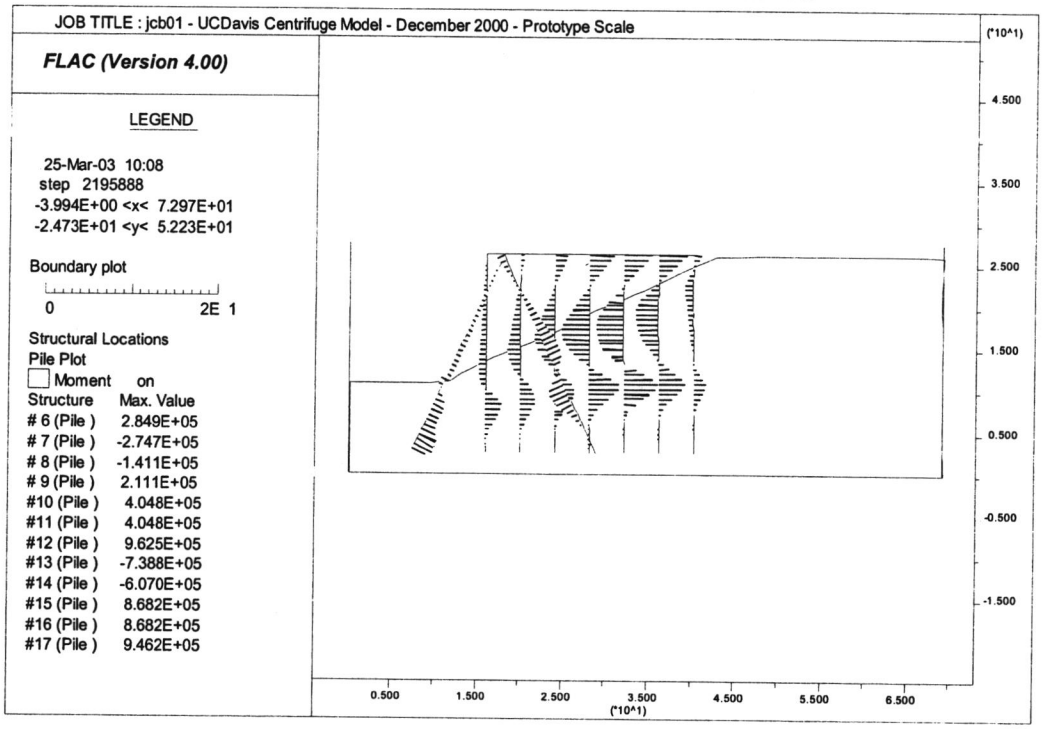

JCB01 – EXCESS PORE PRESSURE GENERATION